ISSN 0021-9673

VOL. 638 NO. 1 MAY 21, 1993

# NAL OF HROMATOGRAPHY

## DING ELECTROPHORESIS AND OTHER SEPARATION METHODS



ELSEVIER

# JOURNAL OF CHROMATOGRAPHY

INCLUDING ELECTROPHORESIS AND OTHER SEPARATION METHODS

**Scope.** The *Journal of Chromatography* publishes papers on all aspects of **chromatography, electrophoresis** and related methods. Contributions consist mainly of research papers dealing with chromatographic theory, instrumental developments and their applications. The section *Biomedical Applications*, which is under separate editorship, deals with the following aspects: developments in and applications of chromatographic and electrophoretic techniques related to clinical diagnosis or alterations during medical treatment; screening and profiling of body fluids or tissues related to the analysis of active substances and to metabolic disorders; drug level monitoring and pharmacokinetic studies; clinical toxicology; forensic medicine; veterinary medicine; occupational medicine; results from basic medical research with direct consequences in clinical practice. In *Symposium volumes*, which are under separate editorship, proceedings of symposia on chromatography, electrophoresis and related methods are published.

**Submission of Papers.** The preferred medium of submission is on disk with accompanying manuscript (see *Electronic manuscripts* in the Instructions to Authors, which can be obtained from the publisher, Elsevier Science Publishers B.V., P.O. Box 330, 1000 AH Amsterdam, Netherlands). Manuscripts (in English; *four* copies are required) should be submitted to: Editorial Office of *Journal of Chromatography*, P.O. Box 681, 1000 AR Amsterdam, Netherlands, Telefax (+31-20) 5862 304, or to: The Editor of *Journal of Chromatography, Biomedical Applications*, P.O. Box 681, 1000 AR Amsterdam, Netherlands. Review articles are invited or proposed in writing to the Editors who welcome suggestions for subjects. An outline of the proposed review should first be forwarded to the Editors for preliminary discussion prior to preparation. Submission of an article is understood to imply that the article is original and unpublished and is not being considered for publication elsewhere. For copyright regulations, see below.

**Publication.** The *Journal of Chromatography* (incl. *Biomedical Applications*) has 40 volumes in 1993. The subscription prices for 1993 are:

*J. Chromatogr.* (incl. *Cum. Indexes, Vols. 601–650*) + *Biomed. Appl.* (Vols. 612–651):
Dfl. 8520.00 plus Dfl. 1320.00 (p.p.h.) (total *ca.* US$ 5622.75)

*J. Chromatogr.* (incl. *Cum Indexes, Vols. 601–650*) only (Vols. 623–651):
Dfl. 7047.00 plus Dfl. 957.00 (p.p.h.) (total *ca.* US$ 4573.75)

*Biomed. Appl.* only (Vols. 612–622):
Dfl. 2783.00 plus Dfl. 363.00 (p.p.h.) (total *ca.* US$ 1797.75).

**Subscription Orders.** The Dutch guilder price is definitive. The US$ price is subject to exchange-rate fluctuations and is given as a guide. Subscriptions are accepted on a prepaid basis only, unless different terms have been previously agreed upon. Subscriptions orders can be entered only by calender year (Jan.–Dec.) and should be sent to Elsevier Science Publishers, Journal Department, P.O. Box 211, 1000 AE Amsterdam, Netherlands, Tel. (+31-20) 5803 642, Telefax (+31-20) 5803 598, or to your usual subscription agent. Postage and handling charges include surface delivery except to the following countries where air delivery via SAL (Surface Air Lift) mail is ensured: Argentina, Australia, Brazil, Canada, China, Hong Kong, India, Israel, Japan*, Malaysia, Mexico, New Zealand, Pakistan, Singapore, South Africa, South Korea, Taiwan, Thailand, USA. *For Japan air delivery (SAL) requires 25% additional charge of the normal postage and handling charge. For all other countries airmail rates are available upon request. Claims for missing issues must be made within six months of our publication (mailing) date, otherwise such claims cannot be honoured free of charge. Back volumes of the *Journal of Chromatography* (Vols. 1–611) are available at Dfl. 230.00 (plus postage). Customers in the USA and Canada wishing information on this and other Elsevier journals, please contact Journal Information Center, Elsevier Science Publishing Co. Inc., 655 Avenue of the Americas, New York, NY 10010, USA, Tel. (+1-212) 633 3750, Telefax (+1-212) 633 3764.

**Abstracts/Contents Lists** published in Analytical Abstracts, Biochemical Abstracts, Biological Abstracts, Chemical Abstracts, Chemical Titles, Chromatography Abstracts, Current Awareness in Biological Sciences (CABS), Current Contents/Life Sciences, Current Contents/Physical, Chemical & Earth Sciences, Deep-Sea Research/Part B: Oceanographic Literature Review, Excerpta Medica, Index Medicus, Mass Spectrometry Bulletin, PASCAL-CNRS, Referativnyi Zhurnal, Research Alert and Science Citation Index.

**US Mailing Notice.** *Journal of Chromatography* (ISSN 0021-9673) is published weekly (total 52 issues) by Elsevier Science Publishers (Sara Burgerhartstraat 25, P.O. Box 211, 1000 AE Amsterdam, Netherlands). Annual subscription price in the USA US$ 4573.75 (subject to change), including air speed delivery. Application to mail at second class postage rate is pending at Jamaica, NY 11431. **USA POSTMASTERS**: Send address changes to *Journal of Chromatography*, Publications Expediting, Inc., 200 Meacham Avenue, Elmont, NY 11003. Airfreight and mailing in the USA by Publications Expediting.

**See inside back cover** for Publication Schedule, Information for Authors and information on Advertisements.

---



0021-9673/93/$06.00



Printed in the Netherlands

VOL. 638, NO. 1 JOURNAL OF CHROMATOGRAPHY MAY 21, 1993

# CONTENTS

*(Abstracts/Contents Lists published in Analytical Abstracts, Biochemical Abstracts, Biological Abstracts, Chemical Abstracts, Chemical Titles, Chromatography Abstracts, Current Awareness in Biological Sciences (CABS), Current Contents/Life Sciences, Current Contents/Physical, Chemical & Earth Sciences, Deep-Sea Research/Part B: Oceanographic Literature Review, Excerpta Medica, Index Medicus, Mass Spectrometry Bulletin, PASCAL-CNRS, Referativnyi Zhurnal, Research Alert and Science Citation Index)*

## REGULAR PAPERS

*Column Liquid Chromatography*



*Gas Chromatography*



*Supercritical Fluid Chromatography*



*(Continued overleaf)*

SHORT COMMUNICATIONS

*Gas Chromatography*



*Electrophoresis*

JOURNAL OF CHROMATOGRAPHY

VOL. 638 (1993)

# JOURNAL of CHROMATOGRAPHY

INCLUDING ELECTROPHORESIS AND OTHER SEPARATION METHODS



ELSEVIER

AMSTERDAM — LONDON — NEW YORK — TOKYO

0021-9673/93/$06.00



Printed in the Netherlands

*Journal of Chromatography*, 638 (1993) 1–8
Elsevier Science Publishers B.V., Amsterdam

CHROM. 24 927

# Electrochemical detection of dipeptides with selectivity against amino acids

Stephen G. Weber* and Hweiyan Tsai

*Department of Chemistry, University of Pittsburgh, Pittsburgh, PA 15260 (USA)*

Mats Sandberg

*Institute of Neurobiology, Department of Histology, Göteborgs Universitet, Medicinaregatan 5, Göteborg (Sweden)*

(First received August 27th, 1992; revised manuscript received February 1st, 1993)

ABSTRACT

Electrolysis of a basic mobile phase containing biuret reagent [Cu(II) and a tartrate salt] at high (>1.2 V *vs.* Ag/AgCl) potentials modifies the glassy carbon electrode. This modified anode oxidizes dipeptides, yielding signals expected for a one-electron transfer, even at low (down to 0.7 V *vs.* Ag/AgCl) potentials and in the absence of intentionally added copper(II) ion in the reagent or mobile phase. The same modification demonstrates a selectivity to $\alpha$-dipeptides over amino acids that is unprecedented. The product of the anodic reaction is reduced at a downstream cathode at low positive potentials. Sensitivities for several amino acids and dipeptides are reported under several conditions. Neither the anodic nor the cathodic signals for the buiret complex of the tripeptide Ala–Ala–Ala are significantly altered because of the modification.

## INTRODUCTION

Detection strategies for chromatographically separated peptides have taken one of two courses. Either detection has been specific for an amino acid functional group or the detection has relied upon the nucleophilicity of the peptide's amine group to form a detectable derivative. An example of the former approach is the electrochemical detection of tyrosine-containing opioid peptides [1], while the fluorescence detection of the reaction product of *o*-phthalaldehyde (OPA) [2] or 2,3-naphthalenedialdehyde and peptides [3,4] are examples of the latter. The primary virtues of these methods are their low detection limits and their established nature; OPA has been used successfully and routinely for the fluorescence determination of amino acids in particular.

Although the genetically coded amino acids are only twenty species, the group of natural non-protein amino and imino acids and derivatives are probably well over 700 [5]. The theoretical number of dipeptides consisting only of protein amino acids is 400, and many of these are chromatographically similar to amino acids [6]. It is evident that routine chromatography of today is incapable of separating, for example, all of the dipeptides from all of the amino acids. A related problem is that chromatographic analysis at trace levels inevitably suffers from the presence of interfering peaks. Methods that are more molecularly selective are urgently needed to help solve both of these problems.

We have begun to develop the biuret reaction in electrochemical detection [7,8]. This reaction

* Corresponding author. Visiting scientist at Institute of Neurobiology, Department of Histology, Göteborgs Universitet, Medicinaregatan 5, Göteborg, Sweden; permanent address at Pittsburgh.

0021-9673/93/$06.00 

creates electroactive species from electroinactive peptides, but not from electroinactive amino acids. Thus, the electrochemical detection shows a significant selectivity for peptides over amino acids [7].

Simple pentapeptides yield stable complexes with Cu(II) in which one amine and three amide nitrogens are donors in the distorted octahedral complexes [9]. This coordination environment supports the Cu(III) oxidation state at remarkably modest potentials [9]. The potential needed to oxidize peptide-bound Cu(II) to Cu(III) becomes more positive as the number of amides becomes smaller; the resultant higher energy Cu(III) forms of smaller peptides are less stable towards intramolecular electron transfer reactions. These intramolecular reactions destroy the complex. Thus, the shorter peptides' Cu(III) complexes have short lifetimes in basic aqueous solution as evidenced by the low collection efficiency in dual-electrode electrochemical detection [8], and values of the ratio of cathodic peak current to anodic peak current in cyclic voltammetry [7]. The lifetimes of Cu(III) complexes of dipeptides are probably very short, though there is no direct chemical evidence to support this speculation. Nonetheless, we found conditions under which dipeptides are detectable using the biuret reagent [8]. The electrochemical detection cell had two electrodes, an upstream anode and a downstream cathode. Our finding was that high potential was required for the oxidation and the lifetime of the Cu(III) peptide formed in the oxidation was short, as expected. Thus, detection at both the anode and the cathode is poorer for the dipeptides than for longer peptides.

Some peptides, such as glutathione and N-acetyl–Asp–Glu [10–12], have been recognized as important to brain function. However, in general there is very little information on the concentration and distribution of dipeptides [13–22] perhaps in part due to the lack of suitable methods. Any method which is developed for peptides should, if possible, exhibit some selectivity over amino acids as the latter are expected to be generally higher in concentration than peptides. Thus, we have reinvestigated the detection of dipeptides with the ultimate purpose of finding conditions suitable for the determination of $\alpha$-dipeptides in the brain and we have also looked into the selectivity of the detection for peptides in comparison to the amino acids.

## EXPERIMENTAL

Chromatographic equipment. A Waters 625 pump [polyetheretherketone (PEEK)] with a 600E controller were used to pump the aqueous mobile phases through the $200 \times 4.6$ mm I.D. column of Nucleosil 5 SB (Macherey–Nagel, Düren, Germany), a 5-$\mu$m diameter silica-based anion-exchange material. The detector was a BAS LC4B with a dual glassy carbon electrode cell. The spacer thickness was 50 $\mu$m. All potentials stated are referred to the Ag/AgCl, 3 *M* NaCl electrode which was also obtained from BAS (through CMA/Microdialysis, Stockholm, Sweden). Data were recorded on a strip chart recorder. Peak areas were approximated as the product of the full width at half height and the peak height.

Mobile phases were aqueous buffers and salt solutions including 500 m*M* $K_2SO_4$, 500 m*M* $Li_2SO_4$, 500 m*M* LiCl and acetate buffers (sodium acetate, lithium acetate, acetic acid.) The LiCl was from BDH (Poole, UK), while all the rest were from Merck (analytical-reagent grade, Darmstadt, Germany). Water was Milli-Q deionized and charcoal filtered. All solutions were filtered through 0.45 $\mu$m filters (type HV; Millipore, Bedford, MA, USA). The LiCl was used both as recieved and after recrystallization from hot water. There was a significant orange color in the filtrate of the hot mother liquor which suggests the presence of iron. Indeed, after using the LiCl in the mobile phase the peaks became broader and the peaks were returned to their symmetrical shape after a couple of injections of 500 m*M* EDTA. Retention times were not noticably changed by this procedure, which was only needed once.

The Waters 625 pump uses four solvent reservoirs. The concentrations of salts in the mobile phases cited in the tables are given as final concentrations as seen by the column. However, the pH value of the individual mobile phase components is stated.

Postcolumn phases were buffered with 4-(2-hydroxyethyl)-1-piperazineethanesulfonic (HEPES) (Sigma, St. Louis, MO, USA), and phosphate ($NaH_2PO_4 \cdot H_2O$ and $Na_2HPO_4 \cdot 2H_2O$), or sodium carbonate–hydrogencarbonate (the latter four compounds were analytical-reagent grade from Merck). The pH meter (Orion, Zurich, Switzerland) was calibrated daily at pH 7.00 and pH 4.00. A pH very close to 8.1 is obtained from a phosphate solution 500 m*M* in the monobasic phosphate salt and 20 m*M* in the dibasic salt; a pH near 8.0 is obtained if the latter value is 30 m*M*. A pH near 9.85 results from 100 m*M* each of sodium carbonate and hydrogencarbonate, and the pH is about 8.9 when there are 180 mmols of hydrogencarbonate to 20 mmols of carbonate per liter. A solution of $CuSO_4$ (anhydrous, Merck) analytical-reagent grade) and potassium sodium tartrate (Merck analytical-reagent grade) was prepared by making separate solutions of the two species and combining them. Molar ratios of 3:1 (tartrate to copper) and 6:1 have been used.

The electrode polishing protocol was to polish with 6 $\mu$m diamond (BAS, W. Lafayette, IN, USA) followed by vigorous squirting of the surface with deionized water, and then several minutes of ultrasonication (Juchheim Laborteknik, Seelbach, Germany) in methanol (Rathburn L.C. grade, Walkerburn, UK). Sometimes this was followed by a polish using 0.3 $\mu$m alumina (Fisher, Pittsburgh, PA, USA), and ultrasonication in methanol again.

Amino acid and peptide solutes were: from Research Plus (Bayonne, NJ, USA), Gly–Leu; from Sigma, Ala, Gly, Ser, Lys, Leu, cystine, Asp, Glu, Arg, Ala–Ala–Ala ($A_3$); from Bachem (Philadelphia, PA, USA), Glu–Lys, Arg–Glu, Asp–Ala, Asp–Glu, Asp–Gly, Asp–Leu. Solutions were prepared in water. They were stable for about a week when refrigerated overnight.

## RESULTS

Sensitivities have been calculated as peak area per mol injected. The units are picocoulombs per picomole. For a one-electron transfer, the maximum value of the sensitivity is just Faraday's constant, about $9.65 \times 10^4$. Thin-layer flow cells of the design used usually detect a few percent of the solute that flows over the electrodes, thus a sensitivity of about 1000 C/mol is expected from an ordinary single-electron transfer detection. In a two-electrode cell, with an upstream generator and a downstream collector, the senstivity of the upstream electrode will be about 1000, while that at the downstream electrode will be about one-third of that if the species formed at the upstream generator is long-lived and survives the journey from the upstream to the downstream electrodes. In the system under discussion, the upstream generator is an anode, while the downstream collector is a cathode. Cathodic sensitivities for three representative peptides, $A_3$, Asp–Ala and Asp–Glu, as a function of pH and Cu(II) concentration in the postcolumn reagent are shown in Table I. The mobile phase, flowing at 1.0 ml/min, was 10 m*M* $K_2SO_4$, 25 m*M* pH 4.62 sodium acetate buffer. The postcolumn phases, identified in Table I, were flowing at 0.5 ml/min. Better sensitivities were recorded for the higher pH, a not unexpected result for an oxidation. However, it is surprising that the sensitivities decrease when the Cu(II) concentration is increased.

To test the effect of Cu(II) on the cathodic sensitivity, the compounds $A_3$ and Asp–Ala were used with a series of postcolumn phases shown in Table II. The Cu(II) seems to play no role in the generation of signal; even in the absence of Cu(II), a significant signal is obtained for the two peptides. At pH near 9 the sensitivity is as good or better than at pH near 10. However, when the postcolumn system was rinsed with a 3% solution of concentrated nitric acid in water for 90 min at 1.0 ml/min, the sensitivity with a pH 8.98 carbonate buffer postcolumn phase declined to about 5% of its initial value.

In a separate experiment, with freshly polished electrodes, the effect of pH and Cu(II) concentration were determined without changing the buffering ion. Thus, carbonate–hydrogencarbonate buffers were used at pH values near 9 and 10, and Cu(II) concentrations of 0.1 and 1.0 m*M* were used. The data for cathodic sensitivities are shown in Table III. Once again, it can be seen that the influence of Cu(II) is to decrease, rather

TABLE I

SENSITIVITIES AT THE CATHODE: EFFECT OF pH AND [Cu(II)]

Mobile phase: 1.0 ml/min 10 m*M* $K_2SO_4$, 25 m*M* pH 4.62 NaOAc. Postcolumn phase: 0.5 ml/min. Potassium sodium tartrate concentration is three times the stated Cu(II) concentration. Potentials: anode 1.1 V, cathode 0.0 V.

| Postcolumn phase | | Sensitivity (C/mol) | | |
|---|---|---|---|---|
| | | Ala–Ala–Ala | Asp–Ala | Asp–Glu |
| Hydrogen carbonate–carbonate | pH 9.85 | | | |
| Cu(II) | 0.1 m*M* | 180 | 260 | 120 |
| | 1.0 m*M* | 160 | 80 | 40 |
| HEPES | pH 7.50 | | | |
| Cu(II) | 0.1 m*M* | 80 | 90 | 110 |
| | 1.0 m*M* | 20 | – | – |

TABLE II

SENSITIVITIES AT THE CATHODE: EFFECT OF [Cu(II)]

Mobile phase: 1.0 ml/min 10 m*M* $K_2SO_4$, 25 m*M* pH 4.62 NaOAc. Postcolumn phase: 0.2 *M* total (carbonate + hydrogencarbonate) as sodium salts. Potassium sodium tartrate concentration is three times the stated Cu(II) concentration. Potentials: anode 0.90 V, cathode 0.15 V.

| pH | Cu(II) (m*M*) | Sensitivity (C/mol) | |
|---|---|---|---|
| | | Ala–Ala–Ala | Asp–Ala |
| 9.85 | 0.2 | 260 | 200 |
| 9.85 | 0.05 | 280 | 220 |
| 9.85 | 0 | 250 | 240 |
| 8.98 | 0 | 320 | 240 |
| | $HNO_3$ rinse | | |
| 8.98 | 0 | 10 | 10 |

than increase, the signal. The sensitivities for the dipeptide Asp–Ala and for the amino acid Asp are more strongly dependent on the Cu(II) concentration than the tripeptide $A_3$.

A sequence of events is recorded in Table IV. The cathodic sensitivity at freshly polished electrodes and an anode potential of 1.0 V is the same in the presence and absence of bicarbonate in the Cu(II)-containing postcolumn phase (data not shown). When the anode is taken to 1.2 V, and then back to 1.0 V, there is much less of a decrement in cathodic sensitivity accompanying the potential change from 1.2 to 1.0 V when there is hydrogencarbonate in the phase. In fact, as can be seen in the table, the carbonate need not be present once the anode has been taken up to 1.2 V in its presence. The sensitivity to the dipeptides remains significant at modest potentials.

TABLE III

SENSITIVITIES AT THE CATHODE AND SELECTIVITY TO Asp–Ala OVER Asp

Mobile phase, postcolumn phase and potentials as in Table II.

| pH | Cu(II) (m*M*) | Sensitivity (C/mol) | | | |
|---|---|---|---|---|---|
| | | Ala–Ala–Ala | Asp–Ala | Asp | Asp–Ala/Asp |
| 8.98 | 0.1 | 330 | 180 | 6 | 30 |
| | 1.0 | 270 | 80 | 0.5 | 160 |
| 9.88 | 0.1 | 470 | 110 | 8 | 14 |
| | 1.0 | 220 | 17 | 0.6 | 26 |

TABLE IV

SENSITIVITIES AT THE CATHODE: EFFECT OF HISTORY

Mobile phase: 1.0 ml/min 5 m*M* pH 4.62 NaOAc, 15 m*M* LiCl. Postcolumn phase: 0.5 ml/min 0.52 *M* pH 7.98 phosphate with added $NaHCO_3$ as stated, 0.1 m*M* $CuSO_4$, 0.6 m*M* potassium sodium tartrate. Potentials: anode as stated, cathode 0.0 V.

| | Anode potential (V) | Sensitivity (C/mol) | | | |
|---|---|---|---|---|---|
| | | Ala–Ala–Ala | Asp–Ala | Asp–Asp | Glu–Glu |
| No $HCO_3^-$ | 1.0 | 270 | 60 | 7 | 7 |
| No $HCO_3^-$ | 1.2 | 240 | 140 | 18 | 10 |
| No $HCO_3^-$ | 1.0 | 200 | 40 | 7 | 3 |
| 0.1 *M* $HCO_3^-$ | 1.2 | 290 | 290 | 13 | 130 |
| 0.1 *M* $HCO_3^-$ | 1.0 | 220 | 220 | 60 | 190 |
| 0.1 *M* $HCO_3^-$ | 0.95 | 260 | 180 | 40 | 60 |
| No $HCO_3^-$ | 0.95 | 260 | 200 | 60 | 50 |

Table V shows anodic sensitivities (cathode not used) determined after the electrode had been anodized in a Cu(II) and bicarbonate containing mobile phase. A sampling of acidic, basic and neutral amino acids, and a selection of neutral and acidic dipeptides were tested. It can be seen that, in general, the peptides are more sensitively determined than the amino acids. Thus, the combined sensitivities of Gly and Leu is about 10, while the sensitivity of the dipeptide Gly–Leu is about 1000. Similarly, the sensitivity for the peptides Asp–Gly, Asp–Leu, Glu–Lys and Arg–Glu are significantly larger than the sum of the sensitivities of the relevant amino acids. The most sensitively detected amino acids, of the limited but representative set chosen for study, are the basic ones.

TABLE V

SELECTIVITY AT THE ANODE

Mobile phase: 1.0 ml/min 3 m*M* pH 3.72 LiOAc, 3 m*M* pH 5.72 LiOAc, 50 m*M* $Li_2SO_4$. Postcolumn phase: 0.5 ml/min pH 8.05 phosphate buffer. Electrode preparation: 50 min at 1.2 V in 1.0 ml/min, 3 m*M* pH 3.72 LiOAc, 3 m*M* pH 5.57 LiOAc, 100 m*M* $Li_2SO_4$, plus 0.5 ml/min 0.52 *M* pH 8.14 phosphate buffer, 0.1 m*M* $CuSO_4$, 0.6 m*M* potassium sodium tartrate, 0.1 *M* $NaHCO_3$. The pH of the combination is about 8. Potential: anode 0.85 V.

| Solute | Sensitivity (C/mol) |
|---|---|
| Ala | 2.5 |
| Arg | 220 |
| Asp | 12 |
| Glu | 7.5 |
| Gly | 2.6 |
| Leu | 7.8 |
| Lys | 34 |
| Ser | 4.8 |
| Asp–Glu | 140 |
| Asp–Leu | 300 |
| Glu–Lys | 490 |
| Gly–Leu | 900 |
| Arg–Glu | 1760 |
| Ala–Ala–Ala | 570 |

In some experiments it was noted that the cathodic selectivity for peptides over amino acids increased when the anodic potential was lower and the pH was lower. The effect of pH has been demonstrated in Table III. The results from a study of the anodic sensitivities are shown in Table VI. Here, a selection of neutral amino acids and peptides have been determined at two pH values and two anode potentials. It appears that the sensitivities for all the species except the tripeptide follow about the same pattern; the sensitivity decreases about a factor of three on changing the potential from 0.90 to 0.85 V at each pH, and at each potential, the sensitivity drops a factor of three in lowering the pH the stated amount. Thus the anodic sensitivity, but not the selectivity, are influenced by pH and potential in the range studied.

The potential dependences of the cathodic signal as the anodic and cathodic potentials

TABLE VI

SENSITIVITY AND SELECTIVITY AT THE ANODE: EFFECT OF pH AND POTENTIAL

Mobile phase: 1.0 ml/min 3 m*M* pH 3.72 LiOAc, 3 m*M* pH 5.72 LiOAc, 25 m*M* $Li_2SO_4$. Post column phase: 0.5 ml/min pH 8.05 phosphate buffer. Electrode preparation: 50 min at 1.2 V in 1.0 ml/min 3 m*M* pH 3.72 LiOAc, 3m*M* pH 5.57 LiOAc, 100 m*M* $Li_2SO_4$, plus 0.5 ml/min 0.52 *M* pH 8.1 phosphate buffer, 0.1 m*M* $CuSO_4$, 0.6 m*M* potassium sodium tartrate, 0.1 *M* $NaHCO_3$. The pH of the combination is about 8.

| Solute | Sensitivity (C/mol) | | | |
|---|---|---|---|---|
| | Anode potential 0.9 V, pH 8.14 | Anode potential 0.85 V, pH 8.14 | Anode potential 0.9 V, pH 7.57 | Anode potential 0.85 V, pH 7.57 |
| Ala | 8.2 | 2.4 | 3.4 | 0.7 |
| Gly | 6.6 | 2.6 | 2.6 | 0.9 |
| Leu | 23 | 7.8 | 6.4 | 3.2 |
| Lys | 100 | 30 | 30 | 8.8 |
| Ser | 16 | 4.8 | 5.6 | 1.6 |
| Arg–Glu | 3240 | 1760 | 1300 | 510 |
| Gly–Leu | 3400 | 750 | 800 | 80 |
| Glu–Lys | 1650 | 540 | 510 | 130 |
| Ala–Ala–Ala | 650 | 490 | 90 | 20 |

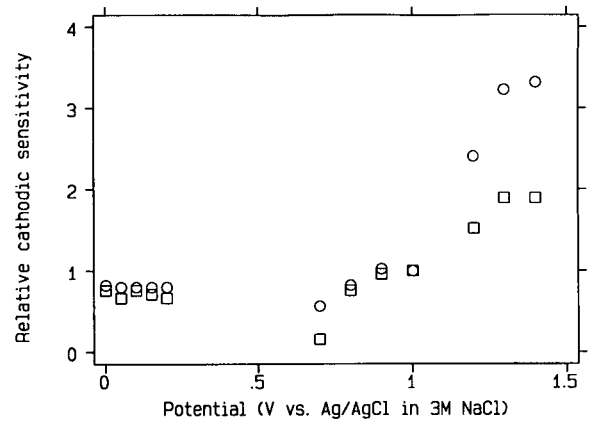


Fig. 1. Cathode sensitivities for $A_3$ (○) and Asp Ala (□). Data plotted from 0 to 0.2 V are taken with varying cathodic potentials and an anodic potential of 0.8 V. Conditions as in Table II. Data plotted from 0.7 to 1.0 V are also taken under conditions as in Table II, but it is the anodic potential that varies, the cathodic potential is 0.0 V. A second set of data, taken under solution conditions in Table V and with cathodic potential = 0, is plotted as the anodic potential changes from 1.0 to 1.4 V. Sensitivities from the two sets of solution conditions are normalized with respect to values found at an anodic potential of 1.0 V and a cathodic potential of 0.0 V.

change are shown in Fig. 1. This is a composite figure, so relative sensitivities to a standard condition (anode = 1.0 V, cathode = 0.0 V) are used. The right side of the diagram shows the response as the anodic potential is changed. There are two waves, one with a half-wave potential around 0.7–0.8 V and the other with a half-wave potential around 1.3 V. Our experience has been that the signal-to-noise ratio is better on the plateau around 0.9–1.0 V than at potentials above 1.4 V. On the left side of the diagram, sensitivities are shown for the cathodic potential changing with a constant anodic potential. In separate experiments we have determined that the signal is negligible when the cathodic potential is 0.5 V. Thus, although it is not well characterized in the figure, the half-wave potential is in the range of 0.4 V.

Fig. 2 shows a chromatogram of dipeptides containing the acidic amino acids. The separa-

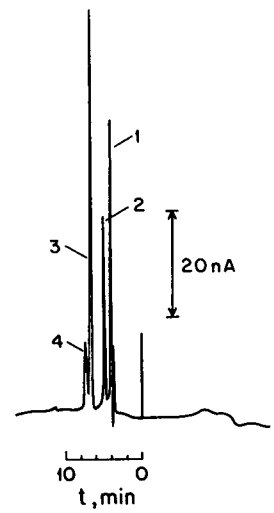


Fig. 2. Chromatogram of (1) Glu–Lys (0.49 nmol), (2) Asp–Gly (0.95), (3) Asp–Asp (0.69), (4) Glu–Glu (0.62). Mobile phase 1.0 ml/min of 6 m*M* acetate buffer pH 4.5, 75 m*M* $Li_2SO_4$. Postcolumn solution pH 8.14, 0.5 *M* phosphate buffer at 0.5 ml/min.

tion based largely on charge is expected of an anion exchange material.

## DISCUSSION

It may be a Cu(II) complex that is detected when Cu(II) is present in the system, but if the primary signal-producing event were the oxidation of Cu(II) bound in a complex, then the law of mass action dictates that the signal must at least remain constant, or perhaps increase, as the Cu(II) concentration increases. The decrease in sensitivity caused by increasing the Cu(II) concentration in the postcolumn reagent, the presence of the signal in the absence of intentionally added Cu(II), and the disappearance of the signal when the postcolumn reactor and flow cell are rinsed with nitric acid, suggest that some surface reaction makes the electrode more sensitive to the peptides. Inspection of the electrodes shows that the anode, but not the cathode, has a film after the potential of the anode has been held at a positive potential ($>1.2$ V).

The data in Table III show that not only is the sensitivity dependent on the Cu(II) concentration, but the relative sensitivity of the dipeptide Asp–Ala to the amino acid Asp is influenced by Cu(II) concentration. At both high and low pH, the selectivity of the detection for the peptide is better with higher Cu(II). This is not due to a relatively greater signal from the dipeptide, but is due to a larger copper-induced decrease in the signal from the amino acid. It is well known that amino acids form complexes with Cu(II) [23]. Certainly tripeptides form the biuret complex [7,9], and, although dipeptides give a signal at the electrochemical detector under conditions which yield the biuret complex from tripeptides [8], they probably do not form a complex with a stable Cu(III) form. An investigation of a single peptide was carried out to explore this.

We have examined the cyclic voltammetry and visible absorbance spectrum of the dipeptide Gly–Leu. The cyclic voltammetry at a glassy carbon electrode in biuret reagent shows a drawn out anodic wave at around 900–1000 mV, with no cathodic wave at 200 mV $s^{-1}$. The visible spectra of Gly–Leu solutions in biuret reagent were recorded with the biuret reagent as a reference. The wavelength of maximum absorbance shifts slightly when the Cu(II)-to-peptide ratio is changed, from 614 nm at 1:5 to 638 nm at 5:1. Biuret complexes have $\lambda_{max}$ at about 550 nm. The molar absorptivity (based on the limiting reagent) is about 50 $M^{-1}$ $cm^{-1}$. The wavelength of maximum absorbance in the excess Cu(II) is consistent with the formation of a 1:1 complex (donor atoms: amine, amido nitrogens, carboxylate and hydroxide oxygens: theoretical $\lambda_{max}$ = 632 nm computed according to Billo [24]).

The electrochemistry and the spectroscopy are consistent in the sense that a stable Cu(III) form is not seen on the time scale used.

The depressing effect of Cu(II) on the signal implies that coordination to Cu(II) lowers the activity of the oxidized species. This effect is more important for the amino acids and dipeptides than for the tripeptide $A_3$ (Tables II and III). It is noteworthy that there is no signal observed (sensitivity $\ll 1$) from N-acetyl–Asp and from N-acetyl–Asp–Glu. These observations imply that the amine group is important to the oxidation of the amino acid and dipeptides.

Recently, a catalytic oxidation by an anodized copper electrode of the amino acids and some peptides has been discussed by Luo *et al.* [25]. This approach seems very promising, as the sensitivity is good, and the electrode is long-lasting. As is the case in the current study, the sensitivity to amino acids depends upon the side chain; amino acid detection limits vary by a factor of 50 in that work. This is similar to the sensitivity variation seen in the current work. Although the data are not explicitly given, it seems that the sensitivity for small peptides with the electrode of Luo *et al.* [25] is about the same as that for the amino acids. The current work is different in two respects. First, the sensitivity to peptides is, in general, higher than for amino acids; in the few examples cited above the dipeptide's sensitivity is always significantly larger than the sum of the sensitivities of the constituent amino acids. Second, the pH required to carry out the reaction is lower. In the work of Luo *et al.* [25] the mobile phase was 0.1 *M* NaOH. In this work, a pH of 8 was shown to be compatible with detection.

## CONCLUSIONS

We do not know yet what the putative electrode modification is, nor do we know why the surface reacts as it does. Nonetheless, we have shown that it is possible to detect dipeptides with some selectivity at a modest potential in weakly alkaline solutions, the latter compatible with most reversed-phase materials, for example. There is, on average, a selectivity for dipeptides over amino acids, though individual exceptions exist (Arg *vs.* Asp–Gly). Future work concerning the application of this detection technique to extracts of rat brain, and work directed towards understanding and optimizing the surface of the anode are underway.

## ACKNOWLEDGEMENTS

We are grateful to the Medical Research Council of Sweden (K91-12V-09772-01 and B93-12X-00164-29B) and the National Institutes of Health (GM-44842) for financial support of the research. M.S. is supported by the Swedish National Science Research Council (B-Bu 1905-308). We also thank CMA/Microdialysis and Millipore-Waters Chromatography Division, Göteborg, Sweden for lending us equipment.

## REFERENCES

1 L.H. Fleming and N.C. Reynolds, Jr., *J. Chromatogr.*, 375 (1986) 65.
2 O. Orwar, S. Folestad, S. Einarsson, P. Andiné and M. Sandberg, *J. Chromatogr.*, 566 (1991) 39.
3 P. de Montigny, J.F. Stobaugh, R.S. Givens, R.G. Carlson, K. Srinivasachar, L.A. Sternson and T. Higuchi, *Anal. Chem.*, 59 (1987) 1096.
4 S.M. Lunte, T. Mohabbat, O.S. Wang and T. Kuwana, *Anal. Biochem.*, 178 (1989) 202.
5 S. Hunt, in G.C. Barrett (Editor), *Chemistry and Biochemistry of the Amino Acids*, Chapman & Hall, London, New York, 1985, pp. 55–138.
6 P.B. Hamilton, *Anal. Chem.*, 35 (1983) 2055.
7 A.M. Warner and S.G. Weber, *Anal. Chem.*, 61 (1989) 2664.
8 H. Tsai and S.G. Weber, *J. Chromatogr.*, 515 (1990) 451.
9 F.P. Bossu, K.L. Chellappa and D.W. Margerum, *J. Am. Chem. Soc.*, 99 (1977) 2195.
10 A.S. Guarda, M.B. Robinson, L. Ory-Lavollée, G.L. Forloni, R.D. Blakely and J.T. Coyle, *Mol. Brain Res.*, 3 (1988) 223.
11 J.R. Moffett, L. Williamson, M. Palkovits and M.A.A. Namboodiri, *Proc. Natl. Acad. Sci. U.S.A.*, 87 (1990) 8065.
12 L.C. Williamson, D.A. Eagles, M.J. Brady, J.R. Moffet, M.A.A. Namboodiri and J.H. Neale, *Eur. J. Neurosci.*, 3 (1991) 441.
13 I. Sano, *Int. Rev. Neurobiol.*, 12 (1970) 235.
14 S.T. Cheung and R. Lin, *Biochim. Biophys. Acta*, 586 (1979) 418.
15 D.C Panish, D.G. Smyth. J.R. Normanton and J.H. Wolstencroft, *Nature*, 306 (1983) 267.
16 J. Bernstein, R.S. Fisher, R. Zaczek and J. Coyle, *J. Neurosci.*, 5 (1985) 1429.
17 J.T. Coyle *et al.*, *Adv. Exp. Med. Biol.*, 203 (1986) 375.
18 G.B. Koelle, *Trends Pharmacol. Sci.*, 9 (1988) 318.
19 G.B. Koelle, K.A. Skau, N.S. Thamp, D.M. Hyme and M.S. Han, *Proc. Nat. Acad. Sci. U.S.A.*, 85 (1988) 6215.
20 E.C. Cropper, D. Price, R. Tenebaum, I. Kupfermann and K. R. Weiss, *Proc. Nat. Acad. Sci. U.S.A.*, 87 (1990) 933.
21 L.B. Piotrovsky, A.P. Garyaev and L.N. Poznyakova, *Neurosci. Lett.*, 125 (1991) 227.
22 I.A. Urgerer, C. Mathis, C. Mélan and J. DeBarry, *Brain Res.*, 549 (1991) 59.
23 A.E. Martell and R.M. Smith, *Critical Stability Constants* Vol. 1, Plenum Press, New York, 1974.
24 E.J. Billo, *Inorg. Nucl. Chem. Lett.*, 10 (1974) 613.
25 P. Luo, Z.F. Zhang and R.P. Baldwin, *Anal. Chem.*, 63 (1991) 1702.

*Journal of Chromatography*, 638 (1993) 9–19
Elsevier Science Publishers B.V., Amsterdam

CHROM. 24 898

# Reversed-phase capillary high-performance liquid chromatography with on-line UV, fluorescence and electrospray ionization mass spectrometric detection in the analysis of peptides and proteins

Timothy G. Heath[☆] and Anne B. Giordani*

*Parke-Davis Pharmaceutical Research Division, Warner Lambert Company, 2800 Plymouth Road, Ann Arbor, MI 48105 (USA)*

(First received November 4th, 1992; revised manuscript received January 22nd, 1993)

ABSTRACT

Analysis of peptide mixtures by reversed-phase capillary HPLC with gradient elution using three detectors in series: UV (214 nm), fluorescence ($\lambda_{exc.} = 280$ nm, $\lambda_{emiss.} = 356$ nm), and electrospray ionization mass spectrometry (ES-MS) is reported. The chromatographic integrity of the system and the detection limits were evaluated. The effect of the mass spectrometer's acquisition rate on the total ion current (TIC) profile was also examined. The utility of fluorescence monitoring with UV and ES-MS detection was demonstrated in the analysis of proteolytic digests of proteins. The native fluorescence character of tryptophan-containing peptides provides selectivity in peptide mapping, while monitoring UV absorption at 214 nm affords detection of the peptide bond. Three tryptophan-containing tryptic peptides of bovine serum albumin were immediately located by fluorescence among many UV peaks and ES-MS provided molecular masses allowing the peptides to be identified.

## INTRODUCTION

The combination of mass spectrometry (MS) and microbore or capillary reversed-phase high-performance liquid chromatography (RP-HPLC) has emerged as a powerful technique for the analysis of complex proteolytic digests of proteins [1–23]. Peptide mapping with mass spectrometric detection is used to validate or confirm deduced protein sequences [2,4]. This strategy relies on comparing measured molecular masses of proteolytic fragments determined by mass spectrometry with theoretical molecular masses of peptides anticipated from the chemical reaction of the enzyme and protein [2].

Electrospray ionization (ES) [1–9] and continuous flow fast atom bombardment (CF-FAB) [1,2,10–23] are two ionization methods which enable a mass spectrometer to be interfaced with HPLC for generating gas-phase ions from peptides in solution. For RP-HPLC, solvents usually consist of aqueous mixtures of acetonitrile or methanol with $\leq 0.1\%$ addition of an ion-pairing agent. A commonly used ion-pairing agent in the analysis of peptides is trifluoroacetic acid (TFA) which is compatible with both ES-MS and CF-FAB-MS. Electrospray ionization mass spectrometry offers several significant advantages over CF-FAB-MS as a detection method for liquid chromatography. One is that mobile phase compositions of this sort work well for ES-MS and do not require modification of the mobile

* Corresponding author.
☆ Present address: Marion Merrell Dow, Inc., Bioanalytical Chemistry Department, P.O. Box 9627, Kansas City, MO 64134-0627, USA.

0021-9673/93/$06.00 

phase prior to mass spectrometric detection. (Involatile buffers, or those with electrolyte content of equivalent conductivity higher than that of $10^{-3}$ *M* NaCl result in reduced sensitivity and spray instability [24].) However, CF-FAB-MS requires a viscous matrix, usually glycerol, at 1–5% in the mobile phase [10–12]. If a viscous matrix is added prior to the column, additional band broadening occurs in the chromatographic separation. Although not as simple to implement, post-column addition of the matrix immediately preceding the CF-FAB probe tip or a coaxial design circumvents this problem [10–12]. However, there still may be memory effects which degrade the total ion current (TIC) profile obtained from the mass spectrometer. The effect that viscous-matrix addition to the mobile phase has on chromatographic integrity has been examined by other investigators [10–12,25,26].

Electrospray ionization mass spectrometry also offers advantages over CF-FAB-MS in the analysis of large peptides and glycopeptides. Detection limits with CF-FAB-MS decrease for peptides with $M_r$ greater than *ca.* 3000 [1,27]. For example, Hemling *et al.* [1] reported that following HPLC separation, glycopeptides with $M_r$ *ca.* 3000–4000 at the 50 pmol level were readily detected by ES-MS whereas CF-FAB failed to detect them. However, CF-FAB-MS with a coaxial interface design apparently overcomes this limitation in the analysis of high mass peptides [23]. Because CF-FAB generates singly and perhaps doubly protonated molecules, the limiting factor in CF-FAB-MS analysis of large peptides can be the mass-to-charge ($m/z$) range of the instrument. In contrast to CF-FAB, electrospray ionization generates multiply protonated molecules [24,28–32] which enables conventional mass spectrometers (quadrupoles, sectors) with limited $m/z$ ranges (*e.g.* 4000 or less) to measure molecular masses of molecules with $M_r > 100\,000$ [31,32]. The ability to analyze peptides and proteins at the low pmol level [1–9], along with the ease with which electrospray ionization mass spectrometry can be interfaced to capillary and microbore HPLC make it an attractive alternative to CF-FAB-MS detection.

Typically in HPLC–MS analyses, on-line UV detection at 214 nm is incorporated for monitoring absorption by the peptide bond. Background ion current may obscure minor components in the TIC profile from mass spectrometric detection. The UV chromatographic trace gives a fingerprint of the peptide map when analyzing complex mixtures. This aids in determining which regions of the chromatogram to examine for the mass spectral information. The native fluorescence emission at $\lambda_{emiss.} = 356$ nm of tryptophan residues following excitation at $\lambda_{exc.} = 280$ nm provides a means to further characterize the peptides in mixtures such as in proteolytic digests [33,34]. Monitoring fluorescence as well as UV absorption reveals which peptides in mixtures contain tryptophan residues while the mass spectrometer measures the molecular masses.

The performance of a system consisting of this combination of three detectors: UV, fluorescence and ES-MS, following gradient separation with a 0.500 mm I.D. reversed-phase capillary $C_{18}$ column is evaluated with respect to chromatographic integrity and detection. The utility of this combination of detectors is demonstrated in the analysis of proteolytic digests of bovine serum albumin (BSA) and stromelysin catalytic domain (SCD) protein expressed in *E. coli*.

## EXPERIMENTAL

### *Instrumentation*

Chromatographic separations were performed using a Michrom BioResources Ultrafast Microprotein Analyzer (Michrom BioResources, Pleasanton, CA, USA) which included a Valco 10-port valve with a 20-$\mu$l injection loop. The solvents are pumped through heated (30°C) precolumns and combined at a micro mixing tee. After mixing, the solvent at a flow of 70 $\mu$l/min, passes through a stainless steel fixed precolumn splitter which directs approximately 14 $\mu$l/min flow to the capillary $C_{18}$ HPLC column (Reliasil $C_{18}$, 5 $\mu$m, 300 Å, 150 mm × 0.5 mm I.D.) and the remainder to waste through a 1 mm I.D. balance column [20,35]. The chromatograph is interfaced to a modified Linear UVis 200 Detector (Linear Instruments, Reno, NV, USA) equipped with a 0.8-$\mu$l, 2-mm pathlength flow cell. Absorbance is monitored at 214 nm. The

outflow from the UV detector is connected by fused-silica capillary tubing (75 μm I.D/150 μm O.D.) to a Gilson 121 Filter Fluorometer (Gilson, Middleton, WI, USA) equipped with a 0.6-μl flow cell. The fluorometer is fitted with a mercury lamp with $\lambda_{exc.} = 280$ nm. A glass filter with wavelength maximum transmission at 356 nm is used in monitoring fluorescence emission. The total dead volume between the UV and fluorescence detector is 5 μl. The sampling interval for both the UV and fluorescent detectors is 0.1 s.

A 1:1 split of the eluent following the fluorescent detector is accomplished by using a PEEK tubing tee and fused-silica capillary (50 μm I.D/150 μm O.D. × 1.25 m; dead volume, 2.5 μl). Flow is delivered at *ca.* 7 μl/min to a Vestec (Houston, TX, USA) electrospray interface fitted to a Finnigan MAT (San Jose, CA, USA) TSQ 70 triple stage quadrupole mass spectrometer (Fig. 1). The Vestec interface uses a heated source block, which was held at 225°C, for desolvation. Prior to performing a gradient HPLC–ES-MS analysis, the needle voltage was set to 2.2 kV, and the solvent composition to 60% A. Then, the distance between the ES needle tip and nozzle aperture of the interface was adjusted until a spray current of *ca.* 0.25 μA was achieved. (A spray current of *ca.* 0.25 μA was found to be optimum in terms of sensitivity). The electrical characteristics of the mobile phase change over the course of the gradient separation due to changes in solvent composition so the needle voltage was adjusted manually during the HPLC runs in order to maintain the spray current. Typically, the needle voltage ranged from *ca.* 2.3 kV at 90% A to *ca.* 1.9 kV at 10% A. The repeller voltage was held at 15–20 V. These interface conditions minimized fragment ion formation. Mass spectra were acquired by scanning the third quadrupole (Q3) from $m/z$ 500–2000 at a rate of 300 $(m/z)$ $s^{-1}$ unless otherwise indicated.

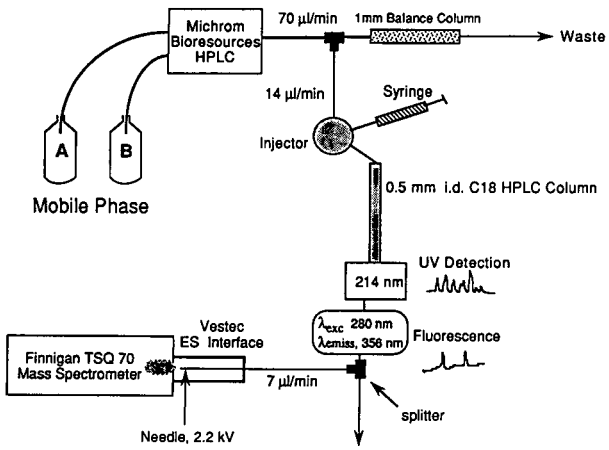


Fig. 1. Capillary HPLC–MS interface.

*Mobile phase*

The mobile phase was prepared from HPLC grade acetonitrile (Mallinckrodt, St. Louis, MO, USA), distilled, deionized water obtained from a Milli-Q system (Millipore, Bedford, MA, USA) and protein sequencing grade trifluoroacetic acid (TFA) (Applied Biosystems, Foster City, CA, USA). Mobile phase A was prepared with a composition of water–acetonitrile (98:2) with 0.1% TFA. Mobile phase B was acetonitrile–water (90:10) with 0.09% TFA.

*Chemicals*

Adrenocorticotropic hormone fragment 1–24 (ACTH 1–24) and BSA were purchased from Sigma (St. Louis, MO, USA). SCD expressed in *E. coli* was provided by Dr. Qi-Zhuang Ye of Parke-Davis (Ann Arbor, MI, USA). Details of the protein expression and purification is found elsewhere [36]. Trypsin-TPCK was from Pierce Chemical (Rockford, IL, USA) and the proteolytic digests (50:1 $w_{substrate}/w_{enzyme}$) were carried out in 0.1 *M* ammonium bicarbonate, pH 8.0, at 37°C for 16 h.

## RESULTS AND DISCUSSION

A typical feature of ES-MS of peptides and proteins is the formation of a series of multiply protonated molecules which are represented as peaks in the mass spectrum. The measured $m/z$ values for the protonated molecules are used to compute the molecular mass of the compound. In mixtures of peptides, hydrophobicity differences can result in pronounced differential ionization when analyzed by FAB. ES does not suffer as severely from this limitation [24], thus

permitting direct mixture analysis with minimal discrimination, although the spectra may be very complex. A separation method preceding ES-MS simplifies data interpretation in mixture analysis and may offer gains in sensitivity due to reduction of both charge competition among mixture components and buffer suppression of ionization [37]. However, Fig. 2 illustrates that a separation method preceding ES-MS analysis of mixtures may be necessary to assure correct interpretation of the mass spectral data. ES mass spectra are simulated for three hypothetical peptides in Fig. 2A–C. Although the peptides have different molecular masses, the simulated ES mass spectral peaks indicate that there are ions with identical $m/z$ values found in the mass spectrum of more than one of the hypothetical peptides. It is a simple task to determine the $M_r$ of the 'pure' peptides from the spectra in Fig. 2A–C. However, the same is not true for the spectrum in Fig. 2D which shows the composite spectrum of the three hypothetical peptides. For example, the peaks at $m/z$ 501, 751 and 1501 could be assigned as $(M + 3H)^{3+}$, $(M + 2H)^{2+}$ and $(M + H)^{+}$, respectively, indicating a species of $M_r$ 1500 while the peaks at $m/z$ 667.7, 1001 and 2001 could be assigned to $(M + 3H)^{3+}$, $(M + 2H)^{2+}$ and $(M + H)^{+}$ for a compound with $M_r$ 2000. Thus the peaks in Fig. 2D may be inadvertently accounted for by components with $M_r$ values of 1500 and 2000. However, because the component with $M_r$ 3000 does not yield a singly protonated molecule (or the $m/z$ range of the mass spectrometer is <3000 so it is not detected), it could easily be overlooked in the composite spectrum obtained by direct analysis. With chromatographic separation, the reconstructed ion chromatograms of individual $m/z$ values would indicate three components. Coupling chromatographic separation with ES-MS simplifies data analysis of mixtures and minimizes the potential of misassignment of molecular masses.

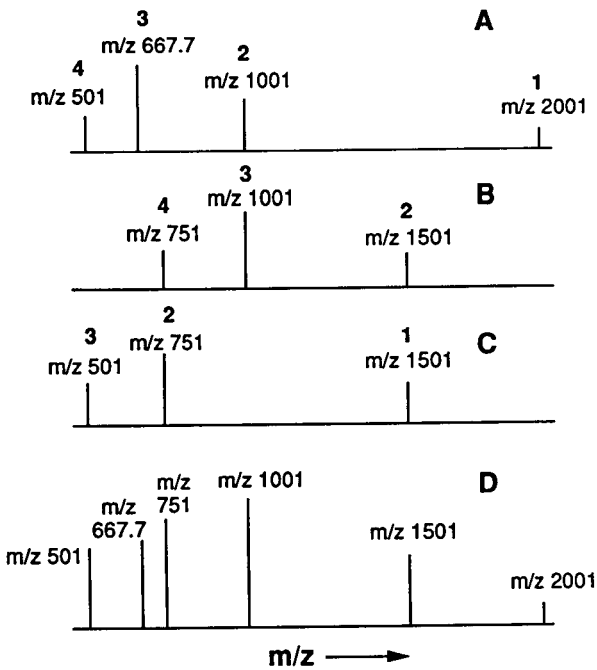


Fig. 2. Simulated electrospray mass spectra for hypothetical peptides with molecular masses of (A) 2000, (B) 3000 and (C) 1500 dalton. Fig. D is the hypothetical composite spectrum of the mixture of the three components in Fig. A–C. The numbers above the $m/z$ labeled peaks in A–C represent the number of protons attached to the molecule represented by the mass spectral peak.

*Chromatographic profile at each detector*

A wide range of capillary columns, from 0.01 mm to 0.5 mm in diameter, have been constructed for HPLC analyses [38]. Commercially available capillary HPLC columns of 0.3 mm I.D. and 0.5 mm I.D. have been used in this laboratory. Although lower detection limits can be achieved with a 0.3 mm I.D. column as the analyte is more effectively concentrated due to lower flow-rates, it has been our experience that the 0.5 mm I.D. columns are more durable, and maintain greater baseline stability with gradient RP-HPLC chromatography. So, for the most part 0.3 mm I.D. columns are reserved for the analysis of very low quantity samples (<5 picomoles). For routine separations, a 0.5 mm I.D. column is the most practical choice in the analysis of 10–500-pmol samples [38] and was selected as the column in measuring chromatographic profiles at each detector.

As a general rule, to ensure minimal extracolumn broadening by the detector, the detector cell volume should be less than one-tenth the volume of the peak of interest [39,40]. In the system described here, the UV and fluorescent detectors each satisfy this rule but there is 5 $\mu$l

dead volume between these two detectors. An important part of the evaluation of the system with three on-line detectors was to evaluate the chromatographic integrity by measuring chromatographic peak width at half heights ($w_{1/2}$) at each detector.

The $w_{1/2}$ values were measured from the chromatographic peak obtained from 25-pmol injections of ACTH (1–24) ($M_r$ 2933.4) into the chromatograph. ACTH (1–24) was selected because the peptide contains a tryptophan residue and therefore is detected by fluorescence under the conditions described in the experimental section. For ES-MS detection, Q3 of the mass spectrometer was repetitively scanned from $m/z$ 730–738 in order to detect only one of the prominent ions in the ES-MS of ACTH (1–24): $(M + 4H)^{4+}$. A scan rate of 80 $(m/z)s^{-1}$, yielding an acquisition rate of 10 scan $\cdot s^{-1}$ was used. Therefore, for this experiment the sampling interval for all three detectors was 0.1 s. A fast acquisition rate ensures that the chromatographic peak widths as observed by ES-MS are not artificially degraded by long sampling intervals while a slow mass spectrometer scan rate improves the signal-to-noise ratio of the peak. The measured $w_{1/2}$ for the chromatographic peak as observed at each detector is shown in Table I. The mixing which occurs in the flow cells along with laminar dispersion in the connecting tubing causes the 26% increase in the fluorescence $w_{1/2}$ *versus* UV, as shown in Table I. As evident by the small increase in $w_{1/2}$ for the TIC trace compared to the fluorescence trace, the data indicates that there is some minimal broadening of the chromatographic zone after fluorescence detection. This broadening occurs in the flow splitter, the connecting tubing prior to the electrospray interface, and in the electrospray interface itself.

TABLE I

MEASURED PEAK WIDTHS ($w_{1/2}$) WITH UV, FLUORESCENCE AND ES-MS DETECTION FOR ANALYSIS OF 25 pmol OF ACTH (1–24)

| Detector | $w_{1/2}$ (s) | % Increase[c] |
|---|---|---|
| UV[a] | 12.5 ± 0.2 | – |
| Fluorescence[a] | 15.7 ± 0.6 | 26 |
| ES-MS[b] | 17.9 ± 0.2 | 14 |

[a] Average of 8 analyses.
[b] Average of 2 analyses.
[c] Represents % increase in $w_{1/2}$ from that measured at the immediately preceding detector.

*Effect of mass spectrometer acquisition rate on chromatographic trace*

The chromatographic peak width observed with mass spectrometric detection is a function of the mass spectrometer's acquisition rate. Increasing the acquisition rate (by shortening the sampling interval) results in a narrower and more accurate characterization of the chromatographic peak because there are more data points to define its shape [41,42]. It has been estimated that using 10–25 cm long columns with efficiencies between $1 \cdot 10^4$ and $2.5 \cdot 10^4$ plates, the sampling interval should be 1 s, preferably between 0.1–0.5 s. Otherwise, there is an apparent loss in chromatographic resolution [41]. If the $m/z$ range scanned is kept constant, increasing the frequency at which mass spectra are collected requires an increase in the scan rate [measured as $(m/z)s^{-1}$]. However, increasing the acquisition rate by scanning faster results in a poorer $S/N$ ratio because the sampling times (sampling time $\equiv$ scan rate$^{-1}$) for each $m/z$ value are shortened. Fig. 3 displays 8-min windows of TIC traces from repetitive injections of 25 pmol of ACTH (1–24). Because the HPLC conditions for these repetitive analyses were identical, the variation in the chromatographic peak observed in the TIC trace is due to the different acquisition and scan rates of the mass spectrometer. The data obtained by scanning the mass spectrometer from $m/z$ 500–2000 at a rate of 150 $(m/z)s^{-1}$, 300 $(m/z)s^{-1}$, 600 $(m/z)s^{-1}$ and 1250 $(m/z)s^{-1}$ is shown in Fig. 3A–D, respectively. Fig. 3A–D compares the measured $w_{1/2}$ for these traces. Of the four traces displayed in Fig. 3A–D, the $w_{1/2}$ in Fig. 3D is the narrowest as is expected because the acquisition rate was highest. However, the increased scan rate results in a decrease in the $S/N$ ratio due to the decrease in sampling times. An alternative way to increase

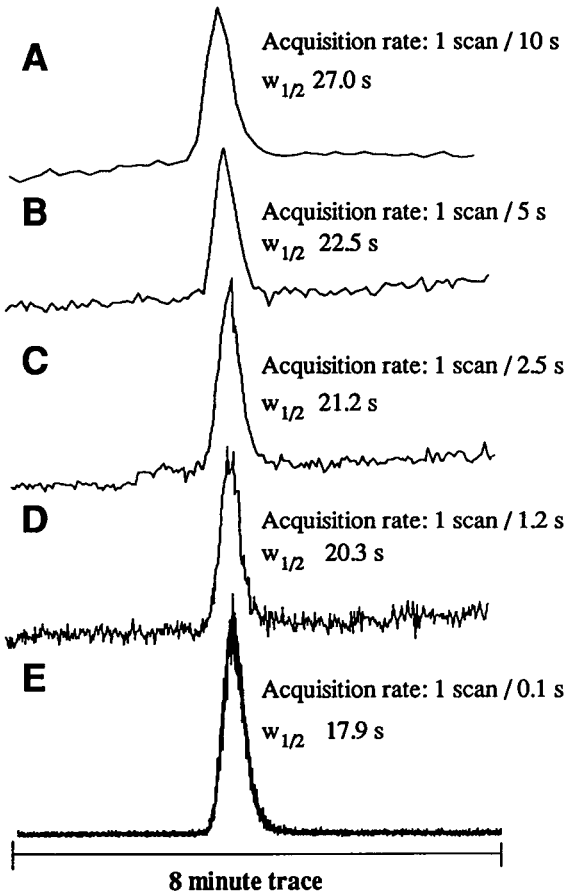


Fig. 3. The TIC chromatogram for analysis of 25 pmol of ACTH (1–24) with the mass spectrometer scanning parameters as follows: (A) $m/z$ 500–2000 at 150 $(m/z)s^{-1}$, sampling time 6.67 ms$(m/z)^{-1}$, (B) $m/z$ 500–2000 at 300 $(m/z)s^{-1}$, sampling time 3.33 ms$(m/z)^{-1}$, (C) $m/z$ 500–2000 at 600 $(m/z)s^{-1}$, sampling time 1.67 ms$(m/z)^{-1}$, (D) $m/z$ 500–2000 at 1250 $(m/z)s^{-1}$, sampling time 0.8 ms$(m/z)^{-1}$ and (E) $m/z$ 730–738 at 80 $(m/z)s^{-1}$, sampling time 12.5 ms$(m/z)^{-1}$. The HPLC conditions were 90% A to 50% A in 25 min followed by re-equilibration at initial conditions.

the acquisition rate is to scan over a narrower mass range. The chromatographic trace displayed in Fig. 3E represents the data obtained at the highest acquisition rate, but the scan rate, 80 $(m/z)s^{-1}$, is the slowest because the mass spectrometer was only scanned from $m/z$ 730–738. Of all the traces displayed in Fig. 3, the profile shown in Fig. 3E reflects the true chromatographic peak shape of the analyte most accurately. However, due to the small scan range, less information is available in the mass spectrum.

*Limits of detection in the analysis of ACTH (1–24)*

The detection limits for each of the three detectors were determined using dilutions of ACTH (1–24). The chromatographic profiles for UV, fluorescence and ES-MS detection following the injection of 1.2 pmol of ACTH (1–24) onto the 0.5-mm $C_{18}$ column are shown in Fig. 4. With a 1:1 split of the eluent following fluorescence detection, approximately 600 fmol is introduced into the electrospray interface. The profiles shown in Fig. 4B and C were obtained when the mass spectrometer was scanned from $m/z$ 500–800 at a rate of 120 $(m/z)s^{-1}$ (1 scan/2.5 s). Although background ion current obscures the

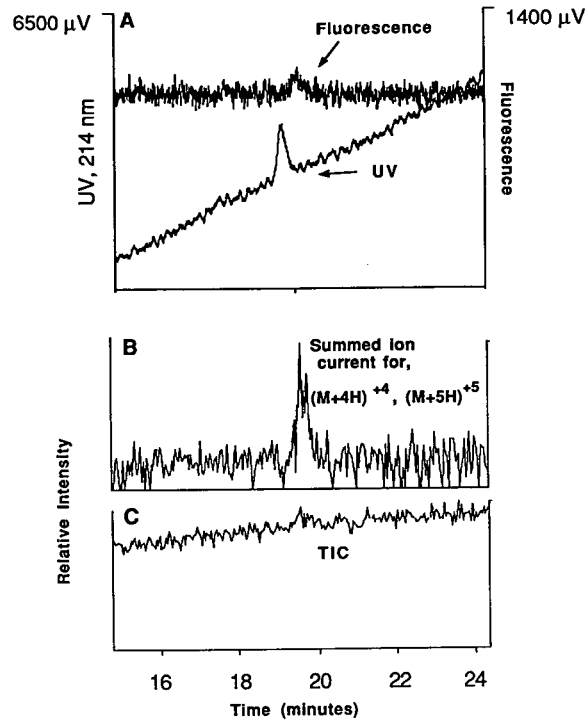


Fig. 4. Chromatographic profiles observed for (A) fluorescence and UV detection, (B) ion current detected at $m/z$ 734 and $m/z$ 588 and (C) TIC with ES-MS following injection of 1.2 pmol of ACTH (1–24) into the chromatograph. For mass spectrometric detection, Q3 was scanned from $m/z$ 500–800 at a rate of 120 $(m/z)s^{-1}$ (acquisition rate, 1 scan/2.5 s).

analyte signal in the TIC trace as seen in Fig. 4C, the analyte signal is observed in the sum of the $(M+4H)^{4+}$ and $(M+5H)^{5+}$ ion current displayed as a function of time as shown in Fig. 4B. The detection limit for analysis of a targeted peptide or protein by HPLC–MS could be further lowered by using selected ion monitoring (SIM) rather than a scanning analysis as in this example. Furthermore, multiple charging with electrospray usually provides more than one $m/z$ value per analyte so that specificity could be enhanced by using a multiple ion monitoring approach.

*Utility of on-line UV, fluorescence and ES-MS detection*

*a) Analysis of BSA tryptic digest.* The utility of this combination of detectors is illustrated in the analysis of the tryptic digest of bovine serum albumin (BSA, $M_r$ 66 500). BSA was digested with trypsin, and a 50 pmol aliquot was injected for analysis. Fig. 5 shows the chromatographic profiles obtained with UV and fluorescence detection. Based on the recently corrected primary sequence of BSA [14], the protein consists of 583 amino acid residues, two of which are tryptophan. The fluorescence detector trace indicates immediately that the peptides eluting at 13.1 min and 14.4 min contain tryptophan. The third highly fluorescent peak (*ca.* 58 min) is undigested BSA. The TIC profile and the $m/z$ values for ion current detected at times corresponding to the fluorescent peptides is displayed in Fig. 6. The reconstructed ion chromatograms shown in Fig. 6B and D indicates the peak at 13.1 min consists of two peptides. The measured $M_r$ values determined for these two peptides are consistent with two anticipated tryptophan-containing tryptic fragments AWSVAR ($M_r$ 688.4) and FWGK ($M_r$ 536.3). The fluorescent peptide eluting at

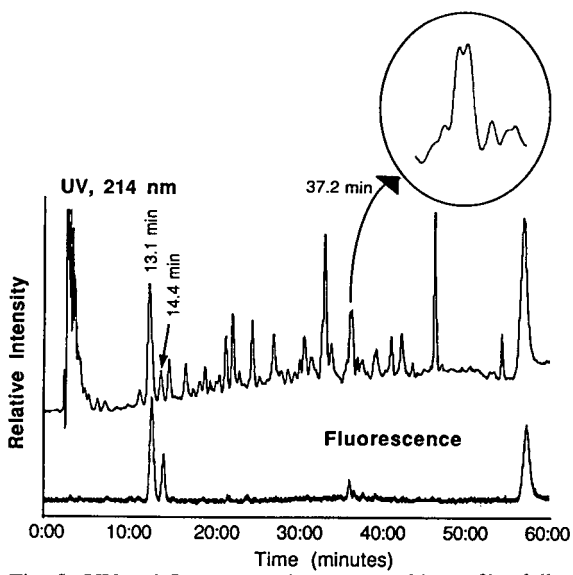


Fig. 5. UV and fluorescent chromatographic profiles following injection of 50 pmol aliquot of BSA tryptic digest. HPLC conditions were 90% A for 4 min, ramped to 40% A at 49 min and to 25% A at 66 min. Inset is a 3-min window centered around the peaks detected with UV at 37.2 min.

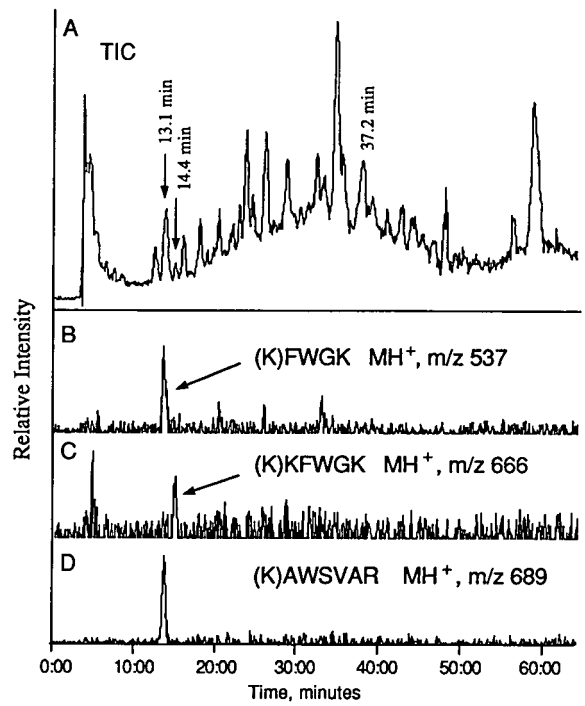


Fig. 6. Chromatographic profile observed for (A) TIC with ES-MS detection, (B) ion current at $m/z$ 537 representing the tryptic peptide FWGK ($M_r$ 536.3), (C) ion current at $m/z$ 666 representing tryptic peptide KFWGK ($M_r$ 664.8) and (D) ion current at $m/z$ 689 representing tryptic peptide AWSVAR ($M_r$ 688.4) for analysis of 50 pmol of BSA tryptic digest. This data was obtained from the same run as the data shown in Fig. 5.

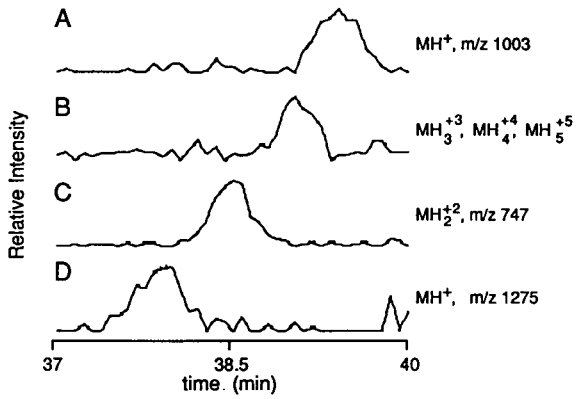


Fig. 7. Reconstructed mass chromatograms for time corresponding to the inset shown in Fig. 5 (37.2 min) for ions detected representing (A) tryptic peptide T 209–217, $M_r$ 1001.6, (B) tryptic peptide with $M_r$ 5262 (sequence uncertain), (C) tryptic peptide T 205–217, $M_r$ 1490.8 and (D) tryptic peptide T 185–196, $M_r$ 1274.4 in the analysis of a tryptic digest of BSA.

14.4 min (Fig. 6C) has a measured $M_r$ of 665 which is consistent with the peptide KFWGK ($M_r$ 664.8) resulting from incomplete digestion.

This analysis also demonstrates how well the resolution provided by the capillary separation is maintained by the three detectors. As evident from the magnification shown in Fig. 5, the peak at 37.2 min in the UV trace consists of multiple components which are not completely resolved. Reconstructed mass chromatograms corresponding to this time frame are shown in Fig. 7 A–D. The computer programs ProComp [43] and MacProMass [44] were used to aid sequence assignments for the peptides detected. Three of the four tryptic peptides detected within this 3-min window were tentatively identified as indicated in Fig. 7. These identifications suggest incomplete digestion. Two of the tryptic fragments represented in Fig. 7, T 205–

TABLE II

SEQUENCE AND MOLECULAR MASSES OF PEPTIDES OBSERVED IN THE HPLC–ES-MS ANALYSIS OF THE TRYPTIC DIGEST OF EXPRESSED SCD

| Peak | $t_R$ (min) | Residues | Sequence | $M_{r(theor)}$ | $M_{r(exp)}$ |
|---|---|---|---|---|---|
| 1 | 7.1 | 10–11 | (K)WR(K) | 360.2 | 360.5 |
| 2 | 7.1 | 10–12 | (K)WRK(T) | 488.3 | 488.4 |
| 3 | 15.6 | 12–18 | (R)KTHLTYR(I) | 917.5 | 918.0 |
| 4 | 23.1 | 3–9 | (R)TFPGIPK(W) | 758.4 | 759.0 |
| 5 | 23.1 | 19–28 | (R)IVNYTPDLPK(D) | 1158.6 | 1159.2 |
| 6 | 26.1 | 10–28 | (K)WRKTHLTYRI VNYTPDLPK(D) | 2401.8 | 2401.2 |
| 7 | 26.1 | 19–37 | (R)IVNYTPDLPKD AVDSAVEK(A) | 2073.0 | 2073.4 |
| 8 | 27.7 | 152–174 | (R)LSQDDINGIQSL YGPPPDSPETP | 2439.1 | 2439.8 |
| 9 | 31.0 | 41–52 | (K)VWEEVTPLTFS R(L) | 1462.7 | 1463.0 |
| 10 | 31.0 | 150–174 | (R)FRLSQDDINGIQSL YGPPPDSPETP | 2742.3 | 2743.4 |
| 11 | 34.3 | 38–52 | (K)ALKVWEEVTPL TFSR(L) | 1775.0 | 1775.8 |
| 12 | 35.2 | 68–106 | (R)EHGDFYPFDGP GNVLAHAYAPGP GINGDAHFDDDEQ WTK(D) | 4255.8 | 4255.3 |
| 13 | 36.5 | 53–67 | (R)LYEGEADIMISF AVR(E) | 1712.8 | 1713.4 |
| 14 | 47.5 | 107–149 | (K)DTTGTNLFLVA AHEIGHSLGLFHS ANTEALMYPLYHS LTDLTR(F) | 4726.4 | 4726.9 |

217 (FGERALKAWSVAR) and T 209–217 (ALKAWSVAR), both contain a tryptophan residue, so the identifications are supported by the fluorescence emission (Fig. 5). The chromatographic traces for $m/z$ values representing singly or multiply protonated tryptic peptides of BSA show how these components may be resolved by mass even though they are not completely resolved by time. This data indicates that the chromatographic resolution, although not perfectly preserved throughout the ES interface, is sufficient to discern incompletely resolved chromatographic peaks.

A problem with the use of multiple detectors is correlation of the data from the different detector traces. Throughout these experiments, the time delay in transfer of the eluent from the UV to the fluorescence to the ES-MS detector was considered in determining which peaks from the different traces represented the same component. To assist in assigning peaks from different traces, a simple mixture containing components detectable by all three detectors but with various retention characteristics can be prepared. Analysis of such a mixture under gradient elution conditions benchmarks the delay times and therefore aids correlation of peaks observed in the analysis of unknown mixtures.

*b) Characterization of expressed SCD.* The metalloproteinase stromelysin is thought to be involved in cartilage degradation in arthritis [36]. SCD was expressed in *E. coli* [36] and introduced into the mass spectrometer by capillary RP-HPLC to remove the urea buffer and to assess sample purity. The $M_r$ of the expressed protein measured by HPLC–ES-MS was 19494.1 ± 0.05%, in good agreement with the theoretical $M_r$ of 19492.7.

The protein was further characterized by digesting some of the material with trypsin. The tryptic map of the expressed material is shown in Fig. 8. As shown in Table II, the $M_r$ values measured for the tryptic fragments are consistent with those anticipated for SCD, and all of the major fluorescent peaks are assigned to tryptic fragments containing a tryptophan residue. The italicized numbers above the chromatographic peaks in the fluorescent and UV traces shown in Fig. 8 correspond to the tryptic peptides listed in Table II. Determining ratios of UV absorbance

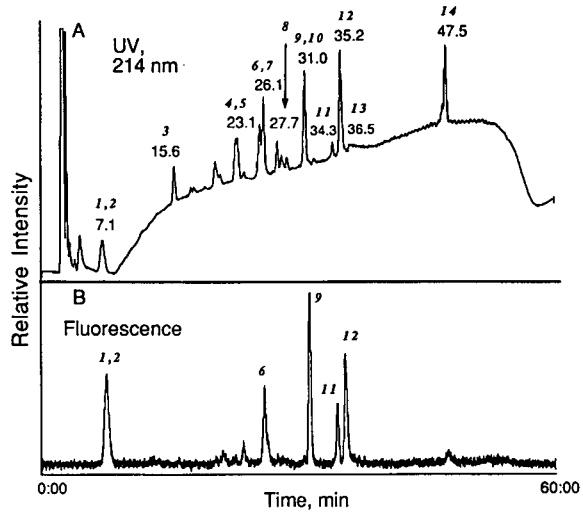


Fig. 8. The (A) UV and (B) fluorescent chromatographic profiles of analysis of tryptic digest of expressed SCD. The sequence for the labeled peaks (italicized numbers) is listed in Table II. The HPLC conditions were 95% A for 4 min followed by 95% A to 35% A from 4 to 40 min and from 35% A to 30% A from 40–45 min. The mobile phase was maintained at 30% A for 5 min before re-equilibration. The mass spectrometer was scanned from $m/z$ 300–2000 at 340 $(m/z)s^{-1}$ which yields an acquisition rate of 1 scan/5 s.

and fluorescence signals may be useful in indicating the number of tryptophan residues, an approach used by other investigators [33], but not examined in this work.

This tryptic map also serves to demonstrate the compatibility of electrospray ionization with gradient elution HPLC. The mass spectra for two tryptic fragments which eluted at 78% $H_2O$ and 36% $H_2O$ are shown in Fig. 9A and B. Electrospray ionization mass spectrometry is able to tolerate a wide range of $CH_3CN$–$H_2O$ compositions, providing good quality mass spectra.

## CONCLUSIONS

On-line combinations of detectors following chromatographic separation by HPLC provides complementary information which is useful in the characterization of proteins/peptides. A novel aspect of this study is the use of fluorescence detection on-line with UV and ES-MS to monitor RP capillary HPLC separations. UV detection at 214 nm provides a complete map or fingerprint of the peptides present in a mixture.

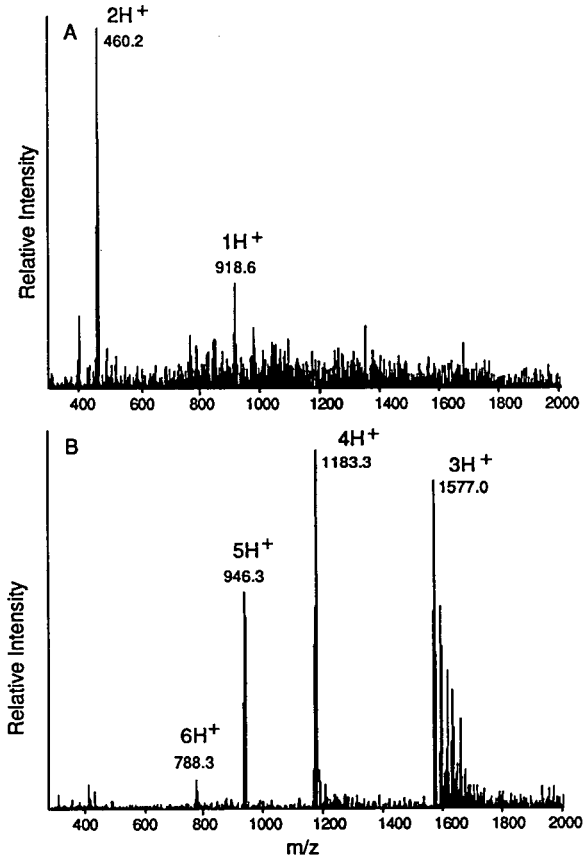


Fig. 9. Electrospray mass spectra obtained in the HPLC–ES-MS analysis of a tryptic digest of expressed SCD for (A) peak 3, which represents the tryptic peptide T 12–18 and has a $M_r$ 917.5 eluting at 78% water and (B) peak 14, which represents the tryptic peptide T 107–149, $M_r$ 4726.4 and elutes when the mobile phase composition is 36% water.

Fluorescence detection affords selective identification of tryptophan containing peptides, and ES-MS provides molecular mass measurements for each peptide. This combination of detectors may prove particularly useful in the analysis of proteins digested with enzymes which lack specificity, such as thermolysin. Knowledge of the presence or absence of tryptophan in a peptide along with the $M_r$ is helpful in assigning a primary sequence. In addition, fluorescence monitoring at the appropriate conditions could provide enhanced detectability and selectivity in the analysis of peptides derivatized with a fluorescent tag [45,46]. As a result of band broadening, some components which were resolved as indicated by the UV trace, may have overlapping profiles in the mass spectrometric trace. However, the mass spectrometric detection allows these components to be resolved by mass. Other detectors in combination with ES-MS, such as electrochemical detection [47] which provides identification of disulfide containing peptides, may be useful in the future for characterization of peptide mixtures.

## REFERENCES

1 M.E. Hemling, G.D. Roberts, W. Johnson, S.A. Carr and T.R. Covey, *Biomed. Environ. Mass Spectrom.*, 19 (1990) 677.
2 S.A. Carr, M.E. Hemling, M.F. Bean and G.D. Roberts, *Anal. Chem.*, 63 (1991) 2802.
3 P.R. Griffin, J.A. Coffman, L.E. Hood and J.R. Yates III, *Int. J. Mass Spectrom. Ion Processes*, 111 (1991) 131.
4 V. Ling, A.W. Guzzetta, E. Canova-Davis, J.T. Stults, W.S. Hancock, T.R. Covey and B.I. Shushan, *Anal. Chem.*, 63 (1991) 2909.
5 E.C. Huang and J.D. Henion, *Anal. Chem.*, 63 (1991) 732.
6 D.F. Hunt, N.Z. Zhu and J. Shabanowitz, *Rapid Commun. Mass Spectrom.*, 3 (1988) 122.
7 S.A. McLuckey, G.J VanBerkel, G.L. Glish, E.C. Huang and J.D. Henion, *Anal. Chem.*, 63 (1991) 375.
8 E.C. Huang and J.D. Henion, *J. Am. Soc. Mass Spectrom.*, 1 (1990) 158.
9 M. Hail, S. Lewis, I. Jardine, J. Liu and M. Novotny, *J. Microcolumn Sep.*, 2 (1990) 285.
10 M.A. Moseley, L.J. Deterding, J.S.M de Wit, K.B. Tomer, R.T. Kennedy, N. Bragg and J.W. Jorgenson, *Anal. Chem.* 61 (1989) 1577.
11 S. Pleasance, P. Thibault, M.A. Moseley, L.J. Deterding, K.B. Tomer and J.W. Jorgenson, *J. Am. Soc. Mass Spectrom.*, 1 (1990) 312.
12 M.A. Moseley, L.J. Deterding, K.B. Tomer and J.W. Jorgenson, *J. Chromatogr.*, 480 (1989) 197.
13 D.B. Kassel, B.D. Musselman and J.A. Smith, *Anal. Chem.*, 63 (1991) 1091.
14 K. Hirayama, S. Akashi, M. Furuya and K. Fukuhara, in Y. Shimonishi (Editor), *Peptide Chemistry 1990*, Protein Research Foundation, Osaka, 1991, p. 177.
15 W.J. Henzel, J.H. Bourell and J.T. Stults, *Anal. Biochem.*, 187 (1990) 228.
16 M.A. Moseley, L.J. Deterding, K.B. Tomer and J.W. Jorgenson, *Anal. Chem.*, 63 (1991) 1467.
17 R.M. Caprioli, W.T. Moore, B. DaGue and M. Martin, *J. Chromatogr.*, 443 (1988) 355.
18 M.J.-F. Suter, B.B. Dague, W.T. Moore, S. Lin and R.M. Caprioli, *J. Chromatogr.*, 553 (1991) 101.
19 R.M. Caprioli, B. DaGue, T. Fan and W.T. Moore, *Biochem. Biophys. Res. Commun.*, 146 (1987) 291.

20 J.E. Coutant, T.-M. Chen and B.L. Ackermann, *J. Chromatogr.*, 529 (1990) 265.
21 D.S. Jones, W. Heerma, P.D. Van Wassenaar and J. Haverkamp, *Rapid Commun. Mass Spectrom.*, 5 (1991) 192.
22 R.M Caprioli, *Anal. Chem.*, 62 (1990) 477A.
23 K.B. Tomer, J.R. Perkins, C.E. Parker and L.J. Deterding, *Biol. Mass Spectrom.*, 20 (1991) 783.
24 M. Mann, *Org. Mass Spectrom.*, 25 (1990) 575.
25 J.-P. Gagné, A. Carrier and M.J. Bertrand, *J. Chromatogr.*, 554 (1991) 47.
26 J.-P. Gagné, A. Carrier and M.J. Bertrand, *J. Chromatogr.*, 554 (1991) 61.
27 G.D. Roberts, W.P. Johnson, M.E. Hemling and S.A. Carr, *Proceedings of the 39th ASMS Conference on Mass Spectrometry and Allied Topics, Nashville, TN, 1991*, ASMS, East Lansing, MI, p. 913.
28 C.K. Meng, M. Mann and J.B. Fenn, *Z. Phys. D.*, 10 (1988) 361.
29 S.F. Wong, C.K. Meng and J.B. Fenn, *J. Phys. Chem.*, 92 (1988) 546.
30 J.B. Fenn, M. Mann, C.K. Meng, S.F. Wong and C.M. Whitehouse, *Mass Spectrom. Rev.*, 9 (1990) 37.
31 J.A. Loo, H.R. Udseth and R.D. Smith, *Anal. Biochem.*, 179 (1989) 404.
32 R.D. Smith, J.A. Loo, R.R. Ogorzalek-Loo, M. Busman and H.R. Udseth, *Mass Spectrom. Reviews*, 10 (1991) 359.
33 T.D. Schlabach and T.C. Wehr, *Anal. Biochem.*, 127 (1982) 222.
34 M. Albin, R. Weinberger, E. Sapp and S. Moring, *Anal. Chem.*, 63 (1991) 417.
35 M.P. Balogh and C.C. Stacey, *J. Chromatogr.*, 562 (1991) 73.
36 Q.Z. Ye, L.L. Johnson, D.J. Hupe and V. Baragi, *Biochemistry*, 31 (1992) 11231.
37 T.R. Covey, E.C. Huang and J.D. Henion, *Anal. Chem.*, 63 (1991) 1193.
38 M.T. Davis and T.D. Lee, *Protein Science*, 1 (1992) 935.
39 M. Saito, K. Hibi, D. Ishii and T. Takeuchi, in D. Ishii (Editor), *Introduction to Microbore High-Performance Liquid Chromatography*, VCH Publishers, New York, 1988. Ch. 2, p. 24.
40 E.S Yeung, in M.V. Novotny and D. Ishii (Editors), *Microcolumn Separations*, Elsevier, New York, 1985, p. 136.
41 G. Guiochon and P.J. Arpino, *J. Chromatogr.*, 271 (1983) 13.
42 C.G. Enke, J. Allison, J.T. Stults, J.D. Pinkston, B. Newcome and J.T. Watson, *Anal Chem*, 55 (1983) 997A.
43 P. Andrews, *ProComp vers. 1.2*, University of Michigan Medical School, Ann Arbor, MI, 1990.
44 T.D. Lee and S. Vemuri, *MacProMass vers. 1.0*, Beckman Research Institute of The City of Hope, Duarte, CA, 1989.
45 T. Sueyoshi, T. Miyata, S. Iwanaga, T. Toyo'oka and K. Imai, *J. Biochem.*, 97 (1985) 1811.
46 M. Kai and Y. Ohkura, *Anal Chim Acta*, 182 (1986) 177.
47 Y. Sun, P.C. Andrews and D.L. Smith, *J. Prot. Chem.*, 9 (1990) 151.

*Journal of Chromatography*, 638 (1993) 21–27
Elsevier Science Publishers B.V., Amsterdam

CHROM. 24 921

# Affinity purification method using a reversible biotinylating reagent for peptides synthesized by the solid-phase technique

Susumu Funakoshi*

*Faculty of Pharamaceutical Sciences, Kyoto University, Sakyo-ku, Kyoto 606 (Japan)*

Hiroyuki Fukuda

*Faculty of Pharmaceutical Sciences, Kyoto University, Sakyo-ku, Kyoto 606 (Japan) and Nihon Millipore Ltd., Shinagawa-ku, Tokyo 140 (Japan)*

Nobutaka Fujii

*Faculty of Pharmaceutical Sciences, Kyoto University, Sakyo-ku, Kyoto 606 (Japan)*

(First received October 16th, 1992; revised manuscript received January 28th, 1993)

ABSTRACT

The specific interaction between biotin and avidin was explored as the basis of an affinity purification procedure for peptides synthesized by the solid-phase technique. In this affinity purification procedure, a reversible biotinylating reagent, 2-[(N-biotinyl)-aminoethylsulphonyl]ethyl *p*-nitrophenyl carbonate (BASEC), was synthesized. Using this reagent, the procedure involves the following sequence of four reactions: (i) attachment of the biotin to the N-terminus of the peptide–resin through a base-labile sulphonylethoxycarbonyl linkage at the final step of solid-phase peptide synthesis; (ii) acid treatment to remove side-chain protecting groups and cleave the biotin-modified peptide from the resin; (iii) affinity purification of the biotinyl-peptide on an avidin–agarose column; and (iv) base (5% ammonia solution) treatment to remove the biotin moiety from the peptide. To facilitate this purification procedure, unreacted amino groups were acetylated in each step during solid-phase synthesis. The usefulness of this method was demonstrated by the purification of several peptides synthesized by the 9-fluorenylmethoxycarbonyl (Fmoc)-based solid-phase technique.

## INTRODUCTION

Improvements in protecting groups, coupling reagents and resin supports have led to significant advances in the field of solid-phase peptide syntheses. In spite of these advances, a condensation reaction yield of over 99% cannot be always obtained, as it depends on the sequence of the target peptide. As a result, peptides with deletions accumulate as impurities. Gel filtration, affinity chromatography, high-performance liquid chromatography and combinations of these methods have been used for the final purification of the desired product [1–8]. However, this step is still a major barrier to obtaining synthetic products in satisfactory yield. Recently, we introduced a novel reversible SH-introducing reagent, 2-{N-[(*p*-methoxybenzylthio)acetyl]aminoethylsulphonyl}ethyl *p*-nitrophenyl carbon-

* Corresponding author.

0021-9673/93/$06.00 

ate, and reported a one-step purification method for the solid-phase synthetic products based on the specific reaction between SH and the iodoacetamide group [9]. Using this method, the target peptide alone can be isolated in high purity and high yield in a short time from a mixture with very similar deleted peptides. The long peptides and proteins, however, could not be isolated effectively because of the too abundant impurities. The chemical affinity of SH–iodoacetamide seemed to be weaker than the biological affinity at such a low concentration. In this event, biotin–avidin affinity chromatography can be a more efficient purification method [10,11]. Lobl *et al.* [12] reported that biotinylation of chemically synthesized protein on resin could be a rapid and efficient purification technique for lower yield products. Their method, however, provided biotinylated protein at the N-terminus as a fully reversible biotinylating reagent was not available.

In this paper, we describe the synthesis of a new reversible biotinylating reagent and introduce a novel biotin–avidin affinity purification technique, using it for peptides synthesized by the solid-phase technique, especially for lower yield synthetic products.

## EXPERIMENTAL

### *Analytical methods*

Thin-layer silica gel (Kieselgel G, Merck) chromatography was conducted with solvent system 1 [chloroform–methanol–water (8:3:1, v/v)]. For $^1$H NMR spectrometry a Bruker AC-300 instrument was used with tetramethylsilane as the internal standard. Fast atom bombardment mass spectrometry (FAB-MS) was carried out with a ZAB SE spectrometer (VG Analytical) and ionspray MS with an API III spectrometer (Perkin-Elmer Sciex). High-performance liquid chromatography (HPLC) was performed with a Model 600E system (Millipore) equipped with a μBondasphere $5C_{18}$ (100 Å) column (150 × 3.5 mm I.D.) (Millipore) using the following two solvent systems: 0.1% trifluoroacetic acid (TFA) in water (solvent A) and 0.1% TFA in acetonitrile (solvent B). Peptide sequence analysis was performed with a Model 6600 protein sequencer (Millipore).

### *Synthesis of the reversible biotinylating reagent*

*Synthesis of 2-[(N-biotinyl)aminoethylsulphonyl]ethanol.* 2-(Aminoethylsulphonyl)ethanol hydrochloride (3.79 g, 20 mmol) was dissolved in dimethylformamide (DMF) (50 ml) together with $Et_3N$ (5.6 ml, 40 mmol) and biotinyl 1-hydroxysuccinimide ester (6.83 g, 20 mmol). After being stirred for 4 h, the solution was filtered and the filtrate was concentrated *in vacuo*. The resulting residue was triturated with ethanol to afford a powder. The crude product was recrystallized from methanol (yield, 5.24 g, 69%), m.p. 126–127°C. Analysis: calculated for $C_{14}H_{25}N_3O_5S_2 \cdot \frac{1}{2}H_2O$, C 43.27, H 6.75, N 10.81; found, C 43.59, H 6.63, N 10.96%. $R_F$ in system 1 = 0.32. FAB-MS: *m/z* 380.3 ($[M + H]^+$); calculated for $C_{14}H_{25}N_3O_5S_2$, 379.5.

*Synthesis of reversible biotinylating reagent (BASEC).* 2-[(N-Biotinyl)aminoethylsulphonyl]-ethanol (3.79 g, 10 mmol) was dissolved in absolute pyridine (30 ml). The solution was cooled at 0°C and *p*-nitrophenyl chloroformate (2.02 g, 10 mmol) was added and stirred. The mixture was then allowed to stand for 5 h at 0°C and subsequently concentrated *in vacuo*. The residue was treated with 1 *M* HCl and diethyl ether, then the product, which immediately crystallized, was collected by filtration and washed with water. The crude product was recrystallized from DMF–ethyl acetate (yield, 3.77 g, 69%), m.p. 104–105°C. Analysis: calculated for $C_{21}H_{28}N_4O_9S_2 \cdot \frac{1}{2}H_2O$, C 45.65, H 5.37, N 10.22; found, C 45.75, H 5.22, N 10.08%. $R_F$ in system 1 = 0.37. $^1$H NMR (300 MHz, DMSO-$d_6$): δ 1.36–1.23 (m, 2H), 1.47–1.37 (m, 1H), 1.58–1.46 (m, 2H), 1.67–1.55 (m, 1H), 2.05 (t, $J$ = 7.3 Hz, 2H) 2.57 (d, $J$ = 12.4 Hz, 1H), 2.81 (dd, $J$ = 12.4 and 5.0 Hz, 1H), 3.08 (ddd, $J$ = 8.2, 6.5 and 4.5 Hz, 1H), 3.32 (t, $J$ = 6.9 Hz, 2H), 3.48 (q, $J$ = 6.7 Hz, 2H), 3.68 (t, $J$ = 5.7 Hz, 2H), 4.11 (ddd, $J$ = 7.8, 4.5 and 2.0 Hz, 1H), 4.29 (dd, $J$ = 7.8 and 5.2 Hz, 1H), 4.62 (t, $J$ = 5.7 Hz, 2H), 6.33 (br, s, 1H), 6.38 (br, s, 1H), 7.58, 8.33 (AA'BB' pattern, $J_{ortho}$ = 9.2 Hz, aromatic H), 8.07 (br, t, $J$ = 5.9 Hz, 1H). FAB-

MS: $m/z$ 545.3 ($[M+H]^+$); calculated for $C_{21}H_{28}N_4O_9S_2$, 544.6.

*Syntheses of model peptides (general method)*

*Synthesis of model peptides.* The model peptides used in this experiment were synthesized by 9-fluorenylmethoxycarbonyl (Fmoc)-based solid-phase synthesis according to the principle of Cameron *et al.* [13], using a Model 9050 automatic peptide synthesizer (Millipore). The following side-chain-protected Fmoc-amino acids were used: Arg(Mtr), Lys(Boc), His(Boc), Glu(OBu$^t$), Asp(OBu$^t$), Ser(Bu$^t$), Thr(Bu$^t$) and Tyr(Bu$^t$), where Mtr 4-methoxy-2,3,6-trimethylbenzenesulphonyl, Boc = *tert.*-butoxycarbonyl and Bu$^t$ = *tert.*-butyl. To make the final purification step easier, the peptide–resin was treated with acetic anhydride after each condensation reaction to ensure the complete termination of the unreacted amino groups. Thus only the mature peptide could be modified at the end of synthesis.

*Introduction of the reversible biotinylating reagent.* The peptide–resin (200 mg) was treated twice with 20% piperidine in DMF (5 ml, for 5 and 15 min) to remove the Fmoc group. Then BASEC (5 equiv.) was condensed to the N-terminal residue of the protected peptide–resin in the presence of 1-hydroxybenzotriazole (5 equiv.) in DMF. The container was shaken until the resin showed a negative Kaiser test [14] (usually for 2 h). The resin was washed with DMF and $CH_2Cl_2$ and dried under reduced pressure.

*Deprotection and purification (general method)*

*Deprotection and cleavage of peptides from the solid-phase support.* The peptide–resin (50 mg) was treated with 1 *M* trimethylsilyl bromide ($Me_3SiBr$)–thioanisole in TFA [15] (10 ml) in the presence of *m*-cresol (200 $\mu$l) and ethanedithiol (200 $\mu$l) at 0°C for 2 h, after which $Me_3SiBr$ and TFA were removed by evaporation and dry diethyl ether was added. The resulting powder was collected by centrifugation.

*Purification.* The crude deprotected peptide was dissolved in PBS(−) buffer (pH 7.5) containing 500 m*M* NaCl and then the solution was filtered. The filtrate was applied to the avidin–agarose column (10 × 1 cm I.D.) (Pierce) at a flow-rate of 1 ml/min and then the column was washed with 20 column volumes of PBS(−) buffer at the same flow-rate. The biotinylated peptide was eluted with 6 *M* guanidine hydrochloride solution (pH 1.5). The eluent was directly treated with 5% ammonia solution (addition of 25% ammonia solution in one quarter the volume of the eluent) at room temperature for 10 min to release the biotin moiety from the peptide. The reaction mixture was then desalted by RP-HPLC or gel filtration.

*Characterization.* The purity of the synthetic peptides was ascertained and/or calculated using HPLC. The peptides obtained were characterized by amino acid sequencing by automated Edman degradation and by FAB-MS or ionspray MS.

## RESULTS AND DISCUSSION

We have developed a new affinity purification method based on the avidin–biotin interaction for isolating a target peptide from a mixture containing many kinds of immature (terminated) peptides. This objective was achieved by the development of not only an acid-stable but also a base-labile biotinylating reagent based on the methylsulphonylethoxycarbonyl (Msc) group [16].

Synthesis of a reversible biotinylating reagent was carried out according to the scheme shown in Fig. 1. The amino group of the 2-aminoethylsulphonylethanol [9] can be attached to biotin by the 1-hydroxysuccinimide active ester method.

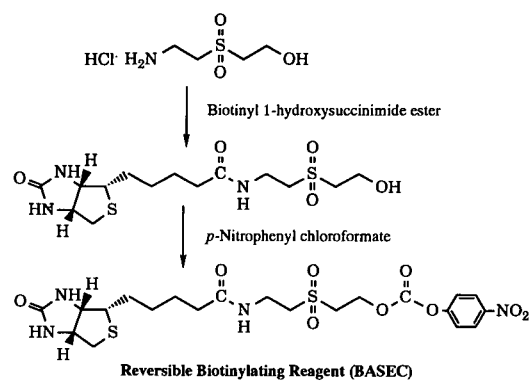


Fig. 1. Scheme for the synthesis of the reversible biotinylating reagent (BASEC).

Then the OH group is converted into active an alkoxy carbonate by treatment with *p*-nitrophenyl chloroformate. This compound (BASEC) is easily introduced to α-amino groups of the peptide–resin within 2 h in the presence of 1-hydroxybenzotriazole at room temperature, and it acts as a urethane-type amino protecting reagent. It is stable to acids, such as trifluoracetic acid, $Me_3SiBr$, hydrofluoric acid, trifluoromethanesulphonic acid and trimethylsilyl trifluoromethanesulphonate, but is easily removed by the β-elimination reaction with a basic reagent (with 0.2 *M* NaOH in 50% MeOH in 5 s or 5% ammonia solution in 50% MeOH in 5 min) (Fig. 2). This indicates that after isolation of the desired product from the deletion peptides, the N-terminal biotin moiety can be removed from the target peptide or protein by mild base treatment.

This reversible biotinylating reagent was allowed to react with the N-terminus of the completely mature peptide at the end of synthesis as shown in Fig. 3. After final deprotection, the biotin-modified target peptide was bound to the avidin–agarose support under neutral conditions. Thus, only the mature peptide could be immobilized on the agarose support with affinity interaction, while terminated peptides and scavengers could be easily washed out from the avidin–agarose column. The biotin-modified target peptide was eluted with 6 *M* guanidine–hydrochloride (pH 1.5). Finally, the eluted peptide was treated with 5% ammonia solution to remove the biotin moiety from the peptide (Fig. 4). The final

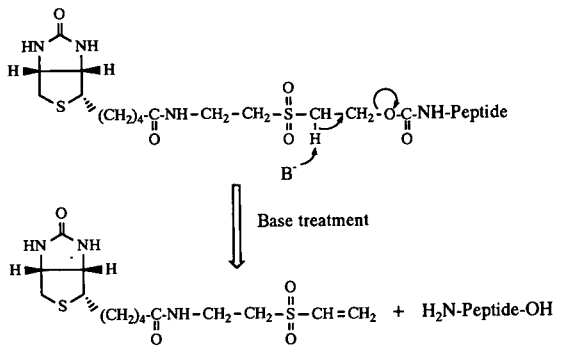


Fig. 2. Schematic representation of the debiotinylation reaction.

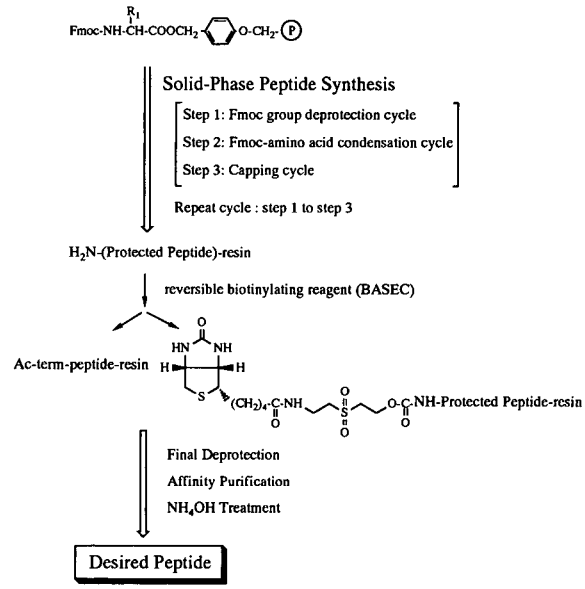


Fig. 3. General scheme for Fmoc-based solid-phase peptide synthesis and affinity purification technique. Step 1, deprotection of Fmoc group treated with 20% piperidine–DMF for 7 min; step 2, coupling of Fmoc-amino acid (5 equiv.) activated with several reagents for 30 min; step 3, capping of unreacted α-amino groups treated with 0.5 *M* acetic anhydride–DMF for 10 min.

purification was performed using RP-HPLC or gel filtration.

To demonstrate the usefulness of this method, magainin 2 [17], a 23-residue peptide, and human growth hormone releasing factor (hGRF) [18,19], a 44-residue peptide amide, were synthesized as model peptides. Syntheses were performed by the Fmoc-based solid-phase method shown in Fig. 3.

As shown in Fig. 5A, the HPLC trace for the crude synthetic magainin 2 showed many failed peptides (content of the desired peptide ≈ 39%), but almost all failed peptides were removed (purity ≈ 87%) by this affinity method. The result of FAB-MS analysis of the obtained peptide was identical with the theoretical value of $m/z$ 2466.6 ($[M+H]^+$) (calculated for $C_{114}H_{180}N_{30}O_{29}S$, 2465.3), and the full amino acid sequence analysis was correct.

With hGRF, the target peptide showed a sharp single peak on HPLC with several small peaks derived from capped terminated peptides (content of the desired peptide ≈ 28%, Fig. 5B).

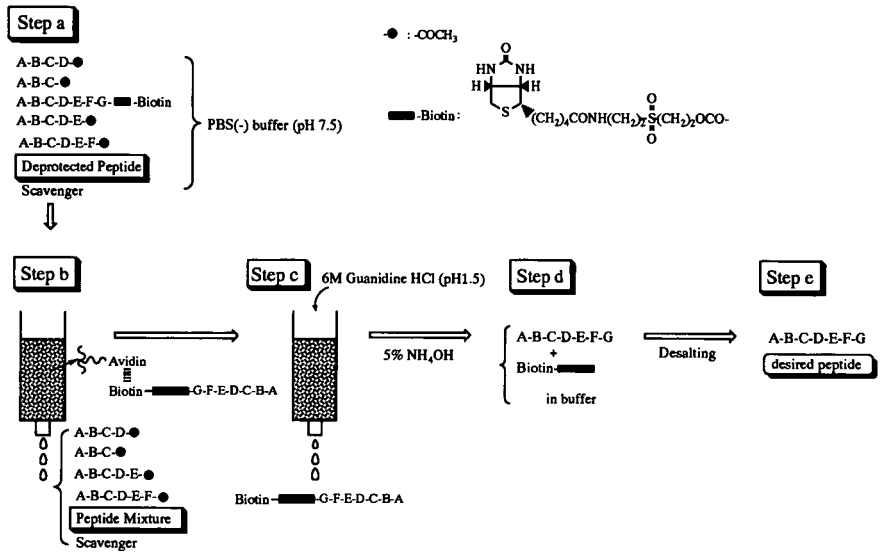


Fig. 4. Deprotection and purification of peptides synthesized by the solid-phase technique. Step a, deprotected peptide mixture dissolved in PBS(−) buffer (pH 7.5); step b, binding to avidin–agarose column; step c, elution of the desired peptide from avidin–agarose column; step d, removal of the biotin moiety; step e, desalting.

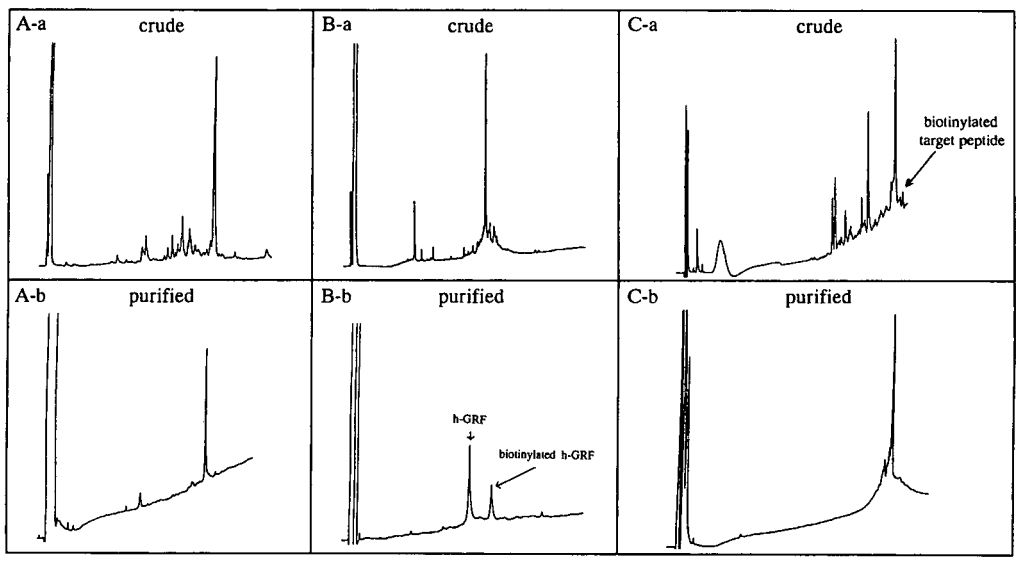


Fig. 5. HPLC elution profile of synthetic peptides. HPLC was performed on a μBondasphere column using two solvent systems (A and B) with a linear gradient of solvent B; flow-rate, 1 ml/min; absorbance monitored at 220 nm. (A) magainin 2: the column was eluted with a linear gradient from 10 to 50% solvent B in 40 min; (a) crude product; (b) purified product. (B) hGRF: (a) crude product, the column was eluted with a linear gradient from 23 to 40% solvent B in 30 min; (b) co-injection of purified product (before and after treatment with 5% ammonia solution), the column was eluted with a linear gradient from 25 to 55% solvent B in 30 min. (C) Acm-transducin γ-subunit 1–67: the column was eluted with a linear gradient from 10 to 40% solvent B in 30 min; (a) crude product; (b) purified biotinylated Acm-Tγ 1–67.

After purification, the hGRF produced in this manner (purity ≈ 85%) showed a retention time identical with that of the peptide obtained by a conventional purification procedure. The full amino acid sequence and FAB-MS result, $m/z$ 5037.8 ($[M+H]^+$) (calculated for $C_{215}H_{358}N_{72}O_{66}S$, 5036.7), agreed with the theoretical values.

We further studied the application of this method to a small protein in synthesizing transducin γ-subunit 1–67 (Tγ 1–67) [20]. For this synthesis, the SH group of the Cys residue was protected with acetamidemethyl (Acm). The procedure was the same as that mentioned above. For Acm-Tγ 1–67, the biotinylated target peptide showed a small peak on HPLC (content of the desired peptide <2%, Fig. 5C) with several large peaks. After purification with the avidin column, the target peptide was isolated as a major component (content of the desired peptide ≈ 65%). The result of ionspray MS analysis of the obtained peptide was identical with the theoretical value of 8052.1 (average mass) (average mass calculated for $C_{354}H_{584}N_{91}O_{113}S_4$, 8050.3), and the amino acid sequence analysis of the N-terminal portion (15 cycles from the $NH_2$-terminus) of the peptide obtained was correct.

These data demonstrated that the proposed method is very useful for separating desired products even at low concentrations from the major part of the non-biotinylated impurities. However, with increase in peptide length, the purity of the recovered peptide decreased owing to a loss of capping efficiency (purity of the final products = 87–65%, Fig. 5). Unfortunately, this method is not effective in purifying peptides that are chemically modified during the synthesis or the final deprotection.

In solid-phase peptide synthesis, it is very common to find many undesired products with random single or multiple point deletions and with very similar chromatographic and isoelectric properties. Therefore, the establishment of an effective technique to purify solid-phase synthetic products is strongly desired. One of the shortfalls of conventional chromatographic purification is that it is troublesome to remove terminated peptides or to isolate the desired peptide when the synthetic yield is very low. The new reversible biotinylating reagent, however, can offer a new type of biotin–avidin affinity chromatography to purify (or isolate) solid-phase synthetic products.

The great advantages of the method are its simplicity and rapidity. It should enable high-purity or constant-purity peptides to be produced, which will be useful in research in the fields of biochemistry, physiology and medicine with respect to the physiological activities and action mechanisms of peptides and proteins.

## ACKNOWLEDGEMENTS

We are grateful to Dr. Hirokazu Tanaka (Fujisawa Pharmaceutical, Tsukuba) for the FAB-MS and Dr. Tetsuroh Shingu (Kobe–Gakuin University, Kobe) and Mrs. Setsuko Funakoshi and Mr. Masami Ono (Kyoto University, Kyoto) for the $^1H$ NMR measurements. This work was supported by the Research Foundation for Pharmaceutical Sciences, Japan.

## REFERENCES

1 D.S. Kemp and D.G. Robert, *Tetrahedron Lett.*, (1975) 4629.
2 R.B. Merrifield and A.E. Bach, *J. Org. Chem.*, 43 (1975) 4808.
3 K. Suzuki, Y. Sasaki and N. Endo, *Chem. Pharm. Bull.*, 24 (1976) 1.
4 R.B. Merrifield, S.B.H. Kent, J.P. Tam, F.S. Tjoeng, V. Sarin, S. Mojsov, N.M. Riemen, T.W. Wong and C. Voss, in E. Gross and J. Meinhofer (Editors), *Peptides, Structure and Biological Function: Proceedings of the 6th American Peptide Symposium*, Pierce, Rockford, IL, 1979, p. 29.
5 H. Ball, C. Grecian, S.B.H. Kent and P. Mascagni, in J.E. Rivier and G.R. Marshall (Editors), *Peptides, Chemistry, Structure and Biology: Proceedings of the 11th American Peptide Symposium*, ESCOM Science, Leiden, 1990, p. 435.
6 D.E. Kriger, B.M. Erikson and R.B. Merrifield, *Proc. Natl. Acad. Sci. U.S.A.*, 73 (1976) 3160.
7 E.A. Bayer and M. Wilchek, *J. Chromatogr.*, 510 (1990) 3.
8 M. Wilchek and T. Miron, in E. Gross and J. Meinhofer (Editors), *Peptides, Structure and Biological Function: Proceedings of the 6th American Peptide Symposium*, Pierce, Rockford, IL, 1979, p. 49.

9 S. Funakoshi, H. Fukuda and N. Fujii, *Proc. Natl. Acad. Sci. U.S.A.*, 88 (1991) 6981.
10 J.A. Swack, G.L. Zander and M.F. Utter, *Anal. Biochem.*, 87 (1978) 114.
11 J. Moss and M.D. Lane, *Adv. Enzymol.*, 35 (1971) 321.
12 T.J. Lobl, R.M. Deibel and A.W. Yen, *Anal. Biochem.*, 170 (1988) 502.
13 L. Cameron, M. Meldal and R.C. Sheppard, *J. Chem. Soc., Chem. Commun.*, (1987) 270; and references cited therein.
14 E. Kaiser, R.L. Colescott, C.D. Bossinger and P.I. Cook, *Anal. Biochem.*, 34 (1970) 595.
15 N. Fujii, A. Otaka, N. Sugiyama, M. Hatano and H. Yajima, *Chem. Pharm. Bull.*, 35 (1987) 3880.
16 G.I. Tesser and I.C. Balvert-Geers, *Int. J. Pept. Protein Res.*, 7 (1975) 295.
17 M. Zasloff, *Proc. Natl. Acad. Sci. U.S.A.*, 84 (1987) 5449.
18 R. Guillemin, P. Brazeau, P. Böhlen, F. Esch, N. Ling and W.B. Wehrenberg, *Science*, 218 (1982) 585.
19 N. Ling, F. Esch, P. Böhlen, P. Brazeau, W.B. Wehrenberg and R. Guillemin, *Proc. Natl. Acad. Sci. U.S.A.*, 81 (1984) 4302.
20 Y. Fukada, T. Takao, H. Oguro, T. Yoshizawa, T. Akino and Y. Shimonishi, *Nature*, 346 (1990) 658.

*Journal of Chromatography*, 638 (1993) 29–34
Elsevier Science Publishers B.V., Amsterdam

CHROM. 24 894

# Separation of sugars by ion-exclusion chromatography on a cation-exchange resin

Lennart Rodén*, Mats Rodén, Hao Yu, Jin Jin and Juliette Greenshields

*P.O. Box 500, University of Alabama at Birmingham, Birmingham, AL 35294 (USA)*

(First received November 17th, 1992; revised manuscript received January 13th, 1993)

ABSTRACT

A method for the separation of N-acetylmannosamine and N-acetylglucosamine is described, which consists of chromatography of the two sugars on a column (30 × 1 cm) of the cation-exchange resin, Dowex 50W-X2, in borate buffer at pH 7.8. N-Acetylmannosamine is eluted near the void volume, while N-acetylglucosamine emerges in a more retarded position. It is postulated that the separation occurs as a result of the combined effects of ion exclusion and gel permeation. Thus, in borate solution, N-acetylmannosamine presumably exists largely as a negatively charged complex and is therefore excluded from the sulfonated polystyrene matrix, while N-acetylglucosamine occurs mainly as the free sugar in the equilibrium mixture and, being a neutral compound, has free access to the porous resin. The proposed mechanism for the separation was supported by the finding that glucose and glucose 6-phosphate could also be separated on a column of the same resin, with water as the eluent.

## INTRODUCTION

Established procedures for the separation of neutral monosaccharides include a group of methods, which are based on the formation of sugar–borate complexes and subsequent fractionation by various techniques originally developed for the separation of charged compounds [1,2]. This approach has been particularly valuable in the analysis of mixtures of monosaccharides that are otherwise difficult to separate, *e.g.*, N-acetylmannosamine and N-acetylglucosamine. Thus, a mixture of these two sugars can easily be resolved by paper electrophoresis in borate buffer [3,4] or by chromatography on an anion-exchange resin in borate form [5]☆. N-Acetylmannosamine migrates faster than N-acetylglucosamine on electrophoresis and binds more tightly to the resin during ion-exchange chromatography, indicating that it forms a borate complex more readily than does N-acetylglucosamine. Yet another expression of the relative strengths of the borate complexes is the difference in $R_F$ values observed on chromatography of the two sugars on borate-treated paper [3,4,7]. N-Acetylmannosamine migrates more slowly than N-acetylglucosamine, presumably because the ionic complexes are less soluble in the mobile phase than the free sugars and N-acetylmannosamine is complexed to a greater extent than N-acetylglucosamine at equilibrium.

We have recently found that N-acetylmannosamine and N-acetylglucosamine may also be separated by chromatography on Sephadex G-15 in borate buffer [8]. Since the borate complexes are larger than the free sugars and N-acetylmannosamine forms the strongest complex, we expected that N-acetylmannosamine would emerge first and that N-acetylglucosamine would be eluted in a more retarded position. This was

* Corresponding author.

☆ The procedure described by Johnson *et al.* [5] was used for fractionation of disaccharides containing N-acetylglucosamine and N-acetylmannosamine but is also applicable to the separation of the two monosaccharides [6].

0021-9673/93/$06.00 

indeed the case. When this experiment was carried out, however, we had not realized that the difference in size between the N-acetylmannosamine–borate complex ($M_r$ 269 for the sodium salt and 246 for the complex ion) and free N-acetylglucosamine ($M_r$ 221) is so small that there had been no reason to expect that complete separation would occur under the conditions chosen. This conclusion was reinforced by the observation that glucose and maltose ($M_r$ 180 and 342, respectively) were separated only partially on the column (117 × 1.5 cm) used in these experiments. We therefore speculated [8] that, besides the molecular mass difference between free N-acetylglucosamine and the N-acetylmannosamine–borate complex, two additional factors contributed to the observed separation: (a) the presence of a hydration shell around the charged borate complex, which increased its apparent molecular mass, and (b) an ion-exclusion phenomenon resulting from complexing of the borate in the buffer with the glucose-containing Sephadex matrix and repulsion of the N-acetylmannosamine–borate complex from the negatively charged beads. If the latter effect were operative, separation should also occur when the two N-acetylhexosamines are chromatographed on a *bona fide* cation-exchange resin with a sufficiently porous matrix that allows entry of the free N-acetylglucosamine into the beads. In the present communication, we report that N-acetylmannosamine and N-acetylglucosamine may indeed be separated by chromatography on the cation-exchange resin, Dowex 50W-X2, in borate buffer.

## MATERIALS AND METHODS

N-Acetylglucosamine was obtained from Pfanstiehl Labs. (Waukegan, IL, USA). N-Acetylmannosamine, glucose, glucose 6-phosphate, N-acetylglucosamine 6-phosphate, *p*-dimethylaminobenzaldehyde, phenol and Dowex 50W-X2-400 (200–400 mesh) were from Sigma (St. Louis, MO, USA). N-Acetyl-[1,6-$^3$H]glucosamine (sp. act., 30–60 Ci/mmol) was purchased from American Radiolabeled Chemicals (St. Louis, MO, USA) and Blue Dextran from Pharmacia LKB Biotechnology (Piscataway, NJ, USA). $^3H_2O$ (sp. act., 5 Ci/g) was from DuPont/New England Nuclear. Other reagents were of analytical grade and were purchased from Fisher Scientific (Atlanta, GA, USA).

Quantitative analysis of N-acetylhexosamines was carried out by the method of Reissig *et al.* [9]. Glucose and glucose 6-phosphate were analyzed by the phenol–sulfuric acid method [10]. Radioactivity was measured by liquid scintillation spectrometry in a Packard Model 2450 instrument, using 0.5 ml of aqueous sample and 4.5 ml of Scintiverse BD (Fisher Scientific).

Chromatography was carried out on Econo-Columns (Bio-Rad Labs., Richmond, CA, USA) as follows. The cation-exchange resin was converted to the $Na^+$ form by washing successively with 4 *M* HCl, water, 2 *M* NaOH, and water again. A column (30 × 1 cm; bed volume, 23.5 ml) was packed and equilibrated with 0.27 *M* sodium borate, pH 7.8, which had been prepared from $H_3BO_3$ and NaOH [5]. Elution was carried out with this buffer at a flow-rate of 10–12 ml/h, unless otherwise indicated, and 0.5- to 1.0-ml fractions were collected. $V_0$ was determined by chromatography of a 200-μl sample (4 mg) of Blue Dextran, and $V_t$ was estimated by chromatography of $^3H_2O$ (50 000 cpm). In some experiments, shorter columns (5.9–6.5 × 1.5 cm) were employed, which had been packed in used PD-10 columns (Pharmacia LKB Biotechnology).

## RESULTS

Calibration of the standard Dowex 50W-X2-400 column (30 × 1 cm; $Na^+$ form) with Blue Dextran and tritiated water as markers for $V_0$ and $V_t$ gave values of 10 and 23 ml, respectively (Fig. 1A). When a mixture of N-acetylmannosamine and N-acetylglucosamine was chromatographed on this column with water as eluent, no separation occurred, and the two sugars emerged as a single peak close to $V_t$, indicating that they had entered the resin beads (Fig. 1B). In contrast, elution with borate buffer gave two completely separated peaks, with effluent volumes of 14 and 18 ml, respectively (Fig. 1C). Since equal weights of the two N-acetylhexosamines had been applied to the column and

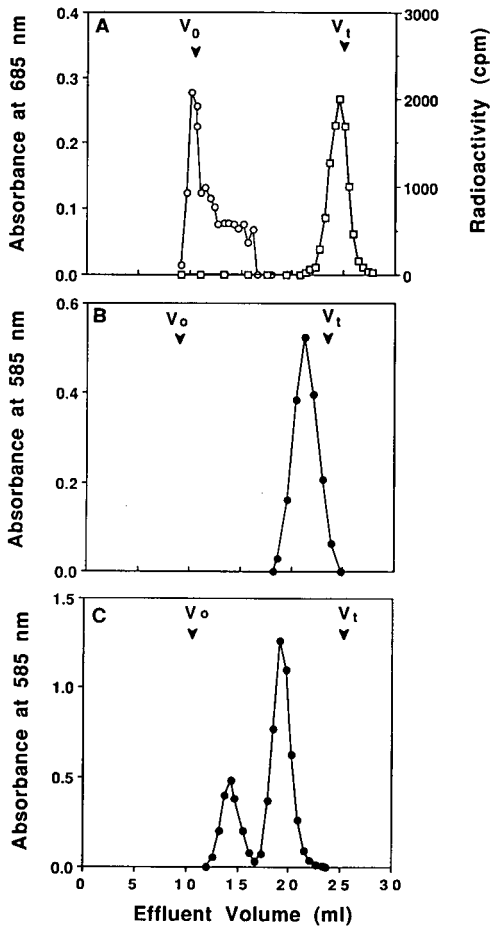


Fig. 1. Separation of N-acetylmannosamine and N-acetylglucosamine on Dowex 50W. A column (30 × 1 cm) of Dowex 50W-X2 ($Na^+$; 200–400 mesh) was used, which was eluted at room temperature at a flow-rate of 10–12 ml/h. (A) After equilibration of the column with 0.27 *M* borate, pH 7.8, a mixture of Blue Dextran (4 mg) and $^3H_2O$ (56 000 cpm) in 0.22 ml of buffer was applied, and the column was eluted with the same buffer. Absorbance at 685 nm (○) and radioactivity (□) in the effluent fractions were measured. (B) After equilibration of the column with water, a mixture of N-acetylglucosamine (0.1 mg) and N-acetylmannosamine (0.2 mg) in 0.3 ml of water was applied to the column, and elution was carried out with water. Fractions were analyzed by the Morgan–Elson procedure (●). (C) After equilibration of the column with borate buffer, a mixture of N-acetylglucosamine (1 mg) and N-acetylmannosamine (1 mg) in 0.2 ml of buffer was applied, and the column was eluted with the same buffer. Fractions were analyzed by the Morgan–Elson procedure (●).

N-acetylmannosamine gives only about half as much color as N-acetylglucosamine in the Morgan–Elson procedure [7], it was concluded that the smaller, earlier peak was N-acetylmannosamine and that the more retarded peak was N-acetylglucosamine.

To establish the identities of the two peaks more directly, a sample of radioactive N-acetylglucosamine was chromatographed in borate buffer, separately and in mixture with non-radioactive N-acetylmannosamine (Fig. 2). As shown in Fig. 2A, a major radioactive peak was observed in the same position as that of the putative N-acetylglucosamine peak in Fig. 1C. In addition, however, at least three minor impurities were present, one emerging with the

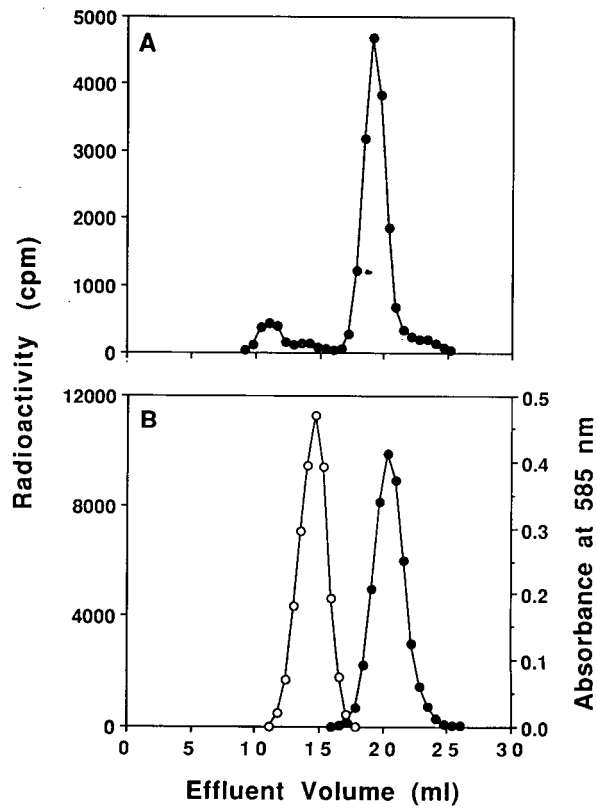


Fig. 2. Analysis of N-acetyl-D-[1,6-$^3$H]glucosamine by chromatography on Dowex 50W. (A) A sample of N-acetyl-D-[1,6-$^3$H]glucosamine (0.2 ml; *ca.* 100 000 cpm) was applied to the column after equilibration with 0.27 *M* borate, pH 7.8. Elution was carried out with the borate buffer, and fractions were analyzed for radioactivity (●). (B) A 1.0-ml sample containing N-acetylmannosamine (2 mg) and purified N-acetyl-D-[1,6-$^3$H]glucosamine (70 000 cpm) was applied to the column after equilibration with borate buffer. Elution was carried out with the same buffer, and fractions were analyzed for N-acetylhexosamine (○) and radioactivity (●).

void volume, a second in the same position as the presumed N-acetylmannosamine peak in Fig. 1C, and a third at the tail end of the major radioactive peak. It is not known whether these impurities were present in the material supplied by the manufacturer or had been formed during storage. After isolation of the major component by fractionation of a larger batch of the radioactive sugar, addition of non-radioactive N-acetylmannosamine and repeated chromatography gave the results shown in Fig. 2B. It is seen that N-acetylmannosamine was eluted first, as indicated by analysis with the Morgan–Elson procedure, and was completely separated from the radioactive N-acetylglucosamine, which now gave a symmetrical peak and showed no signs of the presence of any contaminants. It may be noted that the effluent volume of the N-acetylglucosamine peak in Fig. 2B was slightly larger than that of the major radioactive peak in Fig. 2A; this was probably due mainly to the larger sample volume applied to the column (1.0 *vs.* 0.2 ml).

Since the results described above were in accord with our predictions, the influence of a negative charge on the chromatographic behavior of some other sugars was also explored. When a mixture of glucose and glucose 6-phosphate was chromatographed on a column ($30 \times 1$ cm) of Dowex 50W-X2 in $Na^+$ form, which was eluted with water rather than with borate buffer, complete separation occurred, as illustrated in Fig. 3A. Glucose 6-phosphate emerged with the void volume, while glucose was eluted near $V_t$ of the column, as was established by chromatographing each sugar individually. Similar results were observed on elution with the standard borate buffer or with 0.2 *M* NaCl. Complete separation of N-acetylglucosamine 6-phosphate and N-acetylglucosamine was likewise obtained upon chromatography with water as the eluent (Fig. 3B). It should be noted that the two sugar phosphates were both eluted with the void volume, whereas N-acetylmannosamine, chromatographed in borate buffer, emerged in a more retarded position. This difference was probably an expression of the fact that a portion of the N-acetylmannosamine molecules

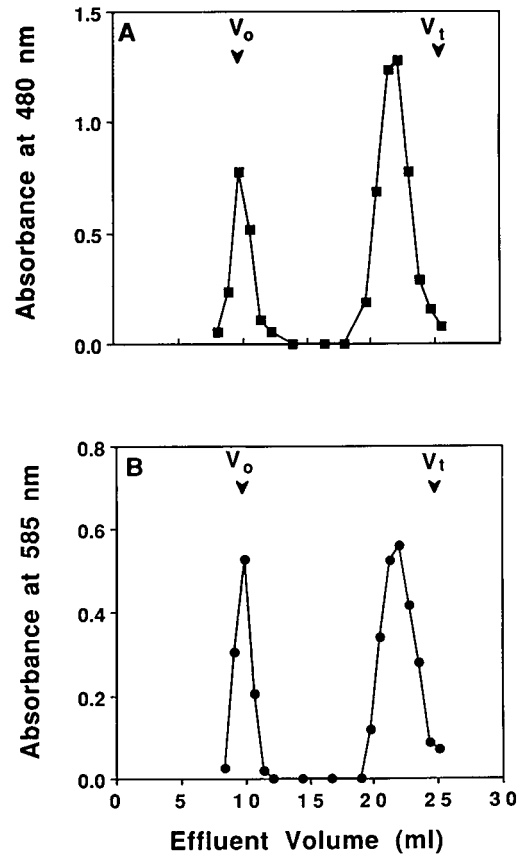


Fig. 3. Isolation of sugar phosphates by chromatography on Dowex 50W. A column ($30 \times 1$ cm) of Dowex 50W ($Na^+$; 200–400 mesh) was equilibrated with water. (A) A mixture of glucose (5 mg) and glucose 6-phosphate (2.5 mg) in 0.15 ml of water was applied to the column, and elution was carried out with water. Fractions were analyzed by the phenol–sulfuric acid method (■). (B) A mixture of N-acetylglucosamine (2 mg) and N-acetylglucosamine 6-phosphate (2 mg) in 0.4 ml of water was chromatographed under the same conditions. Fractions were analyzed by the Morgan–Elson procedure (●).

are not complexed with borate in the equilibrium mixture and therefore are not repelled by the porous resin, leading to an overall slower migration through the column.

In view of the excellent separation between the neutral monosaccharides and their phosphate derivatives, it was of interest to determine whether the procedure could be simplified by use of a shorter column. As shown in Fig. 4A, complete separation of glucose and glucose

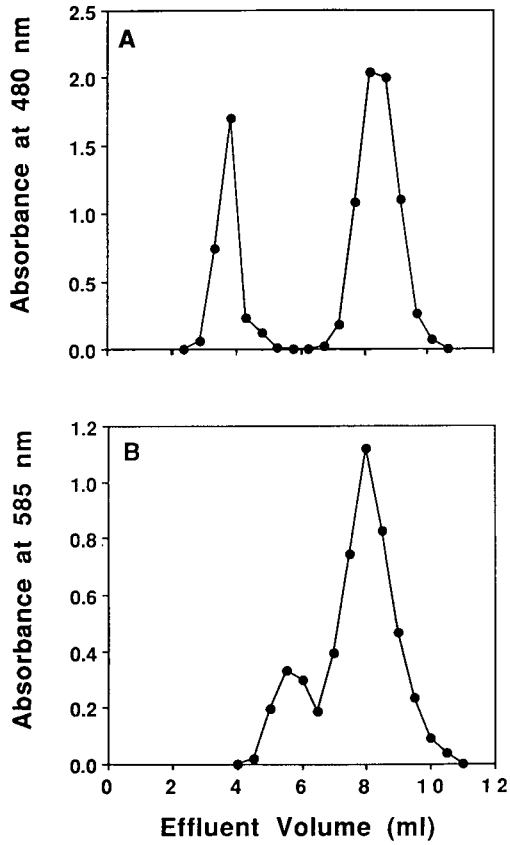


Fig. 4. Chromatography of (A) glucose and glucose 6-phosphate and (B) N-acetylglucosamine and N-acetylmannosamine on a short column of Dowex 50W. (A) A column (6.5 × 1.5 cm) of Dowex 50W-X2 ($Na^+$; 200–400 mesh) was equilibrated with water. A mixture of glucose (5 mg) and glucose 6-phosphate (2.5 mg) in 0.15 ml of water was applied, and the column was eluted with water. Fractions (0.5 ml) were collected and analyzed by the phenol–sulfuric acid method (●). (B) A column (5.9 × 1.5 cm) of Dowex 50W was equilibrated with 0.27 *M* borate, pH 7.8, and a sample (0.2 ml) containing N-acetylglucosamine (2 mg) and N-acetylmannosamine (2 mg) was applied. The column was eluted with borate buffer, and fractions (0.5 ml) were analyzed by the Morgan–Elson procedure (●).

6-phosphate was obtained on a 6.5 × 1.5 cm column of Dowex 50W-X2-400 in the $Na^+$ form, which was eluted with water. The same result was observed when resin in the $H^+$ form was used. N-Acetylmannosamine and N-acetylglucosamine, however, were separated only partially when chromatographed on the shorter column in borate buffer (Fig. 4B).

## DISCUSSION

This study was undertaken to test the hypothesis that ion exclusion might have been a contributing factor in the previously observed separation of N-acetylmannosamine and N-acetylglucosamine, which occurs on chromatography of the two sugars on Sephadex G-15 in borate buffer [8]. The results presented here support this notion, inasmuch as the two N-acetylhexosamines could also be separated by chromatography on the cation-exchange resin, Dowex 50W-X2, provided that the elution was carried out with borate buffer. We envisage that under these conditions the separation occurs by the following process. Most of the N-acetylmannosamine molecules form negatively charged complexes with borate in the equilibrium mixture, and these are repelled by the sulfonated polystyrene matrix, resulting in early elution of the amino sugar. In contrast, the majority of the N-acetylglucosamine molecules presumably remain largely as the free sugar in the equilibrium mixture and, being neutral, have free access to the porous resin and are eluted near $V_t$ of the column. The separation may thus be viewed as the result of a combination of ion exclusion and gel permeation. N-Acetylglucosamine emerged somewhat earlier when the column was eluted with borate rather than with water (*cf.* Fig. 1C and B), and this difference probably reflects the extent of complex formation in borate solution. It seems possible that a quantitative relationship could be established between the equilibrium constants of borate complex formation and the relative elution positions of the sugars, but no attempt to do so was made in the present study.

The observed separation is not only of theoretical interest but represents a practical, new method for the separation of the two N-acetylhexosamines in both analytical and preparative work. The usefulness of the new method is not limited to this particular fractionation, and the complete separation of glucose and N-acetylglucosamine from their respective 6-phosphate derivatives on a short resin column illustrates the broader applicability of the ion-exclusion/gel-permeation principle. In an exten-

sion of these experiments, the Dowex 50 procedure is being used in the development of an alternative assay of hexokinase activity with radioactive glucose as the substrate, and the preliminary results suggest that this approach will be successful.

It is apparent from the results of this study that the new method is well suited for use as an analytical tool. Its usefulness in preparative applications, however, may be limited by the presence of other compounds in the mixtures to be fractionated, and, *e.g.*, anion-exchange chromatography on a resin in the borate form is likely to yield better resolution of multi-component mixtures, since the N-acetylhexosamines and other sugars that form borate complexes are eluted well after the total bed volume of the resin. It should also be pointed out that the experimental conditions chosen in the present study may not be ideal for a particular application and that, *e.g.*, the use of a borate solution of lower concentration may facilitate subsequent desalting of the pooled fractions (see ref. 7).

In summary, we have developed a new method for the separation of N-acetylmannosamine and N-acetylglucosamine, which consists of chromatography on a cation-exchange resin in borate buffer. Cation exchange, however, apparently does not contribute to the observed separation. Rather, the fractionation seems to occur as a result of the combined effects of ion exclusion and gel permeation. Since the method is based on general principles and not only on the unique properties of the two N-acetylhexosamines, it is also applicable to the separation of other mixtures of neutral and negatively charged small molecules.

ACKNOWLEDGEMENTS

This work was supported by grants DE 08252 and NS 27353 from the National Institutes of Health, a grant from DePuy, and by a Grant-in-Aid from the American Heart Association, Alabama Affiliate Inc. Helpful advice from Dr. Y.C. Lee is gratefully acknowledged.

REFERENCES

1 J.X. Khym and L.P. Zill, *J. Am. Chem. Soc.*, 73 (1951) 2399.
2 E.J. Bourne, A.B. Foster and P.M.J. Grant, *J. Chem. Soc.*, (1956) 4311.
3 M.J. Crumpton, *Biochem. J.*, 72 (1959) 479–486.
4 R.D. Marshall and A. Neuberger, in A. Gottschalk (Editor), *Glycoproteins*, Elsevier, Amsterdam, 1972, Ch. 3, Sect. 5, p. 224.
5 G. Johnson, R.T. Lee and Y.C. Lee, *Carbohydr. Res.*, 39 (1975) 271–281.
6 Y.C. Lee, personal communication.
7 C.T. Spivak and S. Roseman, *J. Am. Chem. Soc.*, 81 (1959) 2403–2404.
8 L. Rodén, H. Yu, J. Jin and J. Greenshields, *Anal. Biochem.*, 209 (1993) 188–191.
9 J.L. Reissig, J.L. Strominger and L.F. Leloir, *J. Biol. Chem.*, 217 (1955) 956–966.
10 J.F. McKelvy and Y.C. Lee, *Arch. Biochem. Biophys.*, 132 (1969) 99–110.

*Journal of Chromatography*, 638 (1993) 35–41
Elsevier Science Publishers B.V., Amsterdam

CHROM. 24 867

# Simultaneous determination of alkali, alkaline-earth metal cations and ammonium in environmental samples by gradient ion chromatography

Ewa Dabek-Zlotorzynska* and Joseph F. Dlouhy

*Chemistry Division, River Road Environmental Technology Centre, Environment Canada, 3439 River Road, Ottawa, Ontario K1A 0H3 (Canada)*

(First received August 19th, 1992; revised manuscript received January 6th, 1993)

ABSTRACT

A gradient ion chromatographic method with chemical suppression is described for the simultaneous determination of alkali, alkaline-earth metal cations and ammonium. This fully automated ion chromatographic method was applied to determine these cations in water extracts of ambient air particulates collected on thin PTFE filters. The procedure is also potentially available for any aqueous samples.

## INTRODUCTION

Since the development of ion chromatography (IC) [1], many studies [1–17] have dealt with the determination of monovalent and/or divalent cations.

Monovalent cations such as alkali metal cations and ammonium are easily eluted with dilute nitric or hydrochloric acid [2]. The separation of alkaline-earth metal cations requires the use of stronger driving ions, such as ethylenediamine [4], and are further facilitated by addition of complexing agents to the mobile phase [3,4]. The need for two eluent systems for a complete assay of mono- and divalent cations leads to double the analysis time and expenditure. To date, the simultaneous determination of alkali and alkaline-earth metal cations and ammonium by isocratic elution has been difficult.

A few methods have been reported for simultaneous analysis of alkali and alkaline-earth metal cations by non-suppressed isocratic elution with UV absorption spectrometry or conductivity detection [7–10]. Miyazaki *et al.* [7] reported a simultaneous separation of alkali metals, magnesium and calcium ions, and ammonium utilizing a silica-based cation exchanger with $CuSO_4$ solution as eluent. However, lithium, strontium and barium could not be separated. Sherman and Danielson [8] used a styrene–divinylbenzene copolymer-based cation exchanger and $Ce_2(SO_4)_3$ as an eluent for the separation of $Na^+$, $K^+$, $Rb^+$, $Cs^+$, $Mg^{2+}$ and $Ca^{2+}$ with indirect absorption detection. The isocratic elution of $Na^+$, $NH_4^+$, $K^+$, $Mg^{2+}$ and $Ca^{2+}$ cations using different eluents and conductivity or UV absorption spectrometry detection had been achieved by Sato [9]. With the silica-based weak cation exchanger (Nucleosil) coated with PBDMA [poly(butadiene–maleic acid)] and a tartaric acid or a combination of citric acid and pyridine-2,6-dicarboxylic acid (PDCA) as the

* Corresponding author.

0021-9673/93/$06.00 

eluents, the simultaneous separation of all alkali and alkaline earth cations is reported [10,11].

Ethylenediamine, hydrochloric acid and $Zn^{2+}$ eluent was used as an eluent on a Dionex CS2 separator column for the suppressed IC separation of $Na^+$, $Mg^{2+}$, $Ca^{2+}$ and $Sr^{2+}$ ions [12]. A column-switching method by using two separator columns of different dimensions and capacities, and switching them to change the flow direction during the elution was also proposed for simultaneous determination of alkali and alkaline-earth metal cations [13–16].

A new high-efficiency moderate-capacity cation-exchange column was recently introduced (IonPac CS10 from Dionex). It has been reported that it is possible to carry out an isocratic elution of both alkali and alkaline-earth metal cations [17]. However, a simultaneous determination of $Li^+$, $Na^+$, $NH_4^+$, $K^+$, $Rb^+$, $Cs^+$, $Mg^{2+}$, $Ca^{2+}$, $Sr^{2+}$ and $Ba^{2+}$ with a good resolution of alkali metal cations has been a problem.

An effective way of separating ions of diverse affinities is a gradient elution technique. Gradient IC is still a new field with some problems. Suitable detection methods are difficult to find. With the advent of new high-capacity membrane suppressors, gradient elution was achieved in anion analyses [18]. Gradient elution has generally not been used in cation IC separations, mainly because many important ions can be separated and eluted isocratically. However, Cheam and Chau [19] used a step gradient suppressed IC system for separation of $Li^+$, $Na^+$, $NH_4^+$, $K^+$, $Mg^{2+}$ and $Ca^{2+}$ ions.

The work presented in this study focuses on the use of a suppressed gradient IC method that allows simultaneous separation of $Li^+$, $Na^+$, $NH_4^+$, $K^+$, $Rb^+$, $Cs^+$, $Mg^{2+}$, $Ca^{2+}$, $Sr^{2+}$ and $Ba^{2+}$ ions. This paper describes the fully automated system for the analysis of the above-mentioned ten cations in aqueous extracts of ambient air particulates and in other samples.

## EXPERIMENTAL

### *Apparatus*

A computerized ion chromatography system (Dionex 4500i, Sunnyvale, CA, USA) was used. It consisted of an automated sampler (Dionex), a gradient pump, a micromembrane suppressor (CMMS-II), a conductivity detector (CDM-2) with autoregeneration accessory (Dionex), columns, advanced computer interface module (ACI), personal computer (IBM, PS/2 70), and a dot-module printer (Epson, FX 850).

The separations were carried out on an IonPac CS10 cation-exchange column (250 mm × 4 mm I.D.) with an IonPac CG10 guard column (50 mm × 4 mm I.D.) at a flow-rate of 1.0 ml/min. A cation trap column (CTC-1) filled with a high-capacity low-efficiency cation-exchange resin was placed between the eluent reservoir (40 m*M* HCl) and the pump to remove cation impurities from the eluent.

A cation micromembrane suppressor was used to minimize background conductivity and enhance the analyte conductance. The suppressor was continuously regenerated with a solution of 0.1 *M* tetrabutylammonium hydroxide (TBAOH) at a flow-rate of 10 ml/min. The TBAOH solution was continuously regenerated by an autoregeneration accessory. A 50-$\mu$l loop was used for injection of the samples. All samples were analyzed seven times, unless specified otherwise.

A chromatography data system (Dionex, AI-450) was used for instrument control and for data collection and processing.

### *Reagents*

Hydrochloric acid (J.T. Baker), 2,3-diaminopropionic acid monohydrochloride (Dionex) and 100 m*M* aqueous solution of tetrabutylammonium hydroxide (Dionex) were of analytical reagent-grade quality.

Ultrapure water (18 MΩ/cm resistivity at 25°C) was obtained by treating the tap water in reverse osmosis and with ion-exchange columns (Millipore, RO 20 and SuperQ).

The ammonium standard solution was prepared from ammonium chloride. A stock solution of the other nine cations was prepared from National Institute of Standards and Technology (NIST) standards. Diluted working standard solutions were prepared daily.

All standards, samples, and reagents were prepared and stored in polyethylene containers,

previously cleaned and conditioned following a procedure for trace element determination [21].

*Procedures*

Standards and samples were analyzed by suppressed gradient IC under the operating conditions listed in Table I.

Multilevel calibration was used with linear least-squares best fit regression analysis. Adequacy of linear calibration of the method was tested for both peak area and peak height. Peak areas were found, in general, to have better linearities and better reproducibilities for cations.

Detection limits were calculated by analyzing dilute solutions. They were taken as three times the standard deviation of fifteen replicate analyses of a sample containing analytes with concentration equal to ten times the expected detection limit [22].

The precision of the presented analytical method was verified by replicate analysis of standard solutions containing cations of interest at $\mu$g/l and mg/l levels. These replicate analyses were used for the determination of relative standard deviation (R.S.D.) and ensured accurate reproducibility.

*Sample preparation*

*Filter extracts*. Ambient aerosols collected on thin PTFE filters in virtual dichotomous samplers were obtained from the Pollution Measurement Division, River Road Environmental Technology Centre, Environment Canada.

TABLE I

GRADIENT PROFILE

| Time (min) | Eluent 1[a] (%) | Eluent 2[b] (%) | Comments |
|---|---|---|---|
| 0 | 100 | 0 | Inject sample |
| 3 | 100 | 0 | Start gradient ramp |
| 13 | 40 | 60 | End gradient ramp |
| 39 | 40 | 60 | End isocratic elution |
| 39.5 | 100 | 0 | End run |
| 55 | 100 | 0 | Equilibrate and load |

[a] 40 m*M* HCl.

[b] 40 m*M* HCl–20 m*M* 2,3-diaminopropionic acid monohydrochloride.

The samplers fractionated the aerosol into two aerodynamic size ranges yielding "fine" ($<2$ $\mu$m) and "coarse" ($<10$ $\mu$m) samples [20]. The samples were analyzed first by X-ray fluorescence spectrometry and then by IC.

Because the PTFE surface of the filters and some particulates are hydrophobic, it is necessary to wet the filter initially with methanol (1 ml). Particulates deposited on the filter samples were extracted using water (19 ml) by sonication for 30 min. The analysis was carried out as soon as possible after extraction.

*Soil sample*. A 0.25-g amount of standard reference soil sample SO-2 (Canada Centre for Mineral and Energy Technology CANMET) was acid-digested with nitric acid followed by evaporation to dryness with hydrofluoric and perchloric acids. Fluorides were displaced by heating of residue with 2.5 ml of a saturated boric acid solution and this step was repeated. The residue was then dissolved in 0.5 ml perchloric acid and 20 ml water and the solution transferred to a 100-ml volumetric flask with water.

## RESULTS AND DISCUSSION

Several potential gradient elution profiles were tested to simultaneously separate $Li^+$, $Na^+$, $NH_4^+$, $K^+$, $Rb^+$, $Cs^+$, $Mg^{2+}$, $Ca^{2+}$, $Sr^{2+}$ and $Ba^{2+}$. A moderate-capacity cation-exchange column (IonPac CS10) and eluent solution consisting of hydrochloric acid and diaminopropionic acid mixed in different concentration ratios were used. The procedure summarized in Table I led to the best separation of $Li^+/Na^+$ and $Na^+/NH_4{}^+$. All ten cations were separated with good resolution (see Fig. 1).

*Analytical characteristics*

The analytical characteristics of the developed procedure were determined from calibration graphs constructed for a mixed standard based on peak areas.

The linear least-squares parameters of these plots are summarized in Table II. The response is linear for all components at the concentration levels of interest.

The sensitivity defined as the peak area per

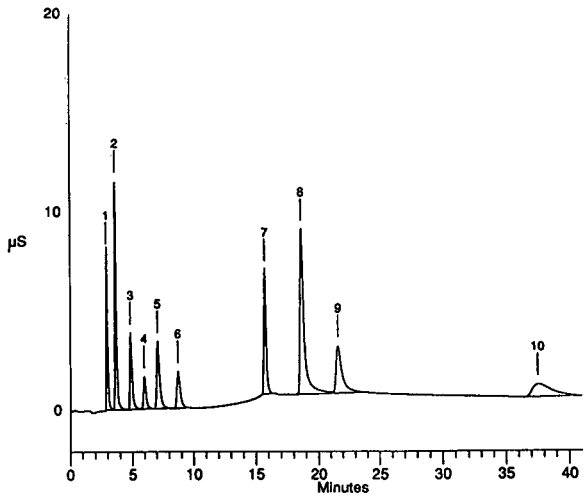


Fig. 1. Simultaneous ion chromatographic separation of alkali, alkaline-earth metal cations and ammonium obtained on the CS10 column by injecting 50 μl of a standard solution. (For elution conditions see Table I). Peaks: 1 = $Li^+$ (0.5 mg/l); 2 = $Na^+$ (2.5 mg/l); 3 = $NH_4^+$ (2.0 mg/l); 4 = $K^+$ (1.0 mg/l); 5 = $Rb^+$ (5.0 mg/l); 6 = $Cs^+$ (5.0 mg/l); 7 = $Mg^{2+}$ (1.0 mg/l); 8 = $Ca^{2+}$ (5.0 mg/l); 9 = $Sr^{2+}$ (5.0 mg/l); 10 = $Ba^{2+}$ (10.0 mg/l).

unit concentration can be easily compared for each cation (Table II). The best response was found for lithium. The day-to-day reproducibility of the slope of each calibration curve depends on the background conductivity. Based on background conductivity values between 2 and 4 μS/cm, the relative R.S.D.s of five values of the slopes was found to be less than 6% for most of the cations under investigation. Only ammonium had a greater R.S.D. of slope (7.72%).

*Blank and limit of detection*

The major problem of this method are the magnesium and calcium impurities in HCl. These ions are concentrated at the front of the column when equilibrating the separator with the weak eluent (40 m*M* HCl). When starting the gradient, they are eluted at their expected retention times. This problem was partly solved by the use of a cation trap column in the weak eluent line. The lowest blank levels observed were 5–10 ng of magnesium and calcium.

Detection limits of analytes (for 50 μl injection volume) using described method are listed in Table II. It can be seen that most of the cations investigated are detectable in the sub-mg/l range. Lower detection limits should be possible using larger injection volumes, a concentrator column or other techniques.

*Accuracy and precision*

Data on the reproducibility of retention times and peak areas are listed in Table III. The R.S.D.s for the retention times of all cations are less than 0.3% and for peak areas at lower concentration level less than 4%. Ammonium was the only cation which had a R.S.D. greater than 4%. Thus, both peak areas and retention times indicate the stability and reproducibility of the system.

TABLE II

PARAMETERS OF CALIBRATION GRAPHS AND DETECTION LIMITS FOR PROPOSED METHOD

| Cation | Concentration range (mg/l) | Slope (area unit/mg/l) | *y*-Intercept (area unit) | Correlation coefficient | Detection limit (mg/l) |
|---|---|---|---|---|---|
| Lithium | 0.05– 1 | $1.41 \cdot 10^8$ | $-4.37 \cdot 10^5$ | 0.9999 | 0.005 |
| Sodium | 0.25– 5 | $4.87 \cdot 10^7$ | $3.24 \cdot 10^5$ | 0.9999 | 0.025 |
| Ammonium | 0.20– 4 | $2.54 \cdot 10^7$ | $2.78 \cdot 10^6$ | 0.9993 | 0.040 |
| Potassium | 0.10– 2 | $2.67 \cdot 10^7$ | $-2.57 \cdot 10^5$ | 0.9999 | 0.010 |
| Rubidium | 0.50–10 | $1.32 \cdot 10^7$ | $-7.44 \cdot 10^5$ | 0.9998 | 0.040 |
| Cesium | 0.50–10 | $7.98 \cdot 10^6$ | $-4.04 \cdot 10^5$ | 0.9999 | 0.050 |
| Magnesium | 0.10– 2 | $7.68 \cdot 10^7$ | $2.75 \cdot 10^6$ | 0.9997 | 0.050 |
| Calcium | 0.50–10 | $4.67 \cdot 10^7$ | $6.38 \cdot 10^6$ | 0.9997 | 0.050 |
| Strontium | 0.50–10 | $2.30 \cdot 10^7$ | $-1.50 \cdot 10^6$ | 0.9998 | 0.040 |
| Barium | 1.0–20 | $1.14 \cdot 10^7$ | $-1.24 \cdot 10^7$ | 0.9997 | 0.400 |

TABLE III

REPRODUCIBILITY OF RETENTION TIMES ($t_R$) AND PEAK AREAS

Reported results are the mean and relative standard deviation of 15 replicates for standard (STD) 1 and 5 replicates for STD 4; STD 1 ($Li^+$ 0.05; $Na^+$ 0.25; $NH_4^+$ 0.20; $K^+$, $Mg^{2+}$ 0.10; $Rb^+$, $Cs^+$, $Ca^{2+}$, $Sr^{2+}$ 0.50 and $Ba^{2+}$ 1.00 in mg/l); STD 4 was twenty times more concentrated than STD 1.

| Cation | STD 1 | | | STD 4 | | |
|---|---|---|---|---|---|---|
| | $t_R$ (min) | R.S.D. (%) | | $t_R$ (min) | R.S.D. (%) | |
| | | $t_R$ | Area | | $t_R$ | Area |
| Lithium | 2.87 | 0.01 | 2.8 | 2.87 | 0.01 | 2.1 |
| Sodium | 3.67 | 0.21 | 3.2 | 3.65 | 0.21 | 2.1 |
| Ammonium | 4.75 | 0.01 | 5.6 | 4.75 | 0.01 | 4.5 |
| Potassium | 5.88 | 0.07 | 3.9 | 5.88 | 0.07 | 2.5 |
| Rubidium | 6.99 | 0.12 | 2.6 | 7.00 | 0.12 | 2.4 |
| Cesium | 8.63 | 0.01 | 3.2 | 8.63 | 0.01 | 2.5 |
| Magnesium | 15.65 | 0.05 | 2.9 | 15.65 | 0.05 | 1.5 |
| Calcium | 18.42 | 0.09 | 1.7 | 18.42 | 0.09 | 1.2 |
| Strontium | 21.30 | 0.09 | 2.1 | 21.30 | 0.09 | 1.9 |
| Barium | 37.25 | 0.18 | 3.0 | 37.23 | 0.18 | 2.6 |

In order to evaluate the quantitative performance and accuracy of the system, a certified soil SO-2 sample was analyzed. The result (see Table IV) is in good agreement with the certified values. The typical chromatogram is shown in Fig. 2.

*Applications*

The proposed method was applied to the simultaneous determination of alkali, alkaline-earth metal cations and ammonium in aqueous extracts of ambient air particulates collected on the thin PTFE filters and other samples.

TABLE IV

ANALYSIS OF SOIL SO-2 BY PROPOSED METHOD

Mean and 95% confidence limits for seven determinations

| Cation | Found | Certified value |
|---|---|---|
| Sodium | 2.11 ± 0.04% | 1.90 ± 0.05% |
| Potassium | 2.48 ± 0.08% | 2.45 ± 0.04% |
| Magnesium | 0.51 ± 0.01% | 0.54 ± 0.03% |
| Calcium | 1.90 ± 0.04% | 1.96 ± 0.10% |
| Strontium | 325 ± 9 μg/g | 340 ± 50 μg/g |
| Barium | 980 ± 52 μg/g | 966 ± 67 μg/g |

Figs. 3 and 4 show the typical chromatograms of coarse and fine filter extracts. All samples of coarse filter extracts contain sodium and calcium as major cations. Ammonium was the major cation in fine filter extracts. It is possible to detect minor peaks attributable to other alkali

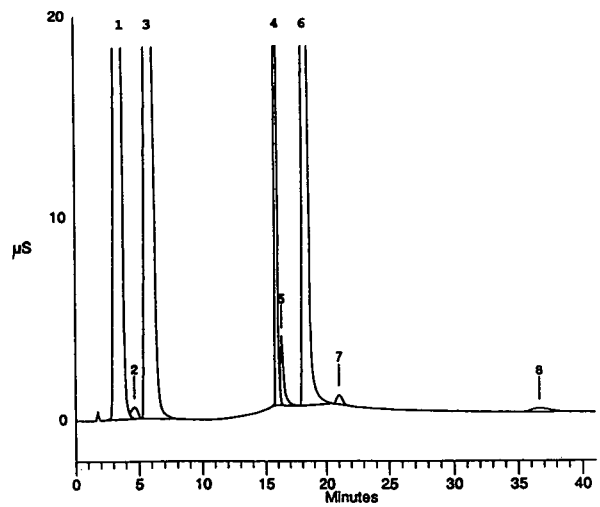


Fig. 2. Determination of alkali and alkaline-earth metal cations in a certified soil SO-2 sample. Conditions as in Table I. Peaks: 1 = $Na^+$; 2 = $NH_4^+$; 3 = $K^+$; 4 = $Mg^{2+}$; 5 = unidentified peak; 6 = $Ca^{2+}$; 7 = $Sr^{2+}$ and 8 = $Ba^{2+}$.

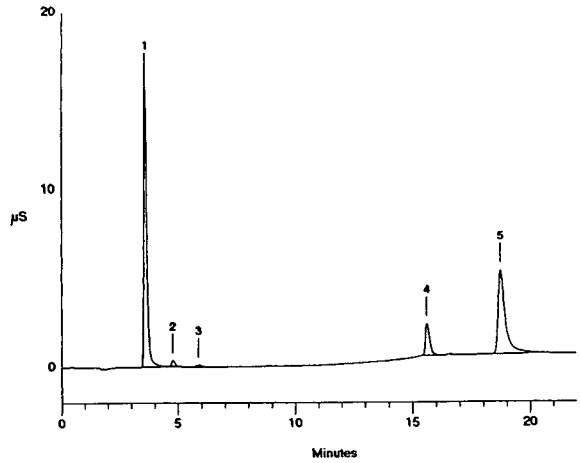


Fig. 3. Ion chromatographic analysis of a coarse air particulates extract. Conditions as in Table I. Peaks: $1 = Na^+$; $2 = NH_4^+$; $3 = K^+$; $4 = Mg^{2+}$; $5 = Ca^{2+}$.

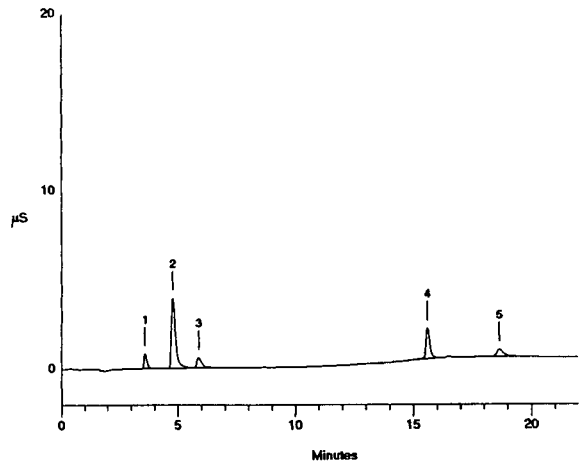


Fig. 4. Ion chromatographic analysis of a fine air particulates extract. Conditions as in Table I. Peaks: $1 = Na^+$; $2 = NH_4^+$; $3 = K^+$; $4 = Mg^{2+}$; $5 = Ca^{2+}$.

and alkaline-earth cations. The concentration of some cations such as $Li^+$, $Rb^+$, $Cs^+$, $Sr^{2+}$ and $Ba^{2+}$ is systematically or frequently under detection limit. Sometimes unidentified peaks are present. Lithium ions were found only in a few coarse filter extracts. The use of the concentrator column improves the detection limits. Strontium and barium cations were detected only in a few extract samples after preconcentration of coarse filter extracts by a factor of 100. Results of the chemical composition (anions and cations) of the aerosols collected on PTFE filters will be reported later [23].

The proposed method was also tested to ascertain its applicability to the determination of alkali, alkaline-earth metal cations and ammonium in a tap water. The tap water sample was spiked with known amount of cation standard solutions. The recovery of all cation spikes was higher than 90% (see Table V).

TABLE V

ANALYSIS OF TAP WATER

| Cation | Tap water, found ($n = 10$) (mg/l ± S.D.) | Spiked tap water | | |
|---|---|---|---|---|
| | | Added (mg/l) | Found (mg/l ± S.D.) | Recovery (%) |
| Lithium | 0.016 ± 0.0003 | 0.10 | 0.107 ± 0.003 | 92.2 |
| Sodium | 7.526 ± 0.229 | 5.00 | 12.501 ± 0.381 | 99.8 |
| Ammonium | | 1.00 | 0.968 ± 0.025 | 96.8 |
| Potassium | 1.589 ± 0.045 | 1.00 | 2.641 ± 0.063 | 102.0 |
| Rubidium | | 1.00 | 0.982 ± 0.015 | 98.2 |
| Cesium | | 1.00 | 0.979 ± 0.017 | 97.9 |
| Magnesium | 18.277 ± 0.276 | 2.00 | 20.013 ± 0.201 | 98.7 |
| Calcium | 39.896 ± 0.737 | 5.00 | 44.425 ± 0.664 | 99.0 |
| Strontium | 0.542 ± 0.014 | 1.00 | 1.408 ± 0.031 | 97.0 |
| Barium | | 2.00 | 1.921 ± 0.096 | 96.0 |

*Advantages and disadvantages*

The main advantage of the proposed method is its applicability for multi-cation analysis of extracts of air particulates in one step. This advantage is valid for any other water sample or solution, where the volume of the sample is limited.

The disadvantage is the analysis time, which is relatively long in comparison to usually reported times for ion chromatography. This disadvantage can be compensated by overnight measurement of samples using a fully automated system.

REFERENCES


1 H. Small, T.S. Stevens and W.C. Bauman, *Anal. Chem.*, 47 (1975) 1801.
2 J.S. Fritz, D.T. Gjerde and R.M. Becker, *Anal Chem.*, 52 (1980) 519.
3 J.S. Fritz, D.T. Gjerde and C.R. Pohlandt, *Ion Chromatography*, Hüthig, New York, 1982.
4 G.J. Sevenich and J.S. Fritz, *J. Chromatogr.*, 347 (1985) 147.
5 H. Shintani, *J. Chromatogr.*, 341 (1985) 53.
6 *Ion Chromatography Cookbook*, Dionex, Sunnyvale, CA, 1987.
7 M. Miyazaki, K. Haykawa and S.G. Choi, *J. Chromatogr.*, 323 (1985) 443.
8 J.H. Sherman and N.D. Danielson, *Anal. Chem.*, 59 (1987) 490.
9 H. Sato, *J. Chromatogr.*, 469 (1989) 339.
10 P. Kolla, J. Kohler and G. Schomburg, *Chromatographia*, 23 (1987) 465.
11 D. Yan and G. Schwedt, *Fresenius' J. Anal. Chem.*, 338 (1990) 149.
12 R.P. Singh, E.R. Pombid, P. Debayle and N.M. Abbos, *Analyst (London)*, 116 (1991) 409.
13 H. Small, *Ion Chromatography*, Plenum, New York, 1990.
14 R.D. Rocklin, M.A. Rey, J.R. Stillan and D.L. Campbell, *J. Chromatogr. Sci.*, 27 (1989) 474.
15 D.L. Campbell, J.R. Stillan, S. Carson, R. Joyce and S. Heberling, *J. Chromatogr.*, 546 (1991) 229.
16 M. Betti, G. Giovannoni, M. Onor and P. Papoff, *J. Chromatogr.*, 546 (1991) 259.
17 *Doc. No. 034341*, Dionex, Sunnyvale, CA, January 1990.
18 R.D. Rocklin, C.A. Pohl and J.A. Shibler, *J. Chromatogr.*, 411 (1987) 107.
19 V. Cheam and A.S. Chau, *Analyst (London)*, 112 (1987) 993.
20 T.G. Dzubay, R.K. Stevens and C.M. Peterson, *X-Ray Fluoroscence Analysis of Environmental Samples*, Ann Arbor Sci. Publ., Ann Arbor, MI, 1977, p. 95.
21 M. Betti, M.P. Colombini, R. Fucco and P. Papoff, *Mar. Chem.*, 17 (1985) 313.
22 E.L. Inman and E.C. Rickard, *J. Chromatogr.*, 447 (1988) 1.
23 E. Dabek-Zlotorzynska and J.F. Dlouhy, *J. Chromatogr.*, in press.

*Journal of Chromatography*, 638 (1993) 43–56
Elsevier Science Publishers B.V., Amsterdam

CHROM. 24 969

# Critical comparison of gas–hexadecane partition coefficients as measured with packed and open tubular capillary columns

Yunke Zhang[☆], Andrew J. Dallas[☆☆] and Peter W. Carr*

*Department of Chemistry, University of Minnesota, Smith and Kolthoff Halls, 207 Pleasant Street S.E., Minneapolis, MN 55455 (USA)*

(First received October 27th, 1992; revised manuscript received February 9th, 1993)

ABSTRACT

The use of gas chromatography to study the thermodynamics of solute–solvent interactions is very well established. Many successful measurements using non-polar solutes have been reported. However, the investigation of the properties of even moderately polar solutes, such as acetone, on porous particles in packed beds is fraught with potential chemical problems including interfacial adsorption at the solid–gas and liquid–solid interfaces. In order to minimize, but likely not eliminate such effects, we have employed fused-silica open tubular capillary columns. This approach affords, relative to other supports, a very inert solid surface with low net area for both the solid–gas and liquid–solid interfaces. Due to the very small amount of stationary phase liquid, it is not possible to measure the absolute value of the partition coefficient. However, it is possible to obtain precise measurements of relative partition coefficients. Using the absolute value of the partition coefficient for some reference solute, obtained by alternative methods, absolute values can be computed. In this work, we show that solute retention on *n*-hexadecane is independent of solute concentration over a usefully wide range in the amount of solute injected. Where the capacity factors do vary with the amount injected, they do so in a direction consistent with a partition dominated process. Values for the partition coefficients for 105 non-polar and polar solutes in *n*-hexadecane are reported and critically compared to literature values.

## INTRODUCTION

Gas–liquid chromatography (GLC) is well established as a rapid method for measuring partition coefficients and other physicochemical parameters [1,2]. The fundamentals governing the measurement of partition coefficients are straightforward. The solute capacity factor measured in a GLC experiment is directly related to the partition coefficient by the following equation:

$$k' = K\phi \quad (1)$$

where $k'$, $K$, and $\phi$ refer to the solute capacity factor, partition coefficient and the phase ratio, respectively.

One assumption in using eqn. 1 is that only partitioning of solutes between the gas and stationary phases contributes to the measured capacity factor. This assumption has been shown to be correct for non-polar solutes with non-polar stationary phases [3–7]. However, adsorption at gas–liquid, gas–solid and liquid–solid interfaces can and do make significant contributions to the measured $k'$ values with polar solutes on non-polar stationary phase and vice versa [3,7–15]. In such cases eqn. 1 must be modified to account for contributions from

* Corresponding author.
☆ Present address: Department of Chemistry, Baylor University, TX, USA.
☆☆ Present address: Donaldson Co., Inc., 9250 W. Bloomington Freeway, Bloomington, MN 55431, USA.

0021-9673/93/$06.00 

adsorption processes. One such modification, proposed by Jonsson and Mathiasson [16] is:

$$V_N = K_L V_L + K_S A_S + K_I A_I + K_A A_A \quad (2)$$

where $K_L V_L$, $K_S A_S$, $K_I A_I$ and $K_A A_A$ represent the contributions to the net retention volume $V_N$ from partitioning, gas–solid, liquid–solid, and gas–liquid interfacial adsorption, respectively. It is clear that the partition coefficient cannot be calculated from the measured net retention volume and stationary phase volume ($V_L$) unless the contribution from these adsorption terms is negligible or can be corrected by empirical or theoretical methods. One obvious method of reducing adsorption contributions is to minimize the area of the gas–solid ($A_S$), liquid–solid ($A_I$), and gas–liquid ($A_A$) interfaces relative to the volume of the stationary phase.

Two different approaches have been developed to separate the contribution due to different retention processes. The first approach is to measure the specific retention volume using a series of columns with different amounts of stationary phase [17]. The specific retention volume is then plotted *versus* $1/V_L$. A "corrected" specific retention volume is said to be obtained by using the value resulting from the extrapolation of this plot to the ordinate, $1/V_L$ equal to zero. This is interpreted as being the specific retention volume obtained on an infinitely thick stationary phase which is said to "correct" for the contributions to retention from interfacial processes. This approach can easily be applied if there is a linear relationship between the specific retention volume and $1/V_L$. This can be true only with constant adsorption effects or a linear absorption contribution, where the absorption effect is so low that the infinite dilution condition can be realized for both the partition and adsorption retention processes. The situation is complicated when adsorption is non-linear, that is when the peak is tailed and the retention time and volume vary with sample size. In such cases where peaks are significantly asymmetrical, the retention volume corresponding to elution at a fixed solute gas concentration, ECP (elution by characteristic point) method [2], rather than the peak maximum volume, has been used as the basis for measurement [17]. This fixed concentration is determined by choosing a point at constant height on the diffuse side of the peak which is then used to obtain a solute's retention volume [18]. One clear disadvantage of this approach is that a series of columns have to be used under the same conditions. Another limitation of the approach is that the relationship between retention volume and the amount of stationary phase may be non-linear. The extrapolation is then much more subjective [19]. Non-linear relationships between retention volume and the volume of stationary phase have been reported [6,20]. These are attributed to cooperative adsorption effects [6] and stationary phase wetting transitions [18].

A second way to handle asymmetric peaks is to inject such a large sample that all adsorption sites become saturated. Retention is then dominated by a non-linear partition process and not by adsorption. This situation is thought to prevail when the retention time increases with sample size [19,21,22]. Retention is measured under partition dominated conditions and the partitioning contribution to retention is obtained by extrapolating the retention volume to zero sample size. The advantage of this approach is that measurements can be made on a single column. However, in order to achieve partitioning dominated retention, very large sample volumes must be used for strongly adsorbed species. Moreover, all measurements are actually made in the region where the partition coefficient becomes sample size dependent. Therefore, it is difficult to estimate the error introduced by using such large amounts of sample.

Jonsson and Mathiasson [22] proposed a similar approach by developing an equation which described retention under the assumption that a single Langmuir-type adsorption process contributes to retention. A series of retention volumes at different sample sizes are measured. The data are then fitted to their equation. The contributions from adsorption and partition processes can then be calculated by extrapolating to zero sample size. Alternatively, the contributions from adsorption and partitioning were separated by Korol *et al.* [23] by assuming a linear relation-

ship between the measured net retention volume and the reciprocal of the logarithm of the peak maximum.

Clearly, accurate measurements of thermodynamic partition coefficient demand that adsorption effects be minimized. Theoretically, this can be done by deactivating the support or minimizing the adsorption surface area. Unfortunately, the methods typically used for the deactivation of support materials produce surfaces that are not completely inert under all conditions. This is primarily attributed to difficulties in covering all adsorption sites on the support surface. In addition, active metal impurities present in the support material can contribute to adsorption. These impurities are very difficult to remove. Even PTFE, which is commonly believed to be inert, is active [24–27]. While glass bead supports have much lower surface areas than do diatomaceous supports their ability to hold the stationary phase is limited. Therefore, they are no better than deactivated white diatomite supports [20,22].

In this study we attempted to measure the gas–hexadecane partition coefficient of 105 solutes, spanning a wide range of functional groups, dipolarity and hydrogen bonding ability. Abraham *et al.* [28] collected literature data for most of the solutes given here as well as a great many others. Our incentive for remeasuring the gas–hexadecane partition coefficients is twofold. First, this molecular property is a very valuable explanatory variable in many linear solvation energy relationships and in a series of related studies we felt that a number of the data reported previously had to be in error [29]. Second, the data set reported by Abraham *et al.* was obtained from a variety of sources, by a variety of methods including gas chromatography on packed columns, head space analysis, and by extrapolations from measured values for lower members of a homolog series. We felt that it would be advisable to use data obtained by a single method on a single type of column in order to minimize differential contributions from determinate errors or at least make these errors internally consistent. Given the strong tendency for interfacial adsorption both at the gas–liquid and the solid interface when a non-polar stationary phase such as *n*-hexadecane is used we felt that the polar solutes would be particularly prone to systematic error.

In preliminary work using porous supports, despite the fact that different supports and deactivation methods were tested, interfacial adsorption was always very evident. We were unable to find a support and/or deactivation method that significantly reduced adsorption for polar and hydrogen bonding solutes. Therefore, we pursued a method that minimized the surface area available for adsorption. Here, we report on the use of deactivated fused-silica capillary columns coated with *n*-hexadecane. To our knowledge, this is the first report using a relatively volatile liquid as a stationary phase for capillary gas chromatography. Fused-silica capillaries were chosen for their high purity (low level of metallic impurities) and nearly inert surface [24,30–34]. It has been shown that the tubing wall can contribute to the retention of solutes when measurements are made at low temperatures (<100°C). Fused silica was the least sorptive of five commercially available tubing materials that we tested in a previous study [24]. An important advantage of a capillary column is the larger ratio of liquid phase volume-to-surface area relative to that of a bed packed with porous particles. Depending on the film thickness the volume-to-area ratio for a capillary column can be more than two orders of magnitude greater than for a packed column [35]. In addition, it should be possible to obtain a more homogeneous surface and a more uniform coating of a non-polar liquid on a capillary column compared to a porous particulate support.

## EXPERIMENTAL

### *Instrument and materials*

A modified Hewlett-Packard 5750 gas chromatograph was used for all measurements. As prescribed by Laub and Pecsok [1] and Conder and Young [2], great efforts were taken to modify the instrument so that high precision measurements could be made. The oven temperature controller was replaced with a YSI (Yellow Springs Instruments, Yellow Springs, OH, USA) Model 72 proportional temperature

controller. A high-resistance heater was substituted for the original low-resistance, high-power heater. This allowed for much tighter control of the oven temperature. The oven was cooled by an air cooling vortex cooler (Model 3210; Exx-air, Cincinatti, OH, USA). This device is able to cool the oven well below room temperature [36]. Auxiliary air was forced into the oven to provide additional convection in order to minimize temperature gradients across the oven. The temperature was controlled to better than ±0.05°C (as measured with a National Bureau of Standards-calibrated thermometer which is readable to the nearest 0.001°C) with a gradient of ±0.2°C across the oven (as measured by a calibrated thermistor). The largest change in the temperature across the oven occurred at the heated injection port and the detector. Essentially, we attempted to isolate these portions of the instrument from the column oven. In addition, the effects of temperature gradients can be minimized by decreasing the diameter of each column coil, thereby increasing the number of coils [37]. The helium carrier gas flow was controlled by two precision pressure regulators (Model 8286; Porter Instruments, Hatfield, PA, USA) attached in series with a flow controller (Model 8744, Brooks) all of which were thermostatted to 35°C (±0.5°C) in a forced air oven using a YSI Model 71A temperature controller [1,2]. During use, the capillary was operated at an inlet pressure of approximately 2.0 p.s.i. (1 p.s.i. = 6894.76 Pa); however, the overall backpressure on the flow controller was 15–20 p.s.i. due to the use of a packed pre-column placed upstream of the injector. The purpose of this packed pre-column was twofold, one of these is described below and the other was to increase the backpressure on the flow controller so as to stabilize its output flow. Typical column dead times during use were 1.06 min, as determined by methane. Problems with using methane as a marker of the dead volume for *n*-hexadecane at 25°C are discussed below. Connection of the capillary to the oven was made with a commercial on-column injection conversion kit from Restek. The deactivated fused-silica capillary column had an I.D. of 0.530 mm (Alltech Assoc.). Chromatograms were recorded with a Hewlett-Packard 3390 integrator and the peak maximum was used as the measure of retention time. A capillary column rinse kit (J&W Scientific) was used to coat the capillary column.

*n*-Hexadecane (99 + %, $H_2O < 0.005\%$) was obtained from Aldrich and kept over $P_2O_5$. All other chemicals were obtained from commercial sources and used as received. All support materials used in the packed column studies were obtained from Supelco.

*Coating of the capillary column*

A dynamic coating method was determined to give the most uniform coating and was used throughout [38–40]. The column was first washed with about 20 ml of the following solvents: methanol, acetone, chloroform and *n*-pentane. After purging the column with dry nitrogen, the column was installed in the oven and the temperature raised to 150°C. The columns was held at this temperature with the helium flow on for at least 8 h. It was then cooled to room temperature and removed. One end of the column was connected to a 10 ft. × 0.320 mm I.D. fused-silica capillary (1 ft. = 30.48 cm). The other end was connected to the washing kit which was pressurized by dry nitrogen. The pressure during the coating process was controlled by a precision pressure regulator in order to deliver a constant flow of *n*-hexadecane to the capillary. About 10 ml of *n*-hexadecane solution in *n*-pentane was forced through both columns. The second column served as a restrictor and ensured a smooth flow of the coating solution through the capillary and prevented an increase in the stationary phase thickness towards the end of the analytical capillary [40–42]. Tight control of the flow of coating solution is necessary in order to control the film thickness and prevent "puddling" of the stationary phase [40,43]. The amount of *n*-hexadecane in the coating solution was varied from 8, 22, 50 to 100% (w/w) to determine conditions that would provide the thickest possible stable film. The best overall performance was obtained with 22% *n*-hexadecane when it was coated at a pressure of 12 p.s.i. and a velocity of about 1.1 cm/s. After the

coating solution passed through the column, pentane was removed by purging the column with helium for approximately 40 min. The column was then installed in the oven at 25°C under a flow of helium until a steady baseline was obtained. To reduce stationary phase loss, a "pre-saturation" tube was installed before the injection port [44,45]. This saturated the carrier gas with *n*-hexadecane. Loss of *n*-hexadecane throughout the experiment was monitored via measurement of the retention of *n*-hexane. Its retention was measured repeatedly each day and minimally after each third solute was examined. All data were corrected for the loss of stationary phase.

Loading of *n*-hexadecane onto porous supports was accomplished by immersing the support in a mixture of *n*-hexadecane and *n*-pentane. *n*-Pentane was slowly removed by applying a vacuum via a rotary-evaporator. All support mesh sizes were 60–80. Chromosorb P AW DMCS (acid-washed, dimethyldichlorosilane deactivated Chromosorb P) and Chromosorb W HP were washed with acetone and dried at 150°C overnight before use. Chromosorb T was washed with acetone and isopropanol and then dried in a vacuum oven at 80°C overnight before use. Coating of Chromosorb T followed the procedure by Kirkland [27] to avoid "clump" formation. These materials were packed into both stainless-steel and glass columns. The glass columns were taken through an extensive on-column silanization procedure at 150°C. Repetitive injections of a commercially available silylation reagent, Silyl 8 (Pierce), was performed until no change in the retention time or peak symmetry was observed [46,47]. This was taken as the point of minimal surface activity.

*Determination of the partition coefficients*

It is difficult to measure directly the amount of stationary phase in a capillary column especially when a volatile stationary phase is used and the evaporation rate is significant. In order to avoid making this measurement, *n*-hexane was used as a standard solute and we assumed that the partition coefficient reported by Abraham *et al.* [28] was correct. The partition coefficient for any solute can then be computed as:

$$K_x = K_{n\text{-hexane}} \cdot \frac{t_{R,x} - t_m}{t_{R,n\text{-hexane}} - t_m} \quad (3)$$

where $t_R$ and $t_m$ denote the retention time of any species and the dead time of the column under the same conditions, respectively. Clearly an estimate of the dead time is needed. The dead time was obtained by the method of Peterson and Hirsch [48]. This method is based on the assumption that within an homolog series there is a linear relationship between the logarithm of the corrected retention time and the solute's carbon number. About 1 $\mu$l of gas phase above a mixture of *n*-pentane, *n*-hexane and *n*-heptane was injected into the column and the dead time was calculated using the following equation:

$$t_m = \frac{t_{C6} - (t_{C5} t_{C7})}{2t_{C6} - (t_{C5} + t_{C7})} \quad (4)$$

where $t_{C5}$, $t_{C6}$, and $t_{C7}$ refer to retention times of pentane, hexane and heptane, respectively. The dead time calculated in this manner is preferred to the retention volume of methane because methane is retained by *n*-hexadecane, its gas–liquid partition coefficient is 0.48 at 25°C [28]. In addition, it has been pointed out that the retention time of methane cannot be used when the column temperature is below 100°C [1]. The linearity between logarithm of the corrected retention times and carbon number of a homologue series is the basis for a more complex method using many members of a homologue series [49]. We decided to use the three alkanes mentioned above because they are all well retained and eluted in a reasonable time frame. Typical dead-times using the three-alkane approach were approximately 1.03 min. This is significantly less than the observed retention time for methane (1.06 min).

It is possible that our choice of Abraham *et al.*'s value for the gas–liquid partition coefficient of *n*-hexane in *n*-hexadecane as a normalizing factor could introduce an error in the partition coefficients reported here. In order to ensure that we are normalizing against the most accurate data available, we have compared this value against several literature values which are

believed to be extremely reliable. McGlashan and Williamson [50] studied the infinite dilution activity coefficient of *n*-hexane in *n*-hexadecane as a function of temperature and composition by the static vapor pressure method. They covered the temperature range 20–60°C in 10°C increments and the mol fraction of *n*-hexane was varied from 0.012 to 0.90. We have interpolated their data to 25°C using their lowest concentration results and have converted the activity coefficient to the gas–liquid partition coefficient using the vapor pressure of *n*-hexane. Cruickshank *et al.* [51] and Chien *et al.* [52] have also determined the infinite dilution activity coefficient at several temperatures using high-precision packed-column GC. In addition, we have made two separate measurements of the partition coefficient of *n*-hexane in *n*-hexadecane by headspace GC [53,54]. The average partition coefficient for *n*-hexane from all of these measurements is 466.1 and the standard error is 1.99 (relative standard deviation 0.42%). Abraham *et al.*'s reported value is 465.6. It is as accurate as any data that are available for this solute. Based on these data, we feel the use of *n*-hexane as a normalization factor should not compromise the accuracy of the partition coefficients reported in this work.

*Measurement precision*

All the partition coefficients reported here were based on at least two measurements for highly retained solutes and three measurements for the rest of the data set. In order to study interfacial adsorption, a series of different sample sizes were used for all polar solutes. When a sample size dependence was observed, four to eight measurements were made using different amounts of solute and the average of the values within the sample size independent region was used to determine the partition coefficient. Repeated measurements of solutes that gave asymmetric peaks were run several times on different days; a deviation of less than ±1% was observed. Despite the fact that we repeatedly measured the retention time of methanol no data are given here since its capacity factor was so low that we deemed the result unreliable. Acetaldehyde, 1,1,1,3,3,3-hexafluoroisopropanol and 2,2,2-trifluoroethanol, the three least retained species reported here, all had capacity factors of less than 0.05.

## RESULTS AND DISCUSSION

*Preliminary experiments using packed columns*

Initial studies were undertaken using deactivated Chromosorb P AW DMCS loaded with 25% *n*-hexadecane as the packing material which was packed into 1/4 in. I.D. (1 in. = 2.54 cm) stainless-steel tubes. Polar solutes such as ketones, alcohols and nitromethane all exhibited severely asymmetric peaks whose retention times depended strongly on sample size. Small amounts of polar solutes could not be detected due to the severity of adsorption. The smallest detectable acetone peak had a retention time approximately four times that observed with a much larger sample. This clearly indicates that when Chromosorb P is used as the support, even after steps have been taken to deactivate the surface, retention of polar solutes is mainly due to adsorption and not partitioning.

In an attempt to decrease the effect of adsorption we switched to Chromosorb W HP which has a lower active metal content and lower surface area than does Chromosorb P AW DMCS. As expected, a significant decrease in peak asymmetry and a reduced dependence of retention on sample size was realized, however, adsorption effects were still very significant. For example, on a 15% (w/w) loaded support the retention time of the smallest detectable acetone peak was 37% higher than that obtained with a much larger sample.

Based on previous studies on the adsorptive strengths of different tubing surfaces [24] we switched from stainless-steel tubing to deactivated glass tubes. Deactivation using Silyl 8 was performed in order to further deactivate an already coated column [46]. A significant improvement was observed for polar solutes injected immediately after the Silyl 8 treatment. However, the decrease in activity towards polar solutes disappeared within a few hours. This leads us to believe that the silanization agent acted to block active sites on the various surfaces by physical adsorption rather than by chemical

reaction. This type of tubing and support material were abandoned due to their activity towards polar solutes.

Chromosorb T, a porous PTFE support, is commonly held to be inert towards polar solutes. When it was loaded with 20% (w/w) *n*-hexadecane, no apparent peak asymmetry or tailing was observed with alcohols and higher ketones. However, repeated measurements at the lowest detectable amount of acetone still gave retention times that were 2% higher than those obtained with a larger amount of solute. Polychloroalkanes showed significant tailing and irreproducible retention on this material. These observations confirm previous reports of the activity of this support towards polar solutes [24–27]. Additionally, nitromethane was irreproducibly retained and double peaks were obtained whereas the same solute gave a single peak on other supports. In addition, most stationary phases have a higher surface tension than PTFE and therefore do not evenly wet its surface. Based on these results, we rejected the premise that PTFE is an inert support and abandoned its further use in this study.

*Partition coefficient measurement using capillary columns*

*Effect of coating concentration and speed.* To minimize the adsorption terms in eqn. 2 relative to the partition terms it is necessary that a thick uniform coating of *n*-hexadecane be present on the column wall. This minimizes the amount of available fused-silica surface and decreases the surface-to-volume ratio, which favors solute partitioning. A column coated with an 8% *n*-hexadecane solution coated under 10 p.s.i. pressure gave a very even coating (as observed through the tubing wall with a microscope). The coating was assumed to be even, if beads were not observed and the intensity of light when directed through the tubing wall did not vary. The calculated film thickness, based on the retention of benzene, was only approximately 0.11 $\mu$m. We found that a thicker film, approximately 0.23 $\mu$m, which was still uniform could be achieved by increasing the concentration of the coating solution to 22% *n*-hexadecane and using a coating pressure of 12 p.s.i. However, increasing the solution concentration to both 50 and 100% *n*-hexadecane solutions gave non-uniform films which were only about 0.29 $\mu$m thick. Soon after the coating was completed the films made from the more concentrated solutions exhibited "pooling" and "beading" of the *n*-hexadecane. It is known that the ability of a phase to wet the tubing wall [55] and the viscosity [56] of the coating solution are critical in coating stable, uniform films on fused-silica surfaces. It is also possible that the solvent, *n*-pentane, acts as a transient wetting agent by reducing the surface energy of the capillary surface which then allowed *n*-hexadecane to coat as a thin uniform film on the tubing wall. A very uniform film with a maximum thickness of 0.29 $\mu$m was obtained using 22.5% (w/w) *n*-hexadecane solutions and coating at a pressure of 12 p.s.i. These were considered to be the optimum coating conditions. It appears that the film thickness is controlled by the coating conditions at lower concentrations of *n*-hexadecane, and by the wettability and viscosity of *n*-hexadecane at higher concentrations [55,56]. Columns prepared under optimum conditions were reasonably stable over a relatively long period of time. However, upon injecting high-boiling polar liquids, a few small "puddles" were observed near the head of the column. This problem was minimized by injecting the head-space vapor above a warm solution of the polar solutes.

The lifetime of a column was limited by the loss of stationary phase. Since the phase ratio is constantly decreasing, it was measured every few hours using a standard mixture of *n*-pentane, *n*-hexane and *n*-heptane as described above. A long term study over eight consecutive days indicated a constant loss rate of approximately 2% per day under the use conditions described here.

*Adsorption of polar solutes on a deactivated fused-silica capillary column.* Preliminary tests of the hexadecane-coated fused-silica capillary column were performed in order to study interfacial adsorption, the sample size dependence and the reproducibility of the retention times for polar solutes. The retention time of acetone was independent of the amount of sample injected. Additionally, more highly retained polar solutes

were studied. Retention times for all solutes, except for the amines (see below), were independent of the amount of sample injected. This sample size independence typically persisted until the sample size was greater than about 10 $\mu$l of the headspace above a warmed solution. When an excessive amount of solute was injected the retention times on the capillary columns increased in contrast to the decreases observed with packed beds. A representative set of results are given in Fig. 1 for a series of alcohols. Retention times are very reproducible and do not vary with sample size until a very large amount is injected. Additionally, we intentionally overloaded the column with 1-pentanol in Fig. 2 in order to emphasize this effect. This result is consistent with the above discussion and results based on studies using headspace gas chromatography and pressure measurements of the partition coefficients [57–61]. This increase in retention times of polar solutes in *n*-hexadecane with the amount of solute injected is due to solute–solute association which increases the solute's gas–liquid partition coefficient which in turn results in an increase in the retention time. This effect is most significant for the alcohols and carboxylic acids. Acetic acid, which is known to be very highly self-associated, gave constant

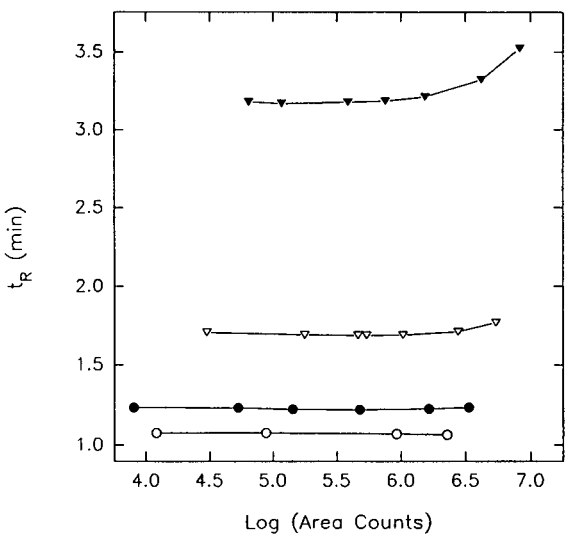


Fig. 1. Effect of injected sample size, as represented by the peak area counts, on the retention time of a series of alcohols. ○ = Ethanol; ● = 1-propanol; ▽ = 1-butanol; ▼ = 1-pentanol.

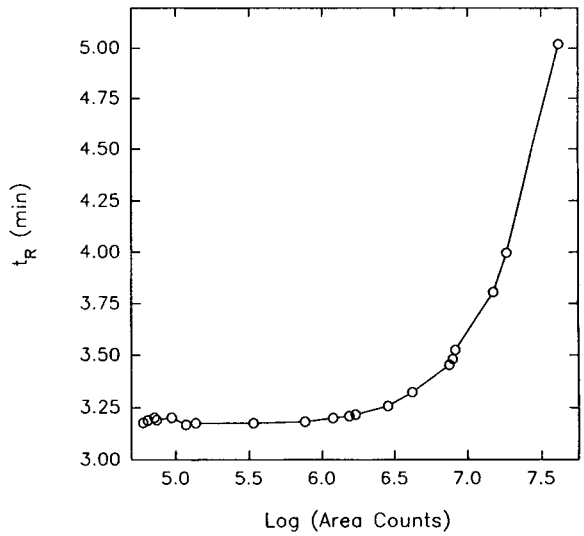


Fig. 2. Effect of injected sample size, as represented by the peak area counts, on the retention time of 1-pentanol.

retention times for small injection volumes on the capillary column whereas asymmetric peaks with varying retention times were obtained with packed columns. In summary, all of the above semi-quantitative observations lead us to believe that our measurements are made under partition-dominated conditions. Based on the above, we believe that the partition coefficients measured in this study are more reliable than those obtained with packed columns regardless of whether mixed retention processes were accounted for in the data analysis.

Although we obtained excellent peak shapes and constant retention times for most solutes, the column is definitely not completely inert. Adsorption, producing tailing peaks and sample size dependent retention, was observed for dimethylformamide, dimethylacetamide, dimethyl sulfoxide and all aliphatic amines. Aniline, pyridine and tertiary amines gave relatively better peaks, but these species were not free from adsorption contributions to retention. This is evident in the poor peak shapes and the increase in retention upon decreasing the amount injected. These observations show that the column still has some activity toward very basic solutes. We expect that the problem with amines can be significantly reduced if special attention is paid to deactivating the fused silica surface before coat-

TABLE I

*n*-HEXADECANE GAS–LIQUID PARTITION COEFFICIENTS

| Solute | Log $L^{16\ a}_{Cap}$ | Log $L^{16\ b}_{Abr}$ | Solute | Log $L^{16\ a}_{Cap}$ | Log $L^{16\ b}_{Abr}$ |
|---|---|---|---|---|---|
| *n*-Pentane | 2.163 | 2.162 | Acetophenone | 4.458 | 4.483 |
| *n*-Hexane | 2.668 (2.670)[d] | 2.668 | Acetonitrile | 1.537 | 1.560 |
| *n*-Heptane | 3.173 | 3.173 | Propionitrile | 1.978 | 1.940 |
| *n*-Octane | 3.677 | 3.677 | Benzonitrile | 3.913 | –[c] |
| *n*-Nonane | 4.176 | 4.182 | Benzyl cyanide | 4.570 | –[c] |
| *n*-Decane | 4.685 | 4.686 | Acetaldehyde | 1.240 | 1.230 |
| Cyclopentane | 2.426 | 2.447 | Propionaldehyde | 1.770 | 1.815 |
| Cyclohexane | 2.906 | 2.913 | Benzylaldehyde | 3.935 | –[c] |
| 2,4-Dimethylpentane | 2.812 | 2.841 | Tetrahydrofuran | 2.521 | 2.534 |
| 2,5-Dimethylhexane | 3.309 | –[c] | *p*-Dioxane | 2.788 | 2.797 |
| Cycloheptane | 3.543 | 3.526 | Diisopropyl ether | 2.561 | 2.559 |
| 2-Methylpentane | 2.507 | 2.549 | Diethyl ether | 2.066 | 2.061 |
| Ethylcyclohexane | 3.767 | –[c] | Dipropyl ether | 2.971 | 2.989 |
| 2,3,4-Trimethylpentane | 3.401 | –[c] | Dibutyl ether | 3.954 | 4.001 |
| Hexene | 2.571 | 2.547 | Anisole | 3.916 | 3.926 |
| Benzene | 2.792 | 2.803 | Methylene chloride | 1.997 | 2.019 |
| Toluene | 3.343 | 3.344 | Chloroform | 2.478 | 2.480 |
| Ethylbenzene | 3.785 | 3.765 | Carbon tetrachloride | 2.822 | 2.823 |
| Propylbenzene | 4.239 | 4.221 | 1,2-Dichloroethane | 2.572 | 2.573 |
| Butylbenzene | 4.714 | 4.686 | Chlorobutane | 2.716 | 2.722 |
| *p*-Xylene | 3.867 | 3.858 | Chloropentane | 3.232 | 3.223 |
| *m*-Xylene | 3.868 | 3.864 | Fluorobenzene | 2.785 | –[c] |
| *o*-Xylene | 3.947 | 3.937 | Chlorobenzene | 3.630 | 3.640 |
| Methanol | (0.975)[d] | 0.922 | Bromobenzene | 4.022 | 4.035 |
| Ethanol | 1.556 (1.425)[d] | 1.485 | Iodobenzene | 4.505 | –[c] |
| *n*-Propanol | 1.975 | 2.097 | *o*-Dichlorobenzene | 4.453 | 4.405 |
| *n*-Butanol | 2.539 | 2.601 | *p*-Dichlorobenzene | 4.405 | –[c] |
| *n*-Pentanol | 3.057 | 3.106 | Dimethylformamide | 2.922 | 3.173 |
| *n*-Hexanol | 3.550 | 3.610 | Dimethylacetamide | 3.357 | 3.717 |
| *n*-Heptanol | 4.067 | 4.115 | Dimethylsulfoxide | 3.110 | 3.437 |
| *n*-Octanol | 4.569 | 4.619 | Ethylamine | 1.646 | 1.677 |
| 2-Propanol | 1.750 | 1.821 | Propylamine | 2.083 | 2.141 |
| Benzyl alcohol | 4.162 | 4.443 | Butylamine | 2.575 | 2.618 |
| 2,2,2-Trifluoroethanol | 1.315 (1.116)[d] | 1.224 | Hexylamine | 3.612 | 3.557 |
| *tert.*-Butanol | 1.994 | 2.018 | Triethylamine | 3.008 | 3.077 |
| 2-Methyl-1-propanol | 2.381 | 2.399 | Diethylamine | 2.386 | 2.395 |
| *sec.*-Butanol | 2.322 | 2.338 | Pyridine | 2.969 | 3.003 |
| Isopentanol | 2.885 | –[c] | Aniline | 3.934 | 3.993 |
| Cyclopentanol | 3.107 | –[c] | N-Methylaniline | 4.492 | –[c] |
| Cyclohexanol | 3.594 | 3.671 | N,N-Dimethylaniline | 4.753 | 4.754 |
| 1,1,1,3,3,3-Hexafluoro-isopropanol | 1.370 | 1.392 | Methyl formate | 1.454 | 1.459 |
| 2-Phenylethanol | 4.552 | –[c] | Methyl acetate | 1.946 | 1.960 |
| 3-Phenylpropanol | 4.663 | –[c] | Ethyl acetate | 2.359 | 2.376 |
| 4-Phenylbutanol | 5.049 | –[c] | Propyl acetate | 2.861 | 2.878 |
| Phenol | 3.641 | 3.865 | Acetic acid | 2.331 | 3.290 |
| *m*-Cresol | 4.187 | 4.329 | Propionic acid | 2.978 | –[c] |
| *p*-Cresol | 4.254 | 4.307 | Butyric acid | 3.427 | –[c] |
| *o*-Cresol | 4.183 | 4.242 | Ethyl propionate | 2.860 | 2.881 |
| Acetone | 1.766 | 1.760 | Nitromethane | 1.839 | 1.892 |
| 2-Butanone | 2.269 | 2.287 | Nitroethane | 2.313 | 2.367 |
| 2-Pentanone | 2.726 | 2.755 | Nitropropane | 2.773 | 2.710 |
| Cyclopentanone | 3.093 | 3.120 | Nitrobenzene | 4.433 | 4.460 |
| Cyclohexanone | 3.580 | 3.616 | | | |

[a] Measured by capillary gas chromatography in this work.
[b] Reported in ref. 28.
[c] Not reported.
[d] Measured by headspace gas chromatography (see ref. 53).

ing. Methods similar to that reported by Biernacki [62] for treating the column support with sodium metanilate which is insoluble in the stationary phase, might be necessary to obtain good peak shapes with very basic compounds. However, such treatment may not produce a support which is inert to the acidic (hydrogen bond donor) solutes and was therefore not used here.

*The partition coefficients for different solutes.* All partition coefficients measured in this work are given in Table I along with the values reported by Abraham *et al.* [28]. Regression of these data against one another gave the following correlation:

$$\log L^{16}_{Cap} = 0.060(\pm 0.046) + 0.967(\pm 0.015) \log L^{16}_{Abr} \quad (5)$$

$n = 85$ S.E. $= 0.129$ $r = 0.9903$

Log $L^{16}_{Cap}$ refers to the data measured in this work and log $L^{16}_{Abr}$ refers to the values reported by Abraham *et al.* The quality of this regressions suggests that there is generally excellent agreement between the two data sets. However, there are a number of very significant outliers, all of which are either good hydrogen bond acceptors or donors. Removal of acetic acid, the single most deviant point, from the regression improves the goodness of fit:

$$\log L^{16}_{Cap} = 0.060(\pm 0.029) + 0.971(\pm 0.009) \log L^{16}_{Abr} \quad (6)$$

$n = 84$ S.E. $= 0.082$ $r = 0.9961$

We believe this excellent correlation confirms the soundness of our measurement conditions. In addition, the points that do not agree are those that are known to be problematic solutes on packed columns. A series of classwise regressions of the two data sets are presented in Table II. It is evident that within the statistics of the fit the data for the alkanes, the "select" solutes (excluding dimethylacetamide, dimethylformamide and dimethylsulfoxide), the non-hydrogen bond donor solutes, the solutes with low hydrogen bond acceptor strength, and the halogenated solutes are in essentially perfect agreement. The

TABLE II

REGRESSION ANALYSIS OF *n*-HEXADECANE GAS–LIQUID *K* VALUES

Regression of log $L^{16}_{Cap}$ *vs.* log $L^{16}_{Abr}$. $r$ = Correlation coefficient; S.E. = standard error of the fit; $n$ = number of data points included in the regression.

| Solute class | Intercept[a] | Slope[b] | | S.E. | $n$ |
|---|---|---|---|---|---|
| Alkanes | −0.020 (0.023) | 1.005 (0.007) | 0.9997 | 0.019 | 12 |
| Aromatic[c] | −0.070 (0.008) | 1.020 (0.002) | 0.99999 | 0.003 | 8 |
| Halogenated[d] | −0.014 (0.020) | 1.003 (0.007) | 0.9999 | 0.011 | 7 |
| Low $\beta$[e] | −0.012 (0.018) | 1.004 (0.006) | 0.9995 | 0.062 | 32 |
| Select[f] | −0.019 (0.016) | 1.002 (0.006) | 0.9993 | 0.028 | 42 |
| N-HBD[g] | −0.023 (0.013) | 1.004 (0.004) | 0.9995 | 0.027 | 55 |
| HBD[h] | 0.070 (0.033) | 0.957 (0.011) | 0.9984 | 0.062 | 26 |
| Oxygenated[i] | 0.054 (0.055) | 0.967 (0.020) | 0.9961 | 0.068 | 20 |
| Amines | −0.024 (0.144) | 0.982 (0.045) | 0.9907 | 0.125 | 11 |

[a] Intercept and in parentheses the standard error of the intercept.
[b] Slope and in parentheses the standard error of the slope.
[c] Non-polar aromatic solutes only.
[d] Halogenated solutes only.
[e] Compounds having $\beta^c_2$ (solute hydrogen bond acceptor basicity) values less than 0.30.
[f] Monopolar aliphatic (non-polyhalogenated) non-hydrogen bond donor solutes, excluding dimethylacetamide, dimethylformamide and dimethyl sulfoxide.
[g] All non-hydrogen bond donor solutes.
[h] Hydrogen bond donor solutes, excluding methanol.
[i] Oxygen containing solutes (carbonyl and ether functionalities), excluding alcohols.

results with the alkanes agree best, but this is hardly surprising since the column was essentially "calibrated" so as to give perfect agreement with Abraham *et al.*'s values for *n*-pentane, *n*-hexane and *n*-heptane. In contrast, there is a very slight systematic deviation observed for the aromatic solutes whereas the hydrogen bond donor, oxygenated, and amine solutes are all less retained on the capillary column relative to Abraham *et al.*'s estimates which come predominantly from measurements made with packed beds of porous particles. Interestingly, the intercept in all cases is essentially zero within the statistics of the fit.

It should be noted that the systematic differences between the gas–liquid $L^{16}$ values reported here and those reported by Abraham *et al.* are not due to errors in estimates of the dead volume. For example, significant deviations with respect to Abraham *et al.*'s reported values are found for dimethylformamide, dimethylacetamide and dimethyl sulfoxide even though all three solutes are well within the range of retentions observed for *n*-pentane to *n*-decane, all of which agree very well with Abraham *et al.*'s values.

Agreement between the alkane and aromatic hydrocarbon series measured in this work and that of Abraham *et al.* [28] is excellent. This is expected since these solutes should not adsorb on packed beds or capillary surfaces. The differences are generally smaller than 0.02 log units, which is within the standard error reported by Abraham *et al.* [28] for a comparison of his data to headspace measurements (which are free from adsorption contributions). However, there are significant deviations for 2-methylpentane and cyclopentane. These solutes, in Abraham *et al.*'s data set, were measured by Kwantes and Rijnders [63] using copper helices as the support. Interpolation of the data for 2-methylpropane, 2-methylbutane and 2-methylhexane, reported by Abraham *et al.*, predicts a value of 2.491, which is in much better agreement with the value of 2.507 in this work than with the value of 2.549 reported by Abraham *et al.* The value reported in this work agrees very well with a recently reported value of 2.516 measured by headspace GC [54]. Additionally, the value reported for 2,4-dimethylpentane by Abraham *et al.*, 2.841, is significantly high relative to the value measured in this work, 2.812. Abraham *et al.*'s value was obtained from ref. 21 by correlation of the data obtained from experiments on *n*-heptadecane at a temperature other than 25°C. Our value agrees well with headspace measurements, 2.816 [54].

The most deviant aromatic hydrocarbon is butylbenzene. Its value is nearly 0.03 log units lower than that measured here. The value quoted by Abraham *et al.* is based on an estimate obtained by extrapolating results from lower homologues. We repeated the correlation and extrapolation and obtained a value of 4.702, which is in very good agreement with our experimental value of 4.714. Also, this data point was reported by Schantz and Martire [64] to be 4.704.

Excellent agreement was also found for halogenated alkanes. No significant deviation between the two data sets was detected.

In contrast to the behavior of the non-polar solutes, considerable systematic differences were observed for many polar solutes. In almost all instances (see below for several exceptions) the partition coefficients of polar species reported by Abraham *et al.* are larger than those observed here. This is the expected direction assuming that the data obtained with the capillary columns are not as strongly influenced by adsorption at the solid surface as are data obtained on packed columns. The gas–liquid $L^{16}$ value for all alcohols (except methanol, ethanol and 2,2,2-trifluoroethanol) were smaller than those given by Abraham *et al.* We do not believe this is a result of interfacial adsorption in our system, but is a result of the exceedingly low retention of these solutes on the capillary column due to the lower surface area to volume ratio. Retention of these species is not significantly different than the dead volume of the column. Therefore, we believe the values listed in Table I for those solutes are in error. Alongside these values we have reported some recently measured headspace GC values for these solutes [see ref. 53] which we prefer to the capillary column measurements.

The largest differences for polar solutes were observed for benzyl alcohol, phenol and an extraordinarily large difference was observed for

acetic acid. All of these solutes are strong hydrogen bond donors. Our measurement of the partition coefficient for benzyl alcohol differs from that of Abraham *et al.* by 48%. To check, we injected a mixture of benzyl alcohol and *p*-xylene, which is known to agree well with Abraham *et al.*'s data. The partition coefficient for *p*-xylene in this particular run differed from our previously measured value and that of Abraham by less than 0.01 log units. This leads us to believe the value measured here is a better estimate of benzyl alcohol's partition coefficient than that reported by Abraham *et al.* The presence of interfacial adsorption in Abraham *et al.*'s value is probably the cause of this difference.

Phenol gave a symmetric peak and a much lower partition coefficient than that reported by Abraham *et al.* We believe this difference is due to the presence of significant interfacial adsorption in Abraham *et al.*'s value. Based on the solute's dipolarity ($\pi_2^{*,c} = 0.77$) and strong hydrogen bond donating ability ($\alpha_2^c = 0.69$) this deviation is expected. Similar solutes such as the cresols, also gave significantly lower partition coefficients than reported by Abraham *et al.* Moreover, the order of increasing partition coefficients for *m*- and *p*-cresol is reversed in our measurements relative to those of Abraham *et al.* Although the boiling point for *m*-cresol is slightly higher than that of *p*-cresol (202.2°C *vs.* 201.9°C) [65], *p*-cresol's vapor pressure at 25°C is higher than that of *m*-cresol (0.143 mmHg and 0.130 mmHg, respectively; 1 mmHg = 133.322 Pa). These observations lead us to believe the higher values in Abraham *et al.*'s compilation for these types of solutes are due to adsorption at the solid and liquid interfaces.

All three aliphatic nitro compounds studied gave very symmetric peaks. The values for nitromethane and nitroethane are lower than Abraham *et al.*'s by 0.05 log units; however, our value for nitropropane is 0.06 log units higher than Abraham *et al.*'s. Based on linearity of the partition coefficients within this homologous series we predict, from the first two members of the series, a value of 2.787 for nitropropane, which is in good agreement with the measured value of 2.773 reported here. The same estimation process was applied to Abraham *et al.*'s data from which a value of 2.842 was calculated for nitropropane, which is much larger than the experimental value of 2.710 reported by Abraham *et al.* Although we do not expect a perfect linear relationship within the series, this approach should at least give a reasonable estimate of the true value. A weak dependence of retention time on sample size was observed with nitrobenzene indicating relatively little interfacial effect. Although peak shapes were good with smaller samples, significant fronting was observed with larger sample sizes.

As mentioned above, the fused-silica surface has an affinity for basic solutes due to the presence of residual silanol groups [24]. Of the amines examined in this study, symmetric peaks were observed only for pyridine, aniline and trimethylamine. $L^{16}$ values for all strong hydrogen bond acceptors reported here, except that of *n*-hexylamine, are smaller than those of Abraham *et al.* The sole exception, *n*-hexylamine, reported by Abraham *et al.* was estimated from the linear relationship between log $L^{16}$ and carbon number for ethyl, propyl and butylamine. We must emphasize that, because of the strong interaction of amines with silanols on the fused-silica surface, the partition coefficients reported here for amines probably contain contributions from interfacial adsorption. These data are given because they are generally lower than the values reported by Abraham *et al.* and are therefore probably closer to the true value.

Some of the other solutes show deviations even greater than those shown by amines. The partition coefficients for dimethylformamide, dimethylacetamide and dimethyl sulfoxide are about 0.3 log units lower than those of Abraham *et al.* Even though we believe these data were obtained under conditions that are not completely partition dominated we still feel they are superior to those obtained using packed columns.

Recently, Abraham *et al.* [66] have reported a new set of log $L^{16}$ values which were obtained by back-calculation from the GC data of McReynolds [67] and Patte *et al.* [68] using an "inverse" multiple linear regression analysis. These calculated data are used by Abraham *et al.* in an attempt to rationalize fundamental issues

regarding solute-solvent interactions as they relate to the solute parameters $\pi_2^*$ (solute dipolarity/polarizability) and $\alpha_2$ (solute hydrogen bond donating acidity). Their calculated log $L^{16}$ are purported to be superior to those used by Li *et al.* [29]. Their use of the cycloalkanones as an example to support this is confusing since Li *et al.* used Abraham *et al.*'s data originally reported in refs. 28 and 69. The data for the two cycloalkanones, cyclopentanone and cyclohexanone, obtained in this work are in reasonably good agreement with Abraham *et al.*'s original data in ref. 28, as well as for cyclopentanone measured by headspace GC [53]. The log $L^{16}_{Cap}$ values for cyclopentanone and cyclohexanone are 3.093 and 3.580, respectively, and those reported in ref. 28 are 3.120 and 3.616, respectively. In contrast, the calculated values are 3.221 and 3.792, respectively; resulting in a difference in the gas–liquid partition coefficient in excess of 25% for cyclopentanone and 50% for cyclohexanone between the three sets of data. These differences are by no means minor or systematic as claimed by Abraham *et al.* [66]. Since the experimentally measured data are in good agreement, we believe that the back-calculated estimates are in error. In support of this we choose to look at *n*-hexane for which the value of log $L^{16}$ is well established, as discussed above. Abraham *et al.*'s back-calculated value is 2.688 ($L^{16} = 487.5$) and the average of six accurate measurements is 2.661 ($L^{16} = 466.1$); this is a 5% difference in $L^{16}$ which is large considering the percent relative standard deviation of the six measurements is 0.42%. Therefore, we suggest that use of back-calculated log $L^{16}$ values should be used with some caution.

## CONCLUSIONS

Gas–liquid partition coefficients on a relatively volatile liquid, *n*-hexadecane, have been measured using capillary gas chromatography. Columns with a film thickness in excess of 0.2 $\mu$m were prepared so as to maximize the ratio of liquid volume to interfacial area and thereby reduce the relative contribution of interfacial adsorption to retention. The problem of measuring the amount of stationary phase was circumvented by making all measurements relative to the partition coefficient of a species (*n*-hexane) whose partition coefficient had been previously established using packed bed chromatography. The data were compared with literature values and deviations are interpreted based on the effect of interfacial adsorption. It is shown that in most instances the literature data for strong hydrogen bond donor and acceptor solutes, especially amines, are significantly influenced by interfacial adsorption effects. The data reported here are shown to be more accurate than the previously reported results.

## ACKNOWLEDGEMENTS

This work was supported by a grant from the National Science Foundation and the Petroleum Research Foundation of the American Chemical Society. The authors would like to thank Richard J. Laub for his helpful discussions regarding the capillary column coating procedures.

## REFERENCES

1 R.J. Laub and R.L. Pecsok, *Physicochemical Applications of Gas Chromatography*, Wiley, New York, 1978.
2 J.R. Conder and C.L. Young, *Physicochemical Measurements by Gas Chromatography*, Wiley, New York, 1979.
3 R.L. Pecsok, A. de Yllana and A. Abdul-Karim, *Anal. Chem.*, 36 (1964) 452.
4 D.E. Martire, in J.H. Purnell (Editor), *Progress in Gas Chromatography*, Plenum Press, New York, 1968, p. 93.
5 V.G. Berezkin and V.N. Returnsky, *J. Chromatogr.*, 292 (1984) 9.
6 J.F. Parcher and L.B. Hung, *J. Chromaotgr.*, 399 (1987) 75.
7 D.E. Martire, *Anal. Chem.*, 38 (1966) 244.
8 R.L. Pecsok and B.H. Gump, *J. Phys. Chem.*, 71 (1967) 2202.
9 P. Urone and J.F. Parcher, *Anal. Chem.*, 38 (1966) 270.
10 J. Serpinet, *Anal. Chem.*, 48 (1976) 2264.
11 J.R. Conder, *Anal. Chem.*, 48 (1976) 917.
12 R.N. Nicolov, *J. Chromatogr.*, 241 (1982) 237.
13 J.R. Conder, *J. High Resolut. Chromatogr. Chromatogr. Commun.*, 3 (1982) 601.
14 A.N. Korol, *J. Chromatogr.*, 67 (1972) 213.
15 V.G. Berezkin, *J. Chromatogr.*, 159 (1978) 359.
16 J.A. Jonsson and L. Mathiasson, in J.A. Jonsson (Editor), *Chromatographic Theory and Basic Principles*, Marcel Dekker, New York, 1987, p. 189.
17 J.R. Conder, *J. Chromatogr.*, 39 (1969) 273.

18 J.R. Conder, N.K. Ibrahim, G.J. Rees and G.A. Oweimreen, *J. Phys. Chem.*, 89 (1985) 2571.
19 H. Liao and D.E. Martire, *Anal. Chem.*, 44 (1972) 498.
20 L. Mathiasson and J.A. Jonsson, *J. Chromatogr.*, 179 (1979) 7.
21 D.E. Martire and P. Riedl, *J. Phys. Chem.*, 72 (1968) 3478.
22 J.A. Jonsson and L. Mathiasson, *J. Phys. Chem.*, 72 (1968) 3478.
23 A.N. Korol, G.M. Belokleytseva and G.V. Flonenko, *Chromatographia*, 12 (1979) 95.
24 A.J. Dallas and P.W. Carr, *Anal. Chim. Acta*, 251 (1991) 83.
25 J.E. Dinunzio, D.D. Bombick and G. Doebler, *Chromatographia*, 15 (1982) 641.
26 J.R. Conder, *Anal. Chem.*, 43 (1971) 367.
27 J.J. Kirkland, *Anal. Chem.*, 35 (1963) 2003.
28 M.H. Abraham, P.L. Grellier and R.A. McGill, *J. Chem. Soc., Perkin Trans. 2*, (1987) 797.
29 J. Li, Y. Zhang, A.J. Dallas and P.W. Carr, *J. Chromatogr.*, 550 (1991) 101.
30 R.D. Dandeneau and E.H. Zerenner, *J. High Resolut. Chromatogr. Chromatogr. Commun.*, 2 (1979) 351.
31 L.G. Blomberg, *J. High Resolut. Chromatogr. Chromatogr. Commun.*, 7 (1984) 232.
32 M.L. Lee and B.W. Wright, *J. Chromatogr.*, 184 (1980) 235.
33 W. Jennings, *J. High Resolut. Chromatogr. Chromatogr. Commun.*, 3 (1980) 601.
34 L. Blomberg, J. Buijten, K. Markides and T. Wannman, *J. Chromatogr.*, 279 (1983) 9.
35 R.N. Lichtenthaler, D.D. Liu and J.M. Prausnitz, *Macromolecules*, 7 (1974) 565.
36 T.J. Bruno, *Anal. Chem.*, 58 (1986) 1595.
37 M. Goedert and G. Guichon, *Anal. Chem.*, 45 (1973) 1180.
38 W. Jennings, *Gas Chromatography with Glass Capillary Columns*, Academic Press, New York, 2nd ed., 1980.
39 T. Czajkowska, *Chromatographia*, 15 (1982) 305.
40 G. Redant, P. Sandra and M. Verzele, *Chromatographia*, 15 (1982) 13.
41 R.J. Laub, personal communication.
42 *Capillary Column Instruction Sheet*, Restek, 1988.
43 G. Alexander and S.R. Lipsky, *Chromatographia*, 10 (1977) 487.
44 C.A. Eckert, B.A. Newman, G.L. Nicolaides and T.C. Long, *AIChE J.*, 27 (1981) 33.
45 E.R. Thomas, B.A. Newman, T.C. Long, D.A. Wood and C.A. Eckert, *J. Chem. Eng. Data*, 27 (1982) 399.
46 B.R. Kersten and C.F. Poole, *J. Chromatogr.*, 399 (1987) 1.
47 J.J. Pesek and J.A. Graham, *Anal. Chem.*, 49 (1977) 133.
48 M.L. Peterson and J. Hirsch, *J. Lipid Res.*, 1 (1959) 132.
49 H.C. Furr, *J. Chromatogr. Sci.*, 27 (1989) 216.
50 M.L. McGlashan and A.G. Williamson, *Trans. Faraday Soc.*, 57 (1961) 588.
51 A.J.B. Cruickshank, B.W. Gainey and C.L. Young, in L.A. Harbourn (Editor), *Gas Chromatography*, Institute of Petroleum, London, 1969, p. 76.
52 C.-F. Chien, M.M. Kopecni, R.J. Laub and C.A. Smith, *J. Phys. Chem.*, 85 (1981) 1864.
53 A.J. Dallas, *Ph.D. Thesis*, University of Minnesota, Minneapolis, MN, 1993.
54 D.I. Eikens, *Ph.D. Thesis*, University of Minnesota, Minneapolis, MN, 1993.
55 K.D. Bartle, *Anal. Chem.*, 45 (1973) 1831.
56 B.W. Wright, P.A. Peaden and M.L. Lee, *J. High Resolut. Chromatogr. Chromatogr. Commun.*, 5 (1982) 413.
57 D.B. Anderson, J.H. Rytting and T. Higuchi, *Int. J. Pharm.*, 1 (1978) 15.
58 J.H. Rytting, B.D. Anderson and T. Higuchi, *J. Phys. Chem.*, 82 (1978) 2240.
59 B.D. Anderson, J.H. Rytting, S. Lindenbaum and T. Higuchi, *J. Phys. Chem.*, 79 (1975) 2340.
60 E.E. Tucker, S.B. Farnham and S.D. Christian, *J. Phys. Chem.*, 73 (1969) 3820.
61 E.E. Tucker and E.D. Becker, *J. Phys. Chem.*, 77 (1973) 1783.
62 W. Biernacki, *J. Chromatogr.*, 50 (1970) 135.
63 A. Kwantes and G.W.A. Rijnders, in D. Desty (Editor), *Gas Chromatography*, 1958, p. 125.
64 M.M. Schantz and D.E. Martire, *J. Chromatogr.*, 391 (1987) 35.
65 J.A. Riddick, W.B. Bunder and T.K. Sakano, *Organic Solvents —Physical Properties and Methods of Purification*, Wiley, New York, 4th ed., 1986.
66 M.H. Abraham, G.S. Whiting, R.M. Doherty and W.J. Shuely, *J. Chromatogr.*, 587 (1991) 213.
67 W.O. McReynolds, *Gas Chromatographic Retention Data*, Preston Technical Abstracts, Evanston, IL, 1966.
68 F. Patte, M. Etcheto and P. Laffort, *Anal. Chem.*, 54 (1982) 2239.
69 M.H. Abraham, P.L. Grellier, D.V. Prior, J.J. Morris and P.J. Taylor, *J. Chem. Soc., Perkin Trans. 2*, (1989) 699.

*Journal of Chromatography*, 638 (1993) 57–63
Elsevier Science Publishers B.V., Amsterdam

CHROM. 24 962

# Explanation of the matrix-induced chromatographic response enhancement of organophosphorus pesticides during open tubular column gas chromatography with splitless or hot on-column injection and flame photometric detection

D.R. Erney, A.M. Gillespie and D.M. Gilvydis*

*Pesticides and Industrial Chemicals Research Center, US Food and Drug Administration, 1560 E. Jefferson Avenue, Detroit, MI 48207 (USA)*

C.F. Poole

*Department of Chemistry, Wayne State University, Detroit, MI 48202 (USA)*

(First received September 11th, 1992; revised manuscript received February 8th, 1993)

ABSTRACT

The observed chromatographic response for organophosphorus pesticides in extracts from milk and butterfat is shown to be matrix dependent. The matrix protects the organophosphorus compounds from adsorption and/or decomposition in hot vaporizing injectors ensuring a more complete transfer from injector to column compared to the results observed when standards dissolved in matrix-free solvent are used. This results in recoveries in excess of 100% for residue-free extracts spiked with organophosphorus pesticides when standards prepared in residue-free solvents are used for calibration. The chromatographic response enhancement is minimized by using hot on-column injection at an optimized injection temperature, but not completely eliminated. The preferred method of calibration is to use matrix standard solutions prepared by adding known amounts of organophosphorus pesticides to residue-free sample matrix of the same character and in similar concentration to the samples to be analyzed.

## INTRODUCTION

Organophosphorus pesticides are widely used in agriculture and are known to accumulate in the fatty receptacles of plant and animal tissues that form a substantial portion of the dietary intake of the world's human population [1]. Organophosphorus pesticides encompass a vast number of chemical species dictating the use of multiresidue methods for the economical screening of foods for contamination. Current methods employ a wide range of sample isolation procedures, reviewed in refs. 2 and 3, followed by gas chromatography and phosphorus element-selective detection, in general, for the separation and detection of the pesticides of typical trace residue levels.

In spite of wide application only a few reports have appeared concerning the influence of the sample matrix on the gas chromatographic properties of the organophosphorus pesticide residues. Using packed columns Carson [4] reported recovery data from 70 to 180% for

* Corresponding author.

0021-9673/93/$06.00 

organophosphorus pesticides in seven non-fatty foods fortified at the 2–10-ppb (w/w) level. Gillespie and Walters [5] noted recoveries in the range of 110–130% for organophosphorus pesticides in fortified samples of vegetable oils and butterfat after cleanup by solid-phase extraction and chromatography on a packed column with flame photometric detection. It was noted that compounds with P=O bonds, such as acephate, methamidophos, azodrin, etc., gave particularly high recoveries. Since degradation of these compounds by gas chromatography has been reported [6], it was speculated that co-injection of residual sample matrix presumably protects the analytes from thermal degradation and/or prevents analyte adsorption by covering active sites in the gas chromatographic system, hence giving a higher response when compared with standards prepared in a matrix-free solvent. Preparing standards in a solution of a residue-free, processed sample, to create a "matrix standard solution" provided a practical means of correcting recovery values to the normal range (80–103%) as reported [5].

The use of modern open tubular columns and injection techniques has not fully resolved the question concerning the matrix-enhanced chromatographic response of the organophosphorus pesticides. Mallet and Mallet [7] obtained response enhancement ratios from 1.09–3.00 relative to standards prepared in a matrix-free solvent for organophosphorus pesticides isolated by solid-phase extraction. Stan and Goebel [8,9] and Stan and Muller [10] have investigated the influence of different sample introduction techniques on the recovery of organophosphorus pesticides by open tubular column gas chromatography. Losses of organophosphorus pesticides in vaporizing injectors was attributed to the thermal stress imposed on the sample and the possibility of adsorption by the liner. These factors vary with the chemical structure of the pesticide and affect individual pesticides differently. They also concluded that substance losses were less using cold on-column injection compared to temperature programmed vaporization, which in turn were less than when hot-splitless injection was used. Hernandez *et al.* [3] studied a number of sample cleanup procedures for fortified peach extracts and obtained recoveries of 72–140% for organophosphorus pesticides using split injection and open tubular column gas chromatography.

The purpose of the present study was to determine the influence of matrix-induced changes in the chromatographic response of organophosphorus pesticides using open tubular column gas chromatography and to explore possible solutions for its irradication or control under conditions suitable for the determination of pesticide residues in fatty foods.

## EXPERIMENTAL

All solvents were Omnisolv grade from EM Science (Gibbstown, NJ, USA). The organophosphorus pesticides methamidophos, acephate, omethoate, diazinon, dimethoate and chlorpyrifos were obtained from the US Environmental Protection Agency Repository (Research Triangle Park, NC, USA). Adsorbex RP-18, 400 mg, solid-phase extraction cartridges were obtained from Bodman (Aston, PA, USA) and used for the milk analysis. Extrelut QE disposable columns, 3 ml capacity, from EM Science and Sep-Pak $C_{18}$, 5 g, cartridges from Millipore (Marlborough, MA, USA) were used for the butterfat analysis. A Visiprep SPE vacuum manifold (Supelco, Bellefonte, PA, USA) was used for sample processing.

A Hewlett-Packard 5880A gas chromatograph with flame photometric detector and Hewlett-Packard 5880A Level Four data station was used for gas chromatography. The standard split/splitless injector was used for splitless injection and hot on-column injection by changing injection liners (J & W Scientific, Folsom, CA, USA). For separations a 2–3 m × 0.53 mm I.D., deactivated retention gap and a 15 m × 0.53 mm I.D., 1.0 $\mu$m film thickness, DB-17 fused-silica open tubular column (J & W Scientific) were used. Operating conditions were varied widely in different studies and the relevant details are given below in the text.

The method used to process the milk extracts [11] and butterfat extracts [5,12,13] are described in detail elsewhere. Briefly, milk solids were precipitated with acetone–acetonitrile, the or-

ganophosphorus pesticides extracted from the supernatant with dichloromethane, and the residue after removal of the solvent taken up in acetonitrile and passed through a $C_{18}$ solid-phase extraction cartridge. After solvent removal final residue containing pesticides was taken up in acetone (1 ml for an original sample size of 10 g of milk).

The butterfat dissolved in hexane was passed through Extrelut QE column which was mounted in series with a $C_{18}$ cartridge. Both columns were eluted with a mixture of methanol–acetonitrile (1:1) saturated with hexane. The $C_{18}$ column was eluted with additional methanol, the eluent evaporated to dryness and reconstituted in acetone to give a final concentration of about 180 mg/ml based on the original mass of butterfat.

## RESULTS AND DISCUSSION

The analysis of fats and oils for residues of pesticides by gas chromatography requires that the contaminants are effectively isolated from the bulk of the fats to prevent contamination of the injector and columns with non-volatile and late eluting material. Solid-phase extraction using short columns (cartridges) packed with octadecylsilanized silica packings have proven particularly useful for isolating organophosphorus pesticides from fats [5,11–15]. The reduced solvent consumption, high sample throughput, low equipment costs, and suitability for multiresidue determinations have quickly promoted this approach to the forefront of pesticide analysis in foods. The milk extracts and butterfat extracts used in this report typically contain less than 2 mg/ml and 4 mg/ml, respectively, of matrix residues, and are suitable for routine analysis, producing little observable contamination of the chromatographic system.

There are features of the general gas chromatographic properties of organophosphorus pesticides which are not well documented in the literature. It has been our experience that several injections of matrix standard solution, are required at the beginning of the day to obtain reproducible peak area responses for the organophosphorus pesticides. During the course of a series of analyses in which standard solutions prepared in an organic solvent are injected interspersed between sample extracts there is generally a gradual but significant increase in the area response for the standards over time. For residue-free extracts spiked with organophosphorus pesticides recoveries between 100–300% have been observed when standards prepared in an organic solvent were used as the basis for the recovery calculation. Both the amount and the type of the matrix can effect the perceived observed recovery, and although the general trends remain true, individual compounds may show different increases in recovery with the same experimental conditions.

Fig. 1 shows comparative chromatograms obtained with the same chromatographic system with the splitless and on-column injection liners installed for the separation of a mixture of organophosphorus pesticides spiked into a residue free milk matrix extract. The peak shapes for on-column injection and the observed detec-

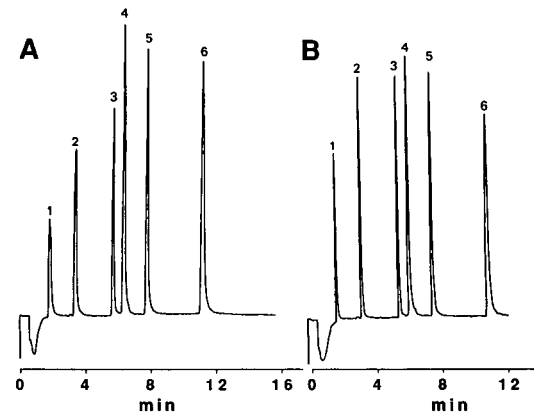


Fig. 1. Comparison of splitless injection (A) and hot on-column injection (B) for the separation and recovery of organophosphorus pesticides spiked into a response free milk extract. A 3 m × 0.53 mm I.D. deactivated retention gap coupled to a 15 m × 0.53 mm I.D. DB-17, 1 $\mu$m film thickness, open tubular column (connected to the detector by a 20 cm × 0.32 mm I.D. deactivated fused-silica capillary column threaded through the detector tube and terminated just below the flame) was used for the separation. Hydrogen was used as the carrier gas at 4 ml/min and the column temperature programmed from 80°C (2 min) at 30°C/min to 200°C (10 min). Peaks: 1 = methamidophos (0.27 ng); 2 = acephate (0.69 ng); 3 = omethoate (1.09 ng); 4 = diazinon (1.16 ng); 5 = dimethoate (1.21 ng); 6 = chlorpyrifos (1.82 ng).

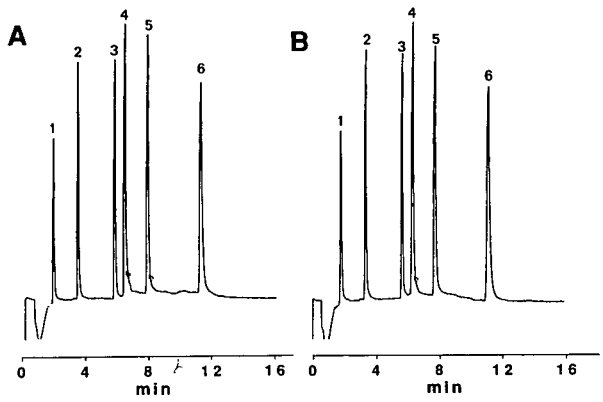


Fig. 2. Comparison of the separation and recovery of organophosphorus pesticides in acetone (A) and spiked into a residue-free butterfat extract (B). Both samples were introduced by hot on-column injection (230°C). Other conditions as for Fig. 1. The chromatographic response enhancement (peak area in chromatogram B/peak area in chromatogram A) is methamidophos (1.01), acephate (1.09), omethoate (1.10), diazinon (1.08), dimethoate (1.02) and chlorpyrifos (1.07). The matrix concentration in (B) was 1.7 mg/ml.

tor response are improved using the hot on-column injection technique. Fig. 2 illustrates the increase in detector response observed for the injection of the same amount of organophosphorus compounds dissolved in acetone and spiked into a residue-free milk matrix extract using hot on-column injection and the same chromatographic parameters. The increase in response observed for the matrix standard solution is discernable. Table I illustrates the observed recoveries determined with reference to a matrix-free standard solution for a mixture of organophosphorus pesticides spiked into milk and butterfat extracts using splitless and hot on-column injection techniques. Comparing the two injection techniques, the level of response enhancement (observed recovery) in excess of 100% is smaller in the case of hot on-column injection. Comparing the two extracts, recoveries for the butterfat are relatively high compared to the milk extract for splitless injection but differences using hot on-column injection are not significant. The influence of peak area response for a standard mixture of organophosphorus pesticides as a function of the injection temperature using hot on-column injection is shown in Fig. 3. There is a gradual increase in the observed response for all compounds as the temperature is increased in the range of 150 to 230°C. Above 230°C a plateau region is reached (chlorpyrifos), a further shallow increase in response is observed (methamidophos, omethoate, dimethoate), or a decrease in response is observed (acephate, diazinon). A compromise temperature of 230°C and hot on-column injection were selected as the most favorable conditions for further comparative experiments reported subsequently.

The above initial experiments provide an adequate framework for a qualitative discussion of the influence of the chromatographic conditions and sample matrix on the recovery of organophosphorus pesticides. The sample matrix has a protective influence on the sample components increasing their transfer to the column by either reducing the thermal stress imposed on the analytes or by blocking active sites within the

TABLE I

OBSERVED CHROMATOGRAPHIC RESPONSE ENHANCEMENT FOR MILK AND BUTTERFAT EXTRACTS WITH ORGANOPHOSPHORUS PESTICIDES USING SPLITLESS AND HOT ON-COLUMN INJECTION

Extraction fortifications were between 0.06 and 0.12 ppm.

| Compound | Milk extract | | Butterfat extract | |
|---|---|---|---|---|
| | Splitless | On-column | Splitless | On-column |
| Acephate | 1.14 ± 4.3% | 1.01 ± 4.7% | 1.36 ± 4.7% | 1.00 ± 1.1% |
| Omethoate | 1.07 ± 6.7% | 1.04 ± 5.3% | 1.33 ± 5.3% | 0.97 ± 4.2% |
| Diazinon | 1.00 ± 4.2% | 0.97 ± 5.1% | 1.25 ± 2.1% | 0.84 ± 5.8% |
| Dimethoate | 1.06 ± 4.2% | 1.03 ± 7.3% | 1.31 ± 4.0% | 0.92 ± 1.1% |
| Chlorpyrifos | 1.04 ± 2.7% | 0.95 ± 5.2% | 1.07 ± 5.3% | 1.04 ± 0.6% |

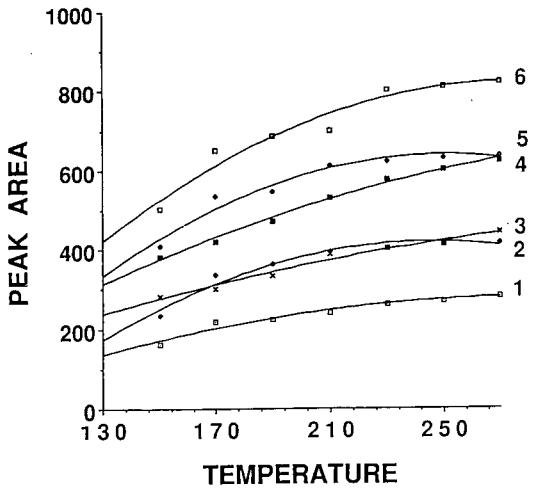


Fig. 3. Plot of peak area response (arbitrary units) as a function of injector temperature (°C) for hot on-column injection of organophosphorus pesticides. Identification: 1 = methamidophos; 2 = acephate; 3 = omethoate; 4 = dimethoate; 5 = diazinon; 6 = chlorpyrifos.

injector that would tend to delay transfer of the analytes to the column. Given that the organophosphorus compounds typically used as pesticide encompass a wide range of physical and chemical properties both factors are likely to be important. Increasing area response with increasing injector temperature, at least up to 230°C, would indicate that adsorption to active sites within the injector is important. Higher temperatures tend to diminish adsorptive forces. Above 230°C reduced area response was observed for some compounds indicating either thermal decomposition and/or enhanced catalytic decomposition on active sites has to be taken into consideration. The results for splitless injection compared to on-column injection show a higher relative observed chromatographic response enhancement since the relatively long residence time of the sample in the vaporization chamber and contact of the sample with a larger (and probably more active surface) result in those conditions most likely to reduce the transfer of the analytes to the column. Releasing the analytes on column results in their vaporization into the column or retention gap where surface activity is likely to be lower and the residence time in the vaporizing chamber much less.

Three potential solutions to the problem suggest themselves. In the absence of matrix the protection effect is not operative and it is true that if samples containing very little matrix are spiked with the organophosphorus compounds there is little if any increase in the detector response. This is perhaps an obvious statement, but is generally not a practical solution. In residue analysis, given the nature of the samples analyzed, matrix contamination cannot be avoided. The extracts obtained by solid-phase extraction are comparatively clean compared to those obtained by other procedures and therefore, increasing the number of steps to minimize the matrix burden is not desirable and would only become feasible if a highly chemically selective isolation procedure for the organophosphorus compounds could be devised. Such a procedure does not exist at present.

A second solution would be to deactivate the chromatographic system to such an extent that the adsorption of the organophosphorus compounds became negligible. Having failed to achieve this chemically by silanization the possibility of achieving permanent or temporary deactivation by the sample matrix itself was evaluated. Injecting milk extract without cleanup by solid-phase extraction and milk extract to which small quantities of corn oil and/or soybean oil had been deliberately added was used to contaminate the chromatographic system in the hope of saturating active sites responsible for sorption of the analytes. As seen from Table II, this was not successful, and the observed recovery increased, in general, with the increasing matrix burden. Also, the changes observed were temporary and required that each sample be contaminated with the crude matrix, which over time resulted in a build up of involatile material increasing the frequency with which retention gaps had to be changed.

The most practical solution is the use of a residue free matrix standard solution prepared to closely resemble the sample extracts in concentration and character. Data presented in Table III for the recovery of the organophosphorus pesticides in butterfat and milk extracts by on-column injection as a function of temperature indicate that if reproducible results are to be obtained both the matrix and injection tempera-

TABLE II

OBSERVED CHROMATOGRAPHIC RESPONSE ENHANCEMENT FOR ORGANOPHOSPHORUS PESTICIDES IN MILK EXTRACTS WITH AN IMPOSED MATRIX BURDEN

| Sample preparation[a] | Chromatographic response enhancement | | | | | |
|---|---|---|---|---|---|---|
| | Methamidophos | Acephate | Omethoate | Diazinon | Dimethoate | Chlorpyrifos |
| A | 1.24 | 1.29 | 1.46 | 1.34 | 1.43 | 1.54 |
| B | 1.25 | 1.55 | 1.68 | 1.68 | 1.54 | 1.59 |
| C | 1.31 | 1.72 | 1.92 | 1.63 | 1.72 | 1.81 |

[a] A = Milk matrix method excluding cleanup step by solid-phase extraction; B = extract A to which one drop of corn oil was added; C = extract B to which one drop of soybean oil was added.

TABLE III

CHROMATOGRAPHIC RESPONSE ENHANCEMENT (MATRIX STANDARD/MATRIX FREE SOLVENT STANDARD) USING HOT ON-COLUMN INJECTION

| Injection temperature (°C) | Matrix extract | Organophosphorus compounds | | | | | |
|---|---|---|---|---|---|---|---|
| | | Methamidophos | Acephate | Omethoate | Diazinon | Dimethoate | Chlorpyrifos |
| 150 | Butterfat | 0.92 | 1.50 | 1.52 | 1.01 | 1.24 | 0.97 |
| | Milk | 1.72 | 1.61 | 1.30 | 1.31 | 1.23 | 1.11 |
| 170 | Butterfat | 1.58 | 1.50 | 1.18 | 1.14 | 1.14 | 1.15 |
| | Milk | 1.92 | 1.67 | 1.79 | 1.26 | 1.32 | 1.33 |
| 190 | Butterfat | 1.20 | 1.41 | 1.37 | 0.97 | 1.15 | 1.04 |
| | Milk | 1.62 | 2.01 | 2.12 | 1.35 | 1.56 | 1.41 |
| 210 | Butterfat | 1.19 | 1.42 | 1.52 | 1.00 | 1.31 | 1.03 |
| | Milk | 1.77 | 1.61 | 1.79 | 1.30 | 1.46 | 1.33 |
| 230 | Butterfat | 1.11 | 1.28 | 1.30 | 1.00 | 1.10 | 0.94 |
| | Milk | 1.82 | 1.59 | 1.58 | 1.20 | 1.24 | 1.23 |
| 250 | Butterfat | 0.93 | 1.20 | 1.23 | 1.14 | 1.16 | 1.16 |
| | Milk | 1.65 | 1.54 | 1.52 | 1.35 | 1.29 | 1.31 |
| 270 | Butterfat | 1.09 | 1.29 | 1.25 | 1.05 | 1.12 | 1.12 |

ture need to be specified. It is not adequate to use a butterfat matrix to correct for matrix enhancement of milk extracts (at least not without correction for the gravimetric differences in the matrix concentrations). The response enhancement seems to be less in all cases around 230°C and this remains the best compromise temperature for sample vaporization.

## CONCLUSIONS

The chromatographic response of organophosphorus pesticides using hot vaporizing injectors is matrix dependent. The matrix protects the analytes from adsorption or alteration during transfer from the injector to the column resulting in a higher observed detector response for the same amount of substance injected in a matrix-modified standard solution compared to a matrix-free standard solution. The protective influence of the matrix is not permanent and probably depends on the nature and concentration of the matrix. To obtain acceptable results either the matrix must be present in low concentration when calibration using matrix-free standards is used or matrix-modified standards

prepared from a residue-free matrix of the same kind and similar concentration to the samples should be used for calibration. In practice, the second alternative will generally be selected when analyzing complex samples such as fatty foods.

## REFERENCES


1 C. Fest and K.J. Schmidt, *The Chemistry of Organophosphorus Pesticides*, Springer, Berlin, 1982.
2 S.M. Walters, *Anal. Chim. Acta*, 236 (1990) 77.
3 F.H. Hernandez, J.M. Grases, J. Beltran and J.V. Sancho, *Chromatographia*, 29 (1990) 459.
4 L.J. Carson, *J. Assoc. Off. Anal. Chem.*, 64 (1981) 714.
5 A.M. Gillespie and S.M. Walters, *Anal. Chim. Acta*, 245 (1991) 259.
6 B.M. McMahon and N.F. Hardin (Editors), *Pesticide Analytical Manual*, US Department of Health and Human Services, Food and Drug Administration, Washington, DC, Vol. 1, 1968, section 314.34.
7 C. Mallet and V.N. Mallet, *J. Chromatogr.*, 481 (1989) 37.
8 H.J. Stan and H. Goebel, *J. Chromatogr.*, 314 (1984) 413.
9 H.J. Stan and H. Goebel, *J. Chromatogr.*, 268 (1983) 55.
10 H.J. Stan and H.M. Muller, *J. High Resolut. Chromatogr. Chromatogr. Commun.*, 11 (1988) 140.
11 D.R. Erney and S.M. Walters, *Laboratory Information Bulletin*, Food and Drug Administration, Washington, D.C., 1991, No. 3583.
12 A.M. Gillespie, S.M. Walters and D.M. Gilvydis, *Laboratory Information Bulletin*, Food and Drug Administration, Washington, D.C., 1991, No. 3633.
13 A.M. Gillespie, S.M. Walters and D.M. Gilvydis, in E. Caples (Editor), *Proc. 63rd Annual NTA Conference, Dallas, July 31–August 3, 1991,* National Technical Association, Dallas, TX, 1991, p. 1.
14 L.G.M.Th. Tuinstra, F.R. Povel and A.H. Roos, *J. Chromatogr.*, 552 (1991) 259.
15 A. DiMuccio, A. Ausili, L. Vergori, I. Camoni, R. Dommarco, L. Gambetti, A. Santilio and F. Vergori, *Analyst*, 115 (1990) 1167.

*Journal of Chromatography*, 638 (1993) 65–69
Elsevier Science Publishers B.V., Amsterdam

CHROM. 24 979

# Assessment by gas chromatography–mass spectrometry of hexenes emitted to air from petrol

Olle Ramnäs, Ulf Östermark and Göran Petersson*

*Department of Chemical Environmental Science, Chalmers University of Technology, 412 96 Gothenburg (Sweden)*

(First received December 9th, 1992; revised manuscript received February 15th, 1993)

ABSTRACT

Hexenes and cyclohexenes in vapours of conventional petrol were separated by gas chromatography on an aluminium oxide column. All hexenes appear in a favourable chromatographic position between hexanes and heptanes. The seventeen isomeric acyclic hexenes were identified by mass spectra and single-ion monitoring on an ion-trap mass spectrometer. The rapidly photooxidant-forming isomers with a non-terminal double bond constitute 70% of the total amount of acyclic hexenes. The proportions of isomers in petrol vapour are similar to those in urban air and in exhaust from petrol-fuelled vehicles.

## INTRODUCTION

Alkenes contribute rapidly and efficiently to the formation of photooxidants in air [1,2]. They are therefore given the highest priority in efforts to prevent environmental photooxidant-related problems by decreasing hydrocarbon emissions. The reactivity of alkenes in air increases with the number of carbon atoms. Pentenes and hexenes are emitted mainly as petrol vapours and as unburnt petrol components in vehicle exhaust.

Alkenes in air polluted with petrol hydrocarbons can be favourably assessed by adsorption sampling and gas chromatographic separation on aluminium oxide columns [3]. Concentrations and proportions of pentenes in petrol vapours have been reported for refuelling of cars with and without vapour recovery [4] and for refuelling with conventional and reformulated petrol [5]. The purpose of the present study was to separate, identify and determine the proportions of the hexenes emitted to air from conventional petrol.

## EXPERIMENTAL

The aluminium oxide–5% potassium chloride gas–solid chromatographic columns (one new and one used in our laboratory for 10 years) were obtained from Chrompack. Their dimensions are 50 m × 0.32 mm I.D. and they are of the porous-layer open tubular (PLOT) type.

The mass spectrometric studies were performed on a Varian Saturn II ion trap GC–MS instrument. The scan rate was one spectrum per second over the range $m/z$ 35–200. Reconstructed ion chromatograms and spectra were obtained from the data-stored scans. Injected gas samples of 10–20 $\mu$l were taken from a laboratory flask, above the surface of commercial petrol (Statoil, RON 98) conditioned to room temperature. The carrier gas was helium and the linear gas velocity through the aluminium oxide

* Corresponding author.

0021-9673/93/$06.00 

column approximately 20 cm $s^{-1}$. The temperature sequence of the column was 40–105°C (20°C $min^{-1}$), 105°C (isothermal, 50 min), 105–200°C (2°C $min^{-1}$) and 200°C (isothermal).

Samples of ambient air were taken by adsorbent sampling and analysed by thermal desorption and gas chromatography as previously described [3]. Hexenes were studied for selected samples of urban air polluted with petrol vapour and vehicle exhaust. The temperature sequence was 30–110°C (10°C $min^{-1}$), 110°C (isothermal, 14 min), 110–200°C (4°C $min^{-1}$) and 200°C (isothermal). The hexenes appear in the temperature range 150–200°C.

## RESULTS AND DISCUSSION

### *Gas chromatographic separation*

The chromatograms given in Fig. 1 demonstrate the separation achieved on the GC–MS system. The structures and chromatographic positions of all seventeen isomeric hexenes are given. In addition, the cyclic hexenes 1-methylcyclopentene and cyclohexene are marked in the total-ion chromatogram. Systematic names, quantitative proportions and relative retentions are given in Table I for all the isomeric non-cyclic hexenes.

On the aluminium oxide–potassium chloride column, the hexenes characteristically appear between the $C_6$ and $C_7$ alkanes. The prominent heptanes in the region MU 6.6–7.0 are dimethylcyclopentanes, methylcyclohexane, dimethylpentanes and methylhexanes. Similarly, the $C_2$–$C_5$ alkenes appear between the corresponding alkanes [3]. The aluminium oxide–potassium chloride column is therefore superior to most columns with other stationary phases for the determination of alkenes in the prevalent applications with higher amounts of alkanes.

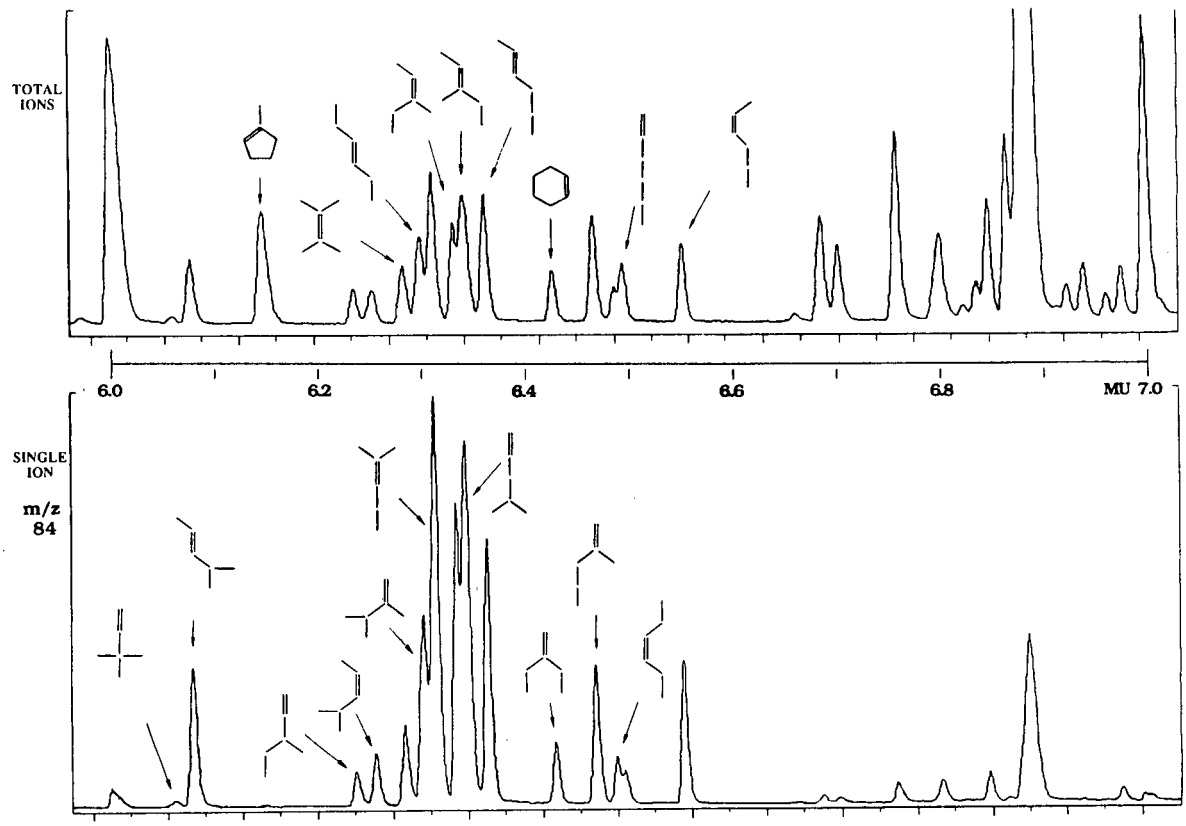


Fig. 1. Chromatographic separation of hexenes in vapours of conventional petrol. Total-ion (above) and single-ion (*m/z* 84, below) reconstructed GC–MS chromatograms. A methylene unit (MU) retention scale between hexane (6.00) and heptane (7.00) is incorporated.

TABLE I

QUANTITATIVE PROPORTIONS AND PHYSICAL DATA OF THE SEVENTEEN ISOMERIC ACYCLIC HEXENES IN VAPOURS OF CONVENTIONAL PETROL

Relative retentions are given for the aluminium oxide column as methylene units, obtained by linear interpolation between hexane (6.00) and heptane (7.00). The boiling points are physical reference data, and the reaction rate ratios are adapted from literature data [1].

| | Quantitative proportions (%) | Relative retention (MU) | Boiling point (°C) | Ions from allylic MS cleavage (*m/z*) | Relative rate for reaction with ozone in air |
|---|---|---|---|---|---|
| 3,3-Dimethyl-1-butene | 1 | 6.06 | 41.2 | 69 | 1 |
| *E*-4-Methyl-2-pentene | 6 | 6.07 | 58.6 | 69 | 20 |
| 3-Methyl-1-pentene | 3 | 6.23 | 54.2 | 55 and 69 | 1 |
| *Z*-4-Methyl-2-pentene | 2 | 6.25 | 56.4 | 69 | 10 |
| 2,3-Dimethyl-2-butene | 3 | 6.28 | 73.2 | – | 100 |
| 2,3-Dimethyl-1-butene | 3 | 6.29 | 55.6 | 69 | 1 |
| *E*-3-Hexene | 4 | 6.29 | 67.1 | 69 | 20 |
| 2-Methyl-2-pentene | 15 | 6.31 | 67.3 | 69 | 50 |
| *Z*-3-Methyl-2-pentene | 9 | 6.33 | 67.7 | 69 | 50 |
| *E*-3-Methyl-2-pentene | 11 | 6.34 | 70.4 | 69 | 50 |
| 4-Methyl-1-pentene | 3 | 6.35 | 53.9 | 41 | 1 |
| *E*-2-Hexene | 13 | 6.36 | 67.9 | 55 | 20 |
| 2-Ethyl-1-butene | 2 | 6.43 | 64.7 | 69 | 1 |
| 2-Methyl-1-pentene | 10 | 6.47 | 62.1 | 55 | 1 |
| *Z*-3-Hexene | 2 | 6.49 | 66.4 | 69 | 10 |
| 1-Hexene | 6 | 6.50 | 63.5 | 41 | 1 |
| *Z*-2-Hexene | 7 | 6.56 | 68.9 | 55 | 10 |

The hexenes elute after the hexanes because of the induced polar interactions between the double bond and the aluminium oxide stationary phase. The MU increment is 0.5 for 1-hexene as compared with hexane. Two alkyl groups in the *Z* (*cis*) or *E* (*trans*) positions at the double bond sterically increase (*Z*) and decrease (*E*) the availability of the $\pi$ electrons for interactions. An MU difference of 0.2 is observed. Alkyl branching at the double bond results in counteracting steric and inductive effects, whereas the unbalanced steric effect of $\beta$-branching evidently decreases retention (3-methyl-1-pentene, 4-methyl-2-pentenes). There is also a general retention-decreasing effect of alkyl branching because of the decreased non-polar interactions of compact molecules.

The relative retentions of the hexenes normally deviated less than 0.01 MU from the tabulated values with the particular temperature programme applied. With different temperature programmes, the MU values still accurately give the retention order of the hexenes, although absolute MU scale shifts of up to 0.05 MU were observed. The MU values for a new aluminium oxide column and one routinely used for about 10 years were very similar. Comparisons with MU values given in a study of alkenes in synthetic mixtures [6] agree well for 1-hexene and the unbranched 2-hexenes. Comparisons also reveal that several other hexenes were incorrectly identified in that study.

On non-polar columns, the hexenes elute essentially in the order of increasing boiling points (Table I), *i.e.* very differently from the aluminium oxide column. Retention data on non-polar stationary phases have been given for most of the hexenes [7,8]. Because of the absence of polar interactions, many hexenes elute unfavourably in the same region as the hexanes on these commonly used phases. On the other hand, complementary separation on a non-polar methylsilicone column was useful for ascertaining the proportions of the hexenes that were not completely resolved on the aluminium oxide column.

*Mass spectrometric identification*

As illustrated in Fig. 1, an abundant molecular ion ($m/z$ 84) permits specific single-ion monitoring of the acyclic hexenes. The heptanes are traced because they give rise to fragment ions of $m/z$ 84 in low abundance. The relative abundance of the $m/z$ 84 molecular ions varies to some extent between the isomeric hexenes. It is low for 1-hexene as illustrated by the relatively larger peak in the total ion chromatogram. The cyclohexenes are not present in the $m/z$ 84 record but were specifically monitored from their abundant $m/z$ 82 molecular ions. The only other hydrocarbons observed in the hexene region were small amounts of pentadienes. These were traced from their mass-specific and very abundant molecular ions of $m/z$ 68. Isoprene elutes near to hexane and the 1,3-pentadienes in the MU 6.20–6.35 region.

Mass spectra were recorded and interpreted for all chromatographic peaks observed in the hexene region. Comparisons with library spectra were made automatically on the MS system. The spectra permit an unambiguous identification of hexenes as a group, whereas the spectral differences between most of the isomers are small. The spectra of *cis* ($Z$) and *trans* ($E$) isomers are almost identical.

A favoured fragmentation of the molecular ion of alkenes is allylic cleavage with loss of an alkyl radical. In Table I, the masses of the primary fragment ions to be expected are given. At the conventional high electron impact energy of 70 eV, the structural specificity of these fragment ions is partly lost by non-specific hydrogen rearrangements and secondary fragmentations. The largest (base) peak in the spectra of most hexene isomers is due to $m/z$ 41 ions. Exceptions are *cis*- and *trans*-2-hexene, for which $m/z$ 55 ions from primary allylic cleavage give rise to the base peak.

The final structural assignments as given in Fig. 1 were made from a combination of mass spectra, structure–retention relationships and comparisons with authentic commercial hexenes.

*Atmospheric chemistry*

In daylight, hydrocarbons are decomposed in air, mainly by reactions with the hydroxyl radical or with ozone. The tropospheric reactions of hydrocarbons were recently reviewed [1].

As seen from Table I, the 1-alkenes react slowly with ozone. The reaction rate of other alkenes increases sharply with the number of alkyl groups adjacent to the double bond. For reaction with the hydroxyl radical, the rate constants of the hexene isomers differ by less than a factor of 5. As a result, the 1-alkenes normally decompose by reaction with the hydroxyl radical, whereas the 2- and 3-methyl-2-pentenes react mainly with ozone if the ambient ozone levels are not too low. The reaction paths and products for the reaction with ozone should be similar to those recently reported for 2-methyl-2-butene [9].

The lifetime of all hexenes in air is normally less than 1 day, and that of the most reactive isomers less than 1 h in the photooxidant season. As a result, the hexenes contribute more efficiently than lower alkenes to locally elevated photooxidant levels. The most reactive isomers do not necessarily produce ozone very efficiently [2], but they give rise to a wide range of other photooxidants [1] such as peroxides, which may be even more harmful.

*Emissions to air*

The results reported refer to vapours from commercial petrol with a conventional content of alkenes from catalytic cracking. The composition and chromatographic separation of the whole range of vapour hydrocarbons, emitted from a similar commercial petrol (RON 95) during refuelling, were recently reported [5]. The portion of the acyclic hexenes was 1.7% of the amount of total hydrocarbons. Although these vapour samples were taken on adsorbent cartridges, and although the temperature programme was more rapid, the proportions of the isomeric hexenes are distinctly similar to those reported here. Similar proportions of the hexene isomers are also seen in a published chromatogram of $C_2$–$C_8$ hydrocarbons from exhaust-polluted urban air [10]. Approximately the same proportions were actually observed in a large number of unpublished chromatograms from samples of petrol vapour, petrol exhaust and vehicle-polluted urban air.

The observed uniform composition of hexene isomers in petrol vapours is obviously explained by the output from the catalytic cracking processes, which deliver most of the alkene-rich fractions mixed into petrol. From Table I, it is seen that 1-alkenes account for almost 30% of the total acyclic hexenes. The reactive 2- and 3-methyl-2-hexenes constitute more than one-third of the total. The somewhat more variable content of cyclohexenes was found to be approximately 10% and 2% for methylcyclopentenes and cyclohexene, respectively, as compared with the total amount of acyclic hexenes. The uniform quantitative proportions of the hexenes permit estimates of all isomers even under conditions when only one or a few of them can be determined reliably.

Hexenes in exhaust from petrol-fuelled vehicles are emitted as unburnt petrol hydrocarbons. This explains the observed similar proportions of hexene isomers in petrol vapours and in urban air that is normally polluted mainly with exhaust hydrocarbons. Obviously, however, exhaust differs from equilibrated vapours by having higher proportions of the less volatile isomers. Not only the $C_6$ but also the $C_5$ alkenes in vehicle exhaust are predominantly unburnt petrol components, whereas ethene, propene and a prominent portion of the butenes are combustion products. The total proportion of hexenes, including the cyclic $C_6$ alkenes, was found to be about the same as that of the pentenes in vehicle-polluted urban air in Sweden. This means approximately 1% of the total amount of $C_2$–$C_8$ hydrocarbons [10].

REFERENCES

1 R. Atkinson, *Atmos. Environ.*, 24A (1990) 1.
2 R.G. Derwent and M.E. Jenkin, *Atmos. Environ.*, 25A (1991) 1661.
3 L. Löfgren, P.M. Berglund, R. Nordlinder, G. Petersson and O. Ramnäs, *Int. J. Environ. Anal. Chem.*, 45 (1991) 39.
4 P.M. Berglund and G. Petersson, *Sci. Total Environ.*, 91 (1990) 49.
5 U. Östermark and G. Petersson, *Chemosphere*, 25 (1992) 763.
6 R. Snel, *Chromatographia*, 21 (1986) 265.
7 S. Boneva and N. Dimov, *Chromatographia*, 21 (1986) 149.
8 C.M. White, J. Hackett, R.R. Anderson, S. Kail and P.S. Spock, *J. High Resolut. Chromatogr.*, 15 (1992) 105.
9 D. Grosjean, *Environ. Sci. Technol.*, 24 (1990) 1428.
10 L. Löfgren and G. Petersson, *Chemosphere*, 24 (1992) 135.

*Journal of Chromatography*, 638 (1993) 71–74
Elsevier Science Publishers B.V., Amsterdam

CHROM. 24 971

# Determination of 3-chloropropane-1,2-diol in hydrolyzed vegetable proteins by capillary gas chromatography with electrolytic conductivity detection

G. Spyres

*A.E. Staley Manufacturing Co., 2200 E. Eldorado, Decatur, IL 62525 (USA)*

(First received October 8th, 1992; revised manuscript received February 10th, 1993)

ABSTRACT

The determination of 3-chloropropane-1,2-diol in hydrolyzed vegetable protein using capillary gas chromatography is improved through the specificity of an electrolytic conductivity detector operated in the halogen mode. The hydrolysate is absorbed onto a Extrelut QE column of kieselguhr, 3-chloropropane-1,2-diol is partitioned into ethyl acetate and is quantitatively measured by gas chromatography using 1-chlorotetradecane as the internal standard. A concentration of 1 mg/kg dry substance is easily determined.

## INTRODUCTION

Hydrolyzed vegetable protein (HVP) is commonly manufactured by the hydrolysis of vegetable protein with hydrochloric acid. The protein sources typically contain residual lipids. Without proper control the potential exists for a reaction between triglycerides and hydrochloric acid to produce 3-chloropropane-1,2-diol (3-MCPD) and 2-chloropropane-1,3-diol (2-MCPD).

Pesselman and Feit [1] used gas chromatography with electron-capture detection to quantitatively measure 3-MCPD in a standard aqueous solution after derivatization with *n*-butylboronic acid and extraction into hexane. Rodman and Ross [2] utilized phenylboronic acid to derivatize 3-MCPD in a non-aqueous media for subsequent determination by gas chromatography.

A method to determine 3-MCPD in HVP by gas chromatography using phenylboronic acid derivatization and solvent extraction was reported by Planting *et al.* [3]. Van Bergen *et al.* [4] recently reported a procedure to determine chloropropanols in protein hydrolysates based on gas chromatography of heptafluorobutyrate derivatives. Limitations of derivatization/extraction procedures for measuring 3-MCPD include a potential for incomplete derivatization, inefficient partitioning of the derivative from the aqueous phase into the organic phase, and short term stability of the derivatives.

This paper reports a method to quantitatively determine 3-MCPD in HVP. The liquid hydrolysate is absorbed on a kieselguhr column, 3-MCPD is partitioned from the column into ethyl acetate and selectively measured by gas chromatography using electrolytic conductivity detection.

## EXPERIMENTAL

### *Apparatus*

Chromatographic measurements were performed with a Tracor Model 560 gas chromatograph equipped with a packed-column injector and a Hall 700A electrolytic conductivity detector. The packed-column inlet was fitted with a

0021-9673/93/$06.00 

SGE on-column adapter to allow direct injection onto a 60 m × 0.75 mm I.D. borosilicate glass Supelcowax 10 column with 1-μm film. The column was fitted with a 50-cm retention gap of 0.53 mm I.D. deactivated fused silica. Helium was used as the carrier gas at a flow-rate of 8 ml/min. The column temperature was 170°C for 5 min, then raised at 5°/min to 250°C and held for 10 min. The injector temperature was 225°C. The electrolytic conductivity detector was operated in the halogen mode.

Hydrogen was used as the reactant gas at a flow-rate of 30 ml/min and 1-propanol was the solvent at a flow through the cell of 0.5 ml/min. Reactor temperature was 900°C with a base temperature of 275°C. Contamination of the reaction tube was minimized by venting flow from the column at all times except for the time during which compounds of interest elute.

Confirmation of peaks observed for 3-MCPD and 2-MCPD was obtained with a Hewlett-Packard Model 5890 II gas chromatograph and a Model 5970B mass-selective detector.

*Reagents*

3-MCPD was obtained from Eastman Kodak (Rochester, NY, USA), 1-chlorotetradecane was obtained from Aldrich (Milwaukee, WI, USA) and ethyl acetate was Burdick & Jackson capillary grade from Baxter Scientific products (McGraw Park, IL, USA).

*Solutions*

A stock solution of 3-MCPD was prepared by weighing 100.0 mg into a 100-ml volumetric flask and diluting to volume with ethyl acetate. This solution was diluted 5 ml/100 ml with ethyl acetate to yield a solution containing 50 μg/ml. The stock solution of 1-chlorotetradecane was prepared by weighing 250 mg into a 50-ml volumetric flask and diluting to volume with ethyl acetate. This solution was diluted 5 ml/100 ml with ethyl acetate to provide a solution containing 250 μg/ml.

*Procedure*

The protein hydrolysate was adjusted as needed with 20% aqueous sodium chloride to obtain a solids content of 36%. A 20-g aliquot was weighed directly into a 20-ml Extrelut column (EM Science, Gibbstown, NJ, USA) and allowed to equilibrate for 15 min. The column was eluted with 150 ml ethyl acetate collecting the eluent in a 250-ml short-neck round-bottom flask with a 24/40 joint. The eluent was concentrated to a volume of approximately 3 ml using a rotary evaporator at 50°C. After the addition of 0.5 ml internal standard solution (250 μg/ml) the eluent was transferred to a 4-dram (1 dram = 3.697 ml) screw cap vial, diluted to a volume of approximately 5 ml, and 1 μl was injected into the gas chromatograph.

*Preparation of standards*

A standard containing 3-MCPD at 4 μg/ml and internal standard at 30 μg/ml was prepared by pipetting 2.0 ml dilute 3-MCPD solution and 3.0 ml dilute internal standard solution into a 25-ml volumetric flask and diluting to volume with ethyl acetate. A second standard containing

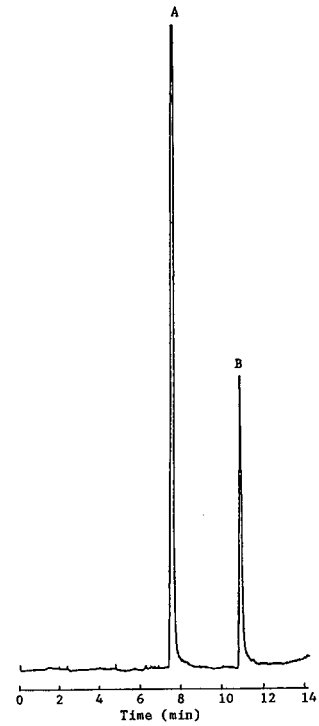


Fig. 1. Chromatogram of standard containing 4 μg/ml of 3-MCPD and 30 μg/ml internal standard. Peaks: A = 1-chlorotetradecane; B = 3-MCPD.

3-MCPD at 20 μg/ml and internal standard at 30 μg/ml was prepared by pipetting 10.0 ml dilute 3-MCPD solution and 3.0 ml dilute internal standard solution into a 25-ml volumetric flask and diluting to volume with ethyl acetate. Calibration was achieved by injecting 1 μl of each standard.

Response factors in reference to the internal standard were calculated for each standard. The amount of 3-MCPD in concentrated sample extracts was calculated using the response factor from a standard exhibiting similar peak areas as the sample.

## RESULTS AND DISCUSSION

A spiked protein hydrolysate was used to measure the efficiency for partitioning 3-MCPD from the Extrelut column into diethyl ether, pentane–diethyl ether (80:20) and ethyl acetate.

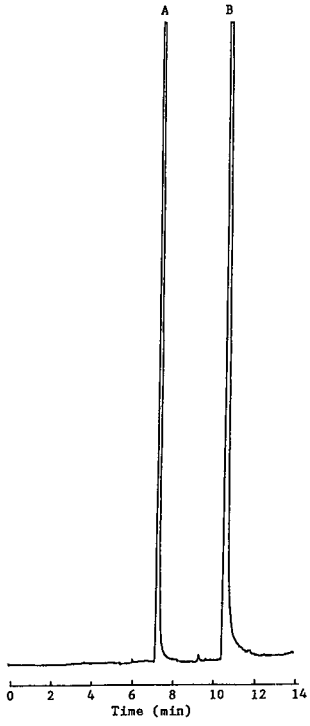


Fig. 2. Chromatogram of standard containing 20 μg/ml of 3-MCPD and 30 μg/ml internal standard. Peaks: A = 1-chlorotetradecane; B = 3-MCPD.

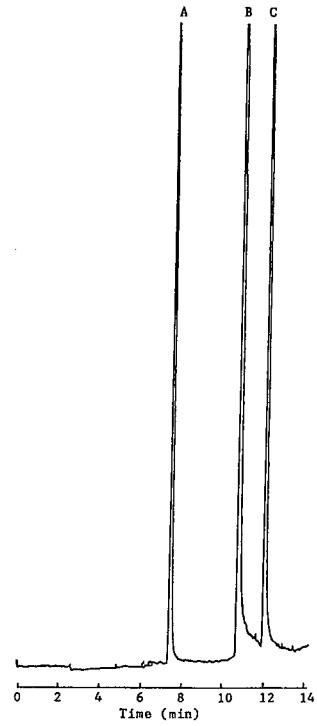


Fig. 3. Chromatogram of concentrated ethyl acetate extract from a sample of HVP. Peaks: A = 1-chlorotetradecane; B = 3-MCPD; C = 2-MCPD.

Highest efficiency was observed with ethyl acetate.

Chromatograms shown in Figs. 1 and 2 are standards containing 3-MCPD at 4 μg/ml and 20 μg/ml with internal standard at 30 μg/ml. The sample chromatogram shown in Fig. 3 exhibits peaks for 3-MCPD and the isomer 2-MCPD.

Standards with 3-MCPD levels between 4 and 2400 μg/ml were chromatographed to determine

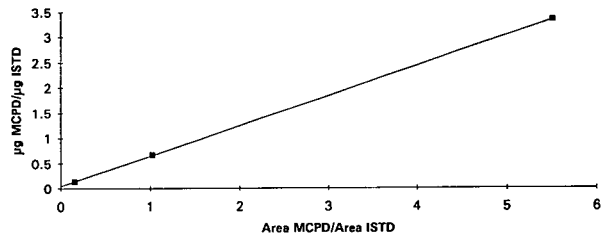


Fig. 4. Plot of the ratio of micrograms 3-MCPD/1-tetrachlorodecane against the ratio of peak area for 3-MCPD/1-tetrachlorodecane.

TABLE I

RECOVERY OF 3-MCPD FROM A SPIKED PROTEIN HYDROLYSATE

| Spike level ($\mu$g/g) | Found ($x \pm$ S.D.) | Recovery (%) |
|---|---|---|
| 0 | 0.82 ± 0.096 | – |
| 1 | 1.80 ± 0.082 | 98 |
| 5 | 5.65 ± 0.208 | 96.6 |

linearity. A plot was made for the ratio of 3-MCPD peak area/internal standard peak area and the ratio for micrograms 3-MCPD/micrograms internal standard. Linearity was observed for the 3-MCPD concentration range of 0 to 100 $\mu$g/ml as shown in Fig. 4. This concentration range was satisfactory for the analysis of samples containing 3-MCPD between 0 and 30 mg/kg. When analyzing samples in excess of 30 mg/kg the extracts were diluted to attain 3-MCPD concentrations within the linear range. An appropriate aliquot of internal standard was added to obtain a concentration of 20–30 $\mu$g/ml.

Table I shows that recoveries obtained with this method for a protein hydrolysate fortified with 3-MCPD at levels of 1 and 5 mg/kg were greater than 95% when corrected for concentrations in the unspiked sample. The detection limit for the method was 0.25 mg/kg sample.

In conclusion, this method is sensitive and precise for routine determination of 3-MCPD in HVP. The halogen-specific detector provides sample chromatograms free of interfering peaks and allows trace level determinations.

REFERENCES

1 R.L. Pesselman and M.J. Feit, *J. Chromatogr.*, 439 (1988) 448–452.
2 L.E. Rodman and R.D. Ross, *J. Chromatogr.*, 369 (1986) 97–103.
3 W.J. Planting, W.G. van Toorn, and G.H.D. van der Stegen, *J. Chromatogr.*, 555 (1991) 311–314.
4 C.A. van Bergen, P.D. Collier, D.D.O. Cromie, R.A. Lucas, H.D. Preston and D.J. Sissons, *J. Chromatogr.*, 589 (1992) 109–119.

*Journal of Chromatography*, 638 (1993) 75–83
Elsevier Science Publishers B.V., Amsterdam

CHROM. 24 984

# Evaluation of microbore and packed capillary column chromatography with an ethylvinylbenzene–divinylbenzene polymeric packing material and supercritical ammonia as the mobile phase

Douglas E. Raynie[☆], Kent M. Payne[☆☆], Karin E. Markides[☆☆☆] and Milton L. Lee*

*Department of Chemistry, Brigham Young University, Provo, UT 84602 (USA)*

(First received July 17th, 1992; revised manuscript received February 16th, 1993)

ABSTRACT

An investigation into the use of ammonia as a mobile phase for high-resolution supercritical fluid chromatography was conducted. A highly cross-linked ethylvinylbenzene–divinylbenzene polymeric packing material (5-$\mu$m diameter) in microbore stainless-steel and nickel capillary tubing demonstrated reasonable efficiencies (*ca.* 10 000–15 000 plates $m^{-1}$, after initial exposure to ammonia) without phase degradation as previously observed when using open-tubular capillary columns. However, ammonia treatment caused an initial rapid loss in efficiency (*ca.* 42%) for reasons as yet undetermined. The polymeric packing materials were much more inert than conventional silica-based packing materials. Separations of polar drugs, underivatized amino acids and defoliant herbicides are shown.

## INTRODUCTION

Supercritical fluid chromatography (SFC) is generally performed with carbon dioxide as the mobile phase. Despite the well-documented advantages of carbon dioxide as an SFC mobile phase, at least two fundamental limitations with the use of this fluid exist. First, with carbon dioxide, moderate and highly polar materials often will not migrate through the chromatographic column. Second, supercritical carbon dioxide, like all solvating mobile phases, has limitations in the molecular weights of compounds which it can solvate. Various approaches have been taken to address these limitations, including organic modifiers, reversed micelle-containing mobile phases, ion-pairing mobile phases, and alternative fluids.

Perhaps the most polar solvent with properties conducive to use as an SFC mobile phase is ammonia. The use of ammonia as a chromatographic mobile phase has been demonstrated [1–9], however its use in capillary SFC is rather restricted since ammonia rapidly degrades most polysiloxane stationary phases [1,2] and more slowly attacks silica. Consequently, packed microcolumns which are fabricated from non-silica materials are preferred for analytical SFC with ammonia as the mobile phase. A new polymeric packing material for packed microcolumn SFC

* Corresponding author.
☆ Present address: The Procter & Gamble Company, Miami Valley Laboratories, P.O. Box 398707, Cincinnati, OH 45239-8707, USA.
☆☆ Present address: G.D. Searle & Company, Research and Development, 4901 Searle Parkway, Skogie, IL 60077, USA.
☆☆☆ Present address: Department of Analytical Chemistry, Uppsala University, S-751 21 Uppsala, Sweden.

0021-9673/93/$06.00 

has been recently reported [10,11] which is resistant to the corrosive action of ammonia. A detailed evaluation of this packing material for SFC is reported in this paper.

*Physical properties and high-pressure studies of ammonia*

Ammonia is a polar material with physical properties compatible with the mobile phase requirements of SFC. The physical properties of ammonia are reviewed in Table I. It is considered to have a hydrogen bonding energy similar to water and a greater proton affinity than water [15]. Consequently, ammonia is a strong hydrogen bond acceptor with little propensity to donate hydrogen bonds, especially in the gas phase [3]. Ammonia possesses a high dielectric constant. Not surprisingly, supercritical ammonia was found [16,17] to have the highest solvatochromic polarity when compared with carbon dioxide, chlorotrifluoromethane, nitrous oxide and carbon dioxide + methanol. The solvating ability which results from these properties should lend itself to unique applications as an SFC mobile phase. One potential problem with the use of ammonia as a chromatographic mobile phase is its reactivity, which may be more pronounced at elevated pressures and temperatures. In chromatography, depending on the nature of the reactions, however, this may function beneficially as a type of on-column derivatization.

TABLE I

PHYSICAL PROPERTIES OF AMMONIA

Data taken from ref. 12.

| | |
|---|---|
| Molecular mass | 17.031 |
| Boiling point | −33.4°C |
| Critical temperature | 132.4°C |
| Critical pressure | 111.3 atm (1 atm = 0.10 MPa) |
| Critical volume[a] | 72.5 ml $mol^{-1}$ |
| Compressibility factor | 0.242 |
| Dipole moment (gas) | 1.47 D |
| Dielectric constant: gas at 0°C | 1.0072 |
| liquid at −33.4°C | 22.4 |
| Acentric factor | 0.250 |
| Solubility factor at liquid density[b] | 16.3 $cal^{1/2}$ $cm^{3/2}$ (1 cal = 4.1868 J) |

[a] Data taken from ref. 13.
[b] Data taken from ref. 14.

Although ammonia is probably the most studied non-aqueous solvent, only a few studies concerning high-pressure ammonia, especially with organic solutes or cosolvents, have been undertaken. The thermodynamic stability of ammonia in the critical region has been studied [18]. Phase equilibria studies of ammonia with nitrogen, argon, helium, water, carbon dioxide, methane, ethane, *n*-butane, ethylene, propylene, benzene, 2,2,4-trimethylpentane, cyclohexane, *trans*-decalin, *o*-xylene, acetylene and biphenyl + dodecane have been reported [19,20]. Potassium and silicon have been found to react with supercritical ammonia to form potassium imidonitridosilicate crystals [21]. The solubility of anthracene [22], and caffeine and theophylline [23,24] in ammonia, and near-critical (20°C) separation of 1-butene and 1,3-butadiene with 2–10% (v/v) ammonia in either ethane or ethylene [25], have been studied. Supercritical ammonia was used for the extraction of ginseng saponins [26] and the extraction of cobalt from hydrotreating catalysts [27]. In addition to these studies, the research group of Smith has used supercritical ammonia for direct fluid injection mass spectrometry [28] and for the extraction of diesel fuel marine sediments [29]. Supercritical fluid injection–time-of-flight mass spectrometry of underivatized peptides, nucleosides, and steroids was accomplished with supercritical ammonia [30].

*Ammonia as a chromatographic mobile phase*

Ammonia was first used as a mobile phase for SFC in 1968 [4,5] when it was shown that supercritical ammonia had solvent characteristics approximately intermediate (except acidity) between water and low-molecular-mass alcohols. It was demonstrated that the ability to form hydrogen bonds favored the solvation of compounds with hydroxylic, amino and related groups by supercritical ammonia. Solutes transported through a packed chromatographic column with ammonia included some waxes, nucleosides, sterols, amino acids, amines, di- and tripeptides, mono- and disaccharides and high-molecular-

mass polyethylene glycols, while proteins, higher polysaccharides and purines did not migrate. Additionally, material stability problems, which resulted in leaks, column plugging, and spiking in the flame ionization detector, were reported.

In capillary SFC, Grolimund *et al.* [6] used ammonia with fluorescence detection for the separation of fluorescent whitening agents containing free sulfonic acid groups. They also reported a variety of material compatibility problems. Kuei *et al.* [1,2] performed a systematic study to alleviate these problems and separated polarizable polycyclic aromatic hydrocarbons (PAHs) greater than ovalene ($M_r = 396$) in a carbon black extract with ammonia as the SFC mobile phase. Also, this mobile phase was applied to the analysis of antidepressant drugs and nucleosides. Ammonia was combined as a modifier with sulfur hexafluoride for the separation of nitrogen-containing polycyclic aromatic compounds and polar drugs [1] and imidazole derivatives [7]. Trifluoromethane with 20 mol% ammonia as the mobile phase was able to produce slightly better resolution of some basic drugs than pure ammonia [1].

Other uses of ammonia as a chromatographic mobile phase include liquid ammonia (30–40°C) for the packed-column separation of alkaloids, and a test mixture of phthalates, biphenyl and *o*-terphenyl [8], and as a carrier gas for capillary GC of aliphatic and aromatic amines [3] and chlorophenols [9]. Compared to nitrogen as carrier gas, ammonia gave improved peak symmetry and decreased capacity factors for primary and secondary amines on both polar (polyethylene glycol) and intermediate polarity (methylphenylcyanopropylsilicone) stationary phases [3]. The effect of ammonia was found to be more pronounced at lower temperatures. With flame ionization detection (FID), the detection limits for these amines were found to be seven to ten times lower with ammonia as the carrier gas than with nitrogen. However, in the analysis of chlorophenols, the capacity factors increased with ammonia relative to when nitrogen was used as carrier gas [9]. The more acidic dichlorophenols were more affected by ammonia than the less acidic monosubstituted ones.

The high pressures and elevated temperatures often associated with SFC have presented certain obstacles in the development of the method. These obstacles are compounded when ammonia is used as the mobile phase, since, as discussed earlier, ammonia is corrosive to many materials. Previous reports emphasized the need to use stainless-steel tubing and PTFE O-rings, gaskets and seals [4,5,8]; however, the work of Kuei *et al.* [1,2] has been the only systematic evaluation of materials for SFC when using ammonia as mobile phase. They found that aluminum supply cylinders provided more pure ammonia (due to fewer particulate contaminants) than when stainless-steel cylinders were used, and stainless-steel tubing should be used for supply lines between the supply cylinder and the pump, and between the pump and the SFC injector. In the assembly of the apparatus, 0.2-$\mu$m in-line filters were placed on both the inlet and outlet sides of the pump. PTFE can be used for pump cylinder piston seals; however, PTFE tends to soften in ammonia at pressures around 240 atm. A PTFE–graphite composite material for the piston seals proved to be more durable. Ferrules made of graphite or Kel-F polymer were used. For injection, Kuei *et al.* [1,2] used the timed-split method with a PTFE spacer in the connection to the injector body. The injector rotor was made from the standard Valcon-H material. Pinched platinum-iridium tubing was used as the restrictor. Detection was accomplished with ultraviolet (UV) absorbance since FID was found to yield significant background noise due to ionization of the ammonia mobile phase. The entire apparatus was placed in a fume hood.

*Stationary phases for ammonia SFC*

As previously mentioned, most of the commonly used polysiloxane stationary phases in capillary SFC are rapidly degraded by supercritical ammonia [1,2]. It was found that *n*-octyl- and *n*-nonyl-substituted polysiloxanes and polyethyleneimine were the only stationary phases studied which could resist the corrosive action of ammonia. Polymethylsiloxane stationary phases containing 50% phenyl, 50% cyanopropyl, 30% biphenyl or 5% phenyl moieties were rapidly degraded by ammonia. It was postulated that the presence of long, easily cross-linkable hydro-

carbon appendages protected the siloxane backbone from attack by ammonia.

Highly cross-linked polymers were reported [8] to be more compatible than silica-based packing materials for use with supercritical ammonia. A new packing material was recently developed [10,11] which is a highly cross-linked ethylvinylbenzene and divinylbenzene (EVB–DVB) polymer. This EVB–DVB, like other polymeric packings, should be more highly resistant to chemical attack than silica-based packings. Because this polymer is more highly cross-linked, it should be degraded less easily than other polymers. The EVB–DVB polymer has an average particle size of 5 $\mu$m, a pore size of about 60 Å, a surface area of about 300 $m^2 g^{-1}$, and was shown to be chemically and physically stable at temperatures and pressures up to at least 200°C and 10 000 p.s.i. (1 p.s.i. = 6894.76 Pa) [11]. The retention mechanism of polar and non-polar compounds on the EVB–DVB polymeric stationary phase was found to be governed by surface adsorption-desorption as a result of non-polar–non-polar interactions. The retention mechanism also was significantly influenced by the $\pi-\pi$ surface interaction with $\pi$-electron-rich solutes because of the high density of $\pi$-electrons associated with the aromatic components of the stationary phase. In this paper, this EVB–DVB polymer was further evaluated for microbore and packed capillary SFC of polar compounds using ammonia as the mobile phase.

## EXPERIMENTAL

For the packed microcolumn work reported here, a Hewlett-Packard Model 5790 gas chromatographic oven (Hewlett-Packard, Avondale, PA, USA), Valco Model CW14 injector (Valco Instruments, Houston, TX, USA), Chiratech Model 203 UV–Vis detector (now produced by Linear Instruments, Reno, NV, USA), and a Varian Model 8500 syringe pump (Varian Associates, Walnut Creek, CA, USA) controlled through a pressure feedback with an Apple IIe computer (Apple Computers, Cupertino, CA, USA) were used with the modifications described by Kuei *et al.* [1,2]. In this study, graphite or graphitized Vespel ferrules were used. Polyether ether ketone (PEEK, Upchurch Scientific, Oak Harbor, WA, USA) tubing was used in connections, although this material is not useful at temperatures above 150°C. Adequate tightening of fittings and connections was extremely important since the polymeric materials tended to soften at elevated temperatures and pressures. Leaks were frequently encountered with fittings involving 1/32 in. O.D. (1 in. = 2.54 cm) tubing when stainless-steel ferrules were used. The use of gold-plated ferrules alleviated this problem. The fused-silica transfer lines from the injector and to the detector were minimized in length and internal diameter since the silica was weakened by the ammonia. The problems previously enumerated [1,2] due to ammonia degradation of the protective polyimide coating on exposed sections of fused-silica were not addressed. With the platinum–iridium restrictor used here, the end of the restrictor tubing was inserted into a small vial of water to collect the ammonia mobile phase and to minimize plugging of the restrictor. Occasional heating of the restrictor tip with a butane cigarette lighter restored flow when the restrictor was partially plugged.

Columns used in this study were microcolumns packed with OmniPAC $\mu$PRN-300 (Dionex, Sunnyvale, CA, USA). Initial experiments with the OmniPAC material were with test columns (15 cm × 750 $\mu$m I.D.) supplied by the manufacturer. Other columns were packed in our laboratory by the slurry packing method [31,32]. Column material of stainless steel, glass-lined stainless steel, fused silica (Polymicro, Phoenix, AZ, USA), and nickel (Valco) tubing with dimensions of 15–75 cm × 0.250–1.0 mm I.D. were used.

## RESULTS AND DISCUSSION

Initially, the OmniPAC columns supplied by the manufacturer were evaluated for efficiency using carbon dioxide, before and after exposure to ammonia, following the procedure of Kuei *et al.* [1,2] (*i.e.*, ammonia at 100 atm and ambient temperature for 15 h, then 200 atm and 145°C for 24 h). The measured efficiency averaged 42%

less after exposure to ammonia. Several columns used in this study were evaluated periodically during their use in the ammonia SFC system. Each column showed similar trends, *i.e.*, a 15–50% loss of efficiency after exposure to ammonia. Efficiency measurements were performed over the course of use of the columns, including after venting the column of ammonia followed by repeated exposure. From this, it appears that the loss in efficiency occurred during the initial 1–2 h following exposure to the ammonia. Minimal additional efficiency loss was observed over the period of use, including up to two weeks of continuous use and *ca.* six weeks of total use. Based on experiments involving purging and venting the columns with ammonia compared to continuous exposure, it does not seem that swelling of the packing material is a significant cause of efficiency loss. Scanning electron microscopy (SEM) of the packing material showed no gross physical changes to the OmniPAC beads due to exposure to ammonia. These SEM results, shown at 9500× magnification, are displayed in Fig. 1. The SEM did show a wide range of particle sizes and a small degree of distortion of the particle shape, even in the material as received from the manufacturer. The erratic efficiencies obtained in ammonia SFC were verified to some extent in carbon dioxide SFC [33]. With columns supplied by the manufacturer, losses in efficiency (up to 50%) were found in most cases. After purging with organic solvents, such as acetonitrile and methanol, some of the efficiency was regained. The highest observed efficiency in our study and in the carbon dioxide study [33] was about 20 000 plates $m^{-1}$. Since the loss in efficiency with these columns occurred during initial exposure, was independent of the mobile phase used (carbon dioxide or ammonia), could only be partially regenerated, and the SEM of the OmniPAC beads showed no gross physical changes due to ammonia exposure, we postulate that the efficiency loss with these columns is due to a redistribution of the packed bed upon pressurization. Swelling of the packing material during exposure to the mobile phase may also be a minor contribution to the efficiency loss.

The initial efficiencies, in ammonia, of these columns were typically 17 000–20 000 plates $m^{-1}$ and the dimensions of the column has no apparent effect on the efficiency of packing. Fused-silica column material yielded particularly erratic efficiency results and became extremely fragile upon exposure to ammonia. Other column materials (stainless steel, glass-lined stainless steel and nickel) gave similar efficiencies. Columns packed in nickel tubing of capillary dimensions (≤500 μm I.D.) were the most reproducible, while the stainless-steel columns were the most durable. Small I.D. columns could be packed to longer dimensions, yielding greater numbers of total plates without deleterious chromatographic effects due to pressure drops. Hence, the nickel and stainless steel columns were preferred.

Silica-based packing materials are often in-

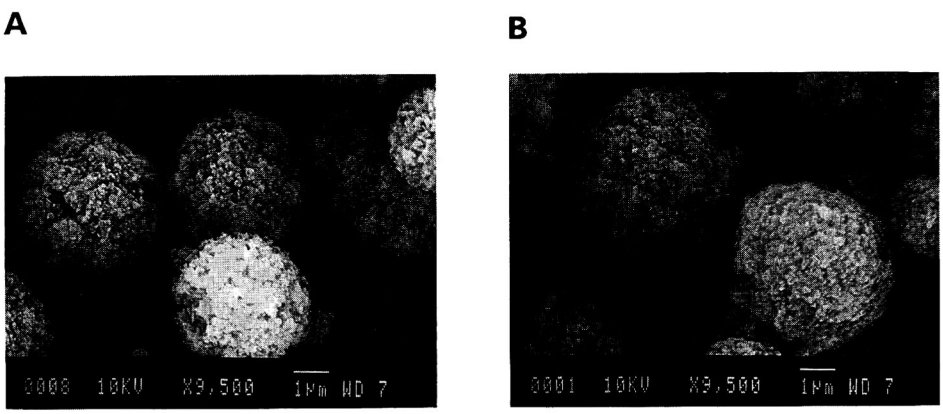


Fig. 1. Scanning electron photomicrographs of OmniPAC μPRN-300 packing material (A) as received and (B) after exposure to supercritical ammonia.

adequate for packed column SFC of polar materials, especially because of the high content of surface silanol groups, even after deactivation. Polymeric packing materials should be much more inert. Therefore, it was of interest to evaluate the surface activity of the polymeric OmniPAC material, especially in ammonia SFC.

Before exposing the OmniPAC material to ammonia, free fatty acids could be separated with good peak shapes [11], as displayed in Fig. 2. After the ammonia purge discussed previously, free fatty acids could not be eluted from the column in supercritical carbon dioxide, both before and after the column was additionally purged with HPLC-grade water for several hours.

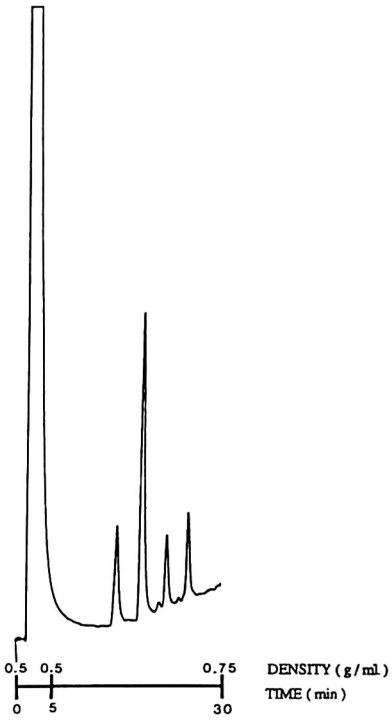


Fig. 2. SFC chromatogram of a mixture of saturated free fatty acids ($C_{12}H_{24}O_2$, $C_{14}H_{28}O_2$, $C_{16}H_{32}O_2$, $C_{18}H_{36}O_2$) using carbon dioxide as the mobile phase prior to exposing the OmniPAC packing to ammonia. Conditions: carbon dioxide, 100°C, 25 cm × 250 μm I.D. OmniPAC μPRN-300, density programmed from 0.50 g $ml^{-1}$ to 0.75 g $ml^{-1}$ following a 5-min isobaric hold, FID. Following exposure to ammonia, the chromatographic integrity of the packing was reduced so that these free fatty acids could not again be eluted with carbon dioxide SFC.

To compare the OmniPAC activity in both carbon dioxide and ammonia mobile phases, a mixture of 15 explosives and related decomposition products was separated using both mobile phases. Two separate OmniPAC columns, each possessing similar efficiencies in the mobile phase in which they were used, were employed. The test mixture contained nitro- and amino-aromatics and other polar materials. The mixture components included 2,6-dinitrotoluene, 2,4-dinitrotoluene, dibenzofuran, *n*-nitrosodiphenylamine, 2,4,6-trinitrotoluene, 2-nitronaphthalene, benz[*a*]anthracene, 1-nitropyrene, benzo[*a*]pyrene, 1,3,5-trinitrobenzene, pyrene, phenol, 2-nitrodiphenylamine, 1-nitronaphthalene and 9-phenylanthracene. The resulting chromatograms, using FID for carbon dioxide SFC and UV detection for ammonia SFC, are presented in Fig. 3. The selectivity of the OmniPAC

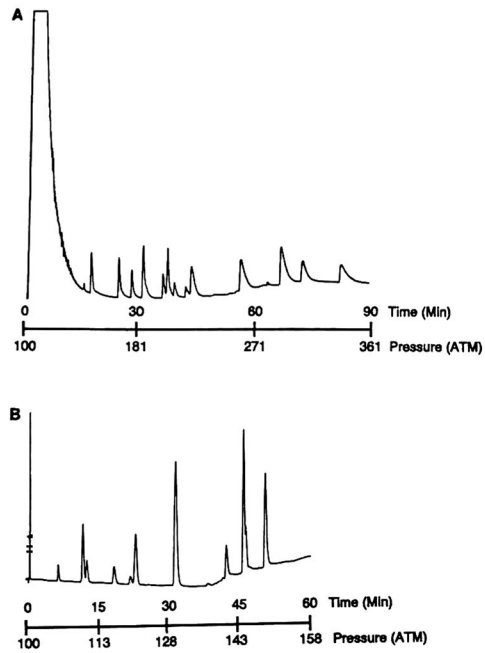


Fig. 3. SFC chromatograms of a mixture of explosives and related decomposition products using (A) carbon dioxide and (B) ammonia as the mobile phase. Conditions: (A) carbon dioxide, 145°C, 30 cm × 250 μm I.D. OmniPAC μPRN-300, pressure programmed from 100 atm to 355 atm at 3 atm $min^{-1}$ following a 5-min isobaric hold, FID; (B) ammonia, 145°C, 25 cm × 500 μm I.D. OmniPAC μPRN-300, pressure programmed from 100 atm to 158 atm at 1 atm $min^{-1}$ following a 2-min isobaric hold, UV at 254 nm.

material in these two mobile phases was not determined, and although no attempt was made to identify the individual peaks and the chromatograms are not directly comparable, it is obvious that the use of ammonia as the mobile phase resulted in dramatically reduced peak tailing and improved peak shape for these compounds.

The value of ammonia as an SFC mobile phase is its applicability for samples too polar to be separated by carbon dioxide SFC. To demonstrate the application to polar materials, three samples were used.

The antidepressant drugs zimelidine and norzimelidine present a difficult separation. These compounds, both hydrochloride salts, cannot be analyzed by GC, and separation of the compounds is difficult to perform by LC. Although zimelidine can be eluted in SFC using carbon dioxide, the formation of the "nor-" derivative imparts enough basicity to the molecule that it cannot be analyzed in the same way. A reasonable separation of these drugs using supercritical ammonia is shown in Fig. 4 with little peak tailing.

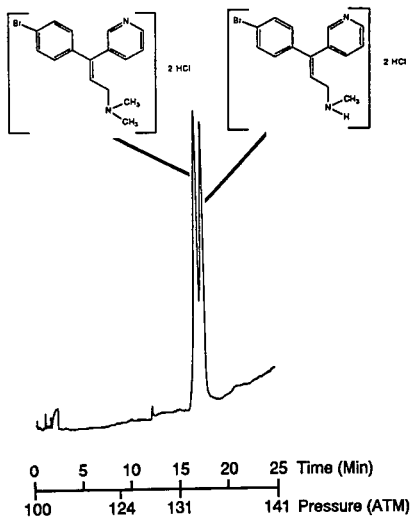


Fig. 4. SFC chromatogram of the antidepressant drugs zimelidine and norzimelidine, using ammonia as the mobile phase. Conditions: ammonia, 145°C, 15 cm × 1 mm I.D. OmniPAC μPRN-300, pressure programmed from 100 atm to 124 atm at 3 atm $min^{-1}$ following a 1-min isobaric hold, then 1 atm $min^{-1}$ to 141 atm, UV at 254 nm.

For the chromatographic analysis of amino acids, they are often derivatized, usually to their phenylthiohydantoin derivatives. The underivatized amino acids, tyrosine and tryptophan, were separated by ammonia SFC (Fig. 5). It has been shown that a wide range of amino acids can be analyzed by ammonia SFC [4,5]. To achieve a separation of a wider range of amino acids than shown in Fig. 5, a selective stationary phase will be needed, as will a more universal detector. In the ammonia SFC of amino acids, ammonia probably reacts with the carboxylic acid moiety of the amino acid to form the corresponding amide. This analysis can be considered as "on-column derivatization" since only one peak is obtained for each compound injected.

The final application is the separation of the defoliant herbicides, diquat dibromide and paraquat dichloride. These compounds are

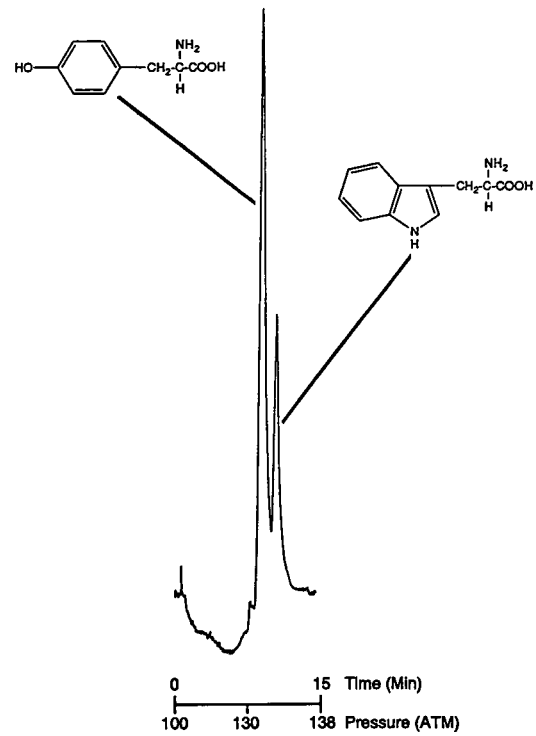


Fig. 5. SFC chromatogram of the amino acids tyrosine and tryptophan using ammonia as the mobile phase. Conditions: ammonia, 145°C, 15 cm × 1 mm I.D. OmniPAC μPRN-300, pressure programmed from 100 atm to 130 atm at 5 atm $min^{-1}$ following a 1-min isobaric hold, then 1 atm $min^{-1}$ to 138 atm, UV at 280 nm.

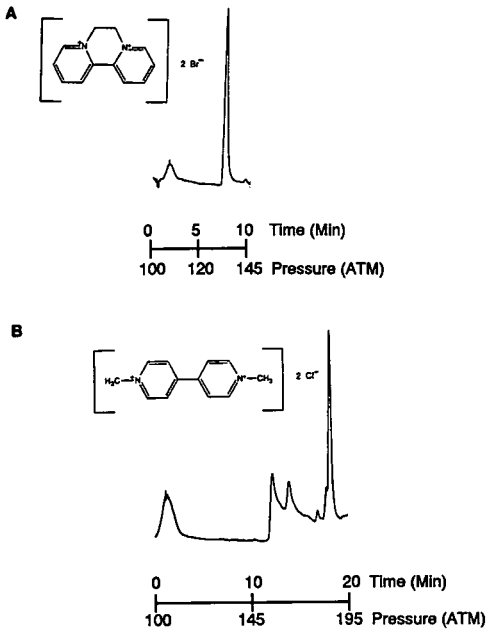


Fig. 6. SFC chromatograms of the defoliant herbicides diquat dibromide (A) and paraquat dichloride (B), using ammonia as the mobile phase. Conditions: ammonia, 145°C, 15 cm × 1 mm I.D. OmniPAC μPRN-300, pressure programmed from 100 atm at 5 atm $min^{-1}$ following a 1-min isobaric hold, UV at 254.

quaternary pyridinium salts of great environmental concern. Due to their nonvolatile nature, these materials cannot be analyzed by GC, and LC usually involves ion chromatography or an ion-pairing mobile phase. The potential for the analysis of these compounds by ammonia SFC is demonstrated in Fig. 6. Several very polar impurities are seen in the chromatogram in Fig. 6B.

These applications have demonstrated the use of ammonia as mobile phase in SFC. While other separation methods can be used for these polar samples, the use of neat mobile phases (such as ammonia) with high efficiency stationary phases (such as OmniPAC) has advantages of simplicity that must be explored further.

## ACKNOWLEDGEMENTS

The authors would like to thank the Dionex Corporation, especially Frank Yang (now with FFFractionation) and Chris Pohl, for gifts of the OmniPAC μPRN-300 columns and packing material, and for helpful discussions, Valco Instruments for gifts of the nickel capillary tubing, the Brigham Young University Department of Botany for performing scanning electron microscopy on the packing material, and Dr. Duane P. Mathees of South Dakota State University for gifts of the diquat dibromide and paraquat dichloride samples.

## REFERENCES

1 J.C. Kuei, *Ph.D. Dissertation*, Brigham Young University, Provo, UT, 1987.
2 J.C. Kuei, K.E. Markides and M.L. Lee, *J. High Resolut. Chromatogr. Chromatogr. Commun.*, 10 (1987) 257–262.
3 M. Abdel-Rehim, M. Hassan and H. Ehrsson, *J. High Resolut. Chromatogr.*, 13 (1990) 252–256.
4 J.C. Giddings, M.N. Myers, L. McLaren and R.A. Keller, *Science*, 162 (1968) 67–73.
5 L. McLaren, M.N. Myers and J.C. Giddings, *Science*, 159 (1968) 197–199.
6 K. Grolimund, W.P. Jackson, M. Joppich, W. Nussbaum, K. Anton and H.M. Widmer, in D. Ishii, K. Jinno and P. Sandra (Editors), *Proc. 7th International Symposium on Capillary Chromatography*, Hüthig, Heidelberg, 1986, pp. 625–636.
7 D. Parlier, D. Thiebaut, M. Caude and R. Rosset, *Chromatographia*, 31 (1991) 293.
8 H.H. Lauer, D. McManigill and R.D. Board, *Anal. Chem.*, 55 (1983) 1370–1375.
9 M. Abdel-Rehim, M. Hassan and H. Ehrsson, *J. High Resolut. Chromatogr.*, 14 (1991) 284–287.
10 F.J. Yang, presented at the *1989 Symposium/Workshop on Supercritical Fluid Chromatography, Snowbird, UT, June 13–15, 1989.*
11 Y. Liu, F. Yang and C. Pohl, *J. Microcol. Sep.*, 2 (1990) 245–254.
12 W. Braker and A.L. Mossman, *Matheson Gas Data Book*, Matheson Gas Products, Secaucus, NJ, 6th ed., 1980.
13 R.C. Reid, J.M. Prausnitz and B.E. Poling, *Properties of Gases and Liquids*, McGraw-Hill, New York, 4th ed., 1987.
14 A.M.F. Barton (Editor), *CRC Handbook of Solubility Parameters and Other Cohesion Parameters*, Chemical Rubber Publishing Co., Boca Raton, FL, 1983.
15 J.J. Lagowski and G.A. Moczygemba, in J.J. Lagowski (Editor), *Acidic and Basic Solvents*, Vol. II, Academic Press, New York, 1967, p. 336.
16 C.R. Yonker, S.L. Frye, K.R. Kalkwalf and R.D. Smith, *J. Phys. Chem.*, 90 (1986) 3022–3026.
17 S.L. Frye, C.R. Yonker, D.R. Kalkwalf and R.D. Smith, in T.G. Squires and M.E. Paulaitis (Editors), *Supercritical Fluids: Chemical and Engineering Principles and Applications (ACS Symposium Series*, No. 329), American Chemical Society, Washington, DC, 1987, pp. 29–41.

18 V.Ya. Baskakov and V.B. Baskakova, *Zh. Fiz. Khim.*, 64 (1990) 1678–1681.
19 H. Lentz and E.U. Franck, *Angew. Chem., Int. Ed. Engl.*, 17 (1978) 728–730.
20 R.E. Fornari, P. Alessi and I. Kikic, *Fluid Phase Equilib.*, 57 (1990) 1–33.
21 D. Peters, E.F. Paulus and H. Jacobs, *Z. Anorg. Allg. Chem.*, 584 (1990) 129–137.
22 G.L. Robing, *Ph.D. Dissertation*, University of Karlsruhe, Karlsruhe, 1981.
23 U. Liedtke and H. Lentz, *Ber. Bunsenges. Phys. Chem.*, 88 (1984) 921.
24 C.R. Yonker and R.D. Smith, *Fluid Phase Equilib.*, 22 (1985) 175–183.
25 D.S. Hacker, in T.G. Squires and M.E. Paulaitis (Editors), *Supercritical Fluids: Chemical and Engineering Principles and Applications* (*ACS Symposium Series*, No. 329), American Chemical Society, Washington, DC, 1987, pp. 213–228.
26 S.O. Oh and H.Y. Seok, *Taehan Hwahakhoe Chi*, 34 (1990) 663–672.
27 J.S. McPartland and R.D. Bautista, *Sep. Sci. Technol.*, 25 (1990) 2045–2055.
28 R.D. Smith and H.R. Udseth, *Anal. Chem.*, 55 (1983) 2266–2272.
29 C.R. Yonker, B.W. Wright, H.R. Udseth and R.D. Smith, *Ber. Bunsenges. Phys. Chem.*, 88 (1984) 908–911.
30 H.M. Pang and D.M. Lubman, presented at the *37th ASMS Conference on Mass Spectrometry and Allied Topics, Miami, FL, May 21–26, 1989.*
31 K.M. Payne, *Ph.D. Dissertation*, Brigham Young University, Provo, UT, 1990.
32 K.M. Payne, B.J. Tarbet, J.S. Bradshaw, K.E. Markides and M.L. Lee, *Anal. Chem.*, 62 (1990) 1379–1384.
33 T. Shaw, Dionex Corporation, Lee Scientific Division, personal communication.

*Journal of Chromatography*, 638 (1993) 85–96
Elsevier Science Publishers B.V., Amsterdam

CHROM. 24 807

# Enantiomer separation by complexation gas and supercritical fluid chromatography on immobilized polysiloxane-bonded nickel(II) bis[(3-heptafluorobutanoyl)-10-methylene-(1*R*)-camphorate] (Chirasil-nickel)

Michael Schleimer and Volker Schurig*

*Institut für Organische Chemie, Universität Tübingen, Auf der Morgenstelle 18, W-7400 Tübingen (Germany)*

(First received September 16th, 1992; revised manuscript received December 10th, 1992)

ABSTRACT

The synthesis of a polysiloxane containing chemically bonded chiral metal complex derived from nickel(II) bis[(3-heptafluorobutanoyl)-10-methylene-(1*R*)-camphorate] (Chirasil-nickel) and its effective immobilization on the inner surface of fused-silica capillaries by thermal treatment is described. As expected, the immobilization properties were found to be dependent on the content of residual reactive Si–R groups in the polymer backbone (R = $OCH_3$, H). The immobilized Chirasil-nickel stationary phase was employed for the analytical enantiomer separation of coordinating solutes by high-resolution capillary gas and supercritical fluid chromatography. The increase in the relative retention monitored for racemic test solutes after rinsing the columns indicates a slight increase in the effective complex concentration which does not affect the chiral separation factor $\alpha$. The temperature limit of analysis was raised to 170–180°C for temperature-programmed runs and to 140–150°C under isothermal conditions, thus extending the scope of *complexation gas chromatography* considerably, as demonstrated by various enantiomer separations performed at elevated temperatures. When Chirasil-nickel is immobilized on the inner surface of short, narrow-bore capillaries (50 $\mu$m I.D.), it can be employed in *complexation supercritical fluid chromatography*, combining the high solvation strength of supercritical carbon dioxide with the benefit of low operating temperatures, enhancing enantioselectivity.

## INTRODUCTION

As a consequence of a steadily refined insight into the relationship between chirality and biological activity, the exact determination of enantiomeric compositions and absolute configurations is an important task not only in research concerned with the synthesis, characterization and use of chiral compounds but also for the evaluation of chiral biologically active compounds (*e.g.*, analysis of chiral pharmaceuticals, flavours, fragrants, pheromones, insecticides and food additives) [1–3]. It is now well appreciated that the separation of enantiomers on chiral, non-racemic stationary phases by capillary chromatography represents a powerful tool for quantitative enantiomer analyses because of the high resolution, speed and sensitivity.

Chiral recognition in chromatography may arise from various types of enantioselective interactions between the solute (selectand) and the chiral, non-racemic moiety (selector), *e.g.*, hydrogen bonding [4], charge transfer [5], dipole–dipole [6], inclusion [7,8] and combinations thereof [9]. *Complexation chromatography* offers a valuable complementary method based on coordination as the formation of the diastereo-

* Corresponding author.

0021-9673/93/$06.00 

meric 1:1 complexes between the lone electron pairs of the selectand and the electronically and coordinatively unsaturated metal-containing selector is due to a rapid and reversible association equilibrium [10,11]. Useful selectors (which were termed Chira-metals) are bis(β-terpeneketoenolates) of manganese(II), cobalt(II), nickel(II), copper(II) and zinc(II) [12–14]. The unique molecular architectures displayed by terpeneketoenolates such as β-perfluoroacylated camphor, carvone, menthone and pulegone [15] provide a broad range in the variation of the enantioselectivity involved in the chiral recognition process.

Thus, racemic ethers, ketones, alcohols, acetals, esters and other classes of compounds have been quantitatively separated into enantiomers employing capillary glass of fused-silica columns coated with an 0.1 *m* (*m* = molal) solution of the chiral metal chelate {*e.g.*, nickel(II) bis[(3-heptafluorobutanoyl)-(1*R*)-camphorate] or other related Chira-metals} in an apolar liquid such as squalane or polysiloxanes [2]. As the maximum operation temperature of Chira-metal columns is limited to about 100°C (in some instances to 130°C for a short period of time) [16], it was desirable to decrease the volatility of the metal chelate by incorporating it in a polysiloxane matrix, thus combining the high enantioselectivity of Chira-metals with the thermostability and excellent coating properties of polysiloxanes reminiscent of Chirasil-Val [4], and related stationary phases [17–20], and Chirasil-Dex [21]. Finally, these chiral polysiloxanes can be cross-linked and/or immobilized on the inner surface of glass or fused-silica columns [19,20,22,23], resulting in non-extractable stationary phases containing chemically bonded chiral metal complexes (Chirasil-metal) suitable for on-column injection modes and for the use of mobile phases with higher density as in supercritical fluid chromatography (SFC) [24] and capillary electrophoresis (CE) [25].

In analogy with the total synthesis of Chirasil-Val [4,22] starting from monomers, and earlier attempt to prepare Chirasil-nickel by hydrolysis–equilibration of nickel(II) bis[(3-heptafluorobutanoyl)-(1*R*)-10-(dimethoxymethylsilyl)methylcamphorate] and diethoxymethylvinylsilane in the presence of trimethylsilanol led to a copolymeric stationary phase possessing clearly enhanced thermal stability [26]; however, attempts to cross-link or immobilize this phase by radical induction were not successful as small amounts of radical starters had an adverse effect on the metal chelate leading to a strong decrease in the observed chiral separation factors α [27].

In this paper, we describe a new synthetic pathway to Chirasil-nickel by a different approach through hydrosilylation of 3-heptafluorobutanoyl-(1*S*)-10-methylenecamphor to a preformed polymer containing Si–H functionalities and subsequent formation of the metal chelate which, after coating on the inner surface of fused-silica columns and thermal treatment, shows no loss in enantioselectivity and is stable against common organic solvents and even supercritical carbon dioxide at high densities [28].

## EXPERIMENTAL

### *Materials*

(1*S*)-10-Camphorsulphonic acid, polymethylhydrosiloxane, hexachloroplatinic acid and china clay were obtained from Aldrich (Steinheim, Germany). Octamethylcyclotetrasiloxane and hexamethyldisiloxane were obtained from ABCR (Karlsruhe, Germany). All solvents employed were of HPLC grade.

### *Instrumentation*

Carlo Erba Fractovap 2350 and 2150 and Mega HRGC 5300 gas chromatographs (Fisons, Mainz, Germany), equipped with flame ionization detectors (250°C), were used. The carrier gas was nitrogen or preferentially helium (both 99.996%) (Messer-Griesheim, Frankfurt, Germany), used without further purification (caution: hydrogen should not be employed as the carrier gas in *complexation gas chromatography*). The splitting ratio at the injector (250°C) was set to 1:100. In order to avoid overloading conditions, the instruments were set to their highest sensitivity at a tolerable signal-to-noise ratio. For SFC measurements a Carlo Erba SFC3000 instrument (Fisons), equipped with a syringe pump, pneumatic injection valve and flame ioni-

zation detector was used. The splitting ratio was set to about 1:40 and the column flow-rate was regulated by a laboratory-made integral-type restrictor (0.5–0.6 cm/s at 10.0 MPa and 80°C, which is about $5u_{opt}$ under these conditions).

*Synthesis of 3-heptafluorobutanoyl-(1S)-10-methylenecamphor (**1**)*

Compound **1** was prepared according to the general procedure of McCreary *et al.* [29] by acylation of 12.1 g (74 mmol) of (1*S*)-10-methylenecamphor [30] with 11 ml (74 mmol) of heptafluorobutanoyl chloride. The crude product was purified by flash-chromatography on 62–200-μm silica [toluene–*n*-hexane (3:1, v/v)], which was extracted with 2,4-pentanedione before use in order to remove traces of iron. The slightly red oil obtained was distilled in a Kugelrohr to yield 10.3 g (38%) of 3-heptafluorobutanoyl-(1*S*)-10-methylenecamphor, b.p. 50–55°C/0.01 mmHg; $\alpha_D^{25}$ +14.4 (0.1 dm; neat); $^1$H NMR ($CDCl_3$, 400 MHz), δ 11.75 and 2.90 (1H, tautomeric proton), 5.80–5.30 (m, 3H), 2.20–1.20 (m, 5H), 0.93 (s, 1H), 0.89 (s, 1H); mass spectrum, *m/z* 361 (16%), 360 ($M^+$, 100%), 317 (24%), 191 (19%), 163 (26%); 135 (29%), 108 (22%), 53 (24%).

*Synthesis of the dimethylpolysiloxane containing 10% hydromethylsiloxane units (**2**)*

In an atmosphere of nitrogen, 5.0 g (2 mmol polymer, 83 mmol Si–H) of polymethylhydrosiloxane (PMHS), 55.74 g (187 mmol) of octamethylcyclotetrasiloxane ($D_4$) and 3.45 g (21.3 mmol) of hexamethyldisiloxane (HMDSO) were mixed with 0.7 g of china clay by vigorous stirring, then 0.5 ml of concentrated sulphuric acid was added and the mixture was held at 100°C for 5 days. After cooling, the china clay was removed by suction of the diluted (150 ml of diethyl ether) reaction mixture through a frit. The solution was washed with water until neutral and the organic layer was separated and dried over anhydrous sodium sulphate, filtered and evaporated. The resulting polymer was held under vacuum ($10^{-3}$ mmHg) at 120°C, yielding 52 g (81%) of a clear viscous fluid. The $^1$H NMR spectrum indicated that the ratio of dimethylsiloxane to methylhydrosiloxane units was 10:1 (9% hydromethylsiloxane units) and titration [31] showed 1.2 mmol of Si–H per gram of prepolymer **2**.

*Hydrosilylation of **1** with polysiloxane **2***

A 3.0-g amount (1 mmol polymer, 3.6 mmol Si–H) of polysiloxane **2** and 1.3 g (3.6 mmol) of 3-heptafluorobutanoyl-(1*S*)-10-methylenecamphor (**1**) were dissolved in 75 ml of dry toluene in an atmosphere of nitrogen. A few droplets of a *ca.* 0.1% solution of hexachloroplatinic acid in dry tetrahydrofuran were added to the refluxing reaction mixture. After 24 h under reflux, the solvent was evaporated and the crude reaction mixture was heated with 25 ml of anhydrous methanol for about 3 h. The methanolic phase was decanted from the polymer, which was then washed several times with portions of anhydrous methanol. In this way 510 mg of **1** were recovered from the combined methanolic phases. Subsequent removal of low-molecular-mass compounds under vacuum ($10^{-3}$ mmHg; 1 mmHg = 133.322 Pa) at 90°C yielded 3.1 g (72%) of a clear polysiloxane (**3**) with a viscosity similar to that of polymer **2**. $^1$H NMR ($CDCl_3$, 400 MHz) δ 0.0–0.09 (m), 0.84 (s), 0.94 (s). The ratio of methyl groups in the polysiloxane to methyl groups of the ligand was found to be 20:1, indicating that about half of the Si–H present were consumed to bind the chiral ligand. IR (thin film, $cm^{-1}$), 2950, 2895, 1725, 1685, 1635, 1405, 1255, 1235, 1100–1010, 855, 790; $[\alpha]_D^{25}$ +22.2 (0.1 dm; $c = 5$, $CHCl_3$).

*Preparation of Chirasil-nickel*

A 2-g amount of the chiral polymer **3** was dissolved in 30 ml of *n*-heptane and a solution of 220 mg of nickel(II) acetate tetrahydrate (a *ca.* tenfold excess) in 20 ml of methanol was added under an atmosphere of nitrogen. The two-phase reaction mixture formed was vigorously stirred and heated at reflux for 30 min. The solvent was removed quantitatively under vacuum and 50 ml of *n*-pentane were added in order to separate the polymer from excess of nickel(II) acetate. Subsequent filtration and washing with several portions of water, followed by drying over anhydrous sodium sulphate and evaporation of the

solvent, yielded a dark-green polymer with increased viscosity. For removal of low-molecular-mass components Chirasil-nickel was dissolved in a small volume of dichloromethane (5 ml per gram of polymer) and precipitated with a 10–20-fold amount of anhydrous methanol. After three precipitation steps, which were accelerated by centrifugation, the residual solvent was removed at 90°C under vacuum ($10^{-3}$ mm Hg), yielding 1.3 g (65%) Chirasil-nickel, which was stored under nitrogen. IR (thin film, $cm^{-1}$), 2950, 2895, 1725, 1645, 1635, 1525, 1405, 1255, 1235, 1150–1000, 855, 790; $[\alpha]_D^{25}$ +26.7 (0.1 dm; $c = 5$, $CHCL_3$); atomic absorption spectrometry (AAS) 10.463 mg of Ni per gram of polymer, corresponding to a complex concentration of 0.205 *m*.

*Open-tubular columns*

Fused-silica tubing of 0.05–0.25 mm I.D. manufactured by Chrompack (Middelburg, Netherlands) was used. Each column was dehydrated at 250°C for 5 h at a very low carrier gas (helium or hydrogen) flow-rate. A solution of Chirasil-nickel in *n*-pentane–dichloromethane (2:1, v/v) (or pure *n*-pentane or diethyl-ether) was prepared and the columns were coated by the static method with a film thickness of 0.25 $\mu$m. The coated columns were installed in a GC oven and conditioned by temperature programming at a rate of 1°C/min from 50 to 160°C and held at the latter temperature overnight.

*Immobilization*

For thermal treatment, the flow-rate of the carrier gas (nitrogen or helium) was adjusted to *ca.* 30 bubbles per minute and the columns were maintained for 24 h at 180°C. When water vapour was added to the carrier gas, it was introduced by passing the carrier gas at room temperature through a vial with distilled water mounted upstream of the injection block [32]. After immobilization the columns were tested and then rinsed with 1 ml of methanol, 15 ml of methylene chloride (≥20 column volumes) and 5 ml of *n*-pentane. The degree of immobilization was calculated from the decrease in $k'$ for *n*-tridecane ($C_{13}$), measured at 90°C before thermal treatment and after rinsing. The $\alpha$ values and relative retentions with respect to *n*-decane determined for 2-methyltetrahydrofuran, 2-methycyclohexanone and 1-phenylethanol at 90°C gave information about changes in enantioselectivity and in concentration of the chiral selector.

## RESULTS AND DISCUSSION

*Synthesis*

As depicted in Fig. 1, the synthesis of Chirasil-metal in a "polymer-analogous rection" involves the introduction of unsaturation into the terpeneketoenolate ligand of the metal complex according to Matlin *et al.* [33]. We selected 3 - heptafluorobutanoyl-(1*S*)- 10 -methylenecamphor (note the formal change of the descriptor as compared with camphor owing to the priority change in the sequence rule of Cahn, Ingold and Prelog [34]) as a versatile ligand for the preparation of Chirasil-metal as it shows a broad range of enantioselectivity in complexation GC [2]. (1*S*)-10-Methylenecamphor prepared according to Fischer and Opitz [30] was perfluoroacylated according to McCreary *et al.* [29]. Subsequent hexachloroplatinic acid-catalysed hydrosilylation [35] of the unsaturated camphor ketoenolate **1**

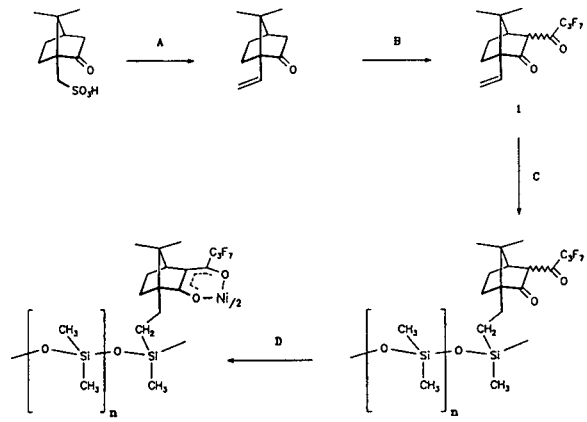


A 1. $SOCl_2$, 2. $CH_2N_2$, 3. > T B 4. LDA, $C_3F_7COCl$
C 5. $H_2PtCl_6$, prepolymer 2 D 6. $Ni(OOCCH_3)_2$ x 4 $H_2O$

Fig. 1. Scheme of synthesis of Chirasil-nickel. >T = higher temperature; LDA = lithium diisopropylamide.

with dimethylpolysiloxane containing Si–H groups (**2**) yielded polysiloxane **3**. The polymeric metal complex was obtained in a vigorously stirred two-phase reaction using *n*-heptane as solvent for the chiral polymer **3** and methanol as solvent for the metal(II) acetate. An excess of the metal(II) acetate was used in order to mediate the deprotonation of the β-diketone to afford Chirasil-nickel in nearly quantitative yield [33].

The nickel content of the polymers was determined by atomic absorption spectrometry to be 1.05%, which, taking into account that one metal complex requires two ligands, corresponds to a molality of 0.205 *m* nickel complex (in this calculation the methylene groups of the ligand directly attached to silicon are assumed to be part of the polymer in order to obtain values comparable to Chira-metal stationary phases). The Chirasil-nickel polymer shows an absorption at $\lambda_{max} = 322$ nm in the ultraviolet spectrum characteristic of the $\pi-\pi^*$ transition of the metal–chelate carbonyl groups. In addition to the dominant absorption of the Si–O–Si group at 1000–1100 $cm^{-1}$, the infrared spectrum of Chirasil-nickel shows bands at 1635, 1645 and 1725 $cm^{-1}$ characteristic of the ketoenolate structure in the metal complex. As it is expected for the paramagnetic nickel(II) ion, all signals of the ligand protons are severly broadened in the $^1H$ NMR spectrum, showing only two relatively sharp signals of methylsilyl (0–0.1 ppm) and methoxysilyl groups (3.45 ppm) from the polymeric backbone.

*Immobilization*

For employment in complexation GC, the fused-silica capillaries coated with Chirasil-nickel have to be conditioned at elevated temperature (160°C) overnight to remove strongly coordinating impurities or solvents such as water from the coordination sites of the metal ion. Immobilization and cross-linking of Chirasil-nickel are achieved by thermal treatment at temperatures above 170°C and reduced flow-rates of the carrier gas (nitrogen or helium; *not* hydrogen), which can be seen form Fig. 2, where the degree of immobilization *I*:

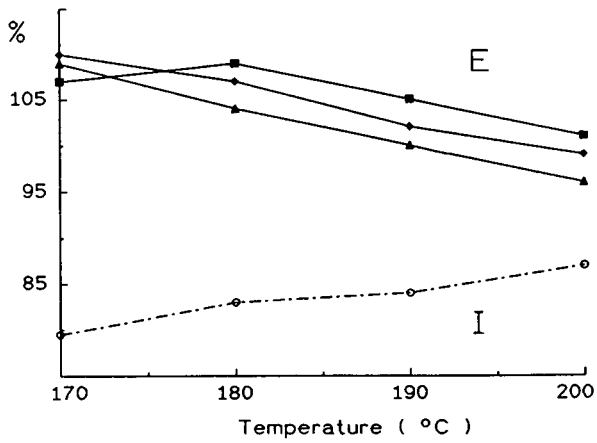


Fig. 2. Degree of immobilization *I* and enantioselectivity factor *E vs.* temperature for the thermal treatment (24 h) of Chirasil-nickel. Conditions: 5 m × 0.25 mm I.D. non-deactivated fused-silica columns (film thickness 0.3 μm); chromatographic measurements were performed at 90°C, 0.3 bar $N_2$. ■ = 2-Methyltetrahydrofuran; ▲ = 2-methylcyclohexanone; ◆ = 1-phenylethanol; ○ = *n*-tridecane.

$$I = 100[k'_{C_{13}}\text{ (after rinsing)}/ k'_{C_{13}}\text{ (before immobilization)}]$$

and the changes in separation factor α for chiral test solutes as expressed by the enantioselectivity factor *E*:

$$E = 100\{[\alpha\text{(after rinsing)} - 1]/[\alpha\text{ (before immobilization)} - 1]\}$$

are shown at different applied temperatures. The low temperature (*ca.* 180°C) needed for the immobilization of Chirasil-nickel is due to the presence of residual reactive sites (SiH, $SiOCH_3$) in the polymetric backbone, well known [36] for the improvement of immobilization during the thermal treatment of polysiloxanes. These reactive sites seem to be mainly methoxysilyl groups as the absorptions of the residual Si–H (IR 2125 $cm^{-1}$, NMR 4.7 ppm) after hydrosilylation change nearly quantitatively to signals of $Si-OCH_3$ groups (3.45 ppm) when the polymer **3** is refluxed with anhydrous methanol in order to hydrolyse undesired silylenol ethers of the β-diketone.

Compared with former batches of Chirasil-nickel, which were prepared by hydrosilylation

of **1** with a dimethylpolysiloxane containing only 4% hydromethylsiloxane units and showed no appreciable immobilization at temperatures below 200°C, good immobilization properties can be achieved easily by increasing the Si–H content of the prepolymer, thus roughly tripling the number of residual reactive sites in the resulting Chirasil-nickel. The low temperature (*ca.* 180°C) now accessible for the immobilization step does not reduce the enantioselectivity of the chiral stationary phase. The washout procedure even improves the observed enantioselectivity of Chirasil-nickel to values of $E \geq 100\%$ (*cf.*, Fig. 2), which does not depend on the time (12–48 h) or the temperature (140–190°C) employed for conditioning of the columns.

Fig. 3 gives more detailed information about the changes in $\alpha$, $k_2'$ and relative retention [10]:

$$r_2 = t_2' - t'_{n\text{-decane}}$$

(the subscript 2 refers to the second-eluted enantiomer) when Chirasil-nickel is immobilized at 180°C. Two methods were employed, differing in the use of carrier gas saturated with water vapour (*cf.*, Fig. 3, open squares) for 12 h instead of only heating the columns for 24 h (*cf.*, Fig. 2, closed squares). In both methods the separation factors $\alpha$ do not show significant changes when measured before thermal treatment and after rinsing, but the capacity factors $k_2'$ and relative retentions $r_2$ of the enantiomers tested increase with a simultaneous decrease in the retention of the *n*-alkane $C_{13}$. The alkane, whose retention is governed by the loss of stationary phase after rinsing and by any changes in the overall polarity during the immobilization procedure, indicates an increase in polarity during the thermal treatment of Chirasil-nickel in the absence of water. As the retention of the enantiomers, which is strongly influenced by the complex concentration due to the high chemical selectivity found in complexation GC [2], is found to decrease under the same conditions, this must be caused by blocking of the metal complex, *e.g.*, with polar by-products of the immobilization reaction. Rinsing of the column extracts the non-immobilized portions of the chiral stationary phase (15–20%), leading to a reduced retention of the alkane, whereas the $k_2'$

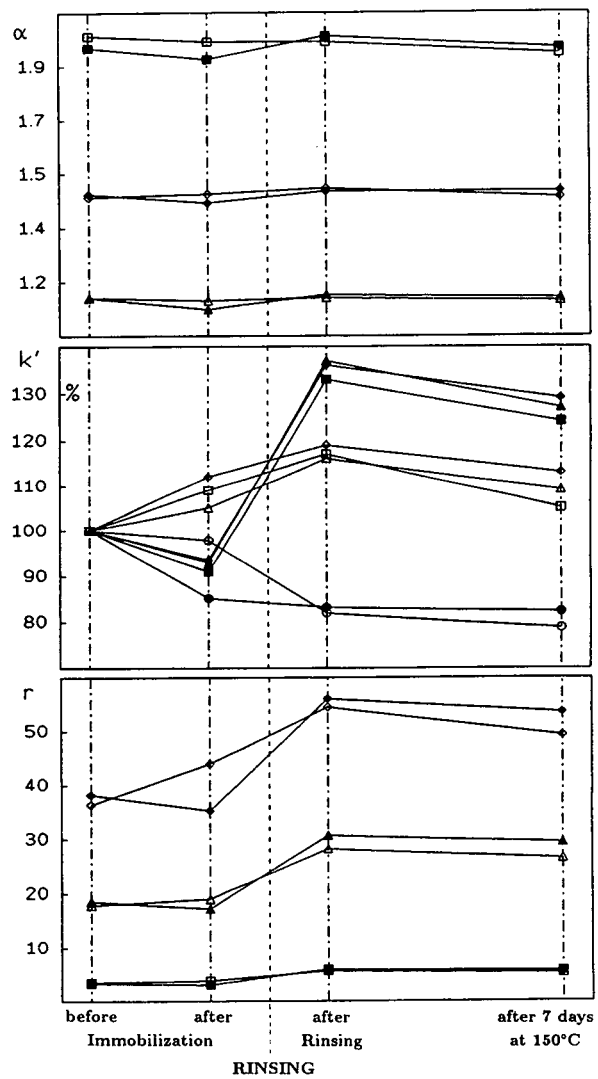


Fig. 3. Changes of $\alpha$ (top), $k_2'$ (middle) and $r_2$ (bottom) during thermal treatment of Chirasil-nickel at 180°C without water vapour (■, 24 h) and in the presence of water vapour (□, 24 h); other symbols as in Fig. 2. Conditions: 10 m × 0.25 mm I.D. non-deactivated fused-silica column (film thickness 0.3 $\mu$m); chromatographic measurements were performed at 90°C, 0.5 bar $N_2$.

and $r_2$ values of the enantiomers tested are found to be increased to 130–180%. The increased effective concentration of the metal complex in immobilized Chirasil-nickel thus monitored is the result of both rinsing out mainly achiral parts of the polymeric stationary phase and possibly an increase in the numbers of non-blocked coordi-

nation sites caused by simultaneously washing out of strongly adsorbed molecules with low vapour pressure which may have been introduced as impurities of the solvents used for synthesis and purification/precipitation of the Chirasil-nickel.

It has been found previously that the addition of water vapour to the carrier gas enhances immobilization rates [32,37]. For Chirasil-nickel the same degree of immobilization was already reached in half the time in the presence of water vapour during the thermal treatment. There were no changes in the chiral separation factors $\alpha$, but surprisingly the water added leads to an increase in the relative retention of the enantiomers during the immobilization procedure (*cf.*, Fig. 3). It is believed that complexed water molecules protect the complexation sites against other polar functionalities in the course of the immobilization reaction. When compared with the immobilization without water, the retention data were found to be always about 10% lower after rinsing of the columns treated with water vapour, indicating that part of the metal complex deteriorates during the contact with water at 180°C.

To summarize, the best conditions for the immobilization of Chirasil-nickel are thermal treatment for 24 h at 180°C with a very low flow-rate of the carrier gas. Although the addition of water vapour reduces the time needed for achieving the same immobilization rate of over 80% without a decrease in enantioselectivity, it leads to slightly lower relative retentions for

TABLE I

ENANTIOMER SEPARATION OF RACEMIC SOLUTES ON CHIRASIL-NICKEL

| Solute | Temperature (°C) | Pressure (bar $N_2$) | $k_1$ [a] | $\alpha$ [b] | $R_s$ [c] | $N$ (plates/m)[d] |
|---|---|---|---|---|---|---|
| Methyloxirane | 70 | 1.0 | 15.34 | 1.04 | 1.46 | 430 |
| Ethyloxirane | 90 | 1.0 | 7.76 | 1.04 | 1.38 | 831 |
| *tert.*-Butyloxirane | 90 | 1.0 | 3.29 | 1.22 | 6.18 | 570 |
| (*E*)-*sec.*-Butyloxirane | 90 | 1.0 | 8.43 | 1.10 | 3.27 | 865 |
| (*Z*)-*sec.*-Butyloxirane | | | 15.69 | 1.11 | 3.59 | 756 |
| 2,2-Dimethyl-3-phenyloxirane | 75 | 1.5 | 22.15 | 1.07 | 1.93 | 680 |
| 2-Methyloxetane | 130 | 1.0 | 5.02 | 1.29 | 10.02 | 915 |
| 2-Methyltetrahydrofuran | 90 | 1.0 | 3.56 | 2.02 | 25.40 | 766 |
| $\gamma$-Pentalactone | 120 | 1.2 | 10.29 | 1.03 | 1.20 | 1027 |
| $\delta$-Hexalactone | 140 | 0.9 | 10.92 | 1.02 | 1.10 | 1883 |
| Camphor | 130 | 1.0 | 7.49 | 1.12 | 4.59 | 1120 |
| Fenchone | 100 | 0.7 | 2.88 | 1.07 | 2.50 | 894 |
| (*E*)-5-Methylhept-2-en-4-one | 90 | 0.8 | 13.73 | 1.03 | 1.60 | 1427 |
| (*E*)-4-Methylheptan-3-ol | 110 | 0.7 | 2.47 | 1.04 | 1.54 | 1290 |
| (*Z*)-4-Methylheptan-3-ol | | | 2.64 | 1.04 | 1.54 | 1313 |
| 2-Methylhept-2-en-6-ol | 120 | 1.0 | 6.73 | 1.10 | 4.50 | 1430 |
| 6-Methylheptan-2-ol | 120 | 1.0 | 6.46 | 1.13 | 4.54 | 1099 |
| Octan-2-ol | 130 | 1.0 | 4.22 | 1.10 | 3.75 | 1190 |
| 1-Phenylethanol | 130 | 1.0 | 3.39 | 1.21 | 7.65 | 1620 |
| 1-Phenylpropanol | 130 | 1.0 | 4.22 | 1.07 | 2.92 | 1083 |
| 2-Octyl acetate | 130 | 1.0 | 2.82 | 1.07 | 2.68 | 1111 |
| 1-Phenyl-1-propyl acetate | 130 | 1.0 | 3.85 | 1.08 | 3.28 | 1123 |
| 1-Methyl-1-phenylbutyronitrile | 165 | 0.8 | 6.56 | 1.03 | 1.53 | 1183 |
| 1-Cyanonorbornan-2-ol | 160 | 1.5 | 14.95 | 1.07 | 2.06 | 763 |

[a] Capacity factor of the first-eluted enantiomer, measured on a 25 m × 0.25 mm I.D. non-deactivated fused-silica column coated with immobilized Chirasil-nickel (film thickness 0.25 $\mu$m).

[b] Chiral separation factor.

[c] Resolution $R_s = 1.177\ (\Delta t_R / \Sigma\ w_{0.5})$.

[d] $N = [5.54(t_1'/w_{0.5})^2]L^{-1}$

the tested enantiomers and was therefore abandoned. In addition, the immobilized Chirasil-nickel obtained by thermal treatment without additional water present exhibits much better long-term stability of all the chromatographic variables investigated. When conditioned after rinsing for 7 days at 150°C and a carrier gas flow-rate usually applied in chromatography (20–30 cm/s nitrogen), the decrease in the relative retention $r_2$ for the tested racemates was always smaller than 5%, whereas the enantioselectivity factor $E$ decreased by 1–10%, depending on the $r_2$ value of the solute employed for testing (*cf.*, Fig. 3).

*Complexation gas chromatography*

Owing to their high chemical selectivity the use of chiral metal complexes for the separation of enantiomers is not that universal when compared with cyclodextrin selectors, but if the separation is successful, the observed enantioselectivity is in most instances higher than

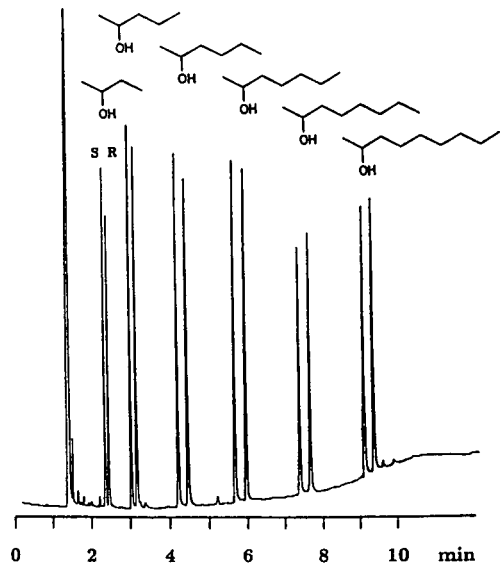


Fig. 5. GC enantiomer separation of homologous 2-alkanols on a 25 m × 0.25 mm I.D. non-deactivated fused-silica column coated with immobilized Chirasil-nickel (film thickness 0.25 μm). Conditions: temperature programmed from 125°C to 165°C at 6.0°C/min after an isothermal period of 3 min at 125°C; 1.0 bar He.

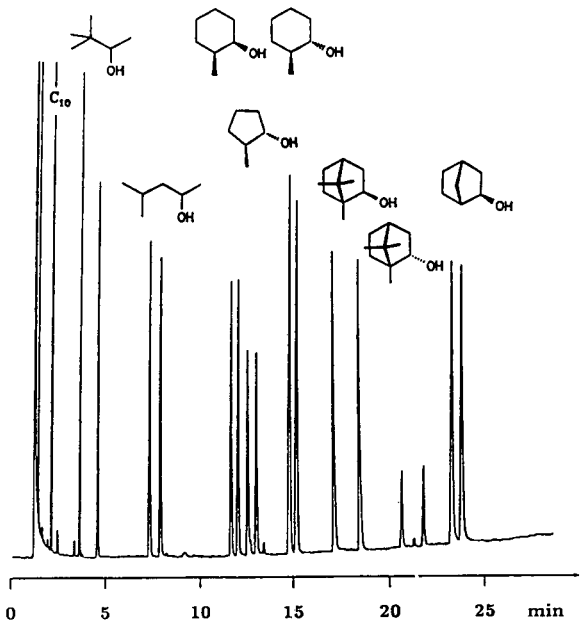


Fig. 4. GC enantiomer separation of acyclic, cyclic and bicyclic alcohols on a 25 m × 0.25 mm I.D. non-deactivated fused-silica column coated with immobilized Chirasil-nickel (film thickness 0.25 μm). Conditions: temperature programmed from 100°C to 145°C at 2.0°C/min after an isothermal period of 3 min at 100°C; 1.3 bar He.

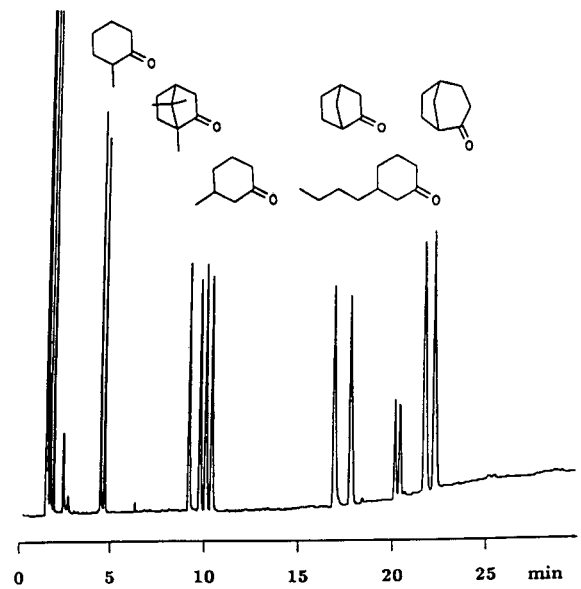


Fig. 6. GC enantiomer separation of cyclic and bicyclic ketones on a 25 m × 0.25 mm I.D. non-deactivated fused-silica column coated with immobilized Chirasil-nickel (film thickness 0.25 μm). Conditions: temperature programmed from 130°C to 170°C at 2.0°C/min after an isothermal period of 5 min at 130°C; 1.0 bar $N_2$.

those found on cyclodextrin columns. Together with the ease of access to both enantiomeric forms of the chiral ligand in the metal complex, which allows the elution order of the separated enantiomers to be reversed, this is of great interest for the tandem-determination of the enantiomeric excess in highly enriched samples [16].

Representative gas chromatograms demonstrating the enantiomer separation of racemates belonging to different classes of compounds obtained on the immobilized Chirasil-nickel are shown in Figs. 4–8 (see also the data in Table I). Although the fused-silica columns were not deactivated prior to coating, cyclic and acyclic alcohols (Figs. 4 and 5) show only slight peak tailing, which is essentially a result of the high complexation strength of alcohols towards the nickel complex, revealing a good coating and separation efficiency. Cyclic and bicyclic ketones (*cf.*, Fig. 6) are separated quantitatively into the enantiomers. Even the enantiomer separation of γ-lactones (*cf.*, Fig. 7), which cannot be readily carried out on Chira-metals [3], is feasible on the Chirasil-nickel stationary phase. For

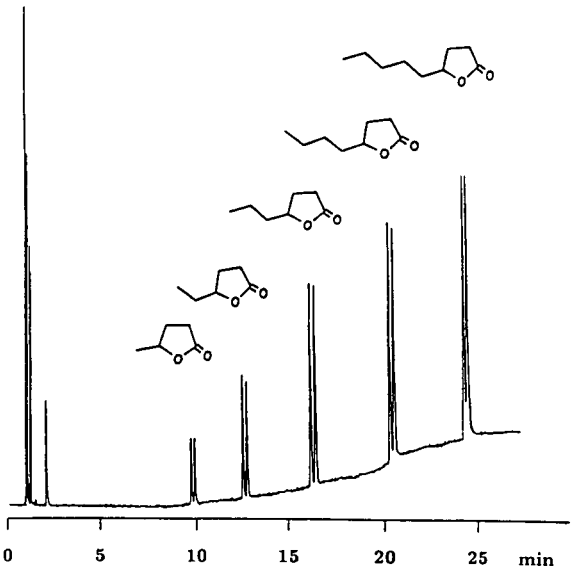


Fig. 7. GC enantiomer separation of homologous γ-lactones on a 25 m × 0.25 mm I.D. non-deactivated fused-silica column coated with immobilized Chirasil-nickel (film thickness 0.25 μm). Conditions: temperature programmed from 115°C to 170°C at 2.0°C/min after an isothermal period of 3 min at 115°C; 2.0 bar He.

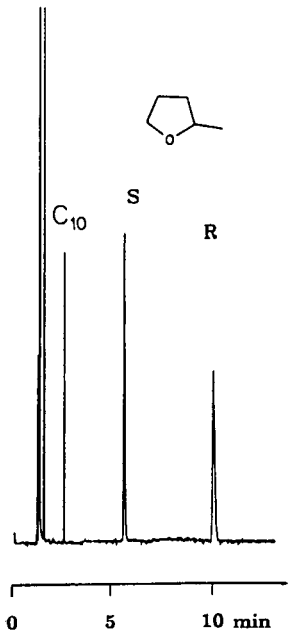


Fig. 8. GC enantiomer separation of 2-methyltetrahydrofuran on a 25 m × 0.25 mm I.D. non-deactivated fused-silica column coated with immobilized Chirasil-nickel (film thickness 0.25 μm). Conditions: temperature isothermal at 90°C; 1.0 bar $N_2$.

2-methyltetrahydrofuran a high separation factor ($\alpha = 2.02$ at 90°C; *cf.*, Fig. 8) was found. The configurationally labile enantiomers of homofuran show a temperature-dependent plateau between the resolved antipodes (enantiomerization) [38,39] during chromatography on Chirasil-nickel. The computer-simulated peak profile analysis [40] of chromatograms obtained between 95 and 130°C showed for the first time an example in complexation GC where the metal complex obviously exerted no catalytic effect of the interconversion of homofuran during chromatography as the rate constants found for mobile and stationary phase are very similar to the values obtained independently by polarimetry.

*Complexation supercritical fluid chromatography*

When coated on the inner surface of small-diameter fused-silica columns, Chirasil-nickel can be employed for *complexation SFC* using carbon dioxide as the mobile phase [28]. It is noteworthy that carbon dioxide, even in the

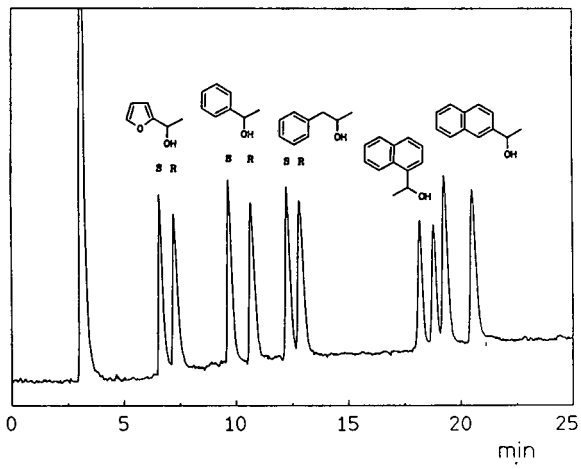


Fig. 9. SFC enantiomer separation of 1-(hetero)aryl functionalized ethanols on a 2.5 m × 0.05 mm I.D. non-deactivated fused-silica column coated with immobilized Chirasil-nickel (film thickness 0.25 μm). Conditions: $CO_2$, density programmed from 0.16 g/ml (9.60 MPa) at 0.015 g/ml · min to 0.46 g/ml (23.0 MPa) after an isothermal period of 5 min at 0.16 g/ml; temperature 120°C; flame ionization detection.

supercritical state, does not compete with solute molecules for coordination sites of the nickel ion. A high degree of immobilization is essential for these stationary phases in order to resist the solvation strength of supercritical carbon dioxide. A representative chromatogram is shown in Fig. 9, where the enantiomer separation of underivatized alcohols was achieved on a 2.5 m × 0.05 mm I.D. non-deactivated fused-silica column, coated with immobilized Chirasil-nickel.

Two features render capillary SFC more favourable than capillary GC for the separation of enantiomers. The low volatility of several compounds is not an obstacle in SFC owing to the strongly enhanced solvation power of supercritical mobile phases. As an example, racemic dimethyl 1,1′-binaphthyl-2,2′-dicarboxylate cannot be separated into enantiomers at the high temperature required for elution in complexation GC but can be quantitatively separated by complexation SFC (*cf.*, Fig. 10). More important, however, in the usual enthalpy-controlled domain of enantioselectivity, separation factors $\alpha$

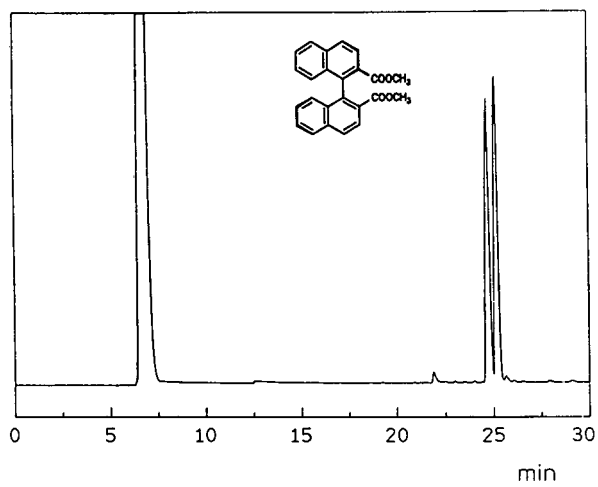


Fig. 10. SFC enantiomer separation of racemic dimethyl-1,1′-binaphthyl-2,2′-dicarboxylate on a 4 m × 0.05 mm I.D. non-deactivated fused-silica column coated with immobilized Chirasil-nickel (film thickness 0.40 μm). Conditions: $CO_2$ from 0.20 g/ml (9.30 MPa) at 0.02 g/ml · min to 0.6 g/ml (23.0 MPa) after an isothermal period of 10 min at 0.20 g/ml; temperature 70°C; flame ionization detection.

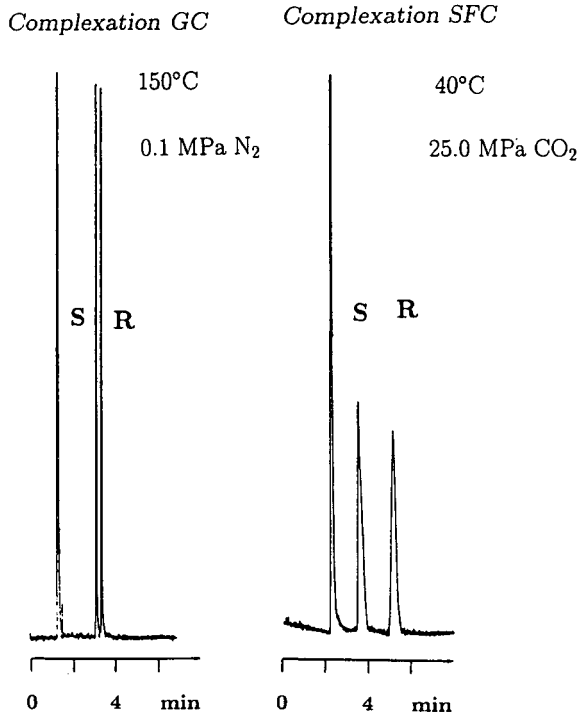


Fig. 11. Comparison of the enantiomer separation of 1-phenylethanol by complexation GC on a 25 m × 0.25 mm I.D. non-deactivated fused-silica column coated with immobilized Chirasil-nickel (film thickness 0.25 μm; temperature 150°C; 1 bar $N_2$) and complexation SFC on a 2 m × 0.05 mm I.D. non-deactivated fused-silica column coated with immobilized Chirasil-nickel [film thickness 0.25 μm; temperature 40°C; 0.883 g/ml (25.0 MPa)].

increase on decreasing the temperature of separation. Consequently, it must be the aim of chromatographic enantiomer separation to lower the analysis temperature in order to enhance enantioselectivity.

Fig. 11 shows the enantiomer separation of 1-phenylethanol in complexation GC and complexation SFC achieved under conditions characteristic for each method. When the resolution

$$R_s = \frac{\sqrt{N}}{4}\left(\frac{\alpha - 1}{\alpha}\right)\left(\frac{k_2'}{k_2' + 1}\right)$$

and overall retention times in both methods are adjusted to comparable values ($R_s = 2.15$, being sufficient for the quantitative enantiomer separation), the low analysis temperature accessible in complexation SFC gives $\alpha = 2.38$ (40°C), compared with 1.13 in complexation GC at 150°C.

For rapid elution of the separated enantiomers in SFC, the density of the supercritical carbon dioxide can be increased to 0.883 g/ml [250 atm (1 atm = 101 325 Pa)]. Although SFC cannot compete with GC with regard to efficiency, it is remarkable that here for the first time is an example where the enantioselectivity observed in GC can be improved considerably under SFC conditions by the use of low analysis temperatures, high mobile phase densities and relatively short, narrow-bore capillaries.

This result, which has also been found for other solutes, is in contrast to the results found for Chirasil-Val [41] and Chirasil-Dex [42]. Both chiral stationary phases show a significant decrease in enantioselectivity when the density of supercritical carbon dioxide is increased, which was explained by interactions of carbon dioxide with the selectors. The absence of such interactions reducing enantioselectivity recommends complexation SFC not only for the chromatography of non-volatile chiral molecules but also for an improvement in the enantioselectivity observed in complexation GC. However, a limiting factor that has to be considered is the decrease in the solute diffusion coefficients, especially at low analysis temperatures and high densities of the carbon dioxide. The observed increase in the separation factor $\alpha$ may thus be adversely compensated for by a decrease in efficiency, notably at higher flow-rates of the supercritical mobile phase.

## CONCLUSIONS

The use of immobilized Chirasil-nickel as enantioselective stationary phase greatly extends the scope of complexation GC and allows SFC to be employed for the analysis of enantiomers. The synthesis of related Chirasil-metals, *e.g.*, with manganese(II) or zinc(II) ions, carried out in the same manner, will further improve the applicability of this chiral stationary phase in complexation chromatography.

## ACKNOWLEDGEMENTS

This work was supported by the Deutsche Forschungsgemeinschaft and the Fonds der chemischen Industrie.

## REFERENCES

1 V. Schurig, in J.D. Morrison (Editor), *Asymmetric Synthesis*, Vol. 1, Academic Press, New York, 1983, p. 59.
2 V. Schurig, *Kontakte (Darmstadt)*, No. 1 (1986) 3.
3 V. Schurig, in P. Schreier (Editor), *Bioflavour '87*, Walther de Gruyter, Berlin and New York, 1988, p. 35.
4 H. Frank, G.J. Nicholson and E. Bayer, *J. Chromatogr. Sci.*, 15 (1977) 174.
5 F. Mikeš, G. Boshart and E. Gil-Av, *J. Chromatogr.*, 122 (1976) 205.
6 W.A. König, K. Stoelting and K. Kruse, *Chromatographia*, 10 (1977) 44.
7 V. Schurig and H.-P. Nowotny, *Angew. Chem., Int. Ed. Engl.*, 29 (1990) 939.
8 W.A. König, *Enantioselective Gas Chromatography on Modified Cyclodextrins*, Hüthig, Heidelberg, 1992.
9 W.H. Pirkle and T.C. Pochapsky, *Chem. Rev.*, 89 (1989) 347.
10 V. Schurig, R. C. Chang, A. Zlatkis and B. Feibush, *J. Chromatogr.*, 99 (1974) 147.
11 V. Schurig and W. Bürkle, *Angew. Chem., Int. Ed. Engl.*, 17 (1978) 132.
12 V. Schurig and W. Bürkle, *J. Am. Chem. Soc.*, 104 (1982) 7573.
13 V. Schurig and R. Weber, *J. Chromatogr.*, 217 (1984) 51.
14 M. Schleimer, *Diplomarbeit*, University of Tübingen, Tübingen, 1989.
15 V. Schurig, W. Bürkle, K. Hintzer and R. Weber, *J. Chromatogr.*, 475 (1989) 23.
16 V. Schurig, *J. Chromatogr.*, 441 (1988) 135.
17 T. Saeed, P. Sandra and M. Verzele, *J. Chromatogr.*, 186 (1979) 611.

18 W.A. König and I. Benecke, *J. Chromatogr.*, 209 (1981) 91.
19 W. Roeder, F.J. Ruffing, G. Schomburg and W.H. Pirkle, *J. High Resolut. Chromatogr. Chromatogr. Commun.*, 10 (1987) 665.
20 P. Peterson, K.E. Markides, D.F. Johnsson, B.E. Rossiter, J.S. Bradshaw and M.L. Lee, *J. Microcol. Sep.*, 4 (1992) 155.
21 V. Schurig, D. Schmalzing, U. Mühleck, M. Jung, M. Schleimer, P. Mussche, C. Duvekot and J. Buyten, *J. High Resolut. Chromatogr.*, 13 (1990) 713.
22 H. Frank, *J. High Resolut. Chromatogr. Chromatogr. Commun.*, 11 (1988) 787.
23 V. Schurig, Z. Juvancz, G.J. Nicholson and D. Schmalzing, *J. High Resolut. Chromatogr.*, 14 (1991) 58.
24 M. Schleimer and V. Schurig, in B. Wenclawiak (Editor), *Analysis with Supercritical Fluids*, Springer, Berlin, 1992, p. 134.
25 S. Mayer and V. Schurig, *J. High Resolut. Chromatogr.*, 15 (1992) 129.
26 V. Schurig and R. Link, in D. Stevenson and I.D. Wilson (Editors), *Chiral Separations*, Plenum Press, London and New York, 1992, p. 91.
27 R. Link, *Thesis*, University of Tübingen, Tübingen, 1987.
28 V. Schurig, D. Schmalzing and M. Schleimer, *Angew. Chem., Int. Ed. Engl.*, 8 (1991) 30.
29 M.D. McCreary, D.W. Lewis, D.L. Wernick and G.M. Whitesides, *J. Am. Chem. Soc.*, 96 (1974) 1038.
30 N. Fischer and G. Opitz, *Org. Synth., Coll. Vol.*, 5 (1973) 877.
31 G. Fritz and H. Burdt, *Z. Anorg. Chem.*, 317 (1962) 35.
32 G. Lai, G.J. Nicholson and E. Bayer, *Chromatographia*, 26 (1988) 229.
33 S.A. Matlin, W.J. Lough, L.C. Chan, D.M.H. Abram and Z. Zhou., *J. Chem. Soc., Chem. Commun.*, (1984) 1039.
34 R.S. Chan, C. Ingold and V. Prelog, *Angew. Chem., Int. Ed. Engl.*, 5 (1966) 385.
35 H. Figge, A. Deege, J. Köhler and G. Schomburg, *J. Chromatogr.*, 351 (1980) 393.
36 F.J. Ruffing, J.A. Lux, W. Roeder and G. Schomburg, *Chromatographia*, 26 (1988) 19.
37 G. Lai, *Thesis*, University of Tübingen, Tübingen, 1991.
38 W. Bürkle, H. Karfunkel and V. Schurig, *J. Chromatogr.*, 288 (1984) 1.
39 M. Jung and V. Schurig, *J. Am. Chem. Soc.*, 114 (1992) 529.
40 V. Schurig, M. Jung, M. Schleimer and F.G. Klärner, *Chem. Ber.*, 125 (1992) 1301.
41 G. Lai, G.J. Nicholson and E. Bayer, *J. Chromatogr.*, 540 (1992) 217.
42 D. Schmalzing, G.J. Nicholson, M. Jung and V. Schurig, *J. Microcol. Sep.*, 4 (1992) 2.

*Journal of Chromatography*, 638 (1993) 97–107
Elsevier Science Publishers B.V., Amsterdam

CHROM. 24 960

# Short Communication

# Determination of 22 protein amino acids as N(O)-*tert.*-butyldimethylsilyl derivatives by gas chromatography

Kang-Lyung Woo*

*Department of Food Engineering, Kyungnam University, 449 Wolyoung-dong, Masan 631-701 (South Korea)*

Duk-Kyu Chang

*Mong-Go Food Co., Ltd, Changwon Charyong Industrial Complex, Changwon City 641-450 (South Korea)*

(First received August 31st, 1992; revised manuscript received January 2nd, 1993)

ABSTRACT

Twenty-two protein amino acids were simultaneously derivatized to N(O)-*tert.*-butyldimethylsilyl derivatives by a single-step reaction at 75°C for 30 min with the silylating reagent N-methyl-N-(*tert.*-butyldimethylsilyl)trifluoroacetamide. All of the derivatives were quantitatively resolved in 41 min by GC on DB-1 capillary column. The relative standard deviations of the relative molar response with regard to the internal standard (pyrene) were less than 5% for all of the derivatives. Calibration graphs showed good linearity in the measured range. Correlation coefficients and regression coefficients for all of the calibration graphs were highly significant ($p < 0.001$). The mass spectra of the derivatives showed that all of the amino acids were derivatized to the N(O)-*tert.*-butyldimethylsilylamino acids.

## INTRODUCTION

The advantages of a gas chromatographic (GC) analysis of amino acids are obviously the low cost, the high sensitivity and the much greater versatility of the instrument compared with specialized amino acids analysers [1]. Moreover, GC offers a relatively simple means of combining the analytical system with mass spectrometry [2]. A disadvantage, however, is the necessity to derivatize the amino acids into more volatile, less polar compounds that are suitable for GC separation. Therefore, not only the development of GC systems but also the concomitant development of suitable derivative reactions are factors that lead to successful separations.

In most of the recent work in this field, the derivatization was carried out by more than two-step reactions, based on acylation of the $\alpha$-amino group and esterification of the carboxyl group. Even though the GC analysis of acylated amino acid alkyl esters has become routine, there are some negative aspects of the derivatization procedures such as two incompatible reaction media with an intermediate evapora-

* Corresponding author.

0021-9673/93/$06.00 

tion step, degradation of the amides, glutamine and asparagine, due to the HCl catalyst, low solubilities of some amino acids in the higher alcohols and high reaction temperatures [3]. Therefore, the quantitative derivatization of all the functional groups of protein amino acids by one-step reaction has been studied. A relatively successful method was the trimethylsilylation (TMS) procedure with the silylating agent bis-(trimethylsilyl)trifluoroacetamide (BSTFA) [4]. However, two different reaction times were required to derivatize quantitatively the protein amino acids. Fourteen amino acids could be silylated in 15 min at 135°C, whereas six amino acids (glutamic acid, arginine, lysine, histidine, tryptophan and cysteine) required 4 h at the same temperature. Glutamine and aspargine were also not detected as TMS derivatives. Glutamine, asparagine and their acids have been successfully derivatized to N(O)-*tert.*-butyldimethylsilyl (tBDMSi) derivatives by N-methyl-N-(*tert.*-butyldimethylsilyl)trifluoroacetamide (MTBSTFA) and quantitatively separated on an SPB-1 fused-silica capillary column by GC [5]. Since then, the analysis of tBDMSi amino acid derivatives by capillary GC have been successfully accomplished for standard protein amino acids [6–9], protein hydrolysates and physiological samples [6,10–13]. Mass spectra of the derivatives were also obtained in several studies [7,8,10,11]. However, we were not able to find a successful report of quantitative analysis and a single-step derivatization method under mild conditions for all 22 protein amino acids. Recently, the GC analysis of N(O,S)-ethoxycarbonyl amino acid ethyl ester derivatives obtained with ethyl chloroformate was accomplished for 21 protein amino acids, but derivatization of arginine was incomplete and it failed to elute from the column [14,15].

The objective of this investigation was to study the derivatization of the 22 protein amino acids simultaneously in one reaction step with MTBSTFA and the quantitative separation of the derivatives on a DB-1 capillary column by GC. To identify the tBDMSi amino acid derivatives mass spectra of the derivatives also were studied.

## EXPERIMENTAL

### *Materials*

N-Methyl-N-(*tert.*-butyldimethylsilyl)trifluoroacetamide (MTBSTFA) was obtained from Aldrich (Milwaukee, WI, USA). Standard amino acids were obtained from Sigma (St. Louis, MO, USA). All other reagents and solvents were of analytical-reagent grade.

### *Derivatization*

A mixture of standard amino acids (10 $\mu$l of solution containing 2.5 $\mu$mol/ml) was placed in a 1-ml conical vial and the solvent was completely evaporated at 50°C with dry nitrogen. Exactly 25 $\mu$l of internal standard (I.S.) solution (2.5 $\mu$mol of pyrene/ml of pyridine), 15 $\mu$l of MTBSTFA and 2 $\mu$l of triethylamine were added in that order. After tightly capping the vial, it was heated at 75°C for 30 min. After cooling to room temperature, the reaction mixture was injected directly on to the GC column.

### *Gas chromatography*

All chromatography was accomplished with a Hitachi 163 gas chromatograph equipped with a capillary injection system with a split injector and a flame ionization detector. A DB-1 (100% methylsiloxane) fused-silica capillary column (60 m × 0.35 m I.D., 0.25 $\mu$m film thickness) (J & W Scientific) was used. The carrier gas (hydrogen) flow-rate was 2 ml/min. The splitting ratio was 5:1. The make up gas was nitrogen at a flow-rate of 30 ml/min.

### *Mass spectrometry*

Mass spectra of tBDMSi amino acid derivatives were obtained using an HP 5971 mass-selective detector operated in the electron impact (EI) ionization mode. The ionization energy was 70 eV. A DB-1 capillary column (30 m × 0.25 mm I.D., 0.25 $\mu$m film thickness) was used. The carrier gas (helium) flow-rate was 0.9 ml/min. The other conditions were same as for GC.

## RESULTS AND DISCUSSION

### *Chromatography*

The chromatographic elution of the derivatives of a mixture of standard amino acids is shown in Fig. 1. All of the 22 protein amino acids were resolved in 41 min. Especially glutamine and asparagine were completely separated from their acids. The results for these four derivatives was similar to those reported previously [6,9–11]. Incompletely resolved derivatives were isoleucine and threonine, hydroxyproline-1 and cysteine and tryptophan and tyrosine. The hydroxyproline derivative showed multiple peaks. The peak of the cystine derivative appeared at about 300°C; this derivative seems less volatile than the others.

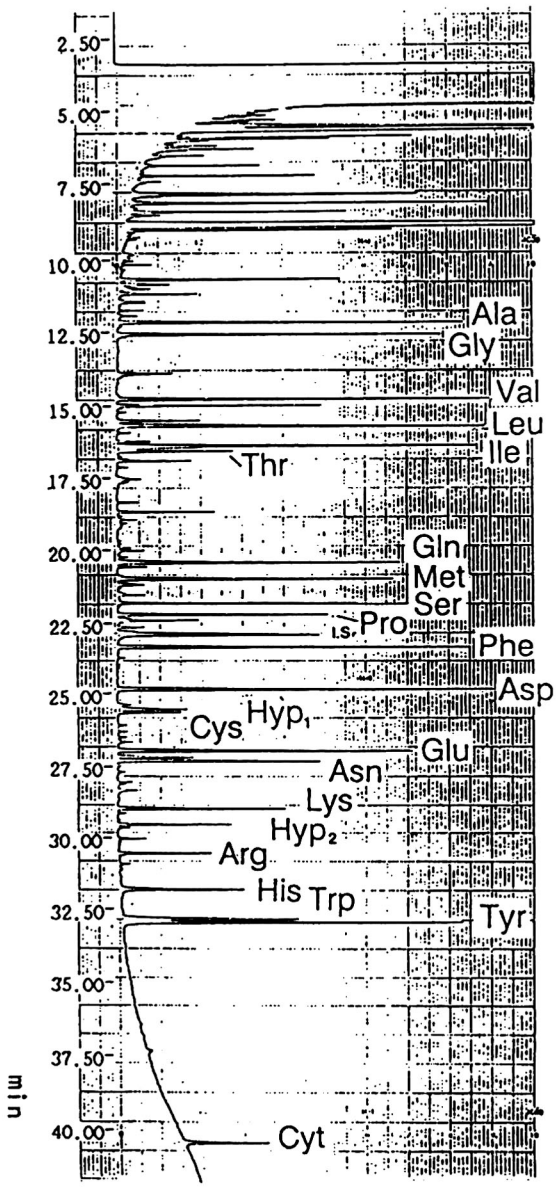


Fig. 1. Gas chromatogram of N(O)-*tert.*-butyldimethylsilyl-amino acids obtained on a DB-1 capillary column. Amount injected, 600 pmol, except cystine (1.2 nmol) and I.S. (750 pmol).

### *Relative molar response (RMR) and calibration graphs*

The molar responses relative to pyrene are given in Table I. Four replicate samples were analysed. The amount of each amino acid injected was 600 pmol and that of pyrene (I.S.) was

TABLE I

RELATIVE MOLAR RESPONSES (RMR) OF N(O)-*tert.*-BUTYLDIMETHYLSILYLAMINO ACID DERIVATIVES

| Amino acid | RMR[a] | S.D.[b] | R.S.D. (%)[b] |
|---|---|---|---|
| Ala | 2.855 | 0.113 | 3.96 |
| Gly | 2.620 | 0.083 | 3.17 |
| Val | 3.190 | 0.015 | 3.61 |
| Leu | 3.343 | 0.108 | 3.23 |
| Ile | 3.293 | 0.155 | 4.71 |
| Thr | 1.178 | 0.058 | 4.92 |
| Gln | 2.430 | 0.048 | 1.98 |
| Met | 2.920 | 0.068 | 2.33 |
| Ser | 1.675 | 0.075 | 4.48 |
| Pro | 1.895 | 0.068 | 3.59 |
| Phe | 3.298 | 0.055 | 1.67 |
| Asp | 3.353 | 0.053 | 1.58 |
| Hyp1 | 0.885 | 0.008 | 0.90 |
| Cys | 0.648 | 0.030 | 4.63 |
| Glu | 2.665 | 0.088 | 3.30 |
| Asn | 1.898 | 0.078 | 4.11 |
| Lys | 1.670 | 0.075 | 4.49 |
| Hyp2 | 0.758 | 0.037 | 4.88 |
| Arg | 0.670 | 0.032 | 4.78 |
| His | 0.815 | 0.008 | 0.98 |
| Trp | 1.928 | 0.060 | 3.11 |
| Tyr | 3.148 | 0.140 | 4.45 |
| Cyt | 0.410 | 0.020 | 4.88 |

[a] Values are relative to pyrene = 1.
[b] $n = 4$.

750 pmol. The relative standard deviations (R.S.D.s) were less than 5% ($n = 4$) for all of the amino acid derivatives. The reproducibility showed high precision. The arginine, hydroxyproline, histidine, cysteine and cystine peaks were relatively small; especially the cystine peak was so small that it could not be detected at levels below 400 pmol. There are several reports that arginine is the most difficult amino acid to derivatize completely [7,8,10], but in our study cystine also seemed to be difficult to derivatize at temperatures below 75°C.

Calibration graphs for all of the amino acid derivatives, obtained by plotting the ratios of their peak areas to that of internal standard, showed good linearity in the range 238–833 pmol, except for the cystine derivative, which showed linearity in the range 476–1900 pmol (Table II). Cystine, proline, histidine and arginine showed poor linearity compared with the other derivatives. The correlation coefficients of the calibration graphs for these derivatives were also highly significant ($p < 0.001$). Typically, the R.S.D.s were lower than 5% ($n = 5$), except for serine, proline, cysteine, arginine, histidine, tryptophan and cystine, which showed higher values but <10%.

*Mass spectra*

The identities of the derivatives were established by EI mass spectrometry. The mass spectra were characterized by the ions M − 15 ($CH_3$), M − 57 [$C(CH_3)_3$], M − 85 [$C(CH_3)_3$ + CO], M − 159 [$COOSi(CH_3)_2C(CH_3)_3$], M − R, $m/z$ 189 [$(CH_3)C(CH_3)_2\overset{+}{S}iO = Si(CH_3)_2$], 147 [$(CH_3)_3\overset{+}{S}iO = Si(CH_3)_2$], 133 [$(CH_3)_2H\overset{+}{S}iO = Si(CH_3)_2$] and 73 [$(CH_3)_3\overset{+}{S}i$]. In sulphur amino acids, additional fragmentations were observed for C–S and S–S bond cleavage with charge retention on either fragment. These fragmentation patterns were similar to those for TMS derivatives [16] and tBDMSi derivatives in other reports [7,8,10,11], where TMS derivatives of aliphatic $\alpha$-amino acids were characterized by molecular ions M − 15 ($CH_3$), M − 43 ($CH_3$ + CO), M − 117 (COOTMS) and M − R [16] and tBDMSi amino acid derivatives by molecular ions, M − 15, M − 57, M − 85, M − 159, M − 302 and M − R [7,10].

TABLE II

LINEAR REGRESSION ANALYSIS OF RELATIVE MOLAR RESPONSE AGAINST AMOUNT INJECTED OF AMINO ACID AS THEIR tBDMSi DERIVATIVES

Internal standard, pyrene: amounts injected, 238, 357, 476, 595, 714 and 833 pmol ($n = 4$).

| Amino acid | Regression line[a] | | |
|---|---|---|---|
| | *s* | *b* | *r* |
| Alanine | 0.0017 | 0.081 | 0.979 |
| Glycine | 0.0017 | 0.022 | 0.989 |
| Valine | 0.0017 | 0.153 | 0.992 |
| Leucine | 0.0019 | 0.129 | 0.991 |
| Isoleucine | 0.0019 | 0.116 | 0.994 |
| Threonine | 0.0009 | −0.108 | 0.992 |
| Glutamine | 0.0014 | 0.097 | 0.983 |
| Methionine | 0.0018 | 0.052 | 0.991 |
| Serine | 0.0014 | −0.060 | 0.969 |
| Proline | 0.0011 | 0.002 | 0.935 |
| Phenylalanine | 0.0021 | 0.018 | 0.989 |
| Aspartic acid | 0.0022 | 0.030 | 0.993 |
| Cysteine | 0.0007 | −0.073 | 0.979 |
| Glutamic acid | 0.0019 | −0.008 | 0.991 |
| Asparagine | 0.0014 | −0.072 | 0.989 |
| Lysine | 0.0014 | −0.164 | 0.992 |
| 2-Hydroxyproline | 0.0005 | 0.056 | 0.968 |
| Arginine | 0.0005 | 0.007 | 0.964 |
| Histidine | 0.0011 | −0.342 | 0.975 |
| Tryptophan | 0.0018 | −0.338 | 0.982 |
| Tyrosine | 0.0024 | −0.102 | 0.992 |
| Cystine | 0.0011 | −0.060 | 0.969 |

[a] $s$ = Slope; $b$ = intercept; $r$ = correlation coefficient.

The relative intensity of the major ions in the EI mass spectra of tBDMSi amino acid derivatives are given in Table III. Molecular ions were not detected except for methionine, lysine and histidine. The relative intensity of the lysine molecular ion was high (7.1%). The fragmented ions of M − 57, M − 85 and $m/z$ 147 and 73 were detected with high intensity for all derivatives. Even though the fragment of $m/z$ 133 was detected with relatively lower intensity than the above fragments, it could be observed in all derivatives.

The $m/z$ 133 fragment was also observed in the chemical ionization mass spectra of the tBDMSi derivatives of glutamine and asparagine in another study [5]. In our study, we considered

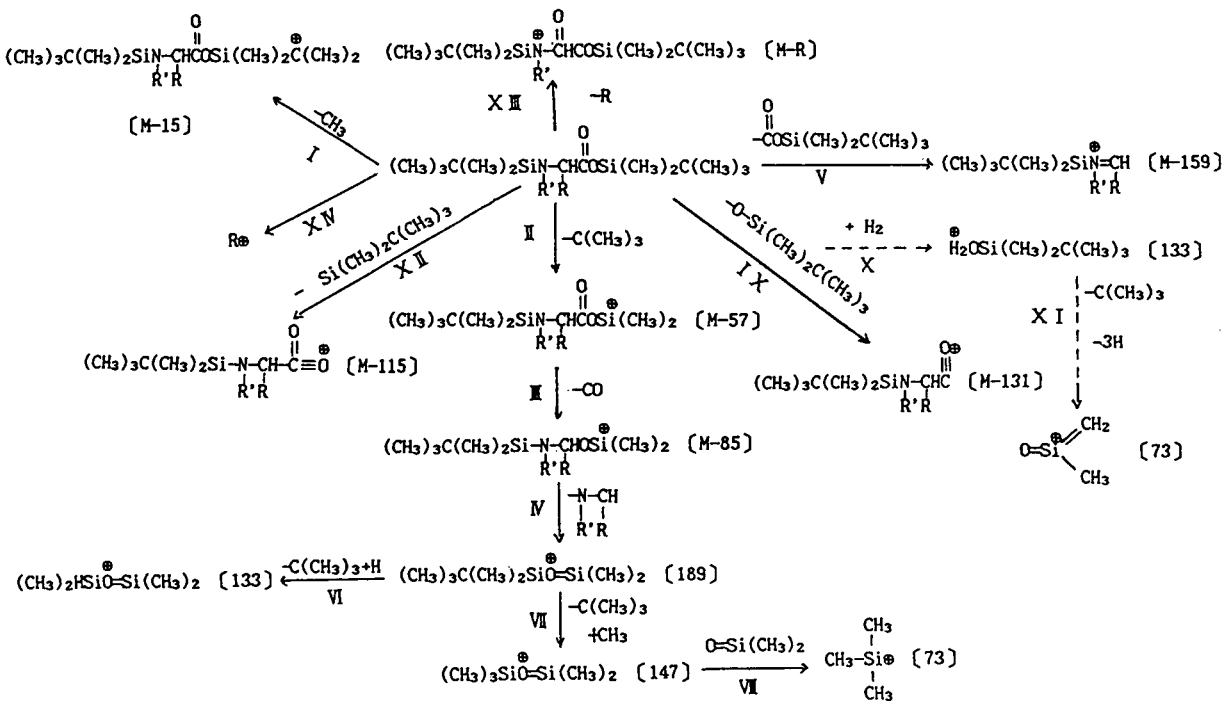

Fig. 2. Possible MS fragmentation pathways of N(O)-*tert.*-butyldimethylsilylamino acids.

that the *m/z* 133 fragment would be produced from pathway VI (Fig. 2), as an intermediate fragment of *m/z* 189 $[(CH_3)_3C(CH_3)_2SiO^+ = Si(CH_3)_2]$ prior to the *m/z* 133 fragment was detected for all the derivatives (Table III). If the *m/z* 133 fragment were $[H_2OSi(CH_3)_2C(CH_3)_3]$, the M − 131 fragment should be detected for all the derivatives, but it was not observed with most of them. We therefore consider that pathways IX, X and XI (Fig. 2) hardly take place. The intensity of the M − 57 fragment was far greater than that of the M − 15 fragment. As neutral radicals have the stability order tertiary > secondary > primary [17], the cleavage pathway would favour pathway II rather than I (Fig. 2).

Mass spectral fragmentations of tBDMSi amino acids are shown in Figs. 3–7. All the derivatives were broken down almost according to the pathways in Fig. 2. The glutamine mass spectrum was consistent with the conversion of glutamine to pyroglutamic acid. It could be concluded, on the basis of the mass spectrum, that the glutamine derivative was a pyroglutamic acid derivative that had been quantitatively converted into pyroglutamic acid during the derivatization reaction [5]. However, glutamine is converted to ammonia and pyroglutamic acid on heating under weakly acidic or alkaline conditions [18,19] and the reaction proceeds slowly even at *ca.* 4°C. Further, there is a report that glutamine can be derivatized with MTBSTFA without loss of the amino moiety and without cyclization to produce a chromatographically stable compound [11]. It appears, therefore, that the conversion to pyroglutamic acid occurred during the storage of standard glutamine in 0.1 *M* hydrochloric acid.

An M − 13 fragment was found for proline and hydroxyproline. We assume that this fragment was produced as follows:

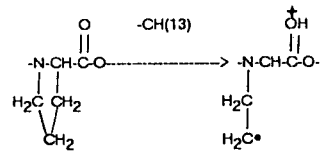

TABLE III

RELATIVE INTENSITIES OF MAJOR IONS IN THE EI MASS SPECTRA OF N(O)-*tert.*-BUTYLDIMETHYLSILYL (tBDMSi) AMINO ACID DERIVATIVES

| Ion | Ala | Gly | Val | Leu | Ile | Thr | Gln | Met | Ser | Pro | Phe | Asp | Hyp1 | Cys | Glu | Asn | Lys | Hyp2 | Arg | His | Trp | Tyr | Cyt |
|---|---|---|---|---|---|---|---|---|---|---|---|---|---|---|---|---|---|---|---|---|---|---|---|
| M | – | – | – | – | – | – | – | 1.4 | – | – | – | – | – | – | – | – | 7.1 | – | – | 0.4 | – | – | – |
| M – $CH_3$ | 2.8 | 3.2 | 2.2 | 1.8 | 1.9 | 1.4 | 7.5 | 3.0 | 4.7 | 0.4 | 3.1 | 2.0 | 0.4 | 2.5 | 3.2 | 1.5 | 1.2 | – | – | 2.1 | – | 2.3 | – |
| M – $C(CH_3)_3$ | 55.3 | 77.3 | 36.6 | 36.8 | 52.9 | 53.4 | 100 | 75.1 | 75.6 | 5.7 | 49.5 | 45.2 | 26.0 | 63.0 | 86.1 | 90.1 | 13.7 | 5.7 | – | 44.4 | 28.9 | 9.5 | 3.3 |
| M – $C(CH_3)_3$ – CO | 56.3 | 74.3 | 40.4 | 37.3 | 37.9 | 5.4 | 79.3 | 83.9 | 67.8 | 20.1 | 45.6 | 20.5 | 17.7 | 54.4 | 9.6 | – | – | 8.8 | – | 1.7 | 5.1 | 4.5 | – |
| M – COOtBDMSi | 100 | 17.2 | 100 | 100 | 100 | 29.4 | 21.1 | 100 | 87.5 | 27.5 | 66.7 | 35.0 | 22.0 | 84.8 | 72.3 | 12.3 | 17.8 | 30.7 | 2.4 | 30.6 | 6.6 | 9.1 | 1.6 |
| M – R | – | – | 15.8 | 36.8 | 52.9 | 42.5 | – | 4.7 | 46.3 | – | 100 | 69.2 | – | 88.5 | – | 33.6 | 66.4 | – | 4.8 | 8.7 | 100 | 100 | 47.8 |
| $R^+$ | – | – | – | – | – | – | – | – | – | – | – | – | – | – | – | – | – | – | 8.4 | 100 | 24.7 | 5.0 | – |
| $(CH_3)_3C(\overset{+}{C}H_3)_2SiO = Si(CH_3)_2$ | 1.8 | 8.0 | 1.3 | 1.0 | 1.7 | 6.6 | 2.4 | 2.4 | 2.1 | 0.5 | 1.3 | 4.7 | 1.0 | 1.5 | 2.6 | 4.4 | 1.5 | 1.0 | 7.1 | 0.2 | 2.0 | 1.0 | 7.7 |
| $(CH_3)_3SiO = Si(CH_3)_2$ | 45.5 | 100 | 23.0 | 18.2 | 19.5 | 25.9 | 15.0 | 46.7 | 31.8 | 14.7 | 29.7 | 27.3 | 19.8 | 25.9 | 35.9 | 30.4 | 23.8 | 23.8 | 14.5 | 5.5 | 9.9 | 6.8 | 19.7 |
| $HSi(CH_3)_2O = Si(CH_3)_2$ | 8.1 | 9.3 | 6.1 | 5.3 | 6.2 | 10.7 | 8.3 | 10.9 | 14.6 | 4.6 | 9.2 | 10.7 | 7.3 | 10.5 | 11.9 | 9.7 | 10.9 | 11.3 | 7.2 | 2.4 | 6.6 | 2.3 | 8.0 |
| $(CH_3)_3Si^+$ | 54.2 | 73.8 | 40.6 | 33.2 | 42.2 | 100 | 79.4 | 85.7 | 100 | 39.8 | 68.6 | 100 | 72.6 | 100 | 100 | 100 | 100 | 92.3 | 100 | 53.3 | 57.4 | 40.9 | 100 |

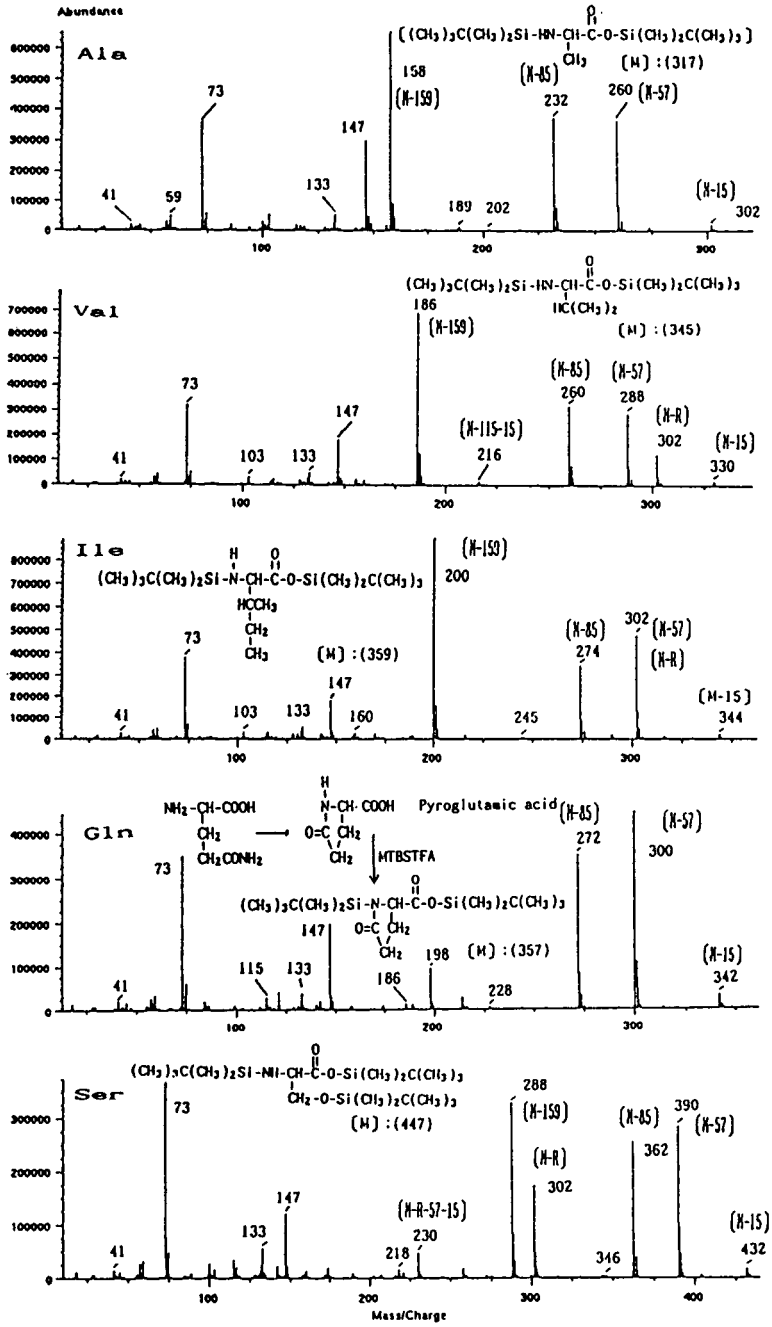


Fig. 3. EI mass spectra of N(O)-*tert.*-butyldimethylsilyl derivatives of alanine, valine, isoleucine, glutamine and serine. M − 15, $CH_3$; M − 57, $C(CH_3)_3$; M − 85, $C(CH_3)_3$ + CO, M − 115, $Si(CH_3)_2C(CH_3)_3$; M − 131, $OSi(CH_3)_2C(CH_3)_3$; M − 159, $COOSi(CH_3)_2C(CH_3)_3$; 189, $(CH_3)_3C(CH_3)_2SiO = Si(CH_3)_2$; 147, $(CH_3)_3Si\text{-}O = Si(CH_3)_2$; 133, $(CH_3)_2HSiO = Si(CH_3)_2$; 73, $(CH_3)_3Si$.

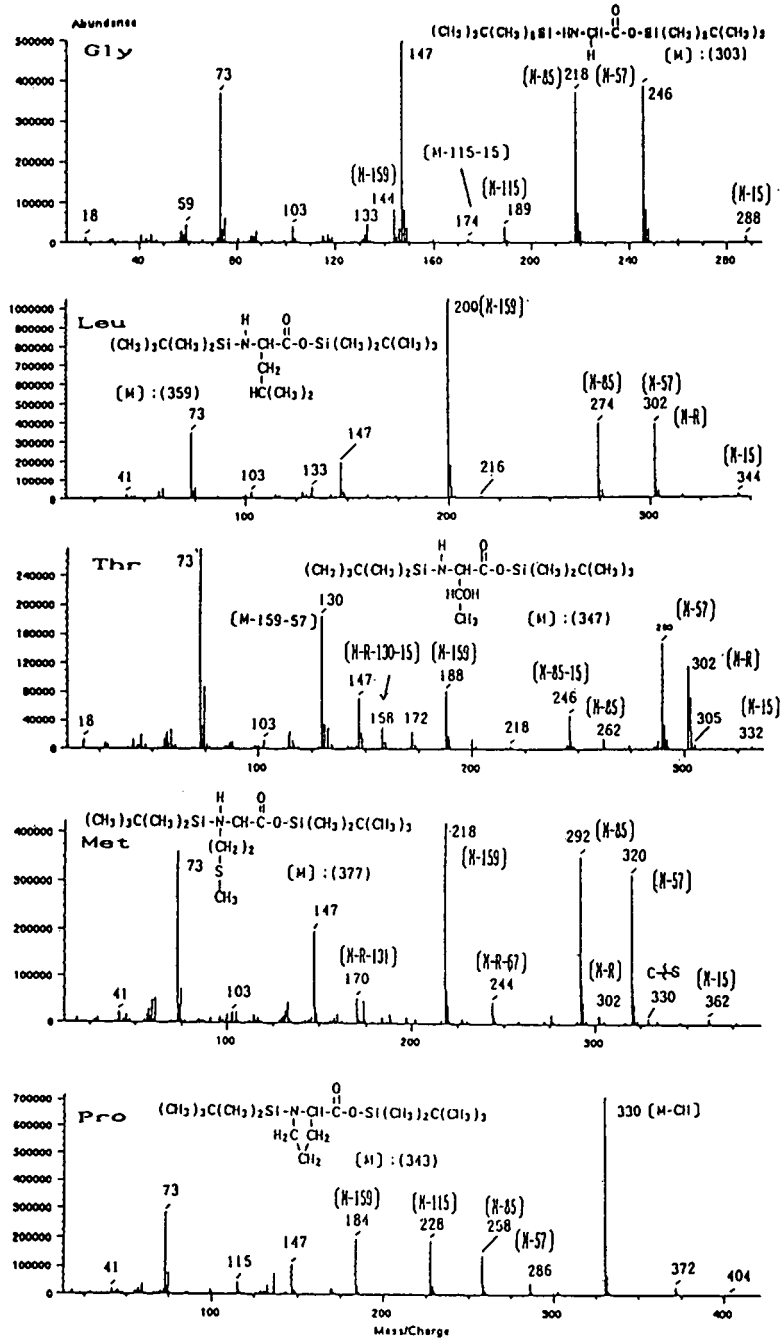


Fig. 4. EI mass spectra of N(O)-*tert.*-butyldimethylsilyl derivatives of glycine, leucine, threonine, methionine and proline.

In the spectrum of arginine, ions of $m/z$ 442 ($M - C_4H_7 - CH_3$), 340 ($M - 172$) and 207 were found with other unusual ions. In the spectrum of cystine, the M/2 ion produced from cleavage of the S–S bond was observed with high intensity.

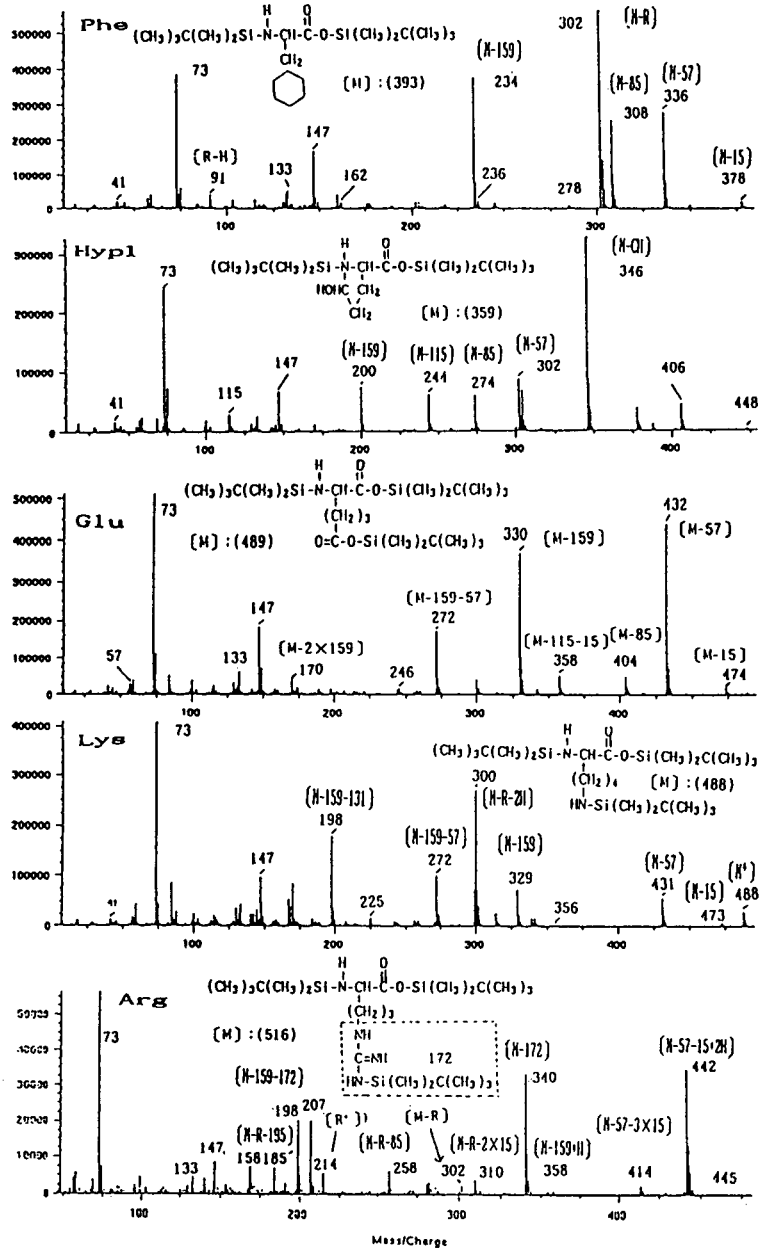


Fig. 5. EI mass spectra of N(O)-*tert.*-butyldimethylsilyl derivatives of phenylalanine, hydroxyproline-1, glutamic acid, lysine and arginine.

## CONCLUSIONS

Amino and carboxyl groups of all protein amino acids can be silylated to the N(O)-*tert.*-butyldimethylsilyl derivatives by a single-step reaction with N-methyl-N-(*tert.*-butyldimethylsilyl) trifluoroacetamide as the silylating reagent.

All 22 protein amino acid derivatives were

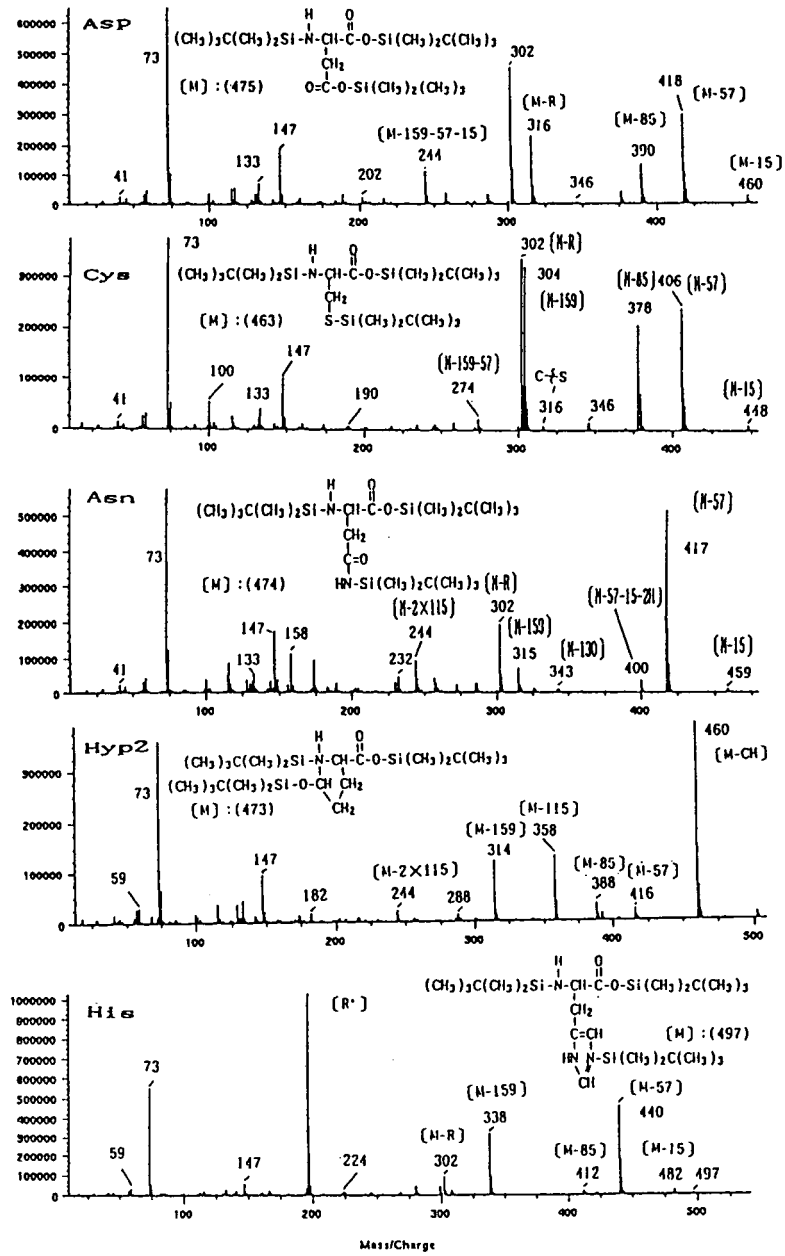


Fig. 6. EI mass spectra of N(O)-*tert.*-butyldimethylsilyl derivatives of aspartic acid, cysteine, asparagine, hydroxyproline-2 and histidine.

successfully separated on a DB-1 capillary column (60 m × 0.35 mm I.D.). Because the R.S.D.s of the relative molar responses were <5% and the calibration graphs showed good linearity, this method could be useful for both the qualitative and quantitative analysis of protein amino acids. The extension of this method to biological amino acids is in progress.

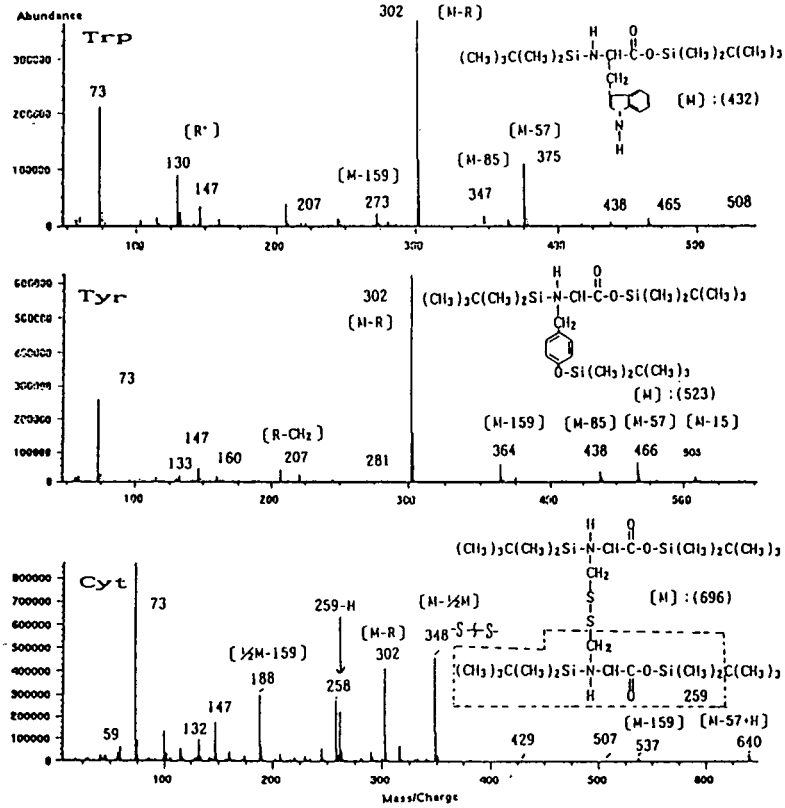


Fig. 7. EI mass spectra of N(O)-*tert.*-butyldimethylsilyl derivatives of tryptophan, tyrosine and cystine.

ACKNOWLEDGEMENT

Financial support for this project from the Korea Research Foundation is gratefully acknowledged.

REFERENCES

1 C.W. Gehrke, L.L. Wall, J.S. Absheer, F.E. Kaiser and R.W. Zumwalt, in R.W. Zumwalt, K.C.T. Kuo and C.W. Gehrke (Editors), *Amino Acid Analysis by Gas Chromatography*, Vol. I, CRC Press, Boca Raton, FL, 1987, p. 2.
2 P. Hušek and K. Macek, *J. Chromatogr.*, 113 (1975) 139.
3 P. Hušek, in R.W. Zumwalt, K.C.T. Kuo and C.W. Gehrke (Editors), *Amino Acid Analysis by Gas Chromatography*, Vol. III, CRC Press, Boca Raton, FL, p. 94.
4 C.W. Gehrke, H. Nakamoto and R.W. Zumwalt, *J. Chromatogr.*, 45 (1969) 24.
5 S.L. MacKenzie and D. Tenaschuk, *J. Chromatogr.*, 322 (1985) 228.
6 C.J. Biermann, C.M. Kinoshita, J.A. Mallet and R.D. Steele, *J. Chromatogr.*, 357 (1986) 330.
7 T.P. Mawhinney, R.S.R. Robinett, A. Atalay and M.A. Madson, *J. Chromatogr.*, 358 (1986) 231.
8 S.L. MacKenzie, D. Tenaschuk and G. Fortier, *J. Chromatogr.*, 387 (1987) 241.
9 C.H. Goh, K.G. Craven, J.R. Lepock and E.B. Dumbroff, *Anal. Biochem.*, 163 (1987) 175.
10 H.J. Chaves das Neves and A.M.P. Vasconcelos, *J. Chromatogr.*, 397 (1987) 249.
11 G. Fortier, D. Tenaschuk and S.L. MacKenzie, *J. Chromatogr.*, 361 (1986) 253.
12 R.J. Early, J.R. Thompson, G.W. Sedgwick, J.M. Kelly and R.J. Christopherson, *J. Chromatogr.*, 416 (1987) 15.
13 H.J. Chaves das Neves, A.M.P. Vasconcelos, J.R. Tavares and P.N. Ramos, *J. High Resolut. Chromatogr. Chromatogr. Commun.*, 11 (1988) 12.
14 P. Hušek and C.C. Sweeley, *J. High Resolut. Chromatogr.*, 14 (1991) 751.
15 P. Hušek, *J. Chromatogr.*, 552 (1991) 289.
16 K.R. Leimer, R.H. Rice and C.W. Gehrke, *J. Chromatogr.*, 141 (1977) 355.
17 K.R. Leimer, R.H. Rice and C.W. Gehrke, *J. Chromatogr.*, 141 (1977) 121.
18 H. Wilson and R.K. Cannan, *J. Biol. Chem.*, 119 (1937) 309.
19 J.P. Greenstein and M. Winitz, *Chemistry of the Amino Acids*, Vol. 3, Wiley, New York, 1961, p. 1934.

*Journal of Chromatography*, 638 (1993) 108–111
Elsevier Science Publishers B.V., Amsterdam

CHROM. 24 983

# Short Communication

# Determination of stabilizers in human serum albumin preparations

Jan Šípoš

*Imuna, 082 22 Šarišské Michal'any (Slovak Republic)*

Anna Ninčáková*

*Faculty of Sciences, P.J. Šafarik University, Moyzesova 11, 041 67 Košice (Slovak Republic)*

(First received September 11th, 1992; revised manuscript received February 5th, 1993)

ABSTRACT

A rapid isotachophoretic method was used for the simultaneous determination of sodium octanoate and N-acetyl-DL-tryptophan, which are used for the stabilization of human serum albumin (HSA) solution. The methods of external calibration and standard addition were used with conductimetric and spectrophotometric detection. The operational system applied is suitable also for the simultaneous determination of organic acids present in HSA solution without further treatment.

## INTRODUCTION

Commercially prepared solutions of 20 or 5% human serum albumin (HSA) concentration are thermally treated in the course of their production in the presence of stabilizers [1], *e.g.*, a mixture of 20 or 5 mmol each of sodium octanoate and N-acetyl-DL-tryptophan. In order to test the quality of the final products, various analytical methods have been utilized [2–10], but all of them require treatment of the samples prior to the analysis. In this paper, a rapid isotachophoretic method without treatment such as extraction or protein precipitation is suggested. The operational system described by Everaerts *et al.* [11] was modified and used for the simultaneous determination of organic acids in the HSA solution.

## EXPERIMENTAL

Samples of albumin were from Imuna (Šarišské Michal'any, Slovak Republic). Sodium octanoate and N-acetyl-DL-tryptophan were supplied by Merck (Darmstadt, Germany), the reagents for the preparation of the operational electrolyte system by Serva (Heidelberg, Germany) and acetate and citrate by Lachema (Brno, Czech Republic).

A CS isotachophoretic analyser (VVZ PJT, Spišská Nová Ves, Slovak Republic) was used. The separation unit was assembled in a coupled-column configuration [12–14] with a 40 × 0.85

* Corresponding author.

0021-9673/93/$06.00 

mm I.D. preseparation column coupled to a 150 × 0.30 mm I.D. analytical column with conductimetric and spectrophotometric (254 nm) detection. The detector signals were automatically recorded and evaluated with a computer using ITP software from KasComp (Bratislava, Slovak Republic). The operational electrolyte system was as follows: the leading electrolyte consisted of 10 mmol/l each histidine and histidine monochloride, with 0.1% hydroxylethylcellulose (HEC) solution added to suppress electroendoosmosis, and the terminating electrolyte contained 5 mmol/l 2-(N-morpholino)ethanesulphonic acid (MES) and 9.6% ethanol. The pH was adjusted to 6.0 by adding tris(hydroxymethyl)aminomethane (Tris).

Samples were prepared by diluting the proteins to a concentration of 0.2% with water and ethanol and analysed without further treatment such as extraction or protein precipitation. A 30-$\mu$l aliquot of the sample was analysed. External calibration and standard addition were used. The calibration solutions contained 0.2% of protein (human albumin), 4.8% (v/v) of ethanol, 0.40–0.05 mmol of sodium octanoate and 0.05–0.40 mmol of N-acetyl-DL-tryptophan. The standard addition solution contained 0.40 mmol of sodium octanoate, 0.40 mmol of N-acetyl-DL-tryptophan, 0.70 mmol of citrate, 0.80 mmol of acetate and 4.8% (v/v) of ethanol. The sample solution was injected into the terminating electrolyte near the boundary between the leading and terminating electrolytes. The driving current in the detection capillary ($I_2$) was 50 $\mu$A.

## RESULTS

The signals were evaluated from the conductimetric detector of the detection capillary in the case of sodium octanoate and from both the conductimetric and UV detectors of the detection capillary in the case of N-acetyl-DL-tryptophane.

Fig. 1 shows the isotachopherogram of 20% HSA diluted 100-fold. The zones of the components determined are perfectly separated, which enables not only sodium octanoate (zone 3) and acetyltryptophan (zone 4) to be deter-

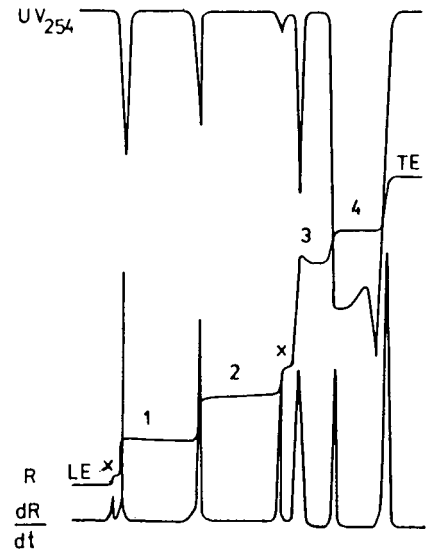


Fig. 1. Isotachopherogram of 20% HSA diluted 100-fold. 1 = citrate; 2 = acetate; 3 = sodium octanoate; 4 = N-acetyl-DL-tryptophan; × = unidentified impurities from electrolyte system. $R$ = response of the conductimetric detector; d$R$/d$t$ = derivative of the conductimetric detector response with time; $A$ = absorbance of the UV detector at 254 nm; $I_1$ = 250 $\mu$A; $I_2$ = 50 $\mu$A; amount of sample = 30 $\mu$l.

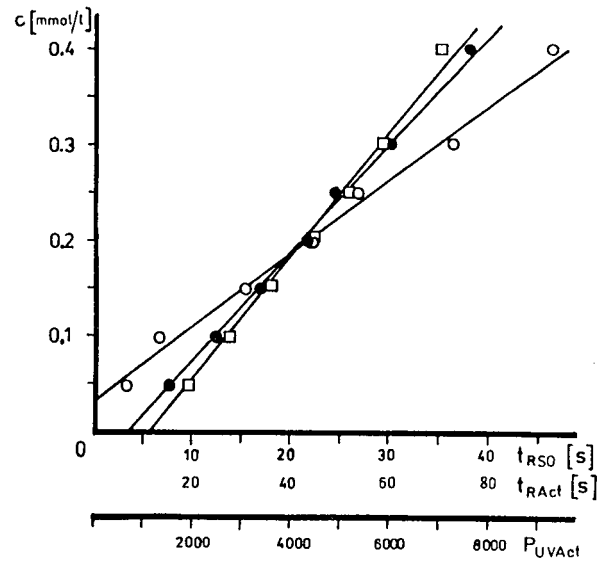


Fig. 2. Calibration graphs for (○) sodium octanoate and (●) N-acetyl-DL-tryptophan, both sets of values from the conductimetric detector, and (□) N-acetyl-DL-tryptophan from the UV detector at 254 nm. The horizontal axis represents zone length in seconds for conductimetric detection and the area of the peaks calculated electronically for UV detection.

mined, but also the citrate and acetate contents (zones 1 and 2, respectively).

For quantitative analysis the calibration graphs covered the range 0.05–0.40 mmol/l, obtained by analysing a series of standard solutions. The calibration graphs (see Fig. 2) were linear in this range and can be expressed by the following equations:

$$c_{RSO} = 0.0077t + 0.034 \quad r = 0.9960$$

$$c_{RAct} = 0.0058t - 0.042 \quad r = 0.9989$$

$$c_{UVAct} = 0.000065P - 0.82 \quad r = 0.9964$$

where $c_{RSO}$ is the sodium octanoate concentration (mmol/l), $c_{RAct}$ and $c_{UVAct}$ are those for N-acetyl-DL-tryptophan obtained from conductimetric and spectrophotometric detection respectively (mmol/l), $t$(s) is the zone length, $P$ is the peak area, and $r$ is the correlation coefficient.

The results for the stabilizer content in the samples of 20% and 5% HSA are summarized in Table I. As can be seen, external calibration gives sufficiently accurate results (the declared values are 20 mmol). In spite of this, it is necessary to use the standard addition method when citrate and acetate in HSA are to be determined. These compounds are usually present in HSA solutions. Analysis is carried out in the presence of proteins, *i.e.*, without their removal prior to the isotachophoretic determination.

The reproducibility of the zone measurements with sodium octanoate is less than 1 s and with N-acetyl-DL-tryptophan less than 2 s. UV detection is more suitable for N-acetyl-DL-tryptophan determination.

## CONCLUSIONS

The method described for the determination of sodium octanoate and N-acetyl-DL-tryptophan in HSA is rapid and simple. The time for one measurement of a multi-component mixture is *ca.* 22 min. It is possible, in addition to the above-mentioned components, to determine simultaneously also citrate and acetate ions. By the standard addition method, twenty samples of HSA were analysed isotachophoretically with a relative error of 1–15%.

## REFERENCES

1 M.W. Yu and J.S. Finlaison, *Vox Sang.*, 47 (1984) 28.
2 K. Nishimura, K. Takeda, K. Haraba, M. Nakayama and A. Sugii, *J. Liq. Chromatogr.*, 15 (1992) 791.
3 V.B. Gavrilov, V.B. Nikolskaja and V.G. Kaler, *Mol. Biol. (USSR)*, 24 (1990) 1211.
4 M.A. Rockas, A.E. Tufenkji, P. Levillain and G. Houin, *Drug Res.*, 41 (1991) 1286.
5 A. M. Ahern and R. L. Garrel, *Langmuir*, 7 (1991) 254.
6 H. Tadshi, T. Kazuniko, K. Hideshi and K. Kakashi, *Jpn. Kokai Tokyo Koho*, JP 02 186 246 (90 186 246) (1990); *C.A.*, 114 (1991) 97778t.
7 M.R. Ladisch, R.L. Hendrikson and K.L. Kohlmann, *Protein Purif. Mol. Mech. Large-Scale Processes (ACS Symposium Series*, No. 427), American Chemical Society, Washington, DC, 1990, pp. 93–103.

TABLE I

STABILIZER CONTENT OF 20% AND 5% HSA

Leading electrolyte: 10 mmol histidine–histidine monochloride (pH 5.95). NAct = N-acetyl-DL-tryptophan; $NAct^+$ = values obtained with UV detection.

| Stabilizer | Stabilizer content (mmol/l) | | | |
|---|---|---|---|---|
| | 20% HSA | | 5% HSA | |
| | External calibration | Standard addition | External calibration | Standard addition |
| Sodium octanoate | 19.8 | 18.2 | 4.9 | 4.2 |
| NAct | 19.0 | 22.3 | 4.9 | 5.2 |
| $NAct^+$ | 20.8 | 20.3 | 4.9 | 4.9 |

8 T. Dengler, S. Kellner and G. Furst, *Infusionstherapie*, 15 (1988) 273.
9 S. Tohru, M. Naka and T. Tsugikazu, *J. Biomater. Sci., Polym. Ed.*, 1, No. 1 (1989) 3.
10 Y. Takashi, K. Tsuneo and H. Nobuo, *Eur. Pat. Appl.*, EP 398 388 (C) (1990); *Jpn. Pat. Appl.*, 89 126 286 (1989), *C.A.*, 115 (1991) 45685m.
11 F.M. Everaerts, J.L. Beckers and Th.P.E.M. Verheggen, *Isotachophoresis —Theory, Instrumentation and Applications* (*Journal of Chromatography Library*, Vol. 6), Elsevier, Amsterdam, Oxford, New York, 1976, p. 295.
12 F.M. Everaerts, Th.P.E.M. Verheggen and F.E.P. Mikkers, *J. Chromatogr.*, 169 (1979) 21.
13 D. Kaniansky, *Thesis*, Komenský University, Bratislava, 1983.
14 D. Kaniansky, I. Zelenský, P. Havaši and M. Cerovský, *J. Chromatogr.*, 367 (1986) 274.

# Capillary Electrophoresis

## Principles, Practice and Applications

*by* **S.F.Y. Li**, *National University of Singapore, Singapore*

Journal of Chromatography Library Volume 52

Capillary Electrophoresis (CE) has had a very significant impact on the field of analytical chemistry in recent years as the technique is capable of very high resolution separations, requiring only small amounts of samples and reagents. Furthermore, it can be readily adapted to automatic sample handling and real time data processing. Many new methodologies based on CE have been reported. Rapid, reproducible separations of extremely small amounts of chemicals and biochemicals, including peptides, proteins, nucleotides, DNA, enantiomers, carbohydrates, vitamins, inorganic ions, pharmaceuticals and environmental pollutants have been demonstrated. A wide range of applications have been developed in greatly diverse fields, such as chemical, biotechnological, environmental and pharmaceutical analysis.

This book covers all aspects of CE, from the principles and technical aspects to the most important applications. It is intended to meet the growing need for a thorough and balanced treatment of CE. The book will serve as a comprehensive reference work and can also be used as a textbook for advanced undergraduate and graduate courses. Both the experienced analyst and the newcomer will find the text useful.

***Contents:***



**1992 xxvi + 586 pages**
**Price: US$ 225.50 / Dfl. 395.00**
**ISBN 0-444-89433-0**

**TO ORDER**

Contact your regular supplier or:

**ELSEVIER SCIENCE PUBLISHERS**
P.O. Box 211
1000 AE Amsterdam
The Netherlands

Customers in the USA & Canada:

**ELSEVIER SCIENCE PUBLISHERS**
Attn. Judy Weislogel
P.O. Box 945
Madison Square Station
New York, NY 10160-0757, USA

*No postage will be added to prepaid book orders. US $ book prices are valid only in the USA and Canada. In all other countries the Dutch guilder (Dfl.) price is definitive. Customers in The Netherlands please add 6% BTW. In New York State please add applicable sales tax. All prices are subject to change without prior notice.*

ELSEVIER
SCIENCE PUBLISHERS

## PUBLICATION SCHEDULE FOR THE 1993 SUBSCRIPTION

*Journal of Chromatography* and *Journal of Chromatography, Biomedical Applications*

| MONTH | 1992 | J | F | M | A | M | J | |
|---|---|---|---|---|---|---|---|---|
| Journal of Chromatography | 623–627 | 628/1<br>628/2<br>629/1<br>629/2 | 630/1 + 2<br>631/1 + 2<br>632/1 + 2<br>633/1 + 2 | 634/1<br>634/2 | 635/1<br>635/2<br>636/1<br>636/2 | 637/1<br>637/2<br>638/1<br>638/2 | 639/1<br>639/2<br>640/1 + 2 | The publication schedule for further issues will be published later. |
| Cumulative Indexes, Vols. 601–650 | | | | | | | | |
| Bibliography Section | | | | 649/1 | | | 649/2 | |
| Biomedical Applications | | 612/1 | 612/2 | 613/1 | 613/2<br>614/1 | 614/2<br>615/1 | 615/2<br>616/1 | |

## INFORMATION FOR AUTHORS

(Detailed *Instructions to Authors* were published in Vol. 609, pp. 437–443. A free reprint can be obtained by application to the publisher, Elsevier Science Publishers B.V., P.O. Box 330, 1000 AH Amsterdam, Netherlands.)

**Types of Contributions.** The following types of papers are published in the *Journal of Chromatography* and the section on *Biomedical Applications:* Regular research papers (Full-length papers), Review articles, Short Communications and Discussions. Short Communications are usually descriptions of short investigations, or they can report minor technical improvements of previously published procedures; they reflect the same quality of research as Full-length papers, but should preferably not exceed five printed pages. Discussions (one or two pages) should explain, amplify, correct or otherwise comment substantively upon an article recently published in the journal. For Review articles, see inside front cover under Submission of Papers.

**Submission.** Every paper must be accompanied by a letter from the senior author, stating that he/she is submitting the paper for publication in the *Journal of Chromatography.*

**Manuscripts.** Manuscripts should be typed in **double spacing** on consecutively numbered pages of uniform size. The manuscript should be preceded by a sheet of manuscript paper carrying the title of the paper and the name and full postal address of the person to whom the proofs are to be sent. As a rule, papers should be divided into sections, headed by a caption (*e.g.*, Abstract, Introduction, Experimental, Results, Discussion, etc.) All illustrations, photographs, tables, etc., should be on separate sheets.

**Abstract.** All articles should have an abstract of 50–100 words which clearly and briefly indicates what is new, different and significant. No references should be given.

**Introduction.** Every paper must have a concise introduction mentioning what has been done before on the topic described, and stating clearly what is new in the paper now submitted.

**Illustrations.** The figures should be submitted in a form suitable for reproduction, drawn in Indian ink on drawing or tracing paper. Each illustration should have a legend, all the *legends* being typed (with double spacing) together on a *separate sheet.* If structures are given in the text, the original drawings should be supplied. Coloured illustrations are reproduced at the author's expense, the cost being determined by the number of pages and by the number of colours needed. The written permission of the author and publisher must be obtained for the use of any figure already published. Its source must be indicated in the legend.

**References.** References should be numbered in the order in which they are cited in the text, and listed in numerical sequence on a separate sheet at the end of the article. Please check a recent issue for the layout of the reference list. Abbreviations for the titles of journals should follow the system used by *Chemical Abstracts.* Articles not yet published should be given as "in press" (journal should be specified), "submitted for publication" (journal should be specified), "in preparation" or "personal communication".

**Dispatch. Before sending the manuscript to the Editor please check that the envelope contains four copies of the paper complete with references, legends and figures. One of the sets of figures must be the originals suitable for direct reproduction. Please also ensure that permission to publish has been obtained from your institute.**

**Proofs.** One set of proofs will be sent to the author to be carefully checked for printer's errors. Corrections must be restricted to instances in which the proof is at variance with the manuscript. "Extra corrections" will be inserted at the author's expense.

**Reprints.** Fifty reprints will be supplied free of charge. Additional reprints can be ordered by the authors. An order form containing price quotations will be sent to the authors together with the proofs of their article.

*Ovomucoid Bonded Column for Direct Chiral Separation*

# ULTRON ES-OVM

**Narrow-Bore Column ( 2.0 I.D. x 150 mm ) for Trace Analyses**
**Analytical Column ( 4.6 I.D. , 6.0 I.D. x 150 mm ) for Regular Analyses**
**Semi-Preparative Column (20.0 I.D. x 250 mm ) for Preparative Separation**

***Analysis of Trace FLURBIPROFEN in Metabolite with NARROW-BORE COLUMN***

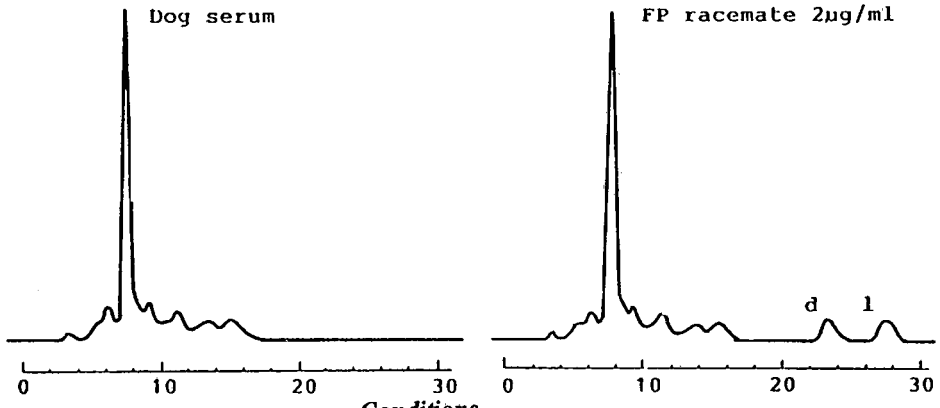


***Conditions***

Column: ULTRON ES-OVM(2.0I.D. x 150mm)
Mobile Phase: 20mMPhosphate Buffer(pH=3.0)/CH3CN =100/15
Flow Rate: 0.1ml/min
Temperature: 25°C
Injection: 5µl
Detection: UV- 247nm(0.05AUFS)

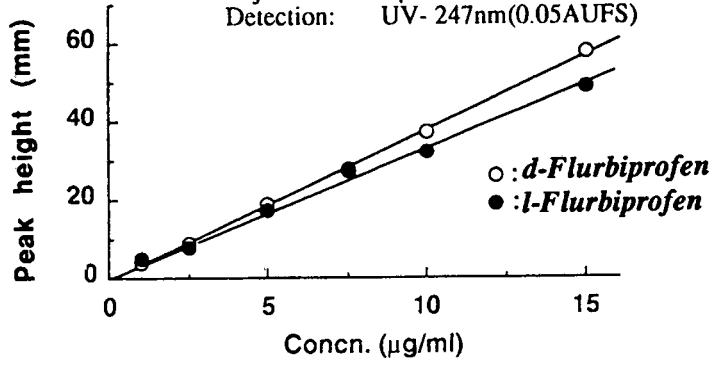


Calibration Curve for Each Enantiomer of Flurbiprofen


## SHINWA CHEMICAL INDUSTRIES, LTD.

**50 Kagekatsu-cho, Fushimi-ku, Kyoto 612, JAPAN**
**Phone:+81-75-621-2360 Fax:+81-75-602-2660**

**In the United States and Europe, please contact:**

## Rockland Technologies, Inc.

**538 First State Boulevard, Newport, DE 19804, U.S.A.**
**Phone: 302-633-5880 Fax: 302-633-5893**


**This product is licenced by Eisai Co., Ltd.**